

**Investigating the mode of action of tuberculosis  
drugs using hypersensitive mutants of  
*Mycobacterium smegmatis***

by

**Richard Laurence Campen**

BSc(Hons.) Victoria University of Wellington

A thesis submitted to the Victoria University of Wellington in fulfilment of the requirements  
for the degree of Doctor of Philosophy in Molecular Microbiology

Victoria University of Wellington

2015



**Primary Supervisor**

Dr Ronan O'Toole

Senior Lecturer, School of Medicine

University of Tasmania

**Victoria Supervisor**

Professor John H. Miller

School of Biological Sciences

Victoria University of Wellington



## Abstract

*Mycobacterium tuberculosis*, the etiological agent of tuberculosis (TB), is the leading cause of death and disease by a bacterial pathogen worldwide. The growing incidence of drug resistant TB, especially multi-drug resistant TB highlights the need for new drugs with novel modes of action. Current treatment of TB involves a multi-drug regimen of four drugs including isoniazid and rifampicin, both of which were discovered over 40 years ago. Bedaquiline is one of the first novel TB drugs to enter clinical trials since the discovery of rifampicin, and has shown excellent activity against drug resistant TB. Although isoniazid and rifampicin are well established anti-TB drugs, significant gaps in knowledge regarding their modes of action exist. Furthermore, little information on the mode of action of the novel drug bedaquiline is known beyond its primary target. Characterisation of drug mode of action facilitates rational modifications of drugs to improve the treatment of TB.

The aim of this study was to identify novel aspects of the modes of action of isoniazid, rifampicin, and bedaquiline by characterising drug hypersensitive mutants of *M. smegmatis* mc<sup>2</sup>155. A sub-saturated *M. smegmatis* mc<sup>2</sup>155 transposon mutant collection with 1.1-fold genome coverage (7680 mutants) was constructed, with this collection estimated to contain mutations in 73.2% of all genes capable of maintaining a transposon insertion (non-essential genes). A high-throughput assay was developed for screening the collection, and mutants related to known drug mode of action were identified for isoniazid (*ahpC* and *eccCa<sub>1</sub>*) and bedaquiline (*atpB*). Additionally, known mechanisms of drug inactivation were identified for isoniazid (*nudC*), rifampicin (*arr* and *lspA*), and bedaquiline (*mmpL5*). The finding that transposon mutants of *nudC* are hypersensitive to isoniazid independently validated the recent discovery of the role of NudC in basal isoniazid resistance by Wang et al. (2011). The remaining genes identified in this thesis represent potentially novel aspects of the modes of action or resistance mechanisms of these drugs.

Cross-sensitivity to other drugs indicated that the mechanism of sensitivity was drug specific for the mutants examined. Differential-sensitivity testing against drug analogues revealed that Arr is involved in resistance to the rifampicin analogue rifapentine as well, indicating that Arr can detoxify rifapentine similar to rifampicin. The *nudC* mutant showed increased sensitivity to a range of isoniazid analogues, indicating that it can detoxify these analogues

similar to the parent compound. Interestingly six analogues were found to be less active against the *nudC* mutant than expected. A number of overexpression strains were tested against these six analogues; a *nudC* overexpression strain, and a strain overexpressing *inhA*, the primary target for isoniazid. Overexpression of *nudC* as well *inhA* increased the resistance of WT to isoniazid, but failed to increase resistance to three of the analogues, NSC27607, NSC33759, and NSC40350. Isoniazid is a prodrug and is activated by the peroxidase/catalase enzyme KatG. Overexpression of *katG* resulted in increased isoniazid sensitivity, as well as increased sensitivity to NSC27607, NSC33759, and NSC40350. Together these results suggest that NSC27607, NSC33759, and NSC40350 are activated by KatG, but that *InhA* is not the primary target. Additionally the inability of *NudC* overexpression to confer resistance suggests these analogues are not acting via a NAD adduct, the mechanism by which isoniazid inhibits *InhA*. These results suggest that there are other toxic metabolites being produced by KatG activation of these three analogues.

In conclusion, characterisation of mutants identified in a high-throughput assay for drug hypersensitivity identified genes involved in the modes of action or resistance mechanisms for isoniazid, rifampicin, and bedaquiline. Additionally, a number of novel genes were identified that have no known connections to the known modes of action or resistance mechanisms for these drugs. Further testing of a *nudC* mutant revealed three isoniazid analogues that appear to inhibit growth of *M. smegmatis* mc<sup>2</sup>155 independent of *InhA*, the primary target of isoniazid. This study has successfully demonstrated that screening for drug hypersensitivity can generate novel information on drug mode of action and resistance mechanisms. This information can ultimately be used to help drive the development of new drugs, and improve treatment of TB.

## **Acknowledgements**

First I would like to thank my primary supervisor Ronan O'Toole for taking me on as a PhD student, and thank you for your support and guidance throughout my project. I would also like to thank my Victoria supervisor Professor John Miller for his support during the later stages of my PhD project, particularly with proof reading my thesis. My gratitude also goes to Associate Professor David Ackerley for taking me in during the later stages of my PhD. Inclusion in your lab group helped me get through the last few years of my project. Thank you also for your help with proof reading my thesis. Thank you also to Dr Joanna Mackichan for sharing her lab space during the last few years of my PhD.

I am also grateful to the fellow O'Toole lab students over the years, Shahista Nisa, Chris Miller, Nathaniel Dasyam, Ian Bassett, Mudassar Altaf, and Sandi Dempsy. Your help and guidance over the years was invaluable. My gratitude also to Yee Suen Low for her help with practical aspects of my project. Thank you also to the Ackerley lab group, including long time office mates Mark Calcott, Katherine Robins, and Becky Edgar, as well as the rest of KK815/816 for their support and friendship throughout my PhD.

Thank you also to our collaborator Professor Greg Cook at the University of Otago, and his post-doc Jen Robson. Thank you for providing a sample of bedaquiline for this study, and for your help with the practical aspects of the bedaquiline assay. Thank you also for flying me down to Otago to discuss my project, and present my work to your research group.

Thank you to my wonderful family and friends for all their support throughout my PhD. Especially thank you to my mother and father for their emotional and financial support, and to my father for sharing his roof with us for the last couple years. Finally, thank you to my amazing wife Kelly. Thank you so much for your love and support, it has been instrumental in me completing this project.





# Table of Contents

<b>Abstract .....</b>	<b>i</b>
<b>Acknowledgements .....</b>	<b>iii</b>
<b>Table of Contents.....</b>	<b>v</b>
<b>List of Figures.....</b>	<b>xi</b>
<b>List of Tables.....</b>	<b>xiii</b>
<b>List of Abbreviations .....</b>	<b>xiv</b>

<b>1. General Introduction.....</b>	<b>1</b>
1.1. Tuberculosis.....	1
1.1.1. Tuberculosis in New Zealand .....	4
1.2. Pathogenesis.....	4
1.3. Mycobacteria .....	6
1.3.1. Physiology.....	6
1.3.2. <i>Mycobacterium tuberculosis</i> .....	8
1.3.3. <i>Mycobacterium smegmatis</i> .....	9
1.4. Treatment of tuberculosis .....	10
1.4.1. Anti-tuberculosis Drugs.....	11
1.4.2. Drug resistance.....	13
1.4.3. Modes of action of the anti-tuberculosis drugs to be examined in this study..	13
1.5. Drug Discovery.....	15
1.5.1. Mode of action identification.....	16
1.5.1.1. Resistance inducing mutations.....	17
1.5.1.2. Altered transcription with drug treatment .....	17
1.5.1.3. Hypersensitivity inducing mutations .....	18
1.6. Random transposon mutagenesis of <i>M. smegmatis</i> .....	19
1.7. Aims of this thesis.....	20
<b>2. Materials and Methods .....</b>	<b>21</b>
2.1. Bacterial strains .....	21
2.2. Plasmids.....	21
2.3. Chemicals and reagents.....	21
2.4. Enzymes.....	22

2.5.	Growth media .....	22
2.5.1.	Media supplements.....	22
2.5.2.	<i>E. coli</i> growth conditions .....	23
2.5.3.	Mycobacteria growth conditions .....	24
2.5.3.1.	<i>M. smegmatis</i> mc <sup>2</sup> 155 .....	24
2.5.3.2.	<i>M. tuberculosis</i> H <sub>37</sub> Rv .....	24
2.6.	Molecular biology .....	25
2.6.1.	DNA isolation and purification .....	25
2.6.1.1.	CTAB genomic DNA isolation .....	25
2.6.1.2.	Plasmid mini-preparation .....	25
2.6.1.3.	Plasmid midi-preparation .....	26
2.6.1.4.	Agarose gel electrophoresis .....	26
2.6.1.5.	Agarose gel DNA extraction.....	26
2.6.1.6.	DNA purification .....	26
2.6.1.7.	DNA quantification .....	26
2.6.2.	DNA sequencing .....	27
2.6.3.	Genetic manipulations .....	27
2.6.3.1.	Primers.....	27
2.6.3.2.	Polymerase chain reaction .....	29
2.6.3.3.	Restriction endonuclease digestions.....	33
2.6.3.4.	Blunting of DNA ends.....	33
2.6.3.5.	DNA phosphatase treatment.....	33
2.6.3.6.	DNA ligations .....	33
2.6.4.	Generation of substrate for inverse PCR .....	33
2.6.5.	Generation of substrate for ligation mediated PCR.....	34
2.6.6.	Transformation of <i>E. coli</i> DH5α .....	34
2.6.6.1.	Generation of chemically competent <i>E. coli</i> cells .....	34
2.6.6.2.	Heat shock transformation of <i>E. coli</i> cells .....	35
2.6.7.	Transformation of <i>M. smegmatis</i> mc <sup>2</sup> 155 .....	35
2.6.7.1.	Generation of electrocompetant <i>M. smegmatis</i> cells.....	35
2.6.7.2.	Electroporation of <i>M. smegmatis</i> cells.....	35
2.6.8.	Construction of strain MRC10 .....	36
2.6.9.	Construction of plasmid pRC20.....	37
2.6.9.1.	Construction of pRC20 gene insert vectors.....	38
2.6.10.	Random transposon mutagenesis of <i>M. smegmatis</i> mc <sup>2</sup> 155.....	39

2.7.	Transposon mutant collection construction .....	39
2.7.1.	Generation of mother stock.....	39
2.7.2.	Generation of daughter stock .....	41
2.7.3.	Generation of mini-hit libraries.....	41
2.8.	Growth-inhibition assays .....	42
2.8.1.	Assay for Drug hypersensitivity.....	42
2.8.1.1.	Primary assay for drug hypersensitivity .....	42
2.8.1.2.	Secondary assay for drug-hypersensitivity.....	44
2.8.2.	Isoniazid analogue screen .....	45
2.8.3.	Dose-response assay .....	46
2.9.	Growth curve assay .....	47
<b>3.</b>	<b>Isolation of drug hypersensitive mutants of <i>M. smegmatis</i> mc<sup>2</sup>155.....</b>	<b>49</b>
3.1.	Introduction.....	49
3.1.1.	Transposon mutagenesis with <i>Tn611</i> .....	49
3.1.2.	Assaying for drug hypersensitivity .....	50
3.1.3.	Objectives of Chapter Three .....	51
3.2.	Methods.....	52
3.2.1.	Estimation of unique mutants versus library size .....	52
3.2.2.	Construction of the transposon mutant collection.....	53
3.2.3.	Primary assay for drug hypersensitivity .....	54
3.2.3.1.	Optimising screening concentrations.....	55
3.2.4.	Secondary assay for drug hypersensitivity.....	56
3.3.	Results.....	56
3.3.1.	Drug screening concentration optimisation .....	56
3.3.2.	Growth of the treated-MRC10 control strain in LB.....	57
3.3.3.	Control strains for quantitating drug hypersensitivity.....	57
3.3.4.	Isoniazid .....	59
3.3.4.1.	Primary assay for drug hypersensitivity .....	59
3.3.4.2.	Secondary assay for drug hypersensitivity .....	61
3.3.4.3.	Quantification of mutant hypersensitivity .....	62
3.3.5.	Rifampicin .....	63
3.3.5.1.	Primary assay for drug hypersensitivity .....	63
3.3.5.2.	Secondary assay for drug hypersensitivity .....	65
3.3.5.3.	Quantification of mutant hypersensitivity .....	66

3.3.5.4.	Growth curve of rifampicin hypersensitive mutant <i>myco4005</i> .....	67
3.3.6.	Bedaquiline .....	68
3.3.6.1.	Primary assay for drug hypersensitivity .....	68
3.3.6.2.	Secondary assay for drug hypersensitivity .....	70
3.3.6.3.	Quantification of mutant hypersensitivity .....	71
3.4.	Discussion .....	72
3.4.1.	Screening for drug hypersensitivity .....	72
3.4.2.	Quantifying drug sensitivity .....	75
3.4.3.	Summary .....	76
<b>4.</b>	<b>Genotypic validation of drug hypersensitive mutants of <i>M. smegmatis</i> .....</b>	<b>77</b>
4.1.	Introduction .....	77
4.1.1.	Transposition site identification.....	77
4.1.2.	Conditional gene expression in mycobacteria .....	78
4.1.3.	Objectives of Chapter Four .....	79
4.2.	Methods.....	80
4.2.1.	Transposon insertion site identification .....	80
4.2.1.1.	Inverse PCR .....	80
4.2.1.2.	Ligation-mediated PCR .....	81
4.2.1.3.	Sequence processing .....	82
4.2.2.	Optimisation of tetracycline concentration for induction of gene expression from plasmid pRC20.....	83
4.2.3.	Complementation of transposon mutants .....	84
4.2.4.	Overexpression of <i>M. smegmatis</i> genes .....	84
4.3.	Results.....	85
4.3.1.	Isoniazid.....	85
4.3.1.1.	Transposon insertion site identification.....	85
4.3.1.2.	Complementation of isoniazid hypersensitive mutants.....	87
4.3.1.3.	Overexpression of genes related to isoniazid hypersensitivity.....	90
4.3.2.	Rifampicin.....	92
4.3.2.1.	Transposon insertion site identification.....	92
4.3.2.2.	Complementation of rifampicin hypersensitive mutants .....	94
4.3.2.3.	Overexpression of genes related to rifampicin hypersensitivity .....	95
4.3.3.	Bedaquiline.....	96
4.3.3.1.	Transposon insertion site identification.....	96

4.4.	Discussion .....	98
4.4.1.	Identification of transposon insertion sites .....	98
4.4.2.	Genetic complementation .....	99
4.4.3.	Gene overexpression.....	100
4.4.4.	Polar effects of <i>Tn611</i> insertion .....	100
4.4.5.	Genotypes related to isoniazid hypersensitivity .....	101
4.4.5.1.	Links to known isoniazid mode of action and resistance mechanisms.....	101
4.4.5.2.	Identification of potentially novel aspects of isoniazid's mode of action....	103
4.4.6.	Genotypes related to rifampicin hypersensitivity.....	106
4.4.6.1.	Links to known rifampicin mode of action and resistance mechanisms.....	106
4.4.6.2.	Identification of potentially novel aspects of rifampicin's mode of action .	107
4.4.7.	Genotypes related to bedaquiline hypersensitivity .....	109
4.4.7.1.	Links to known bedaquiline mode of action and resistance mechanisms...	109
4.4.7.2.	Identification of potentially novel aspects of bedaquiline's mode of action	110
4.4.8.	Summary .....	112
<b>5.</b>	<b>Characterising drug sensitivity phenotypes of <i>Tn611</i> mutants.....</b>	<b>114</b>
5.1.	Introduction .....	114
5.1.1.	Analogues of anti-tuberculosis drugs.....	114
5.1.2.	Isoniazid, rifampicin, and bedaquiline hypersensitive mutants .....	115
5.1.2.	Objectives of Chapter Five .....	116
5.2.	Methods.....	117
5.2.1.	Cross sensitivity testing of transposon mutants to other drugs.....	117
5.2.2.	Differential-sensitivity testing of transposon mutants to drug analogues.....	117
5.2.2.1.	Selection of isoniazid analogues for differential-sensitivity testing.....	118
5.2.3.	Overexpression strains versus isoniazid analogues .....	118
5.2.3.1.	<i>katG</i> overexpression strain versus isoniazid analogues .....	118
5.2.4.	<i>M. tuberculosis</i> H <sub>37</sub> Rv versus isoniazid analogues .....	119
5.3.	Results.....	120
5.3.1.	Cross-sensitivities of hypersensitive mutants.....	120
5.3.2.	Differential-sensitivity of hypersensitive mutants.....	120
5.3.2.1.	Rifapentine versus rifampicin hypersensitive transposon mutants.....	120
5.3.2.2.	Isoniazid analogues tested in isoniazid hypersensitive transposon mutants	121

5.1.1.	Isoniazid analogues versus overexpression strains.....	125
5.1.2.	Activity of isoniazid analogues in wild-type mycobacterial strains .....	129
5.4.	Discussion .....	130
5.4.1.	Cross-sensitivity of hypersensitive transposon mutants .....	130
5.4.2.	Differential-sensitivities of hypersensitive transposon mutants to drug analogues .....	131
5.4.2.1.	Role of KatG in activation of isoniazid analogues .....	134
5.4.3.	Activity of isoniazid analogues against <i>M. tuberculosis</i> .....	135
5.4.4.	Summary .....	136
<b>6.</b>	<b>General Discussion .....</b>	<b>137</b>
6.1.	Research summary .....	138
6.1.1.	Isoniazid.....	138
6.1.2.	Rifampicin.....	142
6.1.3.	Bedaquiline.....	143
6.2.	Critical evaluation of methodology .....	144
6.2.1.	Limitation of using <i>M. smegmatis</i> mc <sup>2</sup> 155 as the genetic model.....	144
6.2.2.	Use of <i>Tn611</i> for transposon mutagenesis .....	145
6.1.1.	Transposon mutant collection coverage.....	146
6.1.2.	Quantifying mutant hypersensitivity .....	148
6.1.3.	Transposon mutant controls .....	149
6.2.	Future directions .....	150
6.3.	Conclusions .....	152
<b>7.</b>	<b>References .....</b>	<b>155</b>
<b>8.</b>	<b>Appendix.....</b>	<b>172</b>
8.1.	Solutions .....	172
8.2.	Routine laboratory procedures .....	173
8.3.	<i>MSMEI</i> and <i>MSMEG</i> annotations .....	174
8.4.	Isoniazid analogues.....	175
8.5.	<i>katG</i> protein alignments.....	183
8.6.	Publications .....	184

## List of Figures

Figure 1.1: Estimated global tuberculosis incidence rates for 2013.....	2
Figure 1.2: Estimated number of global multi-drug resistant tuberculosis cases for 2013.....	3
Figure 1.3: Ziehl-Neelsen-stained <i>M. smegmatis</i> .....	7
Figure 1.4: Structure of the mycobacterial cell wall. ....	8
Figure 2.1: Digestion of pNIT-1 and plasmid maps. ....	36
Figure 2.2: Generation of pKW08 derivative pRC20. ....	38
Figure 2.3: Layout of transposon mutant collection plates. ....	40
Figure 2.4: Layout of mini-hit library plates. ....	42
Figure 2.5: Plate setup for primary assays for drug hypersensitivity. ....	43
Figure 2.6: Plate setup for secondary assays for drug hypersensitivity.....	44
Figure 2.7: Plate layout for isoniazid analogue screen. ....	45
Figure 2.8: Plate layout for dose-response assays. ....	46
Figure 2.9: Growth curve assay plate setup.....	48
Figure 3.1: Plasmid pCG79 and transposition. ....	50
Figure 3.2: Number of unique mutants versus library size. ....	53
Figure 3.3: Comparison of MIC of random mutant control strains. ....	58
Figure 3.4: Mutant library A versus 6 $\mu$ M isoniazid. ....	60
Figure 3.5: Mutant library B versus 6 $\mu$ M isoniazid. ....	61
Figure 3.6: Mutant library A versus 0.26 $\mu$ M rifampicin. ....	64
Figure 3.7: Mutant library B versus 0.26 $\mu$ M rifampicin. ....	65
Figure 3.8: Growth curve of rifampicin hypersensitive strains. ....	68
Figure 3.9: Mutant library A versus 10.8 nM bedaquiline. ....	69
Figure 3.10: Mutant library B versus 10.8 nM bedaquiline. ....	70
Figure 4.1: Tetracycline inducible promoter of plasmid pKW08. ....	79
Figure 4.2: Inverse PCR.....	81
Figure 4.3: Ligation-mediated PCR. ....	82
Figure 4.4: Alignments of pRC20 <i>MSMEI_6092</i> constructs. ....	88
Figure 4.5: Optimisation of inducer concentration for complementation assays.....	89
Figure 4.6: Complementation of isoniazid hypersensitive transposon mutants. ....	90
Figure 4.7: Optimal inducer concentration for MRC20.....	91

Figure 4.8: Dose response curve of MRC20 versus isoniazid $\pm$ inducer.....	91
Figure 4.9: Overexpression strains versus isoniazid. ....	92
Figure 4.10: Dose response curve of MRC20 versus rifampicin $\pm$ inducer. ....	95
Figure 4.11: Overexpression strains versus rifampicin. ....	96
Figure 5.1: Structure of isoniazid analogues active against <i>M. smegmatis</i> mc <sup>2</sup> 155.....	122
Figure 5.2: Growth-inhibition of WT <i>M. smegmatis</i> mc <sup>2</sup> 155 by isoniazid analogues.....	123
Figure 5.3: Overexpression strains tested with isoniazid analogues. ....	127
Figure 5.4: <i>katG<sub>sm</sub></i> overexpression strain versus isoniazid.....	128
Figure 5.5: <i>katG<sub>sm</sub></i> overexpression strain versus isoniazid analogues. ....	129



## List of Tables

Table 1.1: Modes of action of current anti-tuberculosis drugs. ....	12
Table 2.1: Bacterial strains used in this study. ....	21
Table 2.2: Plasmids used in this study. ....	21
Table 2.3: Antibiotic concentrations used for marker selection. ....	23
Table 2.4: Primer sequences used in this study. ....	27
Table 2.5: PCR conditions for product amplification. ....	30
Table 2.6: Two-step PCR thermal cycle. ....	31
Table 2.7: Three-step PCR thermal cycle. ....	31
Table 2.8: Touchdown PCR thermal cycle. ....	32
Table 2.9: Overlap PCR thermal cycle. ....	32
Table 3.1: MIC values for anti-TB drugs versus MRC10 and optimised screening concentrations. ....	57
Table 3.2: Growth-inhibition of top secondary assay hits versus isoniazid. ....	62
Table 3.3: Sensitivity of transposon mutants to isoniazid. ....	63
Table 3.4: Growth-inhibition of top secondary assay hits versus rifampicin. ....	66
Table 3.5: Sensitivity of transposon mutants to rifampicin. ....	67
Table 3.6: Growth-inhibition percentage of top secondary assay hits versus bedaquiline. ....	71
Table 3.7: Sensitivity of transposon mutants to bedaquiline. ....	72
Table 4.1: Transposon insertion sites in isoniazid hypersensitive mutants. ....	86
Table 4.2: Protein similarity matrix of Fur proteins from <i>M. smegmatis</i> mc <sup>2</sup> 155 and <i>M. tuberculosis</i> H <sub>37</sub> Rv. ....	87
Table 4.3: Transposon insertion sites in rifampicin hypersensitive mutants. ....	93
Table 4.4: Transposon insertion site for bedaquiline hypersensitive mutants. ....	97
Table 5.1: Cross-sensitivity of hypersensitive strains. ....	120
Table 5.2: Sensitivity of rifampicin hypersensitive mutants to rifapentine. ....	121
Table 5.3: Sensitivity of <i>Tn::nudC</i> to isoniazid analogues. ....	124
Table 5.4: MICs of isoniazid analogues for WT <i>M. smegmatis</i> and <i>M. tuberculosis</i> . ....	130

## List of Abbreviations

AIDS	Acquired immune deficiency syndrome
ATP	Adenine triphosphate
BLAST	Basic Local Alignment Search Tool
bp	Base pair
CFU	Colony forming unit
BCG	Bacillus Calmette-Guérin
ddH <sub>2</sub> O	Distilled deionised water
DMSO	Dimethyl sulfoxide
DNA	Deoxyribonucleic acid
DTP	Developmental therapeutics program
<i>E. coli</i>	<i>Escherichia coli</i>
EDTA	Ethylenediaminetetraacetic acid
F <sub>I</sub>	Factor of inhibition
gDNA	Genomic DNA
GFP	Green fluorescent protein
HIV	Human immunodeficiency virus
Hyg	Hygromycin B
Hyg <sup>R</sup>	Hygromycin resistance
INH	Isoniazid
Kan	Kanamycin
Kan <sup>R</sup>	Kanamycin resistance
Kb	Kilobase
LA	LB agar
LB	Luria broth
MCS	Multiple cloning site
MIC	Minimum inhibitory concentration
MDR-TB	Multi-drug resistant tuberculosis
<i>M. africanum</i>	<i>Mycobacterium africanum</i>
<i>M. bovis</i>	<i>Mycobacterium bovis</i>
<i>M. canetti</i>	<i>Mycobacterium canetti</i>
<i>M. microti</i>	<i>Mycobacterium microti</i>
<i>M. orygis</i>	<i>Mycobacterium orygis</i>
<i>M. pinnipedi</i>	<i>Mycobacterium pinnipedi</i>
<i>M. smegmatis</i>	<i>Mycobacterium smegmatis</i>
<i>M. tuberculosis</i>	<i>Mycobacterium tuberculosis</i>
mRNA	Messenger RNA
NIH	National Institute of Health
NAD	Nicotinamide adenine dinucleotide
NADH	Nicotinamide adenine dinucleotide hydride
NZ	New Zealand
OADC	Oleic acid, albumin, dextrose, catalase
OD <sub>600</sub>	Optical density at 600 nm
ORF	Open reading frame
OriE	<i>E. coli</i> origin of replication
OriM	Mycobacterial origin of replication

PCR	Polymerase chain reaction
RD1	Region of difference 1
RFU	Relative fluorescence unit
RNA	Ribonucleic acid
rRNA	Ribosomal ribonucleic acid
Spec <sup>R</sup>	Spectinomycin resistance
Strep <sup>R</sup>	Streptomycin resistance
TAE	Tris acetate-EDTA
TB	Tuberculosis
Tc	Tetracycline
TE	Tris-EDTA
ts	Temperature sensitive
v/v	Volume/volume
VUW	Victoria University of Wellington
WHO	World health organisation
WT	Wild-type
w/v	Weight/volume
XDR-TB	Extensively-drug resistant tuberculosis



## **Publications**

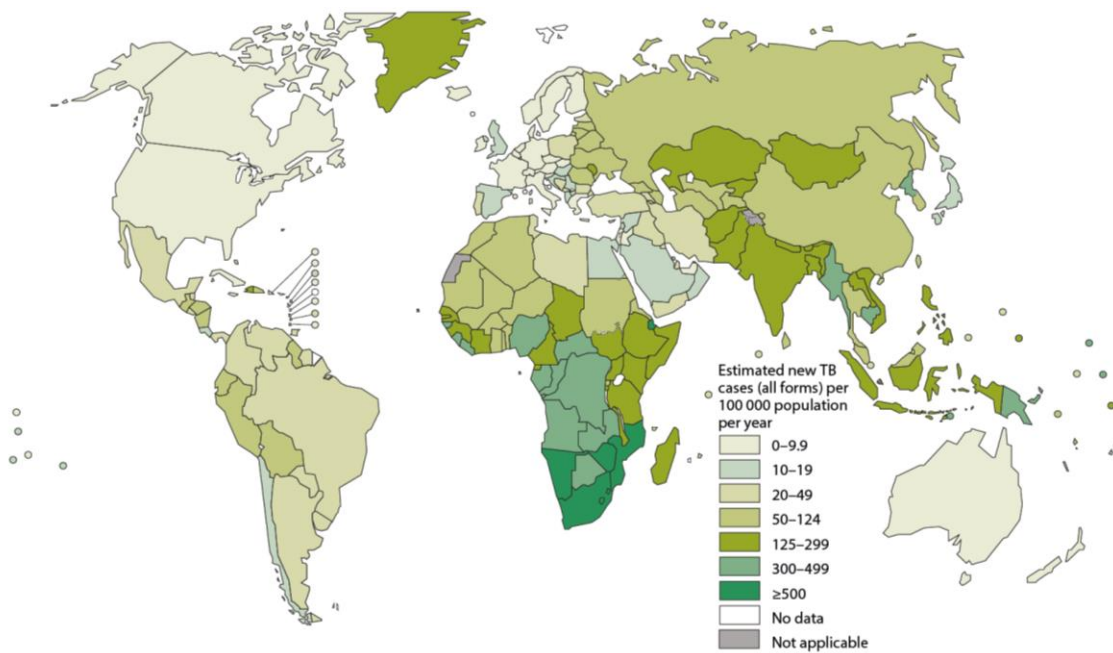
**Campen, R.L.**, Ackerley, D.F., Cook, G.M., and O'Toole, R.F. (2015). Development of a *Mycobacterium smegmatis* transposon mutant array for characterising the mechanism of action of tuberculosis drugs: Findings with isoniazid and its structural analogues. *Tuberculosis Article In Press*.

# 1. General Introduction

## 1.1. Tuberculosis

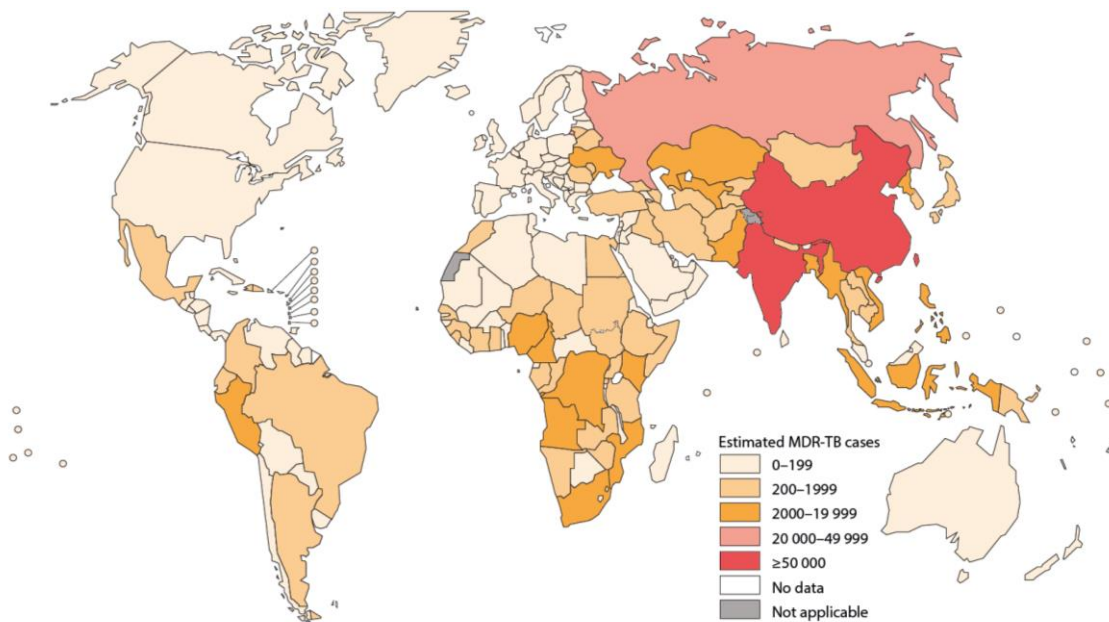
TB is a disease primarily caused by *Mycobacterium tuberculosis*, and is the first equal cause of mortality by a single pathogen along with the human immunodeficiency virus / acquired immune deficiency syndrome (HIV/AIDS) (WHO, 2014). The incidence of TB is worst amongst the poor due to factors such as inadequate health care, overcrowding and malnutrition (Bucher et al., 1999; Marais et al., 2013). As such, improvements in social economic conditions have been shown to improve TB control (Stop TB Partnership, 2006). Other significant risk factors for TB include substance abuse, smoking, chronic lung disease, and the presence of co-morbidities such as HIV and diabetes (Marais et al., 2013). These risk factors either compromise the immune system or lung integrity, increasing the rate of developing active disease, and often affecting treatment outcomes. It is estimated that one third of the world's population is infected with the etiological agent of TB, *M. tuberculosis* (Dye et al., 1999). Susceptibility to TB varies with age, with high rates in young children, lower rates in older children, and higher rates again after adolescence (Dubos and Dubos, 1952). *M. tuberculosis* can be divided into six lineages based upon genetic polymorphisms, with the different lineages varying in terms of geographic distribution, virulence, and drug resistance (Click et al., 2012; Gagneux and Small, 2007; Gagneux et al., 2006; Parwati et al., 2010; Reed et al., 2009).

In 2013 there were an estimated 9 million new cases of TB in the world, and 1.5 million deaths (WHO, 2014). Of the 9 million new cases, approximately 56% of cases occurred in South-East Asia and the Western Pacific region, with China accounting for 11% and India 24% of cases (Figure 1.1). A further 25% of all new cases were from Africa, which had the highest incidence rate along with the highest mortality rate of any region.



**Figure 1.1: Estimated global tuberculosis incidence rates for 2013.** Image reproduced from the Global tuberculosis report 2014 with permission (WHO, 2014).

Resistance to anti-TB drugs is widespread with drug resistant cases reported in all countries surveyed by the World Health Organisation (WHO) (Figure 1.2). Multi-drug resistant TB (MDR-TB), defined as resistant to at least the two front line TB drugs isoniazid and rifampicin, is of significant clinical importance as it has an associated lower cure rate (48% globally in 2011) and higher mortality rate. The incidence of new cases of MDR-TB globally was around 3.5% in 2013 (480,000); however, in some Asian and Eastern European countries the incidence was as high as 35% for new cases, and 75% for previously treated cases. Combined, India, China, and the Russian Federation account for over 50% of all MDR-TB cases. Approximately 9% of MDR-TB cases in 2013 were extensively drug resistant (XDR-TB), which displays additional resistances to fluoroquinolone and a second-line injectable agent. XDR-TB has a much lower cure rate (22% in 2011) and has now been detected in over 100 countries, with several cases of totally drug resistant XDR-TB reported (Udwadia et al., 2012; WHO, 2014).



**Figure 1.2: Estimated number of global multi-drug resistant tuberculosis cases for 2013.** Image reproduced from the Global tuberculosis report 2014 with permission (WHO, 2014).

In the 1980's TB was thought to largely be under control but by the 1990's the HIV pandemic was driving a resurgence of *M. tuberculosis* infection (Murray et al., 1990). This was particularly true in sub-Saharan Africa where HIV/AIDS was becoming a leading cause of morbidity and mortality. HIV infection is associated with increased susceptibility to TB due to the immune-compromising effects of the HIV virus (Hopewell, 1992). HIV co-infection increases the reactivation risk of TB from a 5-10% lifetime risk to a 10% risk per year (Shenoi and Friedland, 2009; Suthar et al., 2012). HIV co-infection also shows a significant association with TB drug resistance, including MDR-TB and XDR-TB (Shenoi and Friedland, 2009). *M. tuberculosis* infection in HIV positive cases represents over 10% of total cases annually, of which 80% occur in Africa, with TB responsible for 25% of deaths in HIV positive individuals (WHO, 2014). A major obstacle in treating HIV/TB co-infected individuals is that the front line TB drug rifampicin activates the cytochrome p450 system that metabolises common anti-retroviral drugs used to treat HIV, thereby reducing their efficacy (L'homme et al., 2009; Niemi et al., 2003). Diabetes is another significant comorbidity for TB, with diabetics three times more likely to develop active TB, primarily due to a defective host immune response (Lönnroth et al., 2014). Additionally, treatment of TB is less effective in diabetics, resulting in lower cure rates and higher mortality (Baker et al., 2011). In 2013, 15% of all adult cases of TB were associated with diabetes. The rates of diabetes in those countries most at risk to TB



has increased over the past decade and is proposed to be in part responsible for the lower than expected reduction in the number of cases of TB in these regions during that time frame.

### **1.1.1. Tuberculosis in New Zealand**

The incidence rate for TB in New Zealand (NZ) is 6.6 cases per 100,000 with a total of 279 new cases in 2012 (Lim and Heffernan, 2013). The majority of these cases (75%) occurred in individuals born outside of NZ, indicating that place of origin is a significant risk factor for TB in NZ. There were four cases of MDR-TB in 2012 in NZ and a total of 32 cases of MDR-TB over the previous 10 years. Of the cases of MDR-TB in NZ only two out of the 32 were NZ born, and it is assumed the other 30 were infected with MDR-TB outside of NZ (Lim and Heffernan, 2013). To date there has only been a single case of XDR-TB, which occurred during 2010. The predominant TB lineage in NZ cases is lineage four (Euro-American), followed by lineages one (Indo-Oceanic), two (East Asian), and three (East African Indian) (Yen et al., 2013). NZ and Pacific Island born patients were predominantly lineage four; whereas, individuals born outside of NZ predominately had lineages common to their place of origin.

## **1.2.Pathogenesis**

*M. tuberculosis* is an obligate pathogen for which humans are the primary host (Saviola and Bishai, 2006). Unlike other infectious mycobacteria such as *M. bovis*, that routinely causes disease in a large number of mammals (including humans); *M. tuberculosis* does not have any significant environmental reservoirs. Disease caused by *M. tuberculosis* most commonly manifests as a pulmonary infection, with 70% of TB cases occurring in the lungs (Harisinghani et al., 2000; Young et al., 2008). Extra-pulmonary TB will occur in 10 – 42% of patients, dependent on additional factors such as age, ethnicity, additional underlying disease, specific *M. tuberculosis* strain, and host immune state (Caws et al., 2008). During HIV co-infection, extra-pulmonary disease can be more common than pulmonary, with little or no lung involvement, and is often diagnosed as another disease and only identified as TB upon autopsy (Mudenda et al., 2012; von Reyn et al., 2011). The characteristic symptoms of

pulmonary TB include a chronic cough, production of sputum, haemoptysis, a loss of appetite, weight loss, and night sweats (Lawn and Zumla, 2011). Infection spreads by inhalation of bacteria-containing droplets expelled from infected individual's lungs. The number of bacteria required to start a new infection has previously been reported to be as few as 1—3 bacilli (Riley, 1957); however, the number required for a successful infection in humans may be significantly higher (Orme, 2014). Once inhaled, the bacilli enter the alveoli of the lungs where they are phagocytosed by resident alveolar macrophages (Clark-Curtiss and Haydel, 2003; Mehta et al., 1996; Saunders and Cooper, 2000). The macrophages are then activated by T cells, stimulating the formation of the acidified phagolysosome, killing the phagocytosed bacteria (Clark-Curtiss and Haydel, 2003). However, *M. tuberculosis* can live within host macrophage phagosomes by preventing their fusion with lysosomes and therefore their acidification (Brown et al., 1969; Mwandumba et al., 2004). The immune system's response to *M. tuberculosis* infection is to wall off the site of infection, forming a granuloma or 'tubercle' within which the tissue undergoes the caseous necrosis characteristic of TB (Saunders and Cooper, 2000).

In 10% of cases, acute disease will continue as the bacilli spread throughout the lung and later into other organ systems including the kidneys, liver, and brain (Caws et al., 2008). In the remaining 90% of cases the infection is either successfully cleared or enters a latent disease state within which the bacteria are believed to be in a dormant growth phase, possibly similar to the sporulation phase exhibited by other bacterial species (Bentrup and Russell, 2001; Parrish et al., 1998). Evidence, however, is mounting that *M. tuberculosis* continues to replicate, albeit at a reduced rate, within the host during chronic infection (Gill et al., 2009). Individuals with latent TB have a 10% lifetime reactivation risk, although this rate becomes much higher if the patient is immunocompromised (Girardi et al., 1999; Selwyn et al., 1989). For example, HIV-positive individuals are 37 times more likely to develop active TB than HIV negative individuals (WHO, 2010), with HIV co-infection increasing reactivation to a 10% per year risk (Shenoi and Friedland, 2009; Suthar et al., 2012). Additionally, individuals with diabetes also have a three-fold higher risk of developing active disease (Dye and Williams, 2010).

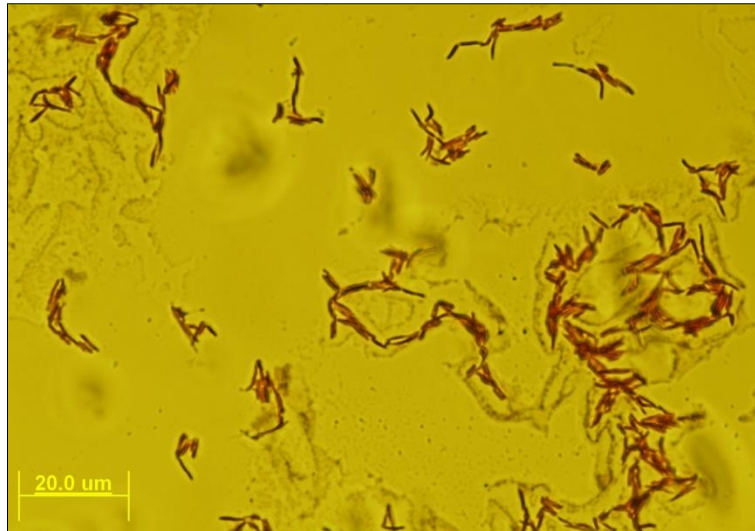
### **1.3.Mycobacteria**

Mycobacteria belong to the family Mycobacteriaceae within the order Actinomycetales and are characteristically acid fast, have a mycolic-acid rich cell wall, and a high GC genome content (61-71%) (Pitulle et al., 1992; Shinnick and Good, 1994). Mycobacteria are commonly divided into two groups, the fast growing and the slow growing mycobacteria, whereby the slow growing mycobacteria are classified as those that take longer than seven days for colonies to appear on solid media; whereas, the colonies of the fast growing species appear in less than seven days (Pitulle et al., 1992; Shinnick and Good, 1994).

The slow growing mycobacteria include those belonging to the *M. tuberculosis* complex that consists of the bacterial species *M. tuberculosis*, *M. bovis*, *M. africanum*, *M. microti*, *M. orygis*, *M. pinnipedi*, and *M. canetti* (Pitulle et al., 1992; Shinnick and Good, 1994). Each member of the *M. tuberculosis* complex has a preferred host, but is capable of causing disease in other mammals (Smith et al., 2006). This is in part due to their very similar genetic makeup, sharing more than 99.9% genetic identity (Fleischmann et al., 2002; Gutacker et al., 2002; Huard et al., 2006). Evidence suggests *M. tuberculosis*-like bacteria have existed for around three million years, evolving in Africa alongside humans (Galagan, 2014). The fast growing mycobacteria, of which approximately 40 species have been identified, are primarily saprophytic and can inhabit a wide variety of habitats in the environment (Saviola and Bishai, 2006; Shinnick and Good, 1994). It was thought for a long time that the fast growers were simply environmental bacteria; however, more species are now demonstrating their ability to cause disease as opportunistic pathogens (Howard and Byrd, 2000).

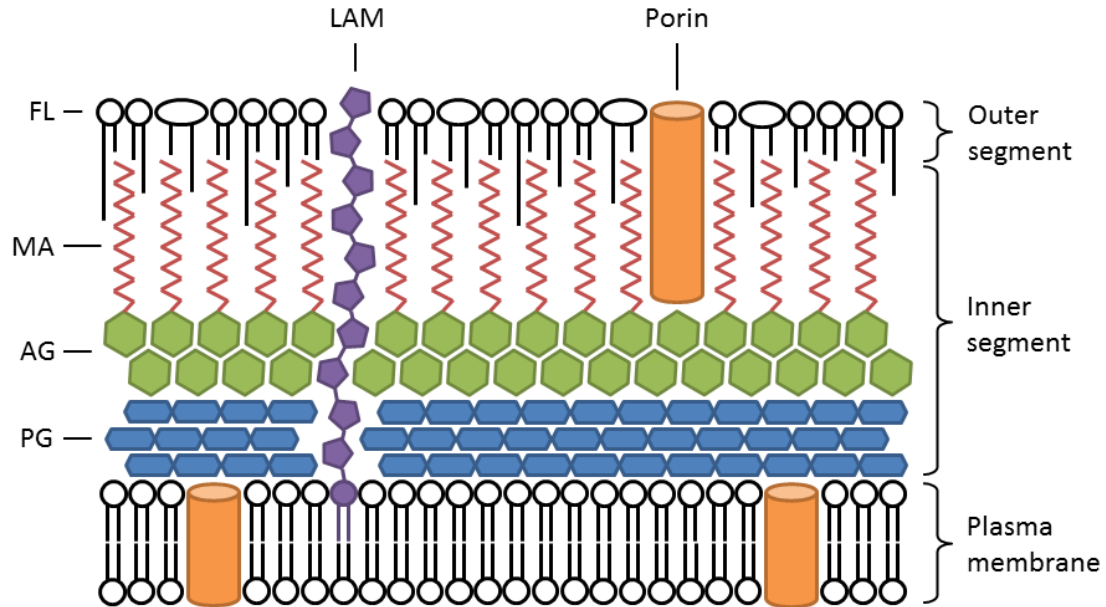
#### **1.3.1. Physiology**

Mycobacteria are aflagellate, irregular rod shaped bacilli of approximately 0.3 - 0.5  $\mu\text{m}$  in diameter with variable length (Figure 1.3)(Martinez et al., 1999; Shinnick and Good, 1994). Mycobacteria are often referred to as gram-positive; however, they have a structurally different cell wall from most gram-positive bacteria and are better defined as acid-fast, as determined by Ziehl-Neelsen staining (Figure 1.3).



**Figure 1.3: Ziehl-Neelsen-stained *M. smegmatis*.** The lipid rich mycobacterial cell wall resists decolourisation during Zeihl-Neelsen staining; therefore, mycobacteria retain the red colour of the primary stain carbol fuchin. Non acid-fast bacteria lose the primary stain and show up blue from the counterstain methylene blue. Characteristic clumping of the mycobacteria can be observed in this image.

The cell wall of mycobacteria is composed of two segments: an inner segment, consisting of the peptidoglycan layer and the arabinogalactan layer with bound mycolic acids, and an outer segment that consists of free lipids (Figure 1.4)(Brennan, 2003). The free lipids in the outer segment along with the mycolic acids in the inner segment form an asymmetric lipid bilayer that gives mycobacteria their characteristic acid fastness. This outer lipid layer also contributes to the innate drug resistance of mycobacteria by limiting drug permeability (Jarlier and Nikaido, 1994).



**Figure 1.4: Structure of the mycobacterial cell wall.** Working outwards, the mycobacterial envelope consists of the plasma membrane, a peptidoglycan (PG) layer, an arabinogalactan (AG) layer, a mycolic acid (MA) layer covalently bound to the arabinogalactan layer, and an outer segment consisting of free lipids (FL). The free lipids include phosphatidylinositol mannoses, dimycolyltrehalose, phthiocerol dimycocerosate, and sulfolipids. The cell wall also contains lipoarabinomannas (LAM) that span the double-layered membrane, and various porins and cell wall proteins.

### 1.3.2. *Mycobacterium tuberculosis*

TB was first identified as a contagious disease in 1868 when it was shown to be transmitted from humans to rabbits (Saviola and Bishai, 2006), although it wasn't until 1882 that Robert Koch first directly observed the bacilli of *M. tuberculosis* responsible for the disease (Adler and Rose, 1996). *M. tuberculosis* belongs to the *M. tuberculosis* complex and is therefore a slow growing mycobacterium, with a doubling time of approximately 24 hours (Shinnick and Good, 1994). The *M. tuberculosis* genome encodes approximately 4000 genes. The genome of the common laboratory strain H<sub>37</sub>Rv was first sequenced in 1998 (Cole et al., 1998). As *M. tuberculosis* is an airborne pathogen, its handling requires specific safety precautions (Alderton and Smith, 2001), and as not all laboratories are equipped to handle virulent *M. tuberculosis*, surrogate strains are often used instead, including the attenuated H<sub>37</sub>Ra strain, *M. bovis* Bacillus Calmette–Guérin (BCG), or the low virulence environmental

mycobacterium *M. smegmatis* (Altaf et al., 2010; Chaturvedi et al., 2007; Steenken et al., 1934).

### **1.3.3. *Mycobacterium smegmatis***

*M. smegmatis* is a soil dwelling saprophyte with a doubling time of approximately four hours, taking around three days for visible colonies to form on rich solid media (Shiloh and DiGiuseppe Champion, 2010). The fast doubling time of *M. smegmatis* makes it a useful surrogate for *M. tuberculosis* in high-throughput drug screening and large scale genetic based assays. Genetic studies of *M. smegmatis* were greatly facilitated by the discovery of a transformation efficient mutant, mc<sup>2</sup>155, that has a 10 - 100,000 increase in efficiency (Snapper et al., 1990). Interestingly, *M. smegmatis* mc<sup>2</sup>155 contains a genomic duplication of approximately 56 kilobases (Kb) not present in the parental strain (Wang et al., 2008). This duplication contains the alcohol dehydrogenase gene *adhC*, a gene previously predicted to be duplicated in the *M. smegmatis* mc<sup>2</sup>155 genome (Galamba et al., 2001). The gene encoding the  $\beta$  subunit of the F<sub>1</sub> domain of the adenosine triphosphate (ATP) synthase, *atpD*, is also predicted to be duplicated in the genome of *M. smegmatis* mc<sup>2</sup>155 (Tran and Cook, 2005). However, *atpD* does not appear to be duplicated in the genome sequence. This suggests there may be more regions of the genome of *M. smegmatis* that are duplicated other than the characterised 56 Kb region. The original *M. smegmatis* reference genome sequence (NCBI Accession CP000480) had 6947 predicted genes, based mostly on homology to other known gene sequences. More recently, efforts to improve the accuracy of *M. smegmatis* mc<sup>2</sup>155's genome annotations led to a newer updated genome sequence (NCBI Accession CP001663). Confirmation of gene sequences with protein sequence data led to refinement of the *M. smegmatis* mc<sup>2</sup>155 genome, and this new reference sequence encodes only 6752 genes (Deshayes et al., 2007; Gallien et al., 2009; Perrodou et al., 2006).

Significant genetic differences exist between *M. smegmatis* and *M. tuberculosis*, whereby approximately half of the *M. smegmatis* genome contains genes that do not have homologues in *M. tuberculosis* (Altaf et al., 2010). This translates into phenotypic differences including different sensitivities to various compounds. However, *M. smegmatis* has a demonstrated ability to identify growth-inhibitory compounds that are active against

*M. tuberculosis* in high-throughput assays (Altaf et al., 2010). Although the number of false positives are higher than when using the closer biological model *M. bovis* BCG, the majority of compounds active against *M. tuberculosis* can be identified using *M. smegmatis*. On balance, the benefits provided by the fast doubling time of *M. smegmatis* outweigh the disadvantages arising from genetic differences to *M. tuberculosis*. Any findings in *M. smegmatis* can ultimately be confirmed in lower throughput validation assays with *M. tuberculosis*.

#### **1.4.Treatment of tuberculosis**

Directly observed therapy, short course (DOTS) was a strategy developed to help control TB, encompassing policies around funding, case detection, treatment, logistics of drug supply, and monitoring (WHO, 2010). The *Stop TB* Strategy was developed as the successor to DOTS with the goal “to dramatically reduce the global burden of TB by 2015 in line with the Millennium Development Goals and the *Stop TB* Partnership targets” (Uplekar et al., 2006). Specifically, the WHO’s Millennium Development Goals are to reverse the incidence of TB by 2015 (WHO, 2010); while, the *Stop TB* partnership has the additional goals of halving the mortality rates by 2015 compared to 1990 levels, and eliminating TB by 2050 (WHO, 2010).

Currently, treatment of drug-susceptible TB consists of a two-month course of isoniazid, rifampicin, pyrazinamide, and ethambutol, followed by a further four months of isoniazid and rifampicin alone (WHO, 2014). Treatment of drug-resistant TB requires the use of alternative second-line drugs that are generally more expensive, less effective, have higher associated toxicities, and lower cure rates. Treatment of drug-sensitive TB has a cure rate of over 90%; while, the cure rate for MDR-TB is lower at only 50-70% (WHO, 2010). Treatment of MDR-TB takes on average two years, while in extreme cases of XDR-TB there is no successful treatment. It is a commonly held belief that the current tools for the treatment and prevention of TB are ineffective, with a great need for drugs that can both reduce the treatment time and effectively treat drug-resistant TB, especially MDR-TB and XDR-TB (Duncan, 2003; O’Brien and Nunn, 2001; WHO, 2010; Young et al., 2008).

### **1.4.1. Anti-tuberculosis Drugs**

Prior to the advent of the first antibiotic, treatment of TB involved travelling to a sanatorium, where it was believed rest and a healthy diet would help to cure patients (Davis, 1996). Streptomycin, discovered in 1945, was the first antibiotic that was successful in treating TB infections (Pyle, 1947). Para-aminosalicylic acid was discovered almost simultaneously and was found to be effective for treating TB, especially in combination with streptomycin (Lienhardt et al., 2012). Isoniazid was discovered in 1951, demonstrating even greater activity against *M. tuberculosis* than either para-aminosalicylic acid or streptomycin and enabling the first three-drug treatment of TB (Pansy et al., 1952). By the mid-1980's, ethambutol and pyrazinamide had replaced para-aminosalicylic acid and streptomycin, and rifampicin had been introduced as well, giving the core first-line multidrug treatment for TB still used today. In cases of drug resistance, second-line drugs are utilised, including the aminoglycosides (including streptomycin), fluoroquinolones (e.g. ciprofloxacin), capreomycin, and the macrolides.

The current anti-TB drugs target a limited range of cellular processes, namely cell wall biosynthesis, DNA replication, transcription, translation, and folate biosynthesis (Table 1.1). Discovery of drugs that can inhibit novel targets is crucial for improving the current treatment regimens of TB, particularly drug-resistant TB (Duncan, 2003; O'Brien and Nunn, 2001; Young et al., 2008).



**Table 1.1: Modes of action of current anti-tuberculosis drugs.**

Drug	Mode of Action	References
Rifamycins (including rifampacin)	Binds to the $\beta$ Subunit of RNA polymerase, inhibiting transcription	(Wehrli et al., 1968)
Isoniazid	Inhibits mycolic acid biosynthesis	(Banerjee et al., 1994)
Ethionamide	Inhibits mycolic acid biosynthesis	(Banerjee et al., 1994)
Ethambutol	Inhibits arabinogalactan layer biosynthesis	(Deng et al., 1995)
D-Cycloserine	Prevents D-serine insertion into peptidoglycan, inhibiting cell wall synthesis	(Prosser and de Carvalho, 2013)
Fluoroquinolones	Inhibits DNA gyrase, inhibiting DNA synthesis	(Fernandes, 1988)
Capreomycin	Interferes with the ribosome inhibiting protein synthesis	(Maus et al., 2005)
Macrolides	Binds the 50s ribosomal subunit, inhibiting translation	(Chopra and Brennan, 1998)
P-aminosalicylic acid	Inhibits dihydropteroate synthetase, inhibiting folate biosynthesis	(Chakraborty et al., 2013)
Aminoglycosides	Binds the 30s ribosomal subunit, inhibiting translation	(Moazed and Noller, 1987)
Pyrazinamide	Inhibits trans-translation	(Shi et al., 2011)

For 40 years after the discovery of rifampicin in the 1950s no new drug classes were developed for the treatment of TB. Research into anti-TB drugs has only become more active in the last decade. There are currently 10 drugs in the various phases of clinical trials, and a further nine in preclinical development (WHO, 2014). Of the 10 drugs currently in clinical trials, four have novel modes of action and are active against MDR-TB: Delamanid, PA-824, bedaquiline, and SQ109. Delamanid, previously known as OPC 67683, is a nitroimidazole that targets mycolic acid biosynthesis, and is similar to another recently discovered nitroimidazole PA-824 (Matsumoto et al., 2006; Singh et al., 2008; Stover et al., 2000). Delamanid is currently undergoing phase III clinical trials, while PA-824 is undergoing phase II clinical trials. Bedaquiline, previously known as TMC207, is a diarylquinoline, a novel class of anti-TB drug that targets the C subunit of the ATP synthase  $F_0$  domain. The two drugs, bedaquiline and delamanid, have been approved for use in treating restricted cases of MDR-TB (Villemagne et al., 2012). The only other anti-TB drug with a novel mode of action currently in clinical trials is SQ109, which is currently in phase II clinical trials. SQ109 inhibits integration of mycolic acid into the cell wall by inhibition of the transporter MmpL3, which

appears to be involved in translocating mycolic acids to outside the cell (Protopopova et al., 2005; Tahlan et al., 2012).

#### **1.4.2. Drug resistance**

Clinical resistance has been reported for all of the drugs used to treat TB, with the first cases identified shortly after the initial use of streptomycin. Spontaneous drug resistance, in the clinical setting or in a laboratory environment, most often occurs from point mutations in the gene encoding the drug's target, reducing the affinity of the drug for its target. For example, mutations in the target of rifampicin, *rpoB*, led to rifampicin resistance (Ramaswamy and Musser, 1998), whereas mutations in the fluoroquinolone targets, the DNA gyrase encoding genes *gyrA* and *gyrB*, led to fluoroquinolone resistance (Kocagöz et al., 1996). Alternatively, if the drug is a prodrug, resistance often occurs from mutations in the prodrug activating enzyme, e.g. mutations in *katG* which encodes the catalase peroxidase enzyme KatG responsible for activating isoniazid lead to isoniazid resistance.

The long treatment time for TB (i.e. 6 months or longer) has been shown to play a significant role in the generation of drug resistance due to treatment non-compliance (Chao and Rubin, 2010; Claxton et al., 2001). This non-compliance selects for drug-resistant populations and has been demonstrated by Saunders et al. (2011) who sequenced serial isolates from a patient who was not adhering to the treatment regimen. Over the course of treatment the isolates developed sequential isoniazid then rifampicin resistance, with only two single nucleotide changes identified in the genome, one in *katG* and one in *rpoB*.

#### **1.4.3. Modes of action of the anti-tuberculosis drugs to be examined in this study**

Isoniazid is an inhibitor of mycolic acid biosynthesis, an important substrate of the mycobacterial cell wall. Specifically, isoniazid inhibits the fatty acid synthase II (FASII) enoyl-acyl carrier protein reductase (InhA). Isoniazid was first shown to have anti-TB activity in 1952, and was far superior to any agents in use at the time (Bernstein et al., 1952; Pansy et al., 1952). Despite its long history of use, little was known about the mode of action of

isoniazid until recently. Loss of catalase activity was long known to accompany isoniazid resistance in mycobacteria, but it was not until the advent of genetic techniques that mutations in the catalase/oxidase *katG* were identified as the cause of both isoniazid resistance and catalase negative phenotypes (Zhang et al., 1992). *InhA* was first identified in the isoniazid mode of action when a catalase positive mutant resistant to isoniazid was identified carrying mutations in *inhA* (Banerjee et al., 1994). Subsequent studies have shown that isoniazid is a pro-drug that is activated by KatG into a reactive species that reacts with nicotinamide adenine dinucleotide (NAD) to form the isoniazid-NAD (INH-NAD) adduct responsible for inhibition of *InhA* (Johnsson and Schultz, 1994; Rozwarski et al., 1998; Wilming and Johnsson, 1999). Other targets have been suggested for isoniazid since, including ketoacyl synthase A (*KasA*) (Mdluli et al., 1998) and dihydrofolate reductase (*Dhfr*) (Argyrou et al., 2006), although the lack of correlation between overexpression of these proteins and increased isoniazid resistance has helped support the hypothesis that *InhA* is the drug's primary target (Larsen et al., 2002; Wang et al., 2010). However, multiple isoniazid radicals have been demonstrated (Wengenack and Rusnak, 2001), as well as a range of secondary radicals (Ito et al., 1992; Timmins et al., 2004; Timperio et al., 2005; Van Zyl and Van Der Walt, 1994) whose activity within the mycobacterial cell supports the idea that the mode of action of isoniazid is broader than just inhibition of *InhA*.

Rifampicin is a transcriptional inhibitor which binds to, and inhibits the  $\beta$  subunit of the DNA dependent RNA polymerase enzyme (*RpoB*) in bacteria (Wehrli et al., 1968), including mycobacteria (Levin and Hatfull, 1993). Rifampicin is a semi-synthetic drug derived from the natural product rifamycin (Maggi et al., 1966). This derivative was found to have improved activity against gram-negative bacteria and the actinobacteria including mycobacteria. Clinical resistance to rifampicin is almost entirely due to mutations in *rpoB*, with 96% of mutations in rifampicin-resistant clinical isolates occurring within an 81 base pair (bp) sequence of the gene (Ramaswamy and Musser, 1998).

Bedaquiline is a diarylquinoline, the first novel class of anti-mycobacterials to be discovered in 40 years (Andries et al., 2005). The primary target for bedaquiline is the C subunit of the  $F_0$  ATP synthase domain encoded by *atpE* (Andries et al., 2005; Koul et al., 2007). Due to its recent discovery, limited work has been done investigating the mode of action of bedaquiline beyond the primary ATP synthase target.

## 1.5. Drug Discovery

The TB drug development pipeline involves identification of compounds that are bacteriostatic or bactericidal against *M. tuberculosis*, development of lead compounds including identification of drug modes of action, and finally progression into clinical trials (Duncan, 2003). These anti-TB compounds are identified from high-throughput screening of chemical libraries against mycobacteria (whole-cell screening), or from screening of isolated enzyme targets (Balganesh et al., 2008). Whole-cell screening has been the most successful approach to drug discovery as it simultaneously assesses all factors related to a drug's efficacy (Lechartier et al., 2014; Payne et al., 2007). Numerous variations on whole cell screening exist using a number of different model systems including macrophage infection, nutrient starvation, non-replicating, latent systems, and incorporating various different animal models. While these approaches have the potential to identify compounds that will be active in the clinic, care needs to be taken as each model makes an assumption about *M. tuberculosis* infection that can lead to misinterpretation of results (Miller et al., 2009; Pethe et al., 2010).

A disadvantage to whole-cell based screening for anti-mycobacterial compounds is that no information on the mode of action of the drug is generated. The absence of any target information from whole-cell screening prevents the rational design of structural modifications to improve drug activity without further investigation of the drug's mode of action (Koul et al., 2011). However, whole-cell screening remains an effective way to identify new anti-TB drugs, including those with new modes of action. Whole-cell screening was used to identify bedaquiline, delamanid, PA-824, and SQ109, (Lechartier et al., 2014).

Screening of isolated enzyme targets has been largely unsuccessful in identifying anti-TB compounds due to difficulty with translating good target inhibition in biochemical assays into good bactericidal or bacteriostatic activity against whole cells (Ioerger et al., 2013). This difficulty largely stems from an incomplete understanding of what makes an enzyme a good drug target. An alternative approach is target-based whole-cell screening, whereby target information is incorporated into the whole-cell screen (Abrahams et al., 2012; Ioerger et al., 2013; Nisa et al., 2010). A common strategy in this type of screen is the conditional repression of a gene of interest with a system such as the tetracycline inducer and repressor

system (Ehrt et al., 2005; Williams et al., 2010). By reducing the levels of the target protein the cells become more sensitive to compounds that inhibit that protein, with specific inhibitors demonstrating differential activity between the conditional mutant and wild-type (WT). This approach has been used to find inhibitors of an enzyme essential for cell division (ParA) (Nisa et al., 2010), an enzyme involved in vitamin B5 biosynthesis (PanC) (Abrahams et al., 2012), and the malate synthase enzyme (Krieger et al., 2012).

### **1.5.1. Mode of action identification**

Mode of action identification studies are essential during development of novel anti-TB drugs, generating information on the primary drug target, secondary off target effects, and mechanisms of drug resistance (Azad and Wright, 2012; Lechartier et al., 2014). Drugs are pleiotropic by nature, and determining the primary and secondary targets provides information on whether drug-drug interactions are likely to occur when the novel drug is used in combination with current drugs, a consideration important in the multi-drug treatment of TB (Ginsberg and Spigelman, 2007). Additionally, identification of the primary and secondary targets enables a rational approach to chemical modifications to drugs to improve their efficacy against both the primary and secondary drug targets (Balganesh et al., 2008; Campbell et al., 2001; Ioerger et al., 2013).

There are three commonly used genetic techniques to investigate the mode of action of a drug: a) identification of genes involved in drug resistance, b) identification of genes whose transcription is altered upon drug treatment, and c) identification of genes involved in drug hypersensitivity. These three different genetic approaches complement each other well, and utilising all of them, combined with biochemical data, gives the most information on drug mode of action. Past studies have focused on the identification of resistance inducing mutations, and altered transcription upon gene treatment. To the best of my knowledge, only two previous studies have examined drug sensitising mutations in mycobacteria, one study by Alexander et al. (2003) looking for rifampicin hypersensitive mutants, and another by Daugherty et al. (2011) looking for mutants hypersensitive to a ubiquitin derived peptide. Therefore, the study of sensitising mutations for current anti-TB drugs has the potential to generate novel information on drug mode of action.

#### **1.5.1.1. Resistance inducing mutations**

The majority of primary targets that have been identified for the current anti-mycobacterial drugs were found by studying genes involved in drug resistance (Andries et al., 2005; Banerjee et al., 1994; Belanger et al., 1996). Resistance to most TB drugs occurs through point mutations in the gene encoding the primary target. Alternatively, resistance can occur due to mutations in genes that are functionally interacting with the drug target. Therefore, identification of point mutations in drug resistant mutants has facilitated target identification. This approach can also identify enzymes responsible for activating pro-drugs when the primary resistance mechanism is loss of pro drug activation (Lechartier et al., 2014). Transposon mutagenesis has been used in a similar manner, although this type of mutation typically causes loss of function and consequently is not useful for determination of the primary targets (Billman-Jacobe et al., 2006). Drug resistance studies have a very narrow focus, singling out individual genes that directly interact with the compound, such as the primary drug target, pro-drug activating enzymes, or enzymes responsible for drug detoxification.

#### **1.5.1.2. Altered transcription with drug treatment**

Investigation into which genes are up/down-regulated in response to drug treatment provides a broader picture of drug mode of action. Transcriptional analysis is useful for identifying pathways that are inhibited by a drug, including both the primary and secondary target pathways. Transcriptional analysis can be performed on a small scale, using quantitative polymerase chain reaction (PCR) to measure changes in messenger RNA (mRNA) expression levels of individual genes, or on a larger scale, using micro-arrays to measure changes in mRNA expression levels of large sets of genes, or even the whole transcriptome (Boshoff, 2004). Large scale transcriptional analysis is useful for grouping compounds with similar modes of actions in mycobacteria. For example, Boshoff et al. (2004) measured the transcriptional response of *M. tuberculosis* to a range of growth inhibitory conditions, including drug treatment, and clustered the transcriptional profiles for each condition. This approach was able to group conditions with similar modes of action, e.g. isoniazid and ethionamide clustered together along with thiolactomycin, three drugs that all inhibit

components of the FASII machinery. More recently, transcriptional profiling identified the mode of action of the novel anti-TB drug PA-824 as involving both inhibition of mycolic acid biosynthesis and nitric oxide induced (NO) respiratory poisoning (Manjunatha et al., 2009).

A limitation of the transcriptional analysis approach is that while affected pathways are determined, the specific gene target cannot be directly identified. Additionally, this approach is only as strong as the size of the gene set against which each new drug is tested. Finally, transcriptional analysis gives an incomplete description of a drug's mode of action (Sasseti et al., 2001). For example, transcriptional analysis does not provide information on constitutively expressed genes, or genes that are post-transcriptionally regulated.

#### **1.5.1.3. Hypersensitivity inducing mutations**

Analysis of mutations that cause drug hypersensitivity provides information on genes that are conditionally essential to maintaining WT drug sensitivity. Similar to transcriptional studies, this approach yields information on which pathways are inhibited by the drug (primary and secondary target pathways), as opposed to the specific molecular target. This approach is routinely used in the budding yeast *Saccharomyces cerevisiae* to study drug mode of action where it is termed chemical genetics (Parsons et al., 2004, 2006). A viable loss of function mutation within a pathway targeted by the drug will sensitise the organism to the drug, thereby identifying that pathway as being involved in the drug's mode of action. This approach also identifies specific proteins responsible for maintaining basal drug resistance, i.e. drug detoxification mechanisms (Alexander et al., 2003). It is necessary to isolate mutants and assay them individually for increased drug-sensitivity as the mutations of interest produce a recessive phenotype. Therefore, a common limitation of this technique is a poor genomic coverage for the collection of mutants being studied. This is especially pertinent when using a mutagenesis approach such as random transposon mutagenesis which is unable to create mutations in essential genes (Griffin et al., 2011; Sasseti et al., 2001, 2003). Despite this limitation, random transposon mutagenesis is routinely used to generate collections of random mutants for phenotypic screening, including screening for drug hypersensitivity, because of the ease of identifying the site of insertion, and the

consistent nature of the mutation (loss of function) (Alexander et al., 2003; Daugherty et al., 2011; Gutacker et al., 2002).

### **1.6.Random transposon mutagenesis of *M. smegmatis***

Assaying for drug hypersensitivity requires the prior construction of a collection of viable mutants. This collection should be randomly generated, with good genome coverage and minimal overlap. Insertional mutagenesis using transposons is favoured for the generation of random bacterial mutants due to the inherent labelling of the site of mutation with the transposon DNA, which facilitates the identification of the genetic basis for the mutant phenotype (Billman-Jacobe et al., 2006; Prod'hom et al., 1998; Sassetti et al., 2001). A transposon insertion into a gene leads to a loss of function of the gene product, which has the important implication that only genes not essential for the organism's survival can harbour a transposon insertion (Sassetti et al., 2001). As such, transposon mutant libraries will only contain those genes that are non-essential for survival in the conditions used. This characteristic has been utilised for determining the varying set of essential genes under a range of conditions, including *in vitro* in various media, intra-macrophage survival, *in vivo* mouse models, and under different drug treatment conditions (Alexander et al., 2003; Billman-Jacobe et al., 2006; Daugherty et al., 2011; McAdam et al., 2002; Rengarajan et al., 2005; Sassetti et al., 2001, 2003).

Two different delivery systems exist for transposon mutagenesis in mycobacteria: phage based, such as  $\phi$ MycoMarT7, which delivers the *Himar1* transposon (Sassetti et al., 2001), or plasmid based systems such as pCG79, which delivers the *Tn611* transposon (Guilhot et al., 1994). Transposon mutagenesis systems often use delivery vectors which are temperature sensitive for replication in mycobacteria, which allows the process of transfection or transformation to be separated from the process of transposition. Transposition is a relatively rare event, but appropriate selection techniques can improve the yield of mutants obtained (Bardarov et al., 1997). Transformed/transfected cells can be plated out at a non-permissive temperature for plasmid/phage replication and only successful transposition events will grow. These strains can then be stored individually for later study.



## 1.7.Aims of this thesis

The aim of this thesis was to generate information on drug mode of action by identifying the genetic basis of drug hypersensitivity in mutants of *M. smegmatis* mc<sup>2</sup>155. To the best of my knowledge, only two previous studies have investigated the mode of action of anti-TB compounds through studying drug hypersensitive mutants, one published after this present study had begun (Alexander et al., 2003; Daugherty et al., 2011). To enable the identification of drug hypersensitive mutants of *M. smegmatis* mc<sup>2</sup>155 we also aimed to develop a high-throughput assay for drug hypersensitivity. *M. smegmatis* mc<sup>2</sup>155 was selected as a model for *M. tuberculosis* in this study as it was able to be used in the physical containment 2 (PC2) laboratories available, and as it provided time advantages over the slow growing models. Transposon mutagenesis was selected for generating the mutants of *M. smegmatis* mc<sup>2</sup>155 due to the reported consistent nature of the mutations, and the ease of identifying the site of the genetic lesion responsible for the hypersensitivity phenotype.

The front line TB drugs isoniazid and rifampicin were selected for this study as the known aspects of their modes of action would enable validation of our methodology. Bedaquiline, which has recently been approved for limited treatment of MDR-TB, was also included in this study as little is known about its mode of action other than the primary target. Due to the absence of prior studies of this nature, there was a large potential to identify novel aspects of the modes of action of these three anti-TB drugs. A better understanding of the modes of action of these drugs would enable rational modifications of the drugs to improve treatment of TB. To this end the following specific aims were addressed:

1. Identification of isoniazid, rifampicin, and bedaquiline hypersensitive transposon mutants of *M. smegmatis* mc<sup>2</sup>155. To achieve this aim the following sub aims were addressed: Construction of a transposon mutant collection in *M. smegmatis* mc<sup>2</sup>155, and development of a high-throughput assay for drug hypersensitivity.
2. Identification and validation of the genotypic basis for the observed drug hypersensitivity to generate information about each drug's mode of action.
3. Characterisation of drug sensitivity phenotypes, including cross-sensitivities and differential-sensitivities to other anti-TB drugs and drug analogues, respectively.

## 2. Materials and Methods

### 2.1. Bacterial strains

Strains used in this study are listed in Table 2.1 along with the relevant genotypic and phenotypic properties. Stocks of all strains were stored at -80 °C in 20% (v/v) glycerol.

**Table 2.1: Bacterial strains used in this study.**

Strain	Genotype and/or phenotype	Reference
<i>E. coli</i> DH5α	F <sup>-</sup> Φ80 <i>lacZ</i> ΔM15 Δ( <i>lacZYA-argF</i> ) U169 <i>recA1 endA1 hsdR17</i> (r <sub>k</sub> <sup>-</sup> , m <sub>k</sub> <sup>+</sup> ) <i>phoA supE44 thi-1 gyrA96relA1 λ</i> <sup>-</sup>	Invitrogen™
<i>M. smegmatis</i> mc <sup>2</sup> 155	High plasmid transformation efficiency strain of <i>M. smegmatis</i>	(Snapper et al., 1990)
<i>M. tuberculosis</i> H <sub>37</sub> Rv	Virulent laboratory reference strain of <i>M. tuberculosis</i>	(Oatway Jr. and Steenken Jr., 1936; Steenken et al., 1934)

### 2.2. Plasmids

Plasmids used in this study are listed in Table 2.2 along with the relevant properties.

**Table 2.2: Plasmids used in this study.**

Plasmid	Properties	Reference
pCG79	OriM (ts pAL5000), Kan <sup>R</sup> , Strep/Spec <sup>R</sup> , <i>Tn611</i> transposon	(Guilhot et al., 1994)
pNIT-1	Mycobacterial conditional expression vector, OriE, OriM, Kan <sup>R</sup> , NIT operon, MCS	(Pandey et al., 2009)
pRC10	Derivative of pNIT-1 with NIT operon removed	This study
pLL192_hsp60	OriE, OriM, Kan <sup>R</sup> , hsp60 driven GFP expression	(Srivastava et al., 2007)
pKW08_Lx	Mycobacterial conditional expression vector, OriE, OriM, Hyg <sup>R</sup> , inducible P <sub>Tet</sub> , MCS, <i>luxAB</i>	(Williams et al., 2010)
pRC20	Derivative of pKW08_Lx with <i>luxAB</i> replaced with GFP	This study

### 2.3. Chemicals and reagents

Unless otherwise specified all general reagents and chemicals were obtained from Sigma-Aldrich. HyperLadder™ 1 Kb DNA ladder and DNA loading dye were obtained from Bioline (Auckland, NZ).

## **2.4.Enzymes**

All restriction endonuclease enzymes were purchased from New England Biolabs (Auckland, NZ), as were Antarctic phosphatase, T4 DNA polymerase, and T4 polynucleotide kinase. The PCR enzyme master mixes BioMix™ Red and AccuSure™ were obtained from Bioline (Auckland, NZ). T4 DNA ligase, Proteinase K and lysozyme were obtained from Invitrogen. Phusion® polymerase was obtained from Thermo-Fisher Scientific.

## **2.5.Growth media**

All media were made up in sterile distilled and deionised H<sub>2</sub>O (ddH<sub>2</sub>O) according to the manufacturer's instructions and sterilised by autoclaving at 121 °C for 30 minutes, unless stated otherwise.

### **Luria Broth**

All Luria Broth (LB) and LB agar (LA) low salt powders (Duchefa Biochemie) were purchased from Total Lab Systems (Auckland, NZ). All agar plates, and liquid media containing antibiotics, were stored at 4 °C; liquid media without antibiotics were stored at room temperature.

### **7H9**

Difco™ Middlebrook 7H9 broth was ordered from Becton Dickson. 7H9 broth was made up according to the manufacturer's instructions in ddH<sub>2</sub>O, containing 0.05% Tween™80 (v/v), 0.05% glycerol (v/v) and 10% oleic acid, albumin, dextrose, catalase (OADC) supplement, and stored at 4 °C.

### **2.5.1. Media supplements**

#### **Tween™ 80**

Tween™ 80 was made up as a 20% (v/v) stock solution using ddH<sub>2</sub>O and sterilised by autoclaving at 121 °C for 30 minutes. Tween™ 80 stocks were stored at room temperature.

### D-arabinose

D-arabinose was made up as a 100 mg·mL<sup>-1</sup> stock solution in ddH<sub>2</sub>O and filter sterilised through a 0.22 µM nylon syringe filter unit. D-arabinose stocks were stored at 4 °C.

### Oleic acid, albumin, dextrose, catalase enrichment (OADC)

OADC was purchased from Fort Richard Laboratories and was stored at 4 °C

### Glycerol

Glycerol was made up as a 10% (v/v) stock and sterilised by autoclaving at 121 °C for 30 minutes. Glycerol stocks were stored at 4 °C.

### Antibiotics

All antibiotics used to select for or maintain plasmids/transposons were made up in ddH<sub>2</sub>O and filter sterilised through a 0.22 µM nylon syringe filter before storage at -20 °C, with the exception of hygromycin B, which was purchased as a 52.5 mg·mL<sup>-1</sup> aqueous solution and stored at 4 °C. Antibiotic concentrations used for different bacterial strains are listed in Table 2.3.

**Table 2.3: Antibiotic concentrations used for marker selection.**

Antibiotic	Strain		
	<i>E. coli</i>	<i>M. smegmatis</i>	
		<i>Tn611</i> Mutants	Other
Ampicillin (Amp)	200 µg·mL <sup>-1</sup>	n/a	n/a
Apramycin (Apr)	50 µg·mL <sup>-1</sup>	25 µg·mL <sup>-1</sup>	25 µg·mL <sup>-1</sup>
Hygromycin B (Hyg)	200 µg·mL <sup>-1</sup>	20 µg·mL <sup>-1</sup>	50 µg·mL <sup>-1</sup>
Kanamycin (Kan)	50 µg·mL <sup>-1</sup>	20 µg·mL <sup>-1</sup>	50 µg·mL <sup>-1</sup>

#### 2.5.2. *E. coli* growth conditions

*Escherichia coli* (*E. coli*) was routinely grown in LB or on LA (section 2.5) at 37 °C. Liquid cultures were aerated with shaking at 200 rpm unless otherwise stated. All *E. coli* strains generated were stored as freezer stocks in 20% glycerol (v/v) at -80 °C. Cultures of *E. coli* were prepared from freezer stocks by streaking out an inoculating loop of cells from the frozen stock onto appropriately supplemented LA plates. Plates were incubated overnight, with single colonies used to inoculate 5 mL of LB broth the next day. These 5 mL starter cultures were grown for a further 24 hours before being diluted 100-fold in fresh LB medium

and grown for a further 24 hours. These cultures were used for generating chemically competent *E. coli*, or for plasmid preparation.

### **2.5.3. Mycobacteria growth conditions**

#### **2.5.3.1. *M. smegmatis* mc<sup>2</sup>155**

*M. smegmatis* mc<sup>2</sup>155 was routinely grown in LB broth or on LA (section 2.5) at 37 °C. Liquid cultures were aerated with shaking at 200 rpm unless otherwise stated. *Tn611* transposon mutants of *M. smegmatis* mc<sup>2</sup>155 were grown at 41 °C with shaking at 150 rpm. Liquid cultures of *M. smegmatis* mc<sup>2</sup>155 were supplemented with 0.05% (v/v) Tween™ 80 and 100 µg·mL<sup>-1</sup> D-arabinose (section 2.5.1) to minimise cell clumping (Allen, 1998; Anton et al., 1996). All *M. smegmatis* strains generated, except the transposon mutant collection, were stored as freezer stocks in 20% glycerol (v/v) at -80 °C. The description of storage of the transposon mutant collection is described in section 2.7. Cultures of *M. smegmatis* mc<sup>2</sup>155 were prepared from freezer stocks by streaking out an inoculating loop of cells from the frozen stock onto appropriately supplemented LA plates. Plates were incubated for 3 – 5 days until colonies appeared. An individual colony was inoculated into 1 mL of appropriately supplemented LB broth and grown for 72 hours. The 1 mL starter cultures were then diluted 100-fold in fresh LB broth and grown for a further 24 hours. These cultures of *M. smegmatis* mc<sup>2</sup>155 were used for the generation of electrocompetant cells, or in assays.

#### **2.5.3.2. *M. tuberculosis* H<sub>37</sub>Rv**

Growth and assaying of *M. tuberculosis* H<sub>37</sub>Rv was performed at University College Dublin, in Dublin Ireland, in the physical containment 3 (PC3) laboratory of Professor Stephen Gordon. *M. tuberculosis* H<sub>37</sub>Rv was routinely grown in 7H9 broth at 37 °C, with liquid cultures aerated with shaking at 200 rpm unless otherwise stated. *M. tuberculosis* H<sub>37</sub>Rv stocks were maintained by continuous culture in roller bottles as described by Bacon and Hatch (2009).

## **2.6.Molecular biology**

### **2.6.1. DNA isolation and purification**

#### **2.6.1.1. CTAB genomic DNA isolation**

Genomic DNA (gDNA) was isolated from bacterial strains using cetyltrimethylammonium bromide (CTAB) as described by Bull et al. (2000). Briefly, 10 mL overnight liquid cultures of *M. smegmatis* mc<sup>2</sup>155 (section 2.5.3.1) were spun down at 2700 xg for 20 minutes to pellet cells, then re-suspended in 400 µL of 1x TE buffer (Appendix section 8.1) and transferred to 1.5 mL micro-centrifuge tubes. Cells were heat killed for 20 minutes at 80 °C in a heat block, then left in a rack to cool to room temperature. Cells were then incubated at 37 °C for one hour with 0.5 mg lysozyme. To the cells 0.15 volumes of 10% SDS (w/v) and 0.01 volumes of 10 mg·mL<sup>-1</sup> proteinase K (Appendix section 8.1) were added before being briefly vortexed then incubated at 65 °C for 10 minutes. Following this, 0.2 volumes of 5 M NaCl and 0.2 volumes of a prewarmed (65 °C) CTAB/NaCl (Appendix section 8.1) solution were added. The cells were vortexed until the solution turned white. The cells were then incubated at 65 °C for 10 minutes. To purify the DNA, 1 volume chloroform was added to the cells followed by brief vortexing then spinning in a micro centrifuge for 8 minutes at 12,000 xg. The aqueous phase was removed and 0.6 volumes of isopropanol was added before a further spin for 15 minutes at 12,000 xg. The supernatant was removed and the DNA pellet washed with 1 mL cold 70% (v/v) ethanol before a final spin for 5 minutes at 12,000 xg. The ethanol was removed and the pellet left to air dry before suspension of the DNA in 50 µL ddH<sub>2</sub>O and storage at -20 °C.

#### **2.6.1.2. Plasmid mini-preparation**

Small scale extraction of plasmid DNA from bacterial cells was performed using either the Zymo Research Zyppy™ Plasmid Mini-Prep kit or the Qiagen QIAprep Spin Miniprep kit according to the relevant manufacturer's instructions. Plasmid DNA was extracted from 3 – 5 mL of an overnight culture of *E. coli* (section 2.5.2), eluted in 50 µL ddH<sub>2</sub>O and stored at -20 °C.

#### **2.6.1.3. Plasmid midi-preparation**

Medium scale extraction of plasmid DNA from bacterial cells was performed using the Invitrogen™ PureLink™ HighPure Plasmid DNA Midi-Prep kit according to the manufacturer's instructions. Plasmid DNA was extracted from 50 – 100 mL of an overnight culture of *E. coli* (section 2.5.2), eluted in 50 µL ddH<sub>2</sub>O and stored at -20 °C.

#### **2.6.1.4. Agarose gel electrophoresis**

DNA samples were run on 1% agarose (w/v) gels in 1x Tris acetate-EDTA (TAE) buffer (Appendix section 8.1). Samples were run with 1x DNA loading buffer and alongside the HyperLadder™ 1 Kb DNA ladder. Samples were electrophoresed using constant voltage at 120 V for 25 – 40 minutes until suitable band separation was achieved.

#### **2.6.1.5. Agarose gel DNA extraction**

DNA bands were extracted from agarose gels following electrophoresis using the Zymoclean™ Gel DNA Recovery Kit (Zymo Research) according to the manufacturer's instructions. DNA was eluted in 12 µL ddH<sub>2</sub>O and stored at -20 °C.

#### **2.6.1.6. DNA purification**

DNA in solution was purified using the DNA Clean & Concentrator™-5 kit (Zymo Research) according to the manufacturer's instructions. DNA was eluted in 12µL ddH<sub>2</sub>O and stored at -20 °C.

#### **2.6.1.7. DNA quantification**

DNA was quantified using a NanoDrop® ND-100 Spectrophotometer (NanoDrop Technologies, Auckland, NZ) and the NanoDrop® 3.1.0 software using the DNA setting. A 1 µL aliquot of ddH<sub>2</sub>O was used to initialise the NanoDrop®. A 1 µL aliquot of ddH<sub>2</sub>O was used to generate a blank reading before DNA concentrations were read at 230 nm using 1 µL

of sample. The ratio of the reading at 260 nm and 280 nm was recorded to assess sample purity.

### **2.6.2. DNA sequencing**

DNA sequencing was performed by Macrogen Inc. (South Korea), using their standard sequencing service. A minimum of 200 ng PCR or plasmid DNA was sent for sequencing in a minimum volume of 10  $\mu$ L. Primers were sent at 10  $\mu$ M concentrations or synthesised by Macrogen Inc. using their primer synthesis service.

### **2.6.3. Genetic manipulations**

#### **2.6.3.1. Primers**

Primers were designed using the Geneious 5.5.6 bioinformatics software and ordered from IDT. Primers were designed to include 15-25 nucleotides of the ends of the DNA sequence to be amplified, a restriction site if applicable, and a 5' CTAG motif. Primers were reconstituted in ddH<sub>2</sub>O to a concentration of 100  $\mu$ M and working stocks of 10  $\mu$ M were made up in ddH<sub>2</sub>O and stored at -20 °C. Primers used in this study are listed in Table 2.4.



**Table 2.4: Primer sequences used in this study.**

Product	Primer Name	Sequence (5' - 3')	$T_m$ (°C)
GFP	GFP_RBS_F	CTAG <u>GGATCCT</u> TTTAAGAAGGAGATATACATATGAGT AAAGGAGAA	60.8
	GFP_R	CTAGGGATCCTTATTATTTGTATAGTTCATCCATGCC	57.6
pRC20 MCS primers	TetRO_int	GCCGACCTCTGCGGTTTGCT	63.2
	GFP_int	AAGGACAGGGCCATCGCCAA	62.0
<i>nudC</i> ( <i>MSMEI_1904</i> )	pRC20_1904_F	CTAGGGATCCATGAGCGAACACCGCACGTTCGG	68.3
	pRC20_1904_R	CTAGGGATCCTCAGTCGAGTGCGGCCAGGATT	68.7
<i>MSMEI_1905</i>	pRC20_1905_F	CTAGGGATCCATGACTACTGCTTCCAGCGAACTCAT CATG	65.7
	pRC20_1905_R	CTAGGGATCCTCAGCCGAGCTTGGCCTTGACCT	68.9
	1905_BamHlnull _59mer	TCAGCCGAGCTTGGCCTTGACCTGCTTGATGGTCGG GTTGGTCAGCGTGGATCCGTCGG	75.2
<i>MSMEI_4267</i>	pRC20_4267_F	CTAGGGATCCATGAAACTCCAGGTCACACA	61.0
	pRC20_4267_R	CTAGGGATCCCTATAGATCGAGTGTTAATTTTCGCG	61.1
<i>MSMEI_6092</i>	pRC20_6092_F	CTAGGGATCCGTGACCACAGTGCAT	62.2
	pRC20_6092_R	CTAGGGATCCCTAGATGGTGCTGCT	61.5
<i>inhA</i> ( <i>MSMEI_3070</i> )	pRC20_3070_F	CTAGGGATCCATGACAGGCCTACTCGAAGG	62.5
	pRC20_3070_R	CTAGGGATCCTCACACAGCTGCGTGCTGG	65.5
<i>arr</i> ( <i>MSMEI_1186</i> )	pRC20_1186_F	CTAGGGATCCGTGGCGAATCCGCCG	66.8
	pRC20_1186_R	CTAGGGATCCCTAGTCATAGATGACCGCCA	63.0
<i>MSMEI_3093</i>	pRC20_3093_F	CTAGGGATCCGTGGACACCCGGTCGAT	66.4
	pRC20_3093_R	CTAGGGATCCTCACAGTGCGTGCCGG	66.2
<i>katG</i> ( <i>MSMEI_6216</i> )	pRC20_6216_F	CTAGGGATCCTTGCCTGAGGATCGCC	61.9
	pRC20_6216_R	CTAGGGATCCTCAGGCGACGTCGAA	61.8
	6216_int_F	CAACGGCAATCCGGACCCGAGGCCTCGGC	73.6
ligation- mediated PCR	6216_int_R	TCCGGATTGCCGTTGGGGCCTTCGGGGTTG	71.7
	Salpt	TCGAGCTCGTGC	47.0
	Salgd	TAGCTTATTCCTCAAGGCACGAGC	58.8
	3053	GAACCGCTTCGCTGCCTTG	45.0
	3054	AACCACCATTTTCGACGAGC	44.0
<i>IS6100</i> primers	OligoF	AAGAATTCATCGTTCGTCGTCCTCAATCTCC	62.9
	OligoG	GAGCGACAGCCTACCTCTGACT	60.4

Sequences of primers used to amplify genes, or used for sequencing, along with their melting temperatures ( $T_m$ ). Underlined bases represent restriction endonuclease recognition sites introduced into the primer. Bases in bold in primer GFP\_RBS\_F represent a shine-dalgarno ribosomal binding site sequence introduced into the primer. Italicised bases in sequences salgd and salpt represent homologous regions of these two oligonucleotides used to generate a linker during ligation-mediated PCR.

#### **2.6.3.2. Polymerase chain reaction**

PCR was run using the conditions as listed in Table 2.5. All PCR mixes were prepared according to the manufacturer's instructions. AccuSure™ mix or Phusion® polymerase was used for reactions requiring high fidelity such as amplification of genes for downstream cloning into expression vectors. AccuSure™ was also used for all touchdown PCR and ligation-mediated PCR reactions. Biomix™ Red was used for inverse PCR and the overlap PCR of *katG*. Specific PCR reaction protocols used are listed in Table 2.6 – Table 2.9. All reactions used 100 – 200 ng of template; plasmid pll192\_hsp60 was used as the template for GFP amplification; *M. smegmatis* mc<sup>2</sup>155 gDNA (section 2.6.1.1) was used as the template for amplification of *M. smegmatis* genes; the left and right amplified fragments of *katG* were used as templates for the *katG* overlap PCR reaction; generation of the template for inverse PCR and ligation-mediated PCR are described in detail in sections 2.6.4 and 2.6.5 respectively.

**Table 2.5: PCR conditions for product amplification.**

Product	Primer pair	Protocol	Enzyme	Annealing Temp. (°C) <sup>a</sup>	Extension time (minutes)
GFP	GFP_RBS_F/GFP_R	Touchdown	AccuSure™	68(-1)/55	1:30
<i>nudC</i> ( <i>MSMEI_1904</i> )	pRC20_1904_F/ pRC20_1904_R	Touchdown	AccuSure™	72(-1)/62	2:10
<i>MSMEI_1905</i> (removing BamHI site)	pRC20_1905_F/ 1905_BamHInull_59mer	Two-step	AccuSure™	n/a	0:40
<i>MSMEI_1905</i>	pRC20_1905_F/ pRC20_1905_R	Touchdown	AccuSure™	71(-1)/59	0:40
<i>MSMEI_4267</i>	pRC20_4267_F/ pRC20_4267_R	Touchdown	AccuSure™	68(-1)/57	2:10
<i>MSMEI_6092</i>	pRC20_6092_F/ pRC20_6092_R	Touchdown	AccuSure™	68(-1)/58	2:00
<i>inhA</i> ( <i>MSMEI_3070</i> )	pRC20_3070_F/ pRC20_3070_R	Touchdown	AccuSure™	68(-1)/57	2:10
<i>arr</i> ( <i>MSMEI_1186</i> )	pRC20_1186_F/ pRC20_1186_R	Two-step	Phusion®	n/a	0:15
<i>MSMEI_3093</i>	pRC20_3093_F/ pRC20_3093_R	Two-step	Phusion®	n/a	0:25
<i>katG</i> left fragment ( <i>MSMEI_6216</i> )	pRC20_6216_F/ 6216_int_R	Two-step	Phusion®	n/a	0:12
<i>katG</i> right fragment ( <i>MSMEI_6216</i> )	6216_int_F/ pRC20_6216_R	Two-step	Phusion®	n/a	0:23
<i>katG</i> ( <i>MSMEI_6216</i> )	pRC20_6216_F/ pRC20_6216_R	Overlap	Biomix™ Red	See Table 2.9	
Inverse PCR	3053/3054	Three-step	Biomix™ Red	44	2:00
Ligation- mediated PCR	salgd/OligoF or OligoG	Three-step	AccuSure™	55	2:20

<sup>a</sup> Times for touchdown PCR reactions are in the format: phase I annealing temperature (temperature change per step) / phase II annealing temperature.

### Two-step PCR

A two-step PCR protocol was used when the  $T_m$  of one or both primers in a primer pair was higher than 70 °C when using Phusion® polymerase, or 72 °C when using any other DNA polymerase.

**Table 2.6: Two-step PCR thermal cycle.**

Step	Temperature (°C) <sup>a</sup>	Time (min) <sup>a</sup>	No. of cycles
Initial Denature	98 / 95	2:00 / 7:00	1
Denaturation	98 / 95	0:30	30
Extension	68 / 72	0:30 / 1:30 Kb <sup>-1</sup>	
Final Extension	68 / 72	10:00	1

<sup>a</sup> Denaturation temperature and time, and extension temperature and time were dependant on the polymerase used (Phusion® / AccuSure™).

### Three-step PCR

A three-step PCR was used when the average  $T_m$  of a primer pair was below 65°C and the  $T_m$  of the primers were within 2°C of each other.

**Table 2.7: Three-step PCR thermal cycle.**

Step	Temperature (°C) <sup>a</sup>	Time (min) <sup>a</sup>	No. of cycles
Initial Denature	95	2:00 / 7:00	1
Denaturation	95	0:30	30
Annealing	See Table 2.5	0:30	
Extension	72	0:30 / 1:30 Kb <sup>-1</sup>	
Final Extension	72	10:00	1

<sup>a</sup> Denaturation and extension time were dependant on the polymerase mix used (Biomix™ Red / AccuSure™).

### Touchdown PCR

A Touchdown PCR was used to amplify targets when the average  $T_m$  of a primer pair was greater than 65 °C and less than 72 °C and/or when the temperature difference within a primer pair was more than 2 °C. All touchdown PCR reactions were performed with AccuSure™.

**Table 2.8: Touchdown PCR thermal cycle.**

Phase	Step	Temperature (°C) <sup>a</sup>	Time (min) <sup>a</sup>	No. of cycles
Phase I	Initial Denature	95	7:00	1
	Denaturation	95	0:30	
	Touchdown			
	Annealing (-1 °C/cycle)	See Table 2.5	0:30	8-15 cycles
	Extension	72	1:30 Kb <sup>-1</sup>	
Phase II	Denaturation	95	0:30	
	Annealing	See Table 2.5	0:30	25 cycles
	Extension	72	1:30 Kb <sup>-1</sup>	
	Final Extension	72	10:00	1

<sup>a</sup> The number of cycles performed during phase I was equal to the number required to get from the phase I annealing temperature to the phase II annealing temperature using 1 °C increments per cycle.

### Overlap PCR

Overlap PCR was used to remove the *Bam*HI restriction site from the *katG* gene *MSMEI\_6216*. Phase I used 1x Biomix™ Red, equimolar *katG* left and right fragments as the template (70 nM each), and ddH<sub>2</sub>O to bring the reaction volume to 25 µL. The *katG* left and right fragments were amplified using the protocols described in Table 2.5, and cleaned and concentrated as described in section 2.6.1.6, before use in the overlap PCR reaction. The primers listed in Table 2.5 were added prior to starting phase II, in a volume equal to that of the reaction in phase I, containing 1x Biomix™ Red and sufficient ddH<sub>2</sub>O to bring the final reaction volume to 50 µL.

**Table 2.9: Overlap PCR thermal cycle.**

Phase	Step	Temperature (°C)	Time (min)	No. of cycles
Phase I	Initial Denature	95	2:00	1
	Denaturation	95	0:30	
	Annealing	39	0:30	15 cycles
	Extension	72	1:00	
95 °C hold to add reagents for phase II				
Phase II	Denaturation	95	0:30	
	Annealing	0:30	0:30	25 cycles
	Extension	72	1:30	
	Final Extension	72	10:00	1

#### **2.6.3.3. Restriction endonuclease digestions**

Restriction endonuclease reactions were run according to the manufacturer's instructions with the supplied buffers unless otherwise specified. Restriction endonuclease reactions were heat inactivated according to the manufacturer's instructions where specified, and cleaned and concentrated as described in section 2.6.1.6. Completed restriction reactions were electrophoresed (section 2.6.1.4) alongside undigested control DNA to confirm successful digestion.

#### **2.6.3.4. Blunting of DNA ends**

T4 DNA polymerase was used to blunt the ends of DNA fragments according to the manufacturer's protocol. NEBuffer 2 was used in place of the supplied CutSmart™ buffer. Blunting reactions were inactivated with 10 mM ethylenediaminetetraacetic acid (EDTA) at 75 °C for 20 minutes.

#### **2.6.3.5. DNA phosphatase treatment**

Antarctic phosphatase was used to remove the phosphates from the 5' ends of DNA fragments according to the manufacturer's protocol.

#### **2.6.3.6. DNA ligations**

T4 DNA ligase was used to ligate DNA fragments together according to the manufacturer's protocol. Ligations were run overnight at room temperature and diluted five-fold prior to use in transforming chemically competent cells.

### **2.6.4. Generation of substrate for inverse PCR**

Inverse PCR was used to identify transposon insertion sites in the genome of *M. smegmatis* mc<sup>2</sup>155 and was performed as described by Billman-Jacobe et al. (2006). Briefly, gDNA was isolated from mutant strains as described in section 2.6.1.1. Digests were performed with 600 ng gDNA and the restriction enzymes *RsaI* or *EagI* in 20 µL reactions according to the

manufacturer's protocol (section 2.6.3.3). The reactions were heat inactivated but not cleaned and concentrated. An 18  $\mu$ L aliquot of the restriction digest was then transferred to a ligation reaction setup according to the manufacturer's instructions (section 2.6.3.6) in a total volume of 50  $\mu$ L. Ligations were incubated overnight at room temperature, and then stored at -20 °C. For inverse PCR reactions 8  $\mu$ L ligation mixture was used in a total reaction volume of 25  $\mu$ L.

### **2.6.5. Generation of substrate for ligation mediated PCR**

Ligation-mediated PCR was used to identify insertion sites in the genome of *M. smegmatis* mc<sup>2</sup>155 and was performed essentially as described by Prod'homme et al. (1998). Briefly, the linker was made by annealing the oligonucleotides salgd and salpt (Table 2.4) in equimolar (25  $\mu$ M) concentrations in 1x Phusion® high-fidelity PCR buffer in a 200  $\mu$ L PCR tube. The mixture was heated to 80 °C in a thermal cycler and cooled to 4 °C over one hour. Digests were performed with 250 ng gDNA isolated from mutants as described in section 2.6.1.1 using the restriction enzyme *Sall* in 20  $\mu$ L reactions according to the manufacturer's instructions (section 2.6.3.3). Digest reactions were heat inactivated but not cleaned and concentrated. The linker was ligated to the *Sall* digested gDNA (section 2.6.3.6) according to the manufacturer's instructions for one hour at 16 °C. Ligation reactions were performed in 10  $\mu$ L volumes containing 5  $\mu$ L of the digest reaction mixture and 25 pmol linker. Ligations were heat inactivated at 65 °C for 10 minutes then re-digested with *Sall* in a 15  $\mu$ L reaction according to the manufacturer's instructions. Digestion reactions were heat inactivated but not cleaned and concentrated, and diluted 10-fold in ddH<sub>2</sub>O. A 5  $\mu$ L aliquot of the diluted restriction digest mixture was used as template in the ligation-mediated PCR (section 2.6.3.2) in a total reaction volume of 50  $\mu$ L.

### **2.6.6. Transformation of *E. coli* DH5 $\alpha$**

#### **2.6.6.1. Generation of chemically competent *E. coli* cells**

Generation of chemically competent *E. coli* DH5 $\alpha$  cells was performed as described by Sambrook & Russell (2001) with the following alterations. Cells were re-suspended in twice

the volume of 0.1 M CaCl<sub>2</sub>, 14% (v/v) glycerol than stated, and frozen in 100 µL aliquots at -80 °C.

#### **2.6.6.2. Heat shock transformation of *E. coli* cells**

Chemically competent *E. coli* DH5α were transformed by heat shocked as described by Sambrook & Russell (2001). Briefly, aliquots of cells stored at -80 °C were thawed on ice for 20 minutes following the addition of up to 10 µL of the DNA to be transformed. A sample of *E. coli* was also transformed with 10 µL ddH<sub>2</sub>O to act as a negative control. Cells were heat-shocked in a heat block at 42 °C for 90 seconds, and then chilled on ice for five minutes. Following heat-shock 900 µL LB was added to the cells before recovery for 1 hour at 37 °C before plating on LA supplemented with the appropriate antibiotics (section 2.5.1).

#### **2.6.7. Transformation of *M. smegmatis* mc<sup>2</sup>155**

##### **2.6.7.1. Generation of electrocompetant *M. smegmatis* cells**

Generation of electroporation competent *M. smegmatis* mc<sup>2</sup>155 cells was performed as described by Goude and Parish (2009). Cells were frozen in 200 µL aliquots at -80 °C.

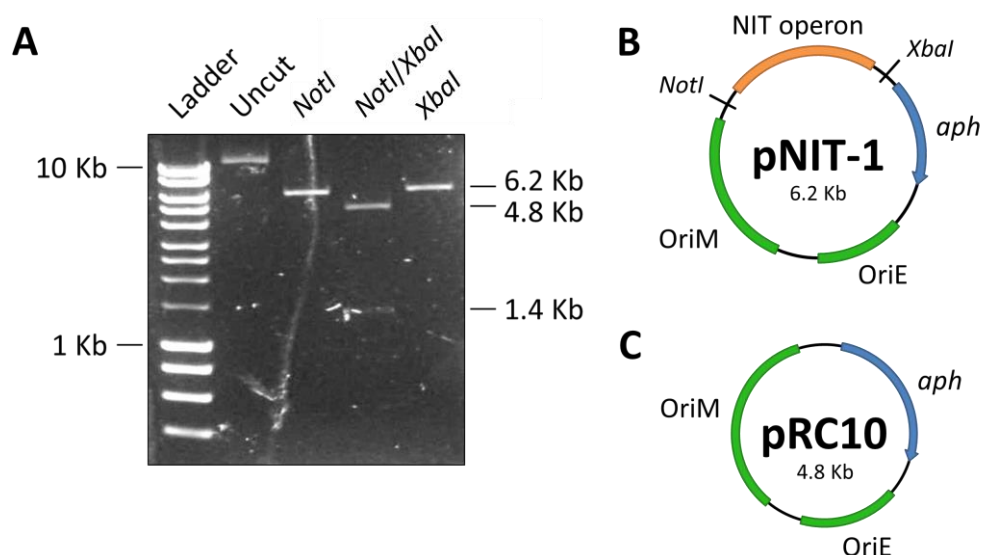
##### **2.6.7.2. Electroporation of *M. smegmatis* cells**

Electrocompetant cells of *M. smegmatis* mc<sup>2</sup>155 were transformed by electroporation as described by Goude and Parish (2009). Briefly, 200 µL 10% glycerol (v/v) cooled to -20 °C was added to 200 µL of frozen cells which were thawed on ice for 1.5 hours in 2 mm gap electroporation cuvettes. A maximum of 5 µL of the plasmid to be transformed was added before electroporation, which was performed at 2500 V, 25 µF, and 1000 Ω. Cells were then added to 600 µL LB in 1.5 mL micro-centrifuge tubes and recovered for two hours at 37 °C before plating on LA supplemented with the appropriate antibiotics (section 2.5.1).



### 2.6.8. Construction of strain MRC10

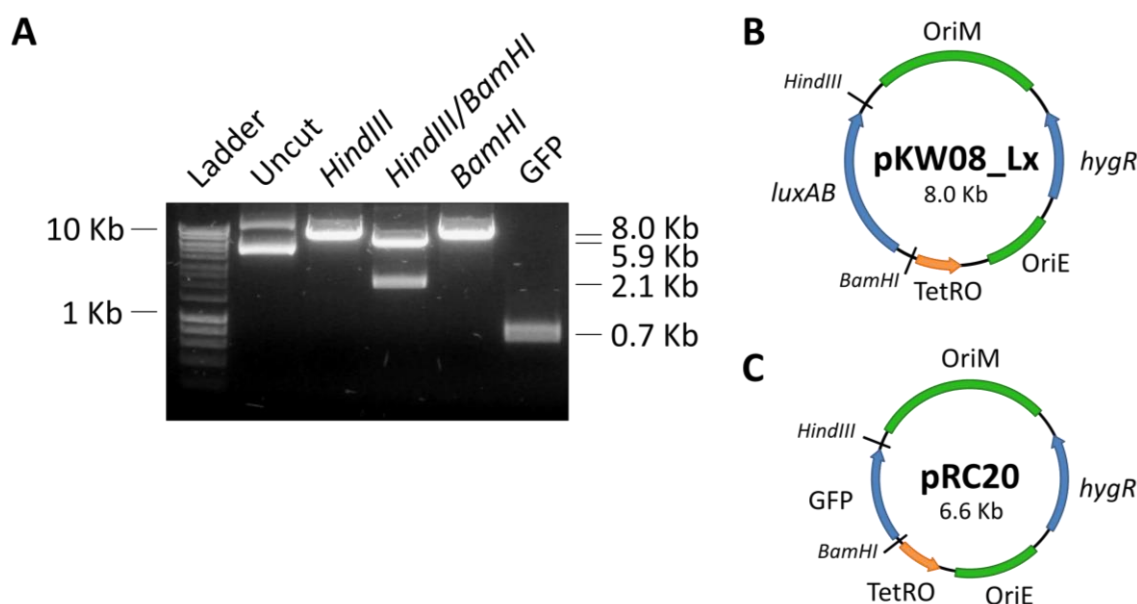
The plasmid pRC10 was constructed by removing the nitrile inducible operon from plasmid pNIT-1 as depicted in Figure 2.2. A digest was setup with 1 µg of plasmid pNIT-1 and the restriction enzymes *Xba*I and *Not*I according to the manufacturer's instructions (section 2.6.3.3). Both single *Xba*I and *Not*I digestion reactions, as well as a double *Xba*I/*Not*I reaction were performed. The 4.8 Kb band in the *Xba*I/*Not*I double digestion reaction, which was the backbone of the pNIT-1 plasmid, was gel extracted (section 2.6.1.5). To blunt the ends of the DNA fragment, 250 ng of the pNIT-1 plasmid backbone was treated with T4 DNA polymerase (section 2.6.3.4). The blunted pNIT-1 plasmid backbone was then ligated with T4 DNA ligase (section 2.6.3.6) under dilute conditions (0.5 ng·mL<sup>-1</sup> DNA) to promote circularisation. Ligation products were transformed into *E. coli* DH5α (section 2.6.6.2), and selected on LA with 50 µg·mL<sup>-1</sup> kanamycin. Several individual transformants were grown up overnight and plasmid mini-prepped (section 2.6.1.2). These plasmids were digested with *Spe*I (section 2.6.3.3), which cuts the pNIT-1 backbone once, to check the size of the plasmid. This plasmid was called pRC10, and was transformed into *M. smegmatis* mc<sup>2</sup>155 (section 2.6.7.2) to generate strain MRC10.



**Figure 2.1: Digestion of pNIT-1 and plasmid maps.** (A) Single and double restriction endonuclease digestions of plasmid pNIT-1. Single digests with *Not*I and *Xba*I resulted in a 6.2 Kb fragment. The double digest resulted in a 4.8 and 1.4 Kb fragment (pNIT-1 plasmid backbone and nitrile inducible operon respectively). Plasmid maps of (B) pNIT-1 and (C) pRC10 with relevant features shown: OriE, *E. coli* pUC origin of replication; OriM, mycobacterial pAL5000 origin of replication; *aph*, kanamycin resistance gene; NIT operon, nitrile inducible operon.

### 2.6.9. Construction of plasmid pRC20

Plasmid pRC20 was constructed to enable tetracycline inducible gene expression in *M. smegmatis* mc<sup>2</sup>155, with semi-quantitative measurement of gene expression provided by a green fluorescent protein (GFP) reporter gene. The plasmid pRC20 was constructed by removing the luciferase genes (*luxAB*) from the plasmid pKW08\_Lx, and replacing it with the GFP gene as depicted in Figure 2.2. A digest was performed with 3 µg of plasmid pKW08\_Lx and the restriction enzymes *Bam*HI and *Hind*III according to the manufacturer's instructions (section 2.6.3.3). Both single *Bam*HI and *Hind*III digestions, as well as a double *Bam*HI/*Hind*III digestion were performed. The 5.9 Kb band that corresponded to the pKW08\_Lx plasmid backbone was gel extracted (section 2.6.1.5). The GFP gene was amplified by PCR from plasmid pLL192\_hsp60 as described in section 2.6.3.2, and digested with *Bam*HI as described in section 2.6.3.3. The GFP PCR product was cleaned and concentrated as described in section 2.6.1.6. GFP was ligated into the backbone of plasmid pKW08\_Lx as described in section 2.6.3.6 using a 3:1 insert to vector molar ratio. Ligations were transformed into *E. coli* DH5α (section 2.6.6.2), and selected on LA with 50 µg·mL<sup>-1</sup> hygromycin B. Several individual transformants were grown up overnight and plasmid midi-prepped (section 2.6.1.3). These plasmids were digested with *Bam*HI (section 2.6.3.3), which cuts the pKW08\_Lx backbone once, to check the size of the plasmid. This plasmid was called pRC20 and was further verified by sequencing with the primer TetRO\_int (Table 2.4) which targets the multiple cloning site, and reads into the downstream GFP gene.



**Figure 2.2: Generation of pKW08 derivative pRC20.** (A) Single and double restriction endonuclease digestions of plasmid pKW08\_Lx were performed. Single digests with *HindIII* and *BamHI* resulted in an 8.0 Kb fragment. A double digest resulted in 5.9 and 2.1 Kb fragments (pKW08\_Lx plasmid backbone and *luxAB* genes respectively). The GFP gene was also digested with *BamHI/HindIII*. Plasmid map of (B) pKW08\_Lx and (C) pRC20 with relevant features shown: OriE, *E. coli* pUC origin of replication; OriM, mycobacterial pAL5000 origin of replication; *hygR*, hygromycin B resistance gene; *luxAB*, luciferase genes A and B; GFP, green fluorescent protein; TetRO, tetracycline regulon including the gene *tetR*, the operator *tetO*, and the promoter  $P_{tet}$ .

#### 2.6.9.1. Construction of pRC20 gene insert vectors

Genes were cloned into pRC20 to generate the expression vectors for the complementation and overexpression assays. Gene inserts were amplified by PCR as described in section 2.6.3.2, and were digested along with plasmid pRC20 with *BamHI* as described in section 2.6.3.3. To decrease self-ligation of the plasmid backbone, pRC20 was treated with Antarctic phosphatase as described in section 2.6.3.5. Gene inserts were then ligated into the pRC20 backbone using T4 DNA ligase as described in section 2.6.3.6, using a 3:1 insert to vector molar ratio. Ligations were transformed into *E. coli* DH5 $\alpha$  (section 2.6.6.2), and selected on LA with 50  $\mu\text{g}\cdot\text{mL}^{-1}$  hygromycin B. Several transformants were selected and grown up in overnight cultures as described in section 2.5.2, with the cultures used for plasmid mini-preparation the next day (section 2.6.1.2). These isolated plasmids were sent for

sequencing using the primer TetRO\_int to confirm gene insert orientation, and sequence fidelity. Correct plasmid constructs were transformed into the relevant strains as described in section 2.6.7.2.

#### **2.6.10. Random transposon mutagenesis of *M. smegmatis* mc<sup>2</sup>155**

Random transposon mutants of *M. smegmatis* mc<sup>2</sup>155 were generated using the pCG79 plasmid as described by Guilhot et al. (1994). Briefly, electrocompetent *M. smegmatis* mc<sup>2</sup>155 cells were transformed with plasmid pCG79 which harbours the *Tn611* transposon (Figure 3.1) and selected on LA supplemented with 20 µg·mL<sup>-1</sup> kanamycin at 30 °C for 4 - 5 days. Several successful transformants were colony purified by re-streaking on fresh LA and left for another 4 – 5 days at 30 °C. Cells were scraped off the plates and re-suspended in supplemented LB (section 2.5) containing 14% glycerol (v/v). Dilutions of 1x10<sup>-2</sup> - 1x10<sup>-6</sup> of the cell suspensions were frozen down at -80 °C. Aliquots of the dilutions were plated in duplicate on fresh LA plates, and incubated at 41 °C to determine the optimal dilution for obtaining individual transposon mutants (approximately 100-200 colonies per plate). Further mutants were then generated by plating the optimal dilution on supplemented LA plates with incubation at 41 °C for 3 – 5 days.

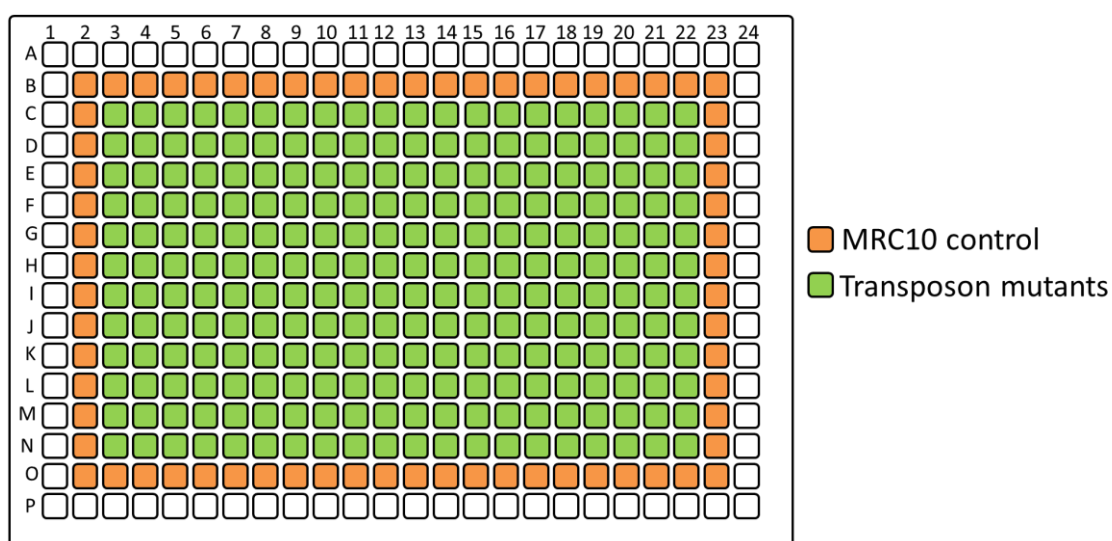
### **2.7. Transposon mutant collection construction**

The transposon mutant collection was generated as a mother stock that was sub inoculated to generate the daughter stock. The daughter stock was used for screening purposes. The mother stock was reserved as a backup for regenerating plates from the daughter stock if a plate was damaged, lost, or contaminated, etc.

#### **2.7.1. Generation of mother stock**

Each plate of the transposon mutant collection contained both random transposon mutants and a control strain MRC10 (section 2.6.8) as depicted in Figure 2.3. The control strain MRC10 was built into the library to provide a standard against which the other mutants on

the plate could be compared, enabling comparison of different mutants across separate plates of the collection, and between different conditions. MRC10 was used as the control as it met the minimum standards for growing under assay conditions (kanamycin resistant). Random transposon mutants of *M. smegmatis* mc<sup>2</sup>155 were generated as described in section 2.6.9.1, and transferred to individual wells of 384-well plates containing 50 µL of supplemented LB (section 2.5) using sterile toothpicks. A 50 µL aliquot of a mid-log phase culture of the control strain MRC10 was added to each of the control wells, and 50 µL ddH<sub>2</sub>O was added to the outside wells. Plates were wrapped in plastic cling film to prevent evaporation, and incubated at 41 °C with shaking at 150 rpm for 48 hours prior to the addition of 35 µL of 80% (v/v) glycerol to each well. Plates were sealed with AlumaSeal® CS aluminium plate seals (Sigma-Aldrich) before brief vortexing, and storage at -80 °C. This process was repeated for 32 separate 384-well plates to generate the mother stock of the complete transposon mutant collection of 7680 mutants. The plates of the mother stock were numbered M01 - M32.



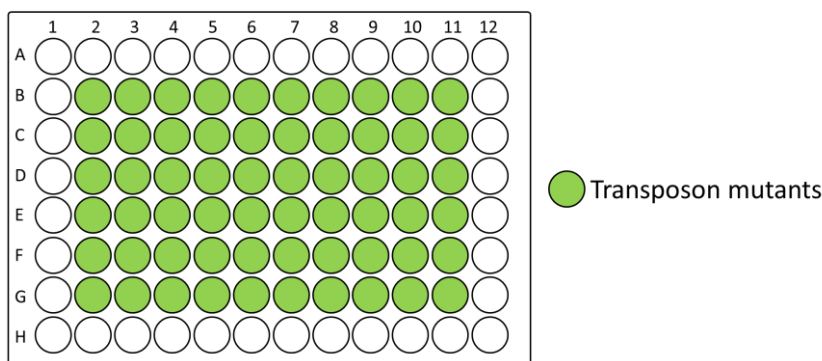
**Figure 2.3: Layout of transposon mutant collection plates.** Each plate of the collection contained 240 individual transposon mutants with each well inoculated with a separate mutant strain. The control strain MRC10 was added to the second outermost ring of wells.

### **2.7.2. Generation of daughter stock**

The daughter stock was generated before the addition of glycerol and freezing down of the mother plates for the first time. Plates of the daughter stock were generated by sub inoculating from the mother stock plates to fresh 384-well plates setup as described in section 2.7.1. Sub inoculation was performed by pinning with 384-pin long pin RePads® (Singer). RePads® were processed after each use as described in appendix section 1. Plates were wrapped in plastic cling film and incubated at 41 °C with shaking at 150 rpm for 48 hours before the addition of glycerol and freezing as in section 2.7.1. This process was repeated to generate a daughter plate for each mother plate of the transposon mutant collection. Plates of the daughter stock were labelled D01 – D32 with the numbers corresponding to the plates in the mother stock.

### **2.7.3. Generation of mini-hit libraries**

The transposon mutant collection was assayed for drug hypersensitivity, as described in section 2.8.1, with the most sensitive mutants from the primary assay transferred to smaller mini-hit libraries. The 120 most sensitive mutants for each drug identified in the primary assay for drug hypersensitivity were picked into mini-hit libraries in the layout described in Figure 2.4. Three mini-hit libraries were constructed, one for isoniazid, one for rifampicin, and one for bedaquiline. The mini-hit libraries consisted of two 96-well plates, each with 60 transposon mutants corresponding to the 60 most sensitive mutants identified from the transposon mutant libraries A and B respectively. The mini-hit libraries plates contained 100 µL supplemented LB (section 2.5) in the inner 60 wells, and 100 µL ddH<sub>2</sub>O in the outermost wells. The 120 most sensitive mutants were picked into individual wells of the mini-hit libraries using sterile toothpicks. Mutants were transferred into the mini-hit library in the order that they appeared in the complete transposon mutant collection. Following strain sub-inoculation from the transposon mutant collection, plates were grown at 41 °C with shaking at 150 rpm for 48 hours. To each well of the mini-hit libraries 70 µL 80% glycerol (v/v) was added, the plates were sealed with AlumaSeal® CS plate seals and briefly vortexed before storage at -80 °C.



**Figure 2.4: Layout of mini-hit library plates.** Each plate of the mini-hit library contained 60 transposon mutants in the internal wells.

## 2.8.Growth-inhibition assays

### 2.8.1. Assay for Drug hypersensitivity

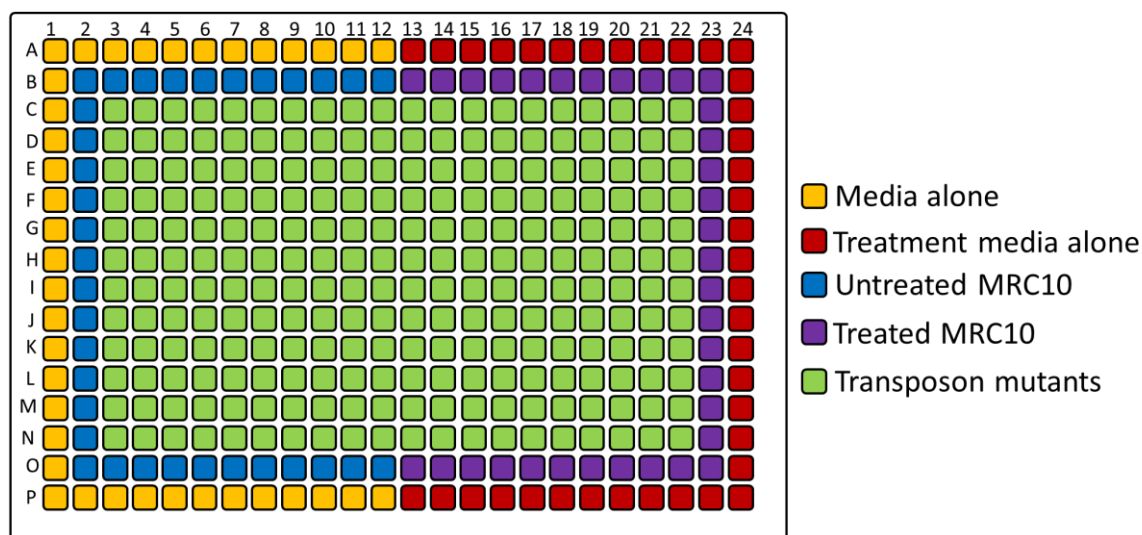
The transposon mutant collection was assayed for drug hypersensitivity using a primary high-throughput assay that utilised resazurin reduction as a surrogate measure of growth-inhibition. A secondary assay was run on the most sensitive mutants identified in the primary assay to validate their sensitivity. The secondary assay used endpoint optical density at 600 nm ( $OD_{600}$ ) to determine growth-inhibition. All assays using transposon mutants were assayed at 41 °C in order to maintain the transposon insertion while under the potential selective pressure caused by drug treatment.

#### 2.8.1.1. Primary assay for drug hypersensitivity

For the primary assay for drug hypersensitivity the transposon mutant collection was split into two halves (Library A and Library B) with 16 plates per library. These libraries were assayed separately and their results processed independently.

The plates of a mutant library were sub-inoculated from the frozen daughter stock by pinning into fresh 384-plates setup as in section 2.7.1. Plates were wrapped in cling film and incubated at 41 °C with shaking at 150 rpm for 72 hours. Plates were then sub-inoculated

into fresh 384-well plates setup identically, and incubated for a further 24 hours. Plates were then used to sub-inoculate 384-well plates setup to assay for drug sensitivity as described in Figure 2.5, using the screening concentration of drug which was determined as described in section 3.2.3.1.



**Figure 2.5: Plate setup for primary assays for drug hypersensitivity.** The outermost wells were split into two halves, the media alone and treatment media controls. The MRC10 controls were also split into two, the untreated MRC10 controls and the treated MRC10 controls. The media alone and untreated MRC10 controls received no drug treatment in all assays, while the treatment media and treated MRC10 controls received the same treatment as the transposon mutants.

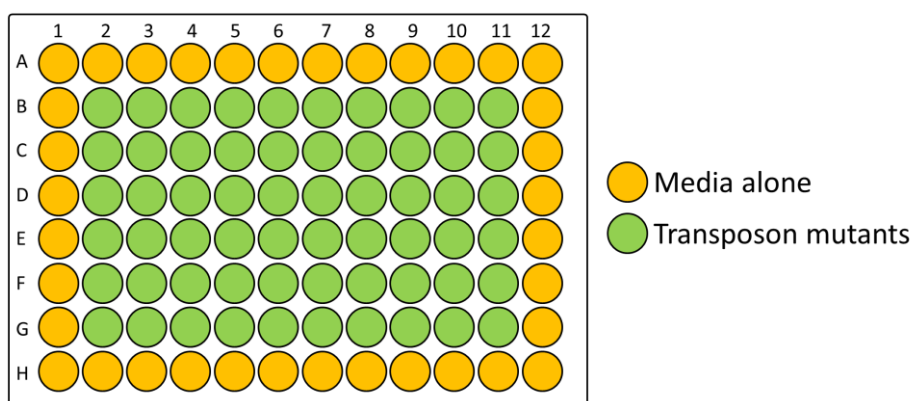
Assay plates were wrapped in cling film then incubated for 48 hours at 41 °C with shaking at 150 rpm. To each well 0.4 volumes of 0.03% resazurin sodium salt (w/v) (appendix section 8.1) was then added. Plates were left for a further two hours at 41 °C without shaking, before reading the fluorescence of the wells of each plate using a PerkinElmer EnSpire®, 2300 multilable reader. Fluorescence measurements were performed at an excitation wavelength of 530 nm and an emission wavelength of 590 nm. The primary assay for drug hypersensitivity was run three independent times for each drug and for media alone. Processing of the resulting data is described in section 3.2.3.



### 2.8.1.2. Secondary assay for drug-hypersensitivity

The mini-hit libraries constructed as described in section 2.7.3 were assayed for drug hypersensitivity using the secondary assay. The same drug concentration was used in the secondary assay as was used in the primary assay (section 3.2.3.1).

The frozen mini-hit library stocks were used to sub-inoculate new 96-well plates setup as described in section 2.7.3. Sub-inoculation of the mini-hit libraries was performed using a metal 96-pin metal pinning tool, which was processed after each pinning as described in appendix section 1. Plates were wrapped in cling film and incubated at 41 °C for 48 hours, before pinning into fresh 96-well plates setup as described in section 2.7.3, and incubated for a further 24 hours. Assay plates were setup containing either 100 µL media, or 100 µL treatment containing the drug at the screening concentration, in every well of a 96-well plate as described in Figure 2.6.



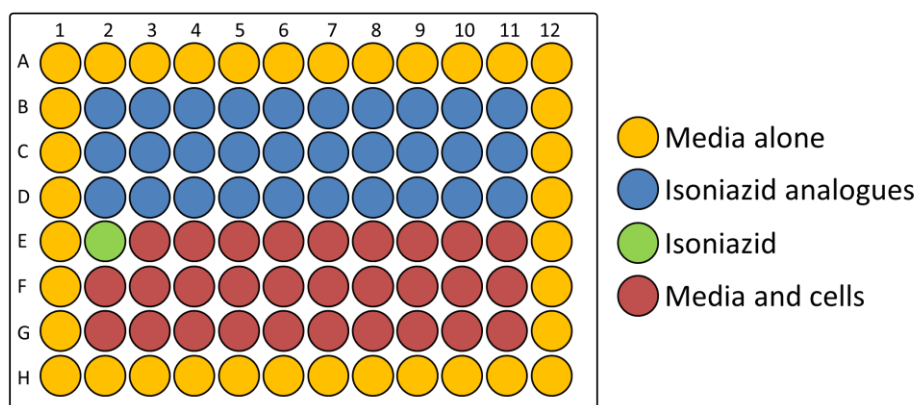
**Figure 2.6: Plate setup for secondary assays for drug hypersensitivity.** The outermost wells contained media alone (treated or untreated), while the inner 60 wells contained the transposon mutants and media (treated or untreated).

The media alone and media with drug assay plates were run in parallel, sub-inoculated from the same overnight mini-hit library plate. Additionally, two of each media alone and treatment assay plate were run at the same time to serve as biological duplicates. The assay plates were inoculated from the overnight mini-hit library plate using the 96-pin tool before incubation at 41 °C for 48 hours. At the assay endpoint the OD<sub>600</sub> of each well of the assay plates was read using the PerkinElmer EnSpire®, 2300 multilable reader. Multiple readings were taken for each well using the three-by-three circular pattern function in the plate-reader software, reading 21 individual points per well, and outputting the average

OD<sub>600</sub> for each well. The experiment was run three independent times for each secondary assay. Assay data was processed as described in section 3.2.4.

### 2.8.2. Isoniazid analogue screen

Isoniazid analogues were tested for their activity against WT *M. smegmatis* mc<sup>2</sup>155. To a 96-well plate 100 µL of LB was added to all wells. As described in Figure 2.7, 100 µg·mL<sup>-1</sup> of each of the 30 analogues as well as an isoniazid control were added to separate wells. A further 50 µL media was added to the outermost wells, and 50 µL of a mid-log phase culture of *M. smegmatis* mc<sup>2</sup>155 diluted to an OD<sub>600</sub> of 0.05 was added to each of the 60 internal wells.

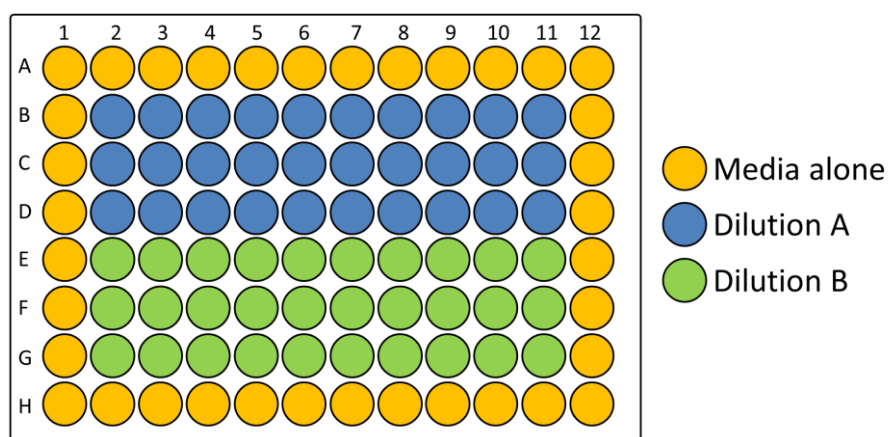


**Figure 2.7: Plate layout for isoniazid analogue screen.** The outermost wells contained media alone, while the inner 60 wells received *M. smegmatis* cells alone, or cells and drug (isoniazid or isoniazid analogue). Each of the blue wells on the figure received a separate isoniazid analogue.

The assay plate was wrapped in plastic cling film and incubated at 37 °C for 48 hours. The endpoint OD<sub>600</sub> was measured using the PerkinElmer EnSpire®, 2300 multilable reader as described in section 2.8.1.2. The OD<sub>600</sub> values for each well were normalised by subtracting the median OD<sub>600</sub> of the media only wells. The growth percentage was calculated for *M. smegmatis* in each of the wells containing isoniazid or an isoniazid analogue compared to the median OD<sub>600</sub> of the media and cells control wells.

### 2.8.3. Dose-response assay

Dose-response assays were performed using serially diluted drug to determine drug minimum inhibitory concentration (MIC). The MIC was defined as the minimum concentration of drug to inhibit growth by more than 90%. Dose-response assays were run in 96-well plates with the plate setup as shown in Figure 2.8. Each plate was divided into two halves (dilutions A and B), with separate drugs run in each half for the basic dose-response assays, or the same drug with and without tetracycline for the complementation and overexpression assays. Each dilution (A or B) provided three technical replicates at each drug concentration, one replicate per row. The three technical replicates were setup using the same bacterial culture. All dose-response assays were setup with mid-log phase cultures at a final OD<sub>600</sub> of 0.05 for *M. smegmatis* mc<sup>2</sup>155 or 0.1 for *M. tuberculosis* H<sub>37</sub>Rv.



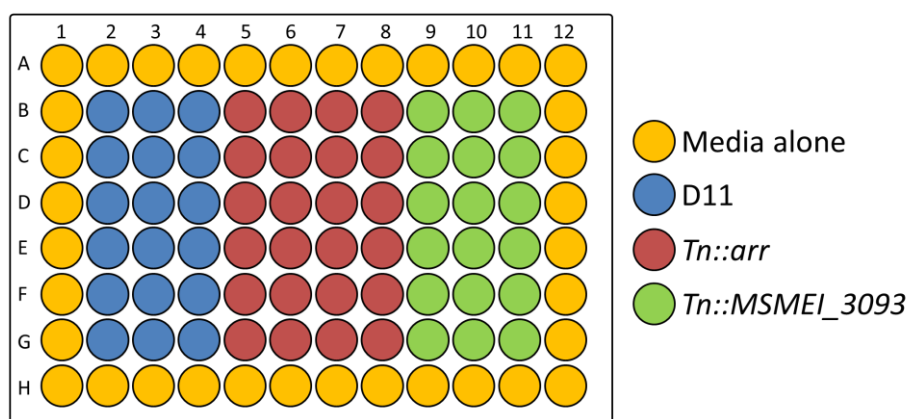
**Figure 2.8: Plate layout for dose-response assays.** The outermost wells contained media alone, columns 2 – 10 contained two-fold serially diluted drug, and column 11 contained no drug and served as the 100% growth control. Cells were added to all 60 internal wells.

To all internal plate wells except column 2, 50 µL media was added, and 100 µL media added to all external wells. To column 2, 100 µL media less the volume of drug to be added was aliquoted. The drug was added to column 2 to give a concentration in the column 2 wells at twice the final desired concentration. The drug was then serially diluted across the plate left to right (column 2 – column 10) transferring 50 µL from column to column with mixing by pipetting up and down 10 times. After mixing the final dilution in row 10, 50 µL was drawn into the pipette and discarded. To each of the internal 60 wells, 50 µL of cells were then added at a concentration twice the desired final concentration (OD<sub>600</sub> of 0.05 for

*M. smegmatis* or an OD<sub>600</sub> of 0.1 for *M. tuberculosis*). Plates were wrapped with cling film and incubated for 48 hours under the conditions specific for each strain as described in section 2.5.3. Endpoint OD<sub>600</sub> was measured with the PerkinElmer EnSpire®, 2300 multilable reader as described in section 2.8.1.2. The OD<sub>600</sub> values were normalised by subtracting the median OD<sub>600</sub> of the media only wells. The OD<sub>600</sub> of each drug dilution triplicate was averaged, and compared to the average OD<sub>600</sub> of the 100% growth control triplicate to calculate the growth-inhibition at each drug concentration. MICs were calculated for each separate assay, with experiments repeated three independent times and the mean MIC calculated across the separate assays.

## **2.9.Growth curve assay**

Growth curve assays were performed in 96-well plates, using the plate setup described in Figure 2.9. To each of the wells 50 µL supplemented LB (section 2.5) was added, with an additional 50 µL added to the outside wells. To the internal 60 wells 50 µL aliquots of an overnight culture for each strain (section 2.5.3.1), diluted to an OD<sub>600</sub> of 0.05, were added. A single culture of each strain was used to setup the assay, with each culture aliquoted into multiple wells to provide biological replicates for each strain, enabling an averaging of the growth rates. Plates were wrapped in plastic cling film and incubated at 41 °C with shaking at 150 rpm for 72 hours total. Every 24 hours, starting at 0 hours, the OD<sub>600</sub> of the wells was measured using the PerkinElmer EnSpire®, 2300 multilable reader as described in section 2.8.1.2. The median OD<sub>600</sub> of the on plate biological replicates for each strain were averaged for each time point. The assay was run three independent times, with the mean OD<sub>600</sub> of each strain averaged across the three assays for each time point.



**Figure 2.9: Growth curve assay plate setup.** The outermost wells contained media alone. The inner 60 wells were divided between the three strains tested, D11, *Tn::arr*, and *Tn::MSMEI\_3093*.

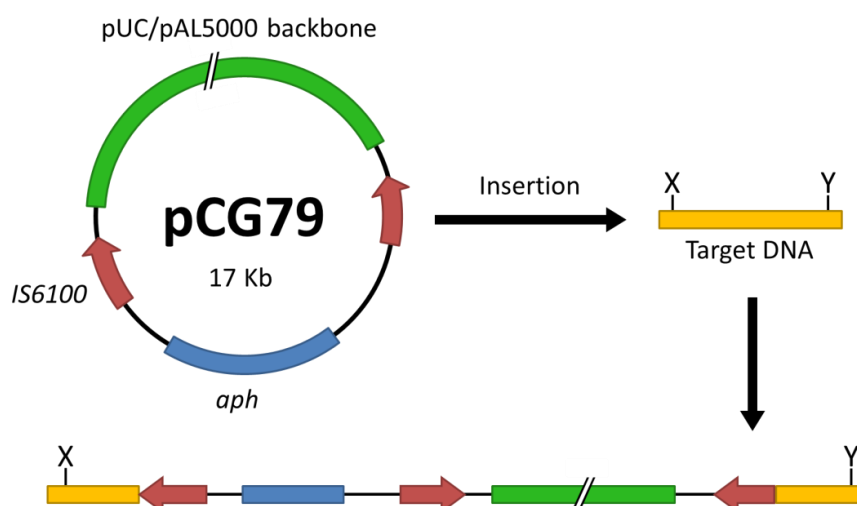
### **3. Isolation of drug hypersensitive mutants of *M. smegmatis* mc<sup>2</sup>155**

#### **3.1.Introduction**

To date, little work has been done on studying drug sensitising mutations for the anti-mycobacterial drugs isoniazid, rifampicin, and bedaquiline, with most research instead focused on studying resistance inducing mutations and altered transcription upon drug exposure. As drug hypersensitivity is a recessive phenotype it cannot be selected for in the same manner as resistant mutants, i.e. in a heterogeneous culture, as sensitive mutants will fail to grow and be lost. This limitation is overcome by the prior construction of a collection of mutants that are then assessed for sensitivity independently. Different methods for the generation of mycobacterial mutant collections for phenotypic screening exist, with transposon mutagenesis favoured due to the inherent labelling of the site of the mutation by the transposon insertion.

##### **3.1.1. Transposon mutagenesis with *Tn611***

*Tn611* is based on the *Tn610* transposon, which has two inverted *IS6100* insertion elements flanking a sulphonamide resistance gene *sul3*, replaced with a gene for kanamycin resistance (*aph*) to generate *Tn611*. Insertion of *Tn611* into a vector that contained both a temperature sensitive pAL5000 mycobacterial origin of replication and an *E. coli* origin (pUC) of replication generated a plasmid named pCG79 (Figure 3.1). This transposon has been shown to insert into the genome of *M. smegmatis* randomly with no insertional hotspots detected (Billman-Jacobe et al., 2006; Guilhot et al., 1994); additionally, insertion is a rare event with only one insertion per cell being reported (Billman-Jacobe et al., 2006; Guilhot et al., 1994). Insertion into the mycobacterial genome occurs by a “copy and paste” mechanism resulting in duplication of one of the insertion elements (Martin et al., 1990), although other possible insertional methods have been reported such as a “cut and paste” mechanism (Guilhot et al., 1994). Insertion of the *Tn611* transposon into the genome has been shown to be stable in the absence of any selective pressure (Guilhot et al., 1994). However, the stability of the insertion under selective pressure is not known.



**Figure 3.1: Plasmid pCG79 and transposition.** Insertion of *Tn611* into the target DNA via a replicative mechanism results in duplication of one of the two *IS6100* elements and insertion of the entire pCG79 vector.

### 3.1.2. Assaying for drug hypersensitivity

Growth-inhibition is commonly measured to assess the inhibitory effect of different conditions in bacteria. A number of techniques are used to measure growth, and therefore growth-inhibition, with direct counting of colony forming units (CFUs) being the gold standard as it is the most direct observation of cell number. However,  $OD_{600}$  is commonly used as a surrogate for CFU measurements as CFU measurements are impractical for higher throughput analyses. Recently, resazurin, a blue weakly fluorescent dye, has been utilised as another alternate method to CFUs for measuring the growth of mycobacteria (Palomino and Portaels, 1999). Resazurin is reduced to the pink, highly fluorescent product resorufin in the presence of NADH, and is used as a measure of oxidative phosphorylation. The dye is commonly used as a viability indicator as only living cells will produce the required NADH, however, recent work has demonstrated a strong correlation between the reduction of resazurin and CFUs for measuring the growth of logarithmic cultures of *M. smegmatis* (Bassett et al., 2013). Measurement of resazurin reduction as an indicator of growth in micro-titre plates is much more suitable for high throughput analyses of mycobacteria than the more direct measure of growth OD. This is because resazurin, and the reduced resorufin, diffuse easily through a liquid medium resulting in a uniform fluorescence and therefore instil a requirement of only one measurement per well. In contrast, OD based measurements

of mycobacteria in micro-titre plates require multiple readings per well to generate reliable measurements of cell growth, owing to the characteristic cell clumping. However, unlike CFU and OD based measurements, the fluorescence generated from the reduction of resazurin is a relative measure of growth, with longer incubation times resulting in different absolute fluorescence values. For the purposes of screening a transposon mutant collection, the inclusion of a standard strain that acts as an untreated (100% growth) control in each library plate allows standardisation of the growth-inhibition as measured by resazurin reduction, enabling the direct comparison between separate library plates. The reduction of resazurin is also affected by the metabolic states of the cultures which, similar to other indirect measure of cell number, can lead to false positives (Petthe et al., 2010). This limitation can be overcome by using a secondary assay to validate the drug hypersensitivity of mutants using an endpoint OD measurement. Although using OD results in a lower throughput assay, using it as a validation assay for a limited number of the most sensitive mutants from the primary assay overcomes this limitation.

### **3.1.3. Objectives of Chapter Three**

The goal of Chapter Three was to generate drug hypersensitive mutants of *M. smegmatis* mc<sup>2</sup>155. These mutants were then studied to identify the underlying genetic basis and the information used to investigate drug mode of action in Chapters Four and Five of this thesis

To achieve this goal the following specific aims were addressed:

- Construction of a random transposon mutant collection in *M. smegmatis* mc<sup>2</sup>155 using *Tn611*
- Development of a high-throughput assay for identifying drug hypersensitive mutants
- Development of a secondary assay to validate mutants identified as drug hypersensitive in the primary assay

Drug hypersensitive mutants were generated in order to identify novel components of the mode of action of the front line anti-TB drugs isoniazid, rifampicin, and bedaquiline. A collection of *M. smegmatis* mc<sup>2</sup>155 transposon mutants were generated in order to assay for increased drug hypersensitivity and identify mutant strains of interest. Sensitivity of these mutants was ultimately characterised in terms of MICs.



## 3.2.Methods

### 3.2.1. Estimation of unique mutants versus library size

The expected number of unique mutants in a random transposon mutant collection was estimated for a range of collection sizes using the Poisson distribution (Equation 3.1 and Equation 3.2), and the following assumptions:

- The percentage of essential genes in *M. smegmatis* mc<sup>2</sup>155 is the same as that previously described for *M. tuberculosis* (Sasseti et al., 2001)
- The *Tn611* transposon inserts into the genome of *M. smegmatis* in a random manner, i.e. lacks insertional hot spots (Guilhot et al., 1994)
- The probability of the transposon inserting into an open reading frame (ORF) is identical for all ORFs regardless of their size

$$P(x) = \frac{e^{-\frac{L}{G}} \cdot (L/G)^x}{x!}$$

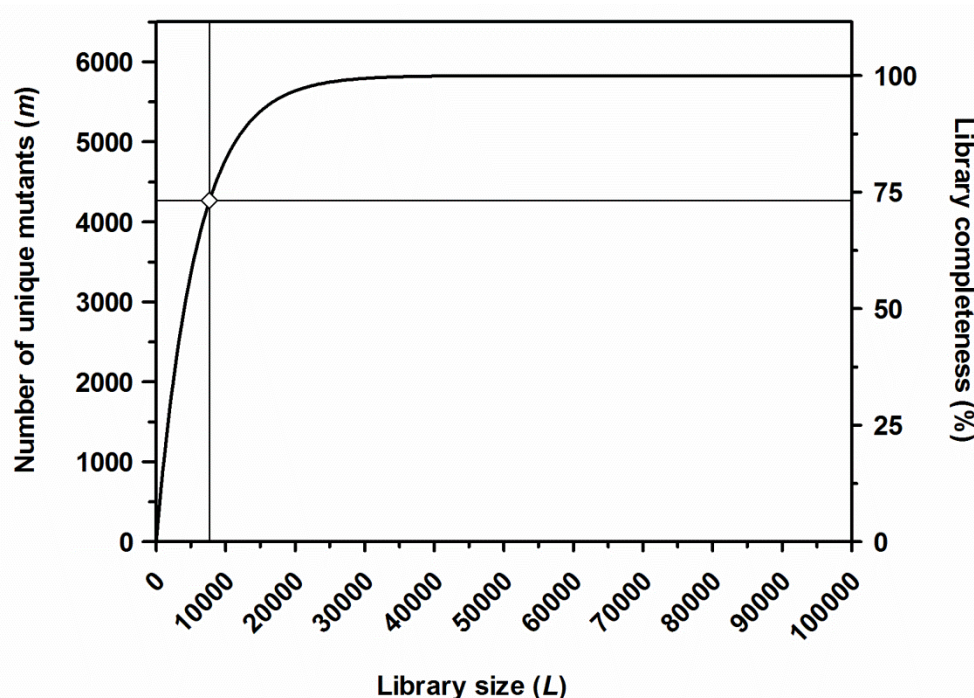
**Equation 3.1: Poisson estimation of the standard distribution.** Where  $L$  is equal to the total number of mutants in the library, and  $G$  is equal to the number of genes in the *M. smegmatis* genome that the transposon can insert into.

$$m = G(1 - e^{-\frac{L}{G}})$$

**Equation 3.2: Calculation for the estimated number of unique mutants in a library of size  $L$ .** For a given library size ( $L$ ) and based upon the above assumptions the number of unique mutants is estimated to be equal to  $m$ .

$G$  was estimated based on the percentage of non-essential genes in *M. tuberculosis* H<sub>37</sub>Rv, i.e. 86.3% of its genome;  $G$  is therefore equal to 86.3% of the 6752 genes in the *M. smegmatis* mc<sup>2</sup>155 genome or 5827 genes. It was determined that a library size of approximately 7680 transposon mutants, which equates to approximately 1.1-fold whole genome coverage, would be suitable for screening for drug hypersensitivity. At this library size it is expected to contain 4267 unique mutants, interrupting 73.2% of the genes predicted to be able to sustain transposon insertions (non-essential genes) (Figure 3.2). In order to increase the proportion of genes knocked out, a significant increase in the number

of mutants would be required. For example, 20,000 or 60,000 mutants would be required to obtain 95% or 100% of genes knocked out, respectively. The aim of this thesis was to identify pathways related to drug mode of action, as opposed to a single gene whose product was affected by a drug and therefore, it was not critical to have every possible gene knocked out within this library. Additionally, the smaller size of the library constructed in this thesis facilitates screening in high-throughput. Libraries with 1.1-fold genome coverage have been used previously for similar studies (Alexander et al., 2003; Daugherty et al., 2011).



**Figure 3.2: Number of unique mutants versus library size.** Line graph describing the expected number of unique mutants ( $m$ ) for a given library size ( $L$ ) estimated using the Poisson distribution. Library completeness is the number of expected mutants ( $m$ ) as a percentage of the number of the predicted non-essential genes for *M. smegmatis*. Line intersect indicates chosen library size of 7680 transposon mutants.

### 3.2.2. Construction of the transposon mutant collection

A collection of 7680 transposon mutants was built in 32 384-well plates, with 240 individual transposon mutants per plate as described in section 2.7. As discussed in the chapter introduction, the fluorescence from resazurin reduction generates a relative measure of growth-inhibition for that plate. In order to compare the fluorescence values and therefore

growth-inhibition of mutants across multiple plates a standard was included in each plate of the library. The selected standard was an untreated control strain (MRC10) that would represent maximal growth (maximal resazurin reduction) for that plate, against which the resazurin reduction of the mutant strains on that plate were standardised. To compare growth-inhibition of mutants across separate plates of a library it was essential the treatment conditions were the same. To test this, half of the MRC10 control strain wells remained untreated, while the other half were treated with the same drug concentration as the transposon mutants, with statistical testing being used to check that the treated-MRC10 control behaved the same across all plates of a library.

### **3.2.3. Primary assay for drug hypersensitivity**

The assays for identifying drug hypersensitive mutants were performed using drug concentrations that gave minor but measureable growth-inhibition, with screening concentrations for each drug optimised as described below in section 3.2.3.1. At these concentrations mutants that displayed hypersensitivity to a drug could be differentiated from the average growth-inhibition levels of the mutant libraries. Drugs were screened against the transposon mutant libraries as described in section 2.8.1. For logistical reasons the 32 plate transposon mutant collection was split into two smaller 16 plate libraries for the purpose of performing the primary assay, Library A and Library B. The data analysis for the primary assays against each library were performed independently to prevent any bias resulting from different assay conditions. To quantify drug sensitivity, a factor of inhibition ( $F_i$ ) was calculated for each mutant strain for each drug. This value is the reciprocal of the growth of the strain when treated versus untreated, with higher values representing increased inhibition in the assay (Equation 3.4). The output from the primary assay was a list of mutants ordered from highest to lowest sensitivity to the drug used.

To calculate the  $F_i$ , the relative fluorescence values from the reduction of resazurin were normalised by removing the background, giving the relative fluorescence units (RFU) for each well of the plate. The in-plate untreated-MRC10 control, which represented maximal resazurin reduction (therefore maximal growth), was averaged to give  $RFU_{UTMRC10}$  that was

used to standardise the RFU values of the treated-MRC10 control and mutant strains across the rest of the plate using Equation 3.3.

$$\text{sRFU}_{\text{myco}} = 100 \cdot \left( \frac{\text{RFU}_{\text{myco}}}{\text{RFU}_{\text{UTMRC10}}} \right)$$

**Equation 3.3: Calculation of standardised RFU values for transposon mutants.** Where  $\text{RFU}_{\text{myco}}$  is the normalised RFU and  $\text{sRFU}_{\text{myco}}$  is the standardised RFU for a given strain.

The  $F_i$  for each mutant strain (and treated-MRC10 control) was calculated according to Equation 3.4. An  $F_i$  value of 1 represented no inhibition while a value greater than 1 represented an increased inhibition, with the greater the  $F_i$  value the greater the strain was inhibited.

$$F_i = \frac{1}{\left( \frac{\mu_{\text{treated}}}{\mu_{\text{untreated}}} \right)}$$

**Equation 3.4: Calculation of  $F_i$  for mutants.** Where  $\mu_{\text{treated}}$  and  $\mu_{\text{untreated}}$  are the mean  $\text{sRFU}_{\text{myco}}$  values with and without drug treatment respectively. Means were calculated over three independent experiments.

The on plate treated-MRC10 control was used to test that all plates for a given condition were behaving the same throughout all experimental replicates. The median  $\text{sRFU}$  values of the treated-MRC10 from each plate of a library were pooled and tested for normal distribution (D'agostino and Pearson omnibus normality test), with data normalised as required using transformations listed in the results sections for each drug. A one-way ANOVA was performed to test if there was a significant difference in the average inhibition of the treated-MRC10 control strain across all plates of a mutant library before directly comparing the growth-inhibition of the mutants to determine the 60 most sensitive. The 60 most sensitive mutants from each library (Library A and Library B), for each drug, were combined into mini-hit libraries as described in section 2.7.3.

### 3.2.3.1. Optimising screening concentrations

Two separate plates from the transposon mutant libraries, selected at random, were grown with and without drug to optimise drug screening concentrations. A range of concentrations

of drug were used, and these were selected by determining the MIC versus MRC10 as a starting reference point, with MICs determined by dose-response assay described in section 2.8.3. The median  $F_i$  for each different drug concentration test plate was determined by averaging the  $F_i$  values for all mutants within a given condition. A drug concentration that gave a median  $F_i$  value in the range of 1.18 - 1.42 was selected as the screening concentration for that drug. This  $F_i$  range represents a median inhibition of 15 - 30%.

#### **3.2.4. Secondary assay for drug hypersensitivity**

The secondary assay was run to reduce the number of false positives resulting from the use of resazurin reduction as a measure of growth, instead using the more biologically relevant measure of growth, OD at 600 nm ( $OD_{600}$ ) as discussed in the introduction to this chapter. The mini-hit libraries comprised of the 60 most sensitive mutants for a give drug from each library (120 total), and were expected to capture most if not all the true positive hits from the initial screen, while minimising the number of mutants for validation. These mini-hit libraries were screened as described in 2.8.1.2. A plate containing only the strain MRC10 was also run against each drug for comparison.

### **3.3.Results**

#### **3.3.1. Drug screening concentration optimisation**

The two frontline anti-TB drugs isoniazid and rifampicin, and the novel anti-mycobacterial bedaquiline, were assayed against the transposon mutant libraries to find drug hypersensitive mutants. The MIC concentrations for these compounds against the control strain MRC10, and the screening concentrations used are listed in Table 3.1. Screening concentrations were chosen as described in section 3.2.3.1. Work on bedaquiline was performed in collaboration with the laboratory of Professor Gregory Cook at the University of Otago.

**Table 3.1: MIC values for anti-TB drugs versus MRC10 and optimised screening concentrations.**

Drug	MIC <sup>a</sup> ± se	Screening concentration
Isoniazid	6.12 ± 0.56 µM	6.00 µM
Rifampicin	0.72 ± 0.12 µM	0.26 µM
Bedaquiline	29.3 ± 7.32 nM	10.8 nM

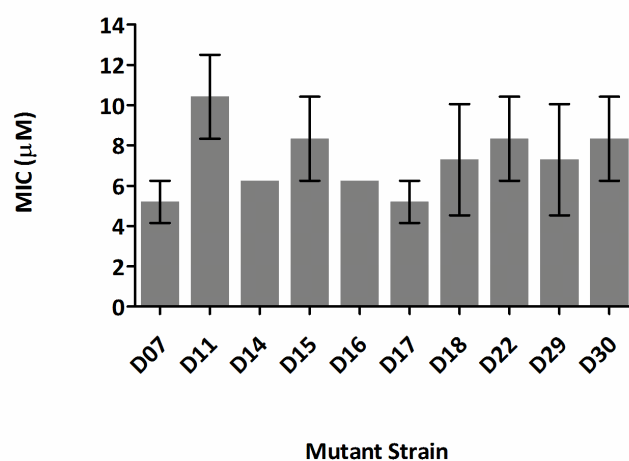
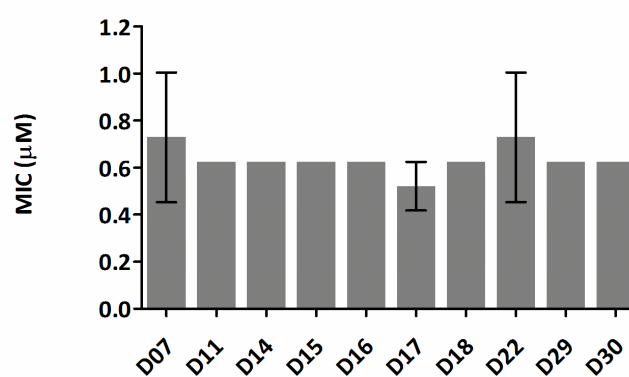
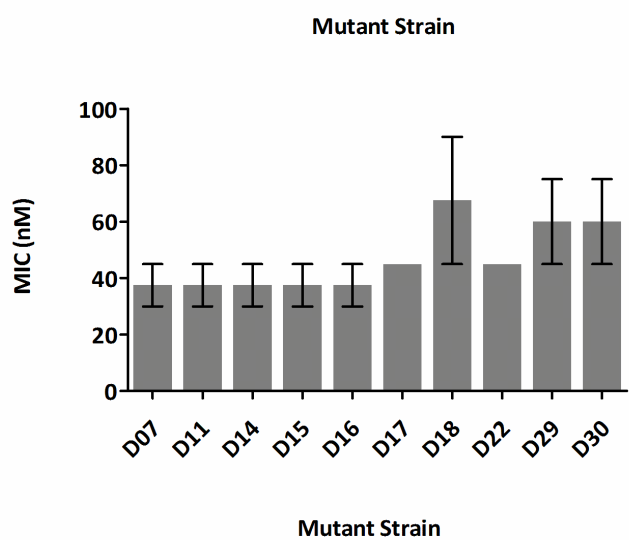
<sup>a</sup>MIC values represent mean values across three independent experiments with standard error (se) presented.

### **3.3.2. Growth of the treated-MRC10 control strain in LB**

The growth of the treated-MRC10 controls were examined for variability between plates within each library when grown in media (LB) alone. The sRFU values of the treated-MRC10 control strain were normally distributed in both libraries, and were examined using a one-way ANOVA. No significant difference between the sRFU values of the treated-MRC10 control strain across the separate plates from the three independent experimental replicates was found for either library; therefore, screening for hypersensitive transposon mutants proceeded.

### **3.3.3. Control strains for quantitating drug hypersensitivity**

Ten mutant strains were randomly selected from the mutant libraries to act as control strains for the dose-response assays. The MICs of these control strains for isoniazid, rifampicin, and bedaquiline were determined (Figure 3.3). The MIC values of the control strains used were consistent for each of the drugs tested (Kruskal-Wallis test; significance cut off of  $p < 0.05$ ). The mean of all 10 control strains was used for the initial dose-response assays to quantify drug hypersensitivity.

**A****B****C**

**Figure 3.3: Comparison of MIC of random mutant control strains.** Average MIC values of 10 random control transposon mutant strains versus (A) isoniazid, (B) rifampicin, and (C) bedaquiline. Mutants are labelled according to the mutant library plate they were picked from. Column heights represent mean MICs across three independent experiments with standard error bars shown.

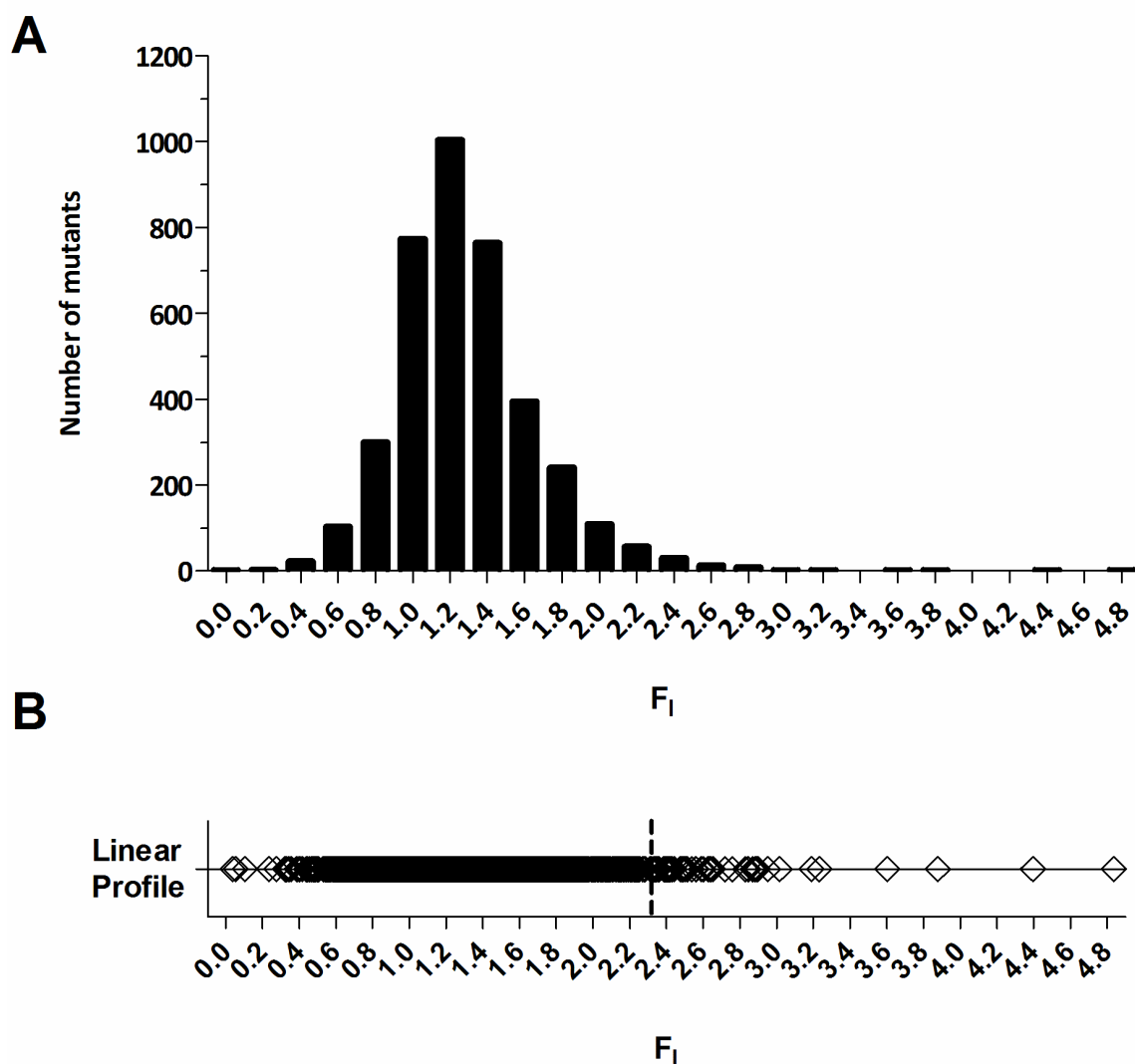
### **3.3.4. Isoniazid**

#### **3.3.4.1. Primary assay for drug hypersensitivity**

The primary assay for isoniazid hypersensitivity was performed at a concentration of 6  $\mu$ M (Table 3.1). As the sRFU values for the treated-MRC10 controls within each library were normally distributed one-way ANOVAs were performed on untransformed data. The one-way ANOVAs did not show a significant difference in mean sRFU for the treated-MRC10 control across all plates within either library (A or B) ( $p > 0.05$ ), therefore analysis of the assay data continued as described in section 3.2.3.

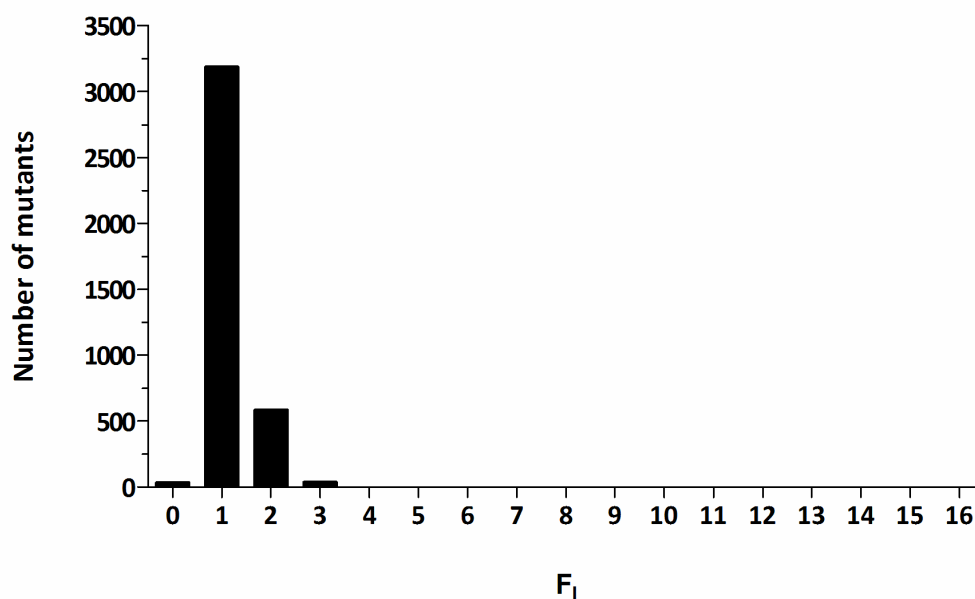
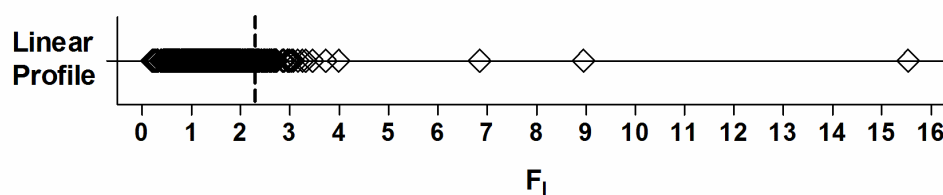
The median inhibition of mutant library A versus isoniazid was approximately 19% (Figure 3.4). The 60 most sensitive mutants from library A, representing mutants that were at least 1.9 times more sensitive to isoniazid than the library median, were picked into the isoniazid mini-hit library.





**Figure 3.4: Mutant library A versus 6  $\mu$ M isoniazid.** (A) Frequency distribution of  $F_1$  values, and (B)  $F_1$  linear profile, from library A versus 6  $\mu$ M isoniazid. The median  $F_1$  across mutant library A was 1.21, and the median  $F_1$  for the treated-MRC10 control was 1.26. The dotted line indicates the cut-off for the 60 most sensitive mutants, and lies at  $F_1 = 2.30$ . The  $F_1$  value for each mutant represents the mean  $F_1$  across three independent experiments.

The median inhibition of mutant library B versus isoniazid was approximately 13% (Figure 3.5). The 60 most sensitive mutants from library B, representing mutants that were at least 2.0 times more sensitive to isoniazid than the library median, were picked into the isoniazid mini-hit library.

**A****B**

**Figure 3.5: Mutant library B versus 6  $\mu$ M isoniazid.** (A) Frequency distribution of  $F_1$  values, and (B)  $F_1$  linear profile, from library B versus 6  $\mu$ M isoniazid. The median  $F_1$  across mutant library B was 1.15, and the median  $F_1$  for the treated-MRC10 control was 1.19. The dotted line indicates the cut-off for the 60 most sensitive mutants, and lies at  $F_1 = 2.29$ . The  $F_1$  value for each mutant represents the mean  $F_1$  across three independent experiments.

### 3.3.4.2. Secondary assay for drug hypersensitivity

A secondary assay was performed in order to validate the hypersensitivity to isoniazid of the 120 most sensitive mutants (60 from each library) identified in the primary assay. Each hypersensitive mutant was tested against the screening concentration of isoniazid (Table 3.1) and growth-inhibition was determined by endpoint  $OD_{600}$  measurement as described in section 3.2.4. The concentration of isoniazid used in the secondary assay was the same as that used in the primary assay (6  $\mu$ M). Table 3.2 shows the 12 most sensitive mutants from

the secondary assay against the isoniazid mini-hit library. The growth-inhibition of mutants in the secondary assay against the isoniazid mini-hit library showed a median growth-inhibition of 23.0%, similar to the growth-inhibition of the MRC10 control strain at 23.6%. Three mutants, *myco7437*, *myco2576*, and *myco5016* stood out, showing greater than 80% inhibition.

**Table 3.2: Growth-inhibition of top secondary assay hits versus isoniazid.**

Strain	Growth-inhibition <sup>a</sup> ± se (%)
<i>myco7437</i>	97.9 ± 0.84
<i>myco2576</i>	87.3 ± 9.29
<i>myco5016</i>	85.5 ± 5.91
<i>myco3113</i>	61.9 ± 19.8
<i>myco0409</i>	54.3 ± 14.3
<i>myco6166</i>	54.2 ± 12.4
<i>myco2100</i>	49.8 ± 13.2
<i>myco1897</i>	49.6 ± 15.6
<i>myco6192</i>	48.7 ± 18.5
<i>myco6482</i>	46.5 ± 12.0
<i>myco2659</i>	45.5 ± 2.78
<i>myco7102</i>	45.2 ± 12.6
MRC10	23.6 ± 5.48

<sup>a</sup>Growth-inhibition values represent mean values across three independent assays with standard errors (se) presented.

### 3.3.4.3. Quantification of mutant hypersensitivity

The isoniazid MIC was determined by dose-response assay (section 2.8.3) for the 12 most sensitive mutants from the secondary assay in order to quantify mutant sensitivity. Isoniazid MICs for the 12 strains were compared to an MIC value averaged across the 10 random transposon mutant control strains (section 3.3.3). All of the 12 isoniazid hypersensitive mutants from the secondary assay showed some level of increased sensitivity compared to the control MIC (Table 3.3). The three mutants that stood out in the secondary assay also showed the greatest change in isoniazid MIC. These mutants, *myco2576*, *myco5016*, and *myco7437*, showed a greatly increased sensitivity to isoniazid with a decrease in MIC of greater than two-fold compared to the control MIC, with *myco2576* and *myco5016* showing a greater than four-fold decrease in MIC.

**Table 3.3: Sensitivity of transposon mutants to isoniazid.**

Strain	MIC $\pm$ se ( $\mu$ M)
<i>myco2576</i>	1.56 $\pm$ 0.00
<i>myco5016</i>	1.56 $\pm$ 0.00
<i>myco7437</i>	3.12 $\pm$ 0.00
<i>myco2100</i>	4.17 $\pm$ 1.04
<i>myco3113</i>	5.21 $\pm$ 1.04
<i>myco0409</i>	5.21 $\pm$ 1.04
<i>myco6166</i>	5.21 $\pm$ 1.04
<i>myco1897</i>	6.25 $\pm$ 0.00
<i>myco6192</i>	6.25 $\pm$ 0.00
<i>myco6482</i>	6.25 $\pm$ 0.00
<i>myco2659</i>	6.25 $\pm$ 0.00
<i>myco7102</i>	6.25 $\pm$ 0.00
Tn Control	7.08 $\pm$ 0.54

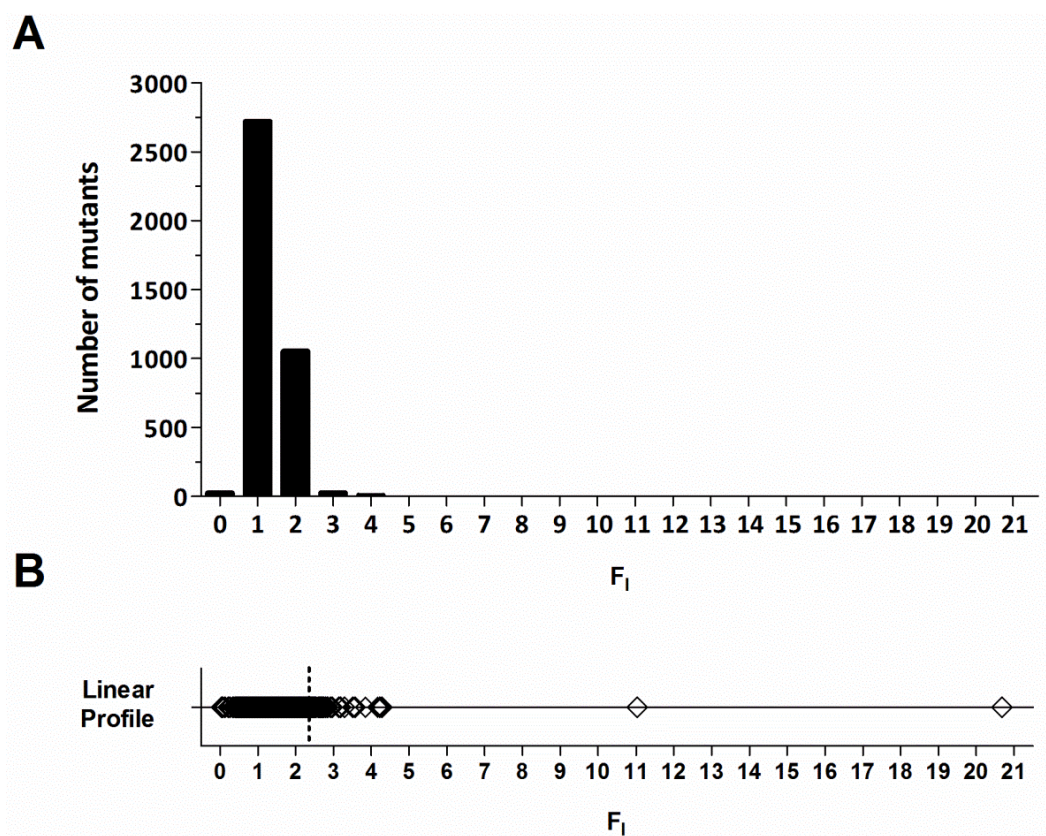
Isoniazid MICs for the 12 mutants most sensitive to isoniazid identified in the secondary assay, averaged over three independent experiments. The transposon (Tn) control value represents the mean of the 10 randomly selected mutant control strains. Standard errors (se) are presented.

### 3.3.5. Rifampicin

#### 3.3.5.1. Primary assay for drug hypersensitivity

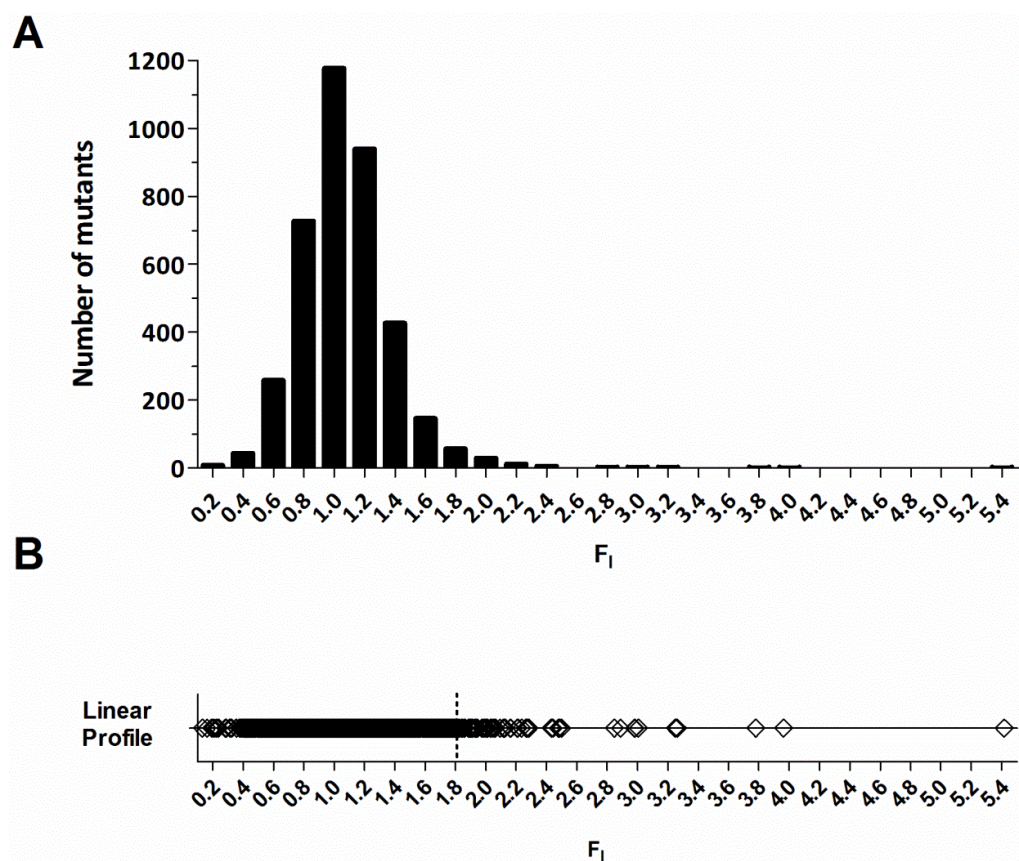
The primary assay for rifampicin hypersensitivity was performed at a concentration of 0.26  $\mu$ M (Table 3.1). As the sRFU values for the treated-MRC10 controls within each library were normally distributed one-way ANOVAs were performed on untransformed data. The one-way ANOVAs did not show a significant difference in mean sRFU for the treated-MRC10 control across all plates of either library A or B ( $p > 0.05$ ), therefore analysis of the assay data continued as described in section 3.2.3.

The median inhibition of mutant library A versus rifampicin was approximately 24% (Figure 3.6). The 60 most sensitive mutants from library A, representing mutants that were at least 1.78 times more sensitive to rifampicin than the library median, were picked into the rifampicin mini-hit library.



**Figure 3.6: Mutant library A versus 0.26  $\mu$ M rifampicin.** (A) Frequency distribution of  $F_1$  values, and (B)  $F_1$  linear profile, from library A versus 0.26  $\mu$ M rifampicin. The median  $F_1$  across mutant library A was 1.32, and the median  $F_1$  for the treated-MRC10 control was 1.60. The dotted line indicates the cut-off for the 60 most sensitive mutants, and lies at  $F_1 = 2.35$ . The  $F_1$  value for each mutant represents the mean  $F_1$  across three independent experiments.

The median inhibition of mutant library B versus rifampicin was approximately 5% (Figure 3.7). The 60 most sensitive mutants from library B, representing mutants that were at least 1.72 times more sensitive to rifampicin than the library median, were picked into the rifampicin mini-hit library.



**Figure 3.7: Mutant library B versus 0.26  $\mu\text{M}$  rifampicin.** (A) Frequency distribution of  $F_1$  values, and (B)  $F_1$  linear profile, from library B versus 0.26  $\mu\text{M}$  rifampicin. The median  $F_1$  across mutant library B was 1.05, and the median  $F_1$  for the treated-MRC10 control was 1.36. The dotted line indicates the cut-off for the 120 most sensitive mutants, and lies at  $F_1 = 1.81$ . The  $F_1$  value for each mutant represents the mean  $F_1$  across three independent experiments.

### 3.3.5.2. Secondary assay for drug hypersensitivity

A secondary assay was performed in order to validate the hypersensitivity to rifampicin of the 120 most sensitive mutants (60 from each library) identified in the primary assay. Each hypersensitive mutant was tested against the screening concentration of rifampicin (Table 3.1) and growth-inhibition was determined by endpoint  $\text{OD}_{600}$  measurement as described in section 3.2.4. The concentration of rifampicin used in the secondary assay was the same as that used in the primary assay (0.26  $\mu\text{M}$ ). Table 3.4 shows the 12 most sensitive mutants from the secondary assay against the rifampicin mini-hit library. The median growth-inhibition of the entire mini-hit library was 8.46%, compared to 13.4%

growth-inhibition for the control strain MRC10. The mutant with the highest sensitivity was *myco2694*, which showed greater than 95% inhibition. In addition, two mutants *myco1030* and *myco4003*, stood out with greater than 60% inhibition.

**Table 3.4: Growth-inhibition of top secondary assay hits versus rifampicin.**

Strain	Growth-inhibition <sup>a</sup> ± se (%)
<i>myco2694</i>	97.7 ± 1.92
<i>myco4005</i>	70.0 ± 22.0
<i>myco1030</i>	61.0 ± 19.1
<i>myco5231</i>	45.0 ± 17.2
<i>myco0163</i>	39.1 ± 20.0
<i>myco7011</i>	38.1 ± 31.9
<i>myco891</i>	38.0 ± 25.8
<i>myco5826</i>	35.2 ± 21.6
<i>myco6762</i>	35.1 ± 33.8
<i>myco6859</i>	33.6 ± 4.56
<i>myco2642</i>	31.3 ± 11.3
<i>myco5883</i>	31.1 ± 0.73
MRC10	13.4 ± 0.30

<sup>a</sup>Growth-inhibition values represent mean values across three independent assays with standard errors (se) presented.

### 3.3.5.3. Quantification of mutant hypersensitivity

The rifampicin MIC was determined by dose-response assay (section 2.8.3) for the 12 most sensitive mutants from the secondary assay in order to quantify mutant sensitivity. Rifampicin MICs for the 12 strains were compared to an MIC value averaged across the 10 random transposon mutant control strains (section 3.3.3). In general, the mutant strains showed an increased sensitivity to rifampicin compared to the control strain with 11 of the 12 strains showing a decrease in MIC compared to the control MIC (Table 3.5). The two most sensitive mutants from the secondary assay had the greatest decrease in rifampicin MIC, whereby *myco2694* showed an almost eight-fold decrease in MIC, while mutant *myco4005* showed a four-fold decrease in MIC. The remaining mutants showed a two-fold or less decrease in MIC to rifampicin compared to the control strain.

**Table 3.5: Sensitivity of transposon mutants to rifampicin.**

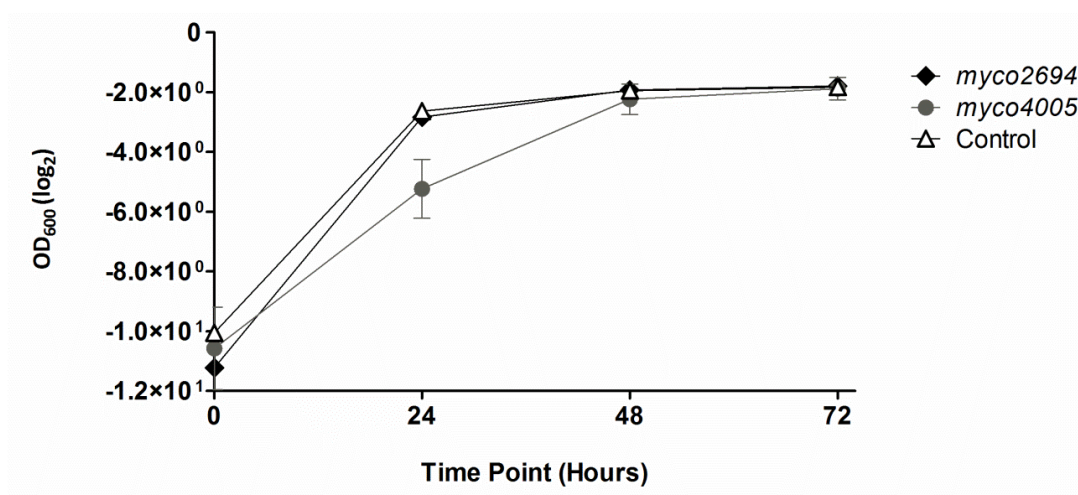
Strain	MIC $\pm$ se ( $\mu$ M)
<i>myco2694</i>	0.09 $\pm$ 0.03
<i>myco4005</i>	0.16 $\pm$ 0.00
<i>myco5826</i>	0.26 $\pm$ 0.05
<i>myco6762</i>	0.26 $\pm$ 0.05
<i>myco1030</i>	0.31 $\pm$ 0.00
<i>myco0163</i>	0.31 $\pm$ 0.00
<i>myco7011</i>	0.31 $\pm$ 0.00
<i>myco5231</i>	0.52 $\pm$ 0.10
<i>myco891</i>	0.52 $\pm$ 0.10
<i>myco2642</i>	0.52 $\pm$ 0.10
<i>myco5883</i>	0.52 $\pm$ 0.10
<i>myco6859</i>	0.63 $\pm$ 0.00
Tn Control	0.64 $\pm$ 0.04

Rifampicin MICs for the 12 mutants most sensitive to rifampicin identified in the secondary assay, averaged over three independent experiments. The transposon (Tn) control value represents the mean of the 10 randomly selected mutant control strains. Standard errors (se) are presented.

#### **3.3.5.4. Growth curve of rifampicin hypersensitive mutant *myco4005***

Interestingly, it was noticed that the rifampicin hypersensitive strain *myco4005* (with a four-fold reduction in MIC) took longer to grow than all other rifampicin hypersensitive mutant strains. A growth curve experiment (section 2.9) was performed to measure the reduced growth rate. A control strain (random transposon mutant strain D11), and the rifampicin hypersensitive mutant *myco2694* reached stationary phase by 24 hours, whereas the strain *myco4005* took approximately 24 hours longer (48 hours total) to reach stationary phase (Figure 3.8).





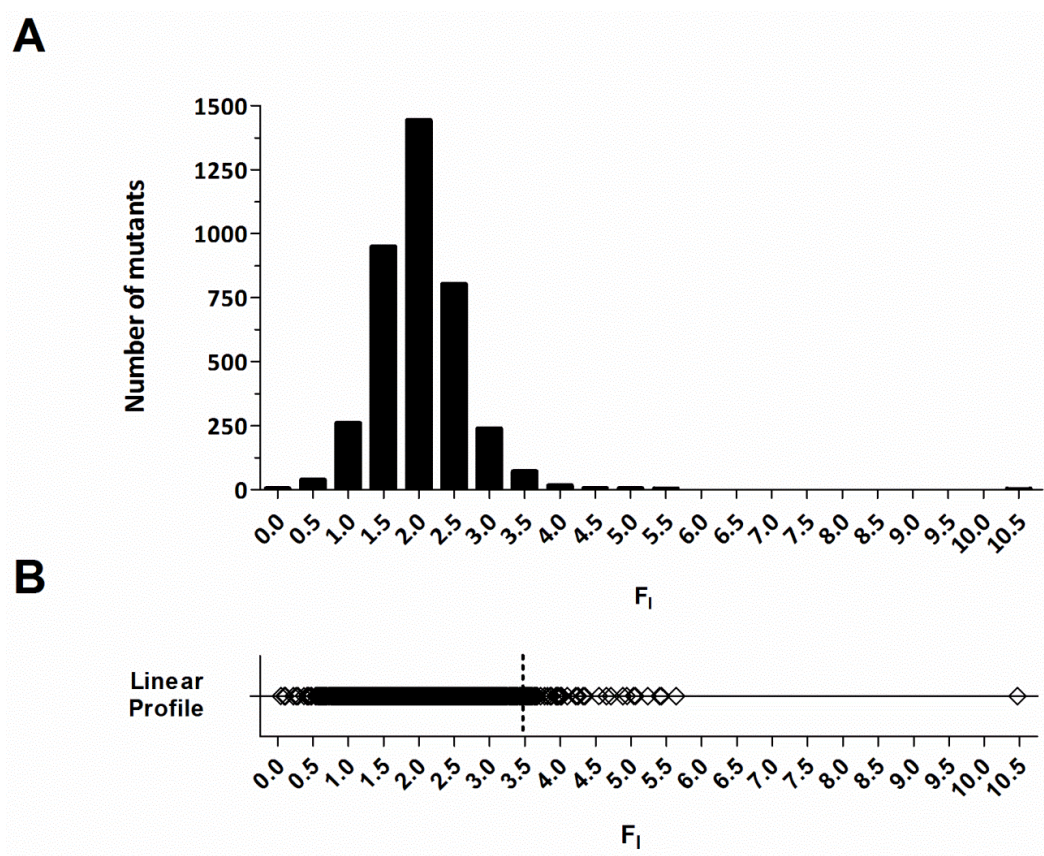
**Figure 3.8: Growth curve of rifampicin hypersensitive strains.** Growth of the rifampicin hypersensitive strains *myco2694* and *myco4005*, and the random transposon mutant control strain D11, was measured every 24 hours by OD<sub>600</sub> up to 72 hours. Values shown are log<sub>2</sub> transformed mean OD<sub>600</sub> values across three independent experiments with standard error bars.

### 3.3.6. Bedaquiline

#### 3.3.6.1. Primary assay for drug hypersensitivity

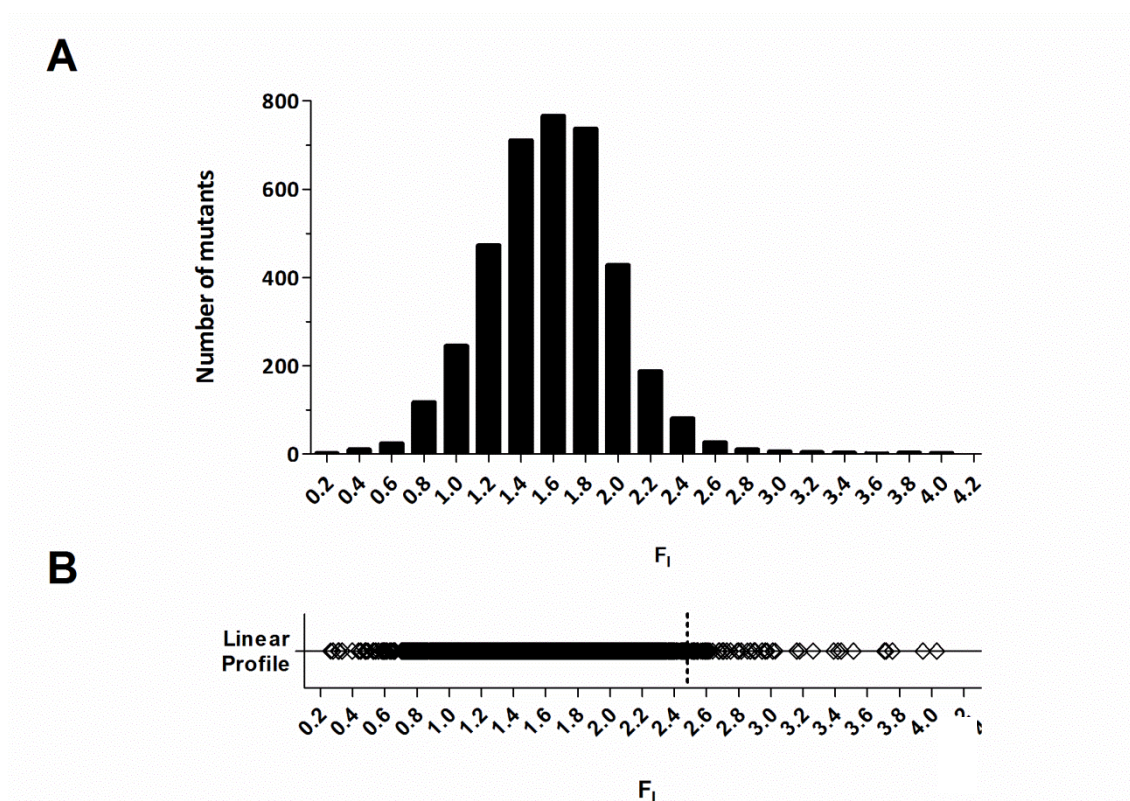
The primary assay for bedaquiline hypersensitivity was performed at a concentration of 10.8 nM (Table 3.1). As the sRFU values for the treated-MRC10 controls within each library were normally distributed one-way ANOVA were performed on untransformed data. The one-way ANOVAs did not show a significant difference in mean sRFU for the treated-MRC10 control across all plates or either library A or B ( $p > 0.05$ ), therefore analysis of the assay data continued as described in section 3.2.3.

The median inhibition of mutant library A versus bedaquiline was approximately 49% (Figure 3.9). The 60 most sensitive mutants from library A, representing mutants that were at least 1.76 times more sensitive to bedaquiline than the library median, were picked into the bedaquiline mini-hit library.



**Figure 3.9: Mutant library A versus 10.8 nM bedaquiline.** (A) Frequency distribution of  $F_I$  values, and (B)  $F_I$  linear profile, from library A versus 10 nM bedaquiline. The median  $F_I$  across mutant library A was 1.97, and the median  $F_I$  for the treated-MRC10 control was 2.37. The dotted line indicates the cut-off for the 60 most sensitive mutants, and lies at  $F_I = 3.47$ . The  $F_I$  value for each mutant represents the mean  $F_I$  across three independent experiments.

The median inhibition of mutant library B versus bedaquiline was approximately 37% (Figure 3.10). The 60 most sensitive mutants from library B, representing mutants that were at least 1.6 times more sensitive to bedaquiline than the library median, were picked into the bedaquiline mini-hit library.



**Figure 3.10: Mutant library B versus 10.8 nM bedaquiline.** (A) Frequency distribution of  $F_1$  values, and (B)  $F_1$  linear profile, from library B versus 10.8 nM bedaquiline. The median  $F_1$  across mutant library B was 1.58, and the median  $F_1$  for the treated-MRC10 control was 1.90. The dotted line indicates the cut-off for the 60 most sensitive mutants, and lies at  $F_1 = 2.53$ . The  $F_1$  value for each mutant represents the mean  $F_1$  across three independent experiments.

### 3.3.6.2. Secondary assay for drug hypersensitivity

A secondary assay was performed in order to validate the hypersensitivity to bedaquiline of the 120 most sensitive mutants (60 from each library) identified in the primary screen. Each hypersensitive mutant was tested against the screening concentration of bedaquiline (Table 3.1) and growth-inhibition was determined by endpoint  $OD_{600}$  measurement as described in section 3.2.4. The concentration of bedaquiline used in the secondary assay was the same as that used in the primary assay (10.8 nM). Table 3.6 shows the 12 most sensitive mutants from the secondary assay against the bedaquiline mini-hit library. Data for the mutant *myco2908* is included as sequencing by collaborators at the University of Otago revealed that it had a transposon insertion in *atpB*. This gene encodes the A subunit of the ATPase  $F_0$  domain, linking it to the target of bedaquiline, the C subunit of the ATPase  $F_0$  domain.

Mutant *myco2908* was the 18<sup>th</sup> most sensitive mutant identified in the secondary assay for bedaquiline. The mutants in the secondary assay against the bedaquiline mini-hit library showed a median inhibition of 39.3% compared to only 15.5% inhibition for the control MRC10. Three mutants, *myco3011*, *myco5040*, and *myco6564*, stood out, showing greater than 80% inhibition, while the remaining 10 mutants all showed over 50% inhibition.

**Table 3.6: Growth-inhibition percentage of top secondary assay hits versus bedaquiline.**

Strain	Growth-inhibition <sup>a</sup> ± se (%)
<i>myco3011</i>	83.8 ± 2.94
<i>myco5040</i>	83.5 ± 5.68
<i>myco6564</i>	82.7 ± 0.96
<i>myco2833</i>	77.2 ± 1.67
<i>myco4393</i>	73.4 ± 3.98
<i>myco1994</i>	72.5 ± 6.19
<i>myco3491</i>	70.5 ± 9.21
<i>myco2664</i>	70.5 ± 5.07
<i>myco1917</i>	69.5 ± 0.52
<i>myco2176</i>	68.4 ± 5.41
<i>myco0934</i>	61.5 ± 6.75
<i>myco6539</i>	61.1 ± 8.37
<i>myco2908</i>	54.3 ± 8.65
MRC10	15.5 ± 2.40

<sup>a</sup>Growth-inhibition values represent mean values across three independent assays with standard error (se) presented.

### 3.3.6.3. Quantification of mutant hypersensitivity

The bedaquiline MIC was determined by dose-response assay (section 2.8.3) for the 12 most sensitive mutants from the secondary assay in order to quantify mutant sensitivity. Bedaquiline MICs for the 12 strains were compared to an MIC value averaged across the 10 random transposon mutant control strains (section 3.3.3). Of the 12 mutants most sensitive to bedaquiline from the secondary assay, only nine showed some level of increased sensitivity when quantified according to their MIC (Table 3.7). Two strains showed a two-fold or greater decrease in MIC compared to the control strain, *myco1994* and *myco2908*. Interestingly, three strains, *myco934*, *myco4393*, and *myco6539* had higher MIC values than the control mutant average (Table 3.7).

**Table 3.7: Sensitivity of transposon mutants to bedaquiline.**

Strain	MIC $\pm$ se (nM)
<i>myco1994</i>	18.6 $\pm$ 3.75
<i>myco2908</i>	22.5 $\pm$ 0.00
<i>myco2833</i>	26.3 $\pm$ 9.92
<i>myco2664</i>	33.8 $\pm$ 11.3
<i>myco3011</i>	33.8 $\pm$ 11.3
<i>myco3491</i>	37.5 $\pm$ 7.50
<i>myco5040</i>	37.5 $\pm$ 7.50
<i>myco6564</i>	37.5 $\pm$ 7.50
<i>myco1917</i>	37.5 $\pm$ 7.50
<i>myco2176</i>	37.5 $\pm$ 7.50
Tn Control	45.8 $\pm$ 3.25
<i>Myco0934</i>	60.0 $\pm$ 15.0
<i>myco4393</i>	60.0 $\pm$ 15.0
<i>myco6539</i>	75.0 $\pm$ 15.0

Bedaquiline MICs for the 12 mutants most sensitive to bedaquiline identified in the secondary assay, and *myco2908*, averaged over three independent experiments. The transposon (Tn) control value represents the mean of the 10 randomly-selected mutant control strains. Standard errors (se) are presented.

### 3.4.Discussion

The aim of this chapter was to identify mutants of *M. smegmatis* mc<sup>2</sup>155 that were hypersensitive to isoniazid, rifampicin, and bedaquiline. To this end, a library of random *Tn611* transposon mutants was constructed and screened for drug hypersensitivity. Mutants that were hypersensitive were identified for all three drugs and the sensitivities quantified by MIC for the 12 mutants most sensitive in each secondary assay.

#### 3.4.1. Screening for drug hypersensitivity

The assay undertaken in this thesis to identify drug hypersensitive mutants in a *Tn611* transposon mutant collection was successful, with mutants identified that were sensitive to all of the drugs tested (isoniazid, rifampicin, and bedaquiline). The assay was run at a concentration of drug that caused minor growth-inhibition across the mutant libraries, allowing those mutants that were hypersensitive to the drug to be differentiated from the rest of the transposon mutants. The original target was to use a drug concentration that

caused 15 –30% median growth-inhibition across a library, however after performing the assays it became apparent that greater variation in the compound's screening concentration can still successfully identify hypersensitive mutants. Specifically, the lowest average inhibition was 5% in the rifampicin versus library B assay; and the highest was 49% in the bedaquiline versus library A assay. These results indicate the assay for drug hypersensitivity developed in this thesis was more sensitive than initially suspected. This conclusion is also supported by the increased number of rifampicin hypersensitive mutants identified in this assay compared to a previous one performed by Alexander et al. (2003). In the previous study only one mutant was isolated that showed increased rifampicin sensitivity, and is likely a combined effect of the different type of assay and drug concentration used. Other factors such as library coverage may have also had an impact; both the collection of mutants used in this assay, and that by Alexander et al. (2003) contained 7680 mutants, therefore there would likely be a large, but not complete overlap between the two different libraries. The assay by Alexander et al. (2003) used an endpoint metric that was the presence or absence of growth on solid media containing antibiotic compared to the assay setup used in this study, where a strain's growth does not need to be completely inhibited to be detected. This demonstrates the general higher sensitivity achieved with a qualitative endpoint growth-inhibition assay compared to a quantitative growth versus no growth metric.

The assay for drug hypersensitivity was designed for high-throughput with the reduction of resazurin used as the endpoint measure of growth-inhibition. As discussed in the introduction resazurin reduction provides a relative measure of growth-inhibition, with other factors including incubation time with the dye affecting the absolute fluorescence achieved by a culture. The library plates were designed to contain an in-plate control strain, MRC10, to enable standardisation whereby the fluorescence of untreated MRC10 was used as the maximum fluorescence standard to which all other strains on the plate were compared. The reliability of this control was confirmed when the libraries were grown in LB alone and the median standardised fluorescence of the treated-MRC10 showed no significant difference across all plates within a library. The treated-MRC10 controls were also compared for the assays against isoniazid, rifampicin, and bedaquiline, and showed no significant differences within either library for all drugs. This result indicates that the treatment conditions were the same for all plates within a library, and that it was valid to

directly compare the sensitivity of the mutants between separate plates within a library. As the libraries were screened separately the data analysis was also performed separately to avoid any library bias due to different treatment conditions between libraries A and B. It was noted that the treatment conditions were significantly different between the assays against Library A and Library B for rifampicin and bedaquiline, therefore a library bias would have existed had the data been analysed together.

As discussed in the chapter introduction, the use of resazurin, while useful in improving assay throughput, also added a risk of introducing false positives. To overcome this, a secondary assay that used endpoint OD<sub>600</sub> was used to validate the sensitivity of the 60 most sensitive mutants from each library for each drug. It was expected that this number of mutants would contain most if not all the true positives, while being small enough to screen in the lower throughput of OD<sub>600</sub> based measurement of growth. To this end, the median growth-inhibition of the mini-hit libraries for each of the three drugs was compared to the MRC10 control. It was observed that the median inhibition of the isoniazid and rifampicin mini-hit libraries by the respective drugs was approximately equal to the inhibition of MRC10. This suggests that the majority of mutants within these mini-hit libraries were not sensitive to the drugs and were false positives. Interestingly, median inhibition of the bedaquiline mini-hit library was approximately twice that of the MRC10 strain, suggesting that most of the mutants in the bedaquiline mini-hit library were true positives and hypersensitive to bedaquiline. This high true positive rate may be due to the mode of action of bedaquiline, which inhibits the ATPase enzyme, with mutations in many of the pathways that utilise ATP potentially sensitising the bacteria to bedaquiline (Andries et al., 2005; Koul et al., 2007). These results confirm the original assumption that the top 60 mutants from each library would contain most if not all of the true hits.

It was observed that the growth-inhibition values generated from the secondary assay had relatively large errors associated with them, likely due to the way in which the assay was setup. In order to sub-inoculate the 96-well plates for the secondary assay, a 96 well pinning tool was used in order to replicate the manner in which the primary assay was setup. This pinning resulted in the occasional transfer of visible clumps of cells, and this variation in starting cell number likely affected the final growth measurement. Two biological replicates were performed for each assay replicate, however increasing this to three or four biological

replicates would likely have reduced the errors; additionally, sub-inoculation of the assay plates by pipetting would have likely decreased variation in the assay. Despite these larger errors the secondary assay was successfully used to validate the sensitivity of the mutants identified in the primary assay.

### **3.4.2. Quantifying drug sensitivity**

MICs were determined for the top 10% of sensitive mutants (12 strains) from the secondary assays for each of the drugs tested, and were used as a convenient metric for quantifying drug sensitivity. For bedaquiline an additional mutant, *myco2908*, was included as it contained a transposon insertion within *atpB*, a gene associated with the known mode of action of bedaquiline, as identified by collaborators at the University of Otago. The control for this assay was an averaged MIC across 10 random mutant strains from the transposon libraries. The random mutant strains were included to account for differences in basal sensitivity between a transposon mutant and the non-transposon mutant control MRC10 as a result of the transposon insertion. These 10 mutant control strains were not identified as hypersensitive to isoniazid, rifampicin, or bedaquiline in either the primary or secondary assays. However, to eliminate the likelihood of accidentally choosing a single random transposon mutant strain that had an altered sensitivity to one of the drugs, an average across the 10 strains was used. It was found that there was no significant difference in the MIC values between the control strains for isoniazid, rifampicin, or bedaquiline.

Most of the top 10% of drug hypersensitive mutants from the secondary assay examined showed a two-fold or less decrease in MIC compared to the control average. Several mutants with a greater than two-fold difference in MIC were identified for each respective drug: three for isoniazid, two for rifampicin, and two for bedaquiline. These were fewer mutants than expected, possibly representing a limitation of using MIC to quantify the sensitivity of these mutants. Additionally, the transposon control average MIC to bedaquiline was found to be lower than that of several validated bedaquiline sensitive mutants. This would indicate that the 10 random mutant control strains may also be hypersensitive to bedaquiline, which would agree with the high true positive rate observed for the secondary



assay for bedaquiline. Therefore, these random transposon strains may not have been the most reliable control for the assay determining MIC values for bedaquiline.

### **3.4.3. Summary**

A transposon mutant collection was constructed in a 384-well format and was screened in high-throughput for mutants that were hypersensitive to isoniazid, rifampicin, and bedaquiline. For each drug, 12 validated hypersensitive mutants had their sensitivities quantified by determining their MICs for the relevant drug, with three mutants from the isoniazid assay, two from the rifampicin assay, and one mutant from the bedaquiline assay, standing out. The genotypic basis for drug hypersensitivity for these 36 validated mutants will be further examined in Chapter Four.

## **4. Genotypic validation of drug hypersensitive mutants of *M. smegmatis***

### **4.1.Introduction**

As discussed in Chapter Three, the advantage of transposon mutagenesis is that the site of the genetic mutation responsible for the drug hypersensitivity is labelled by the transposon sequence. Rapid identification of the transposon insertion site facilitates downstream genetic analysis including complementation of the transposon mutant with an intact plasmid-borne copy of the gene, or overexpression of the identified gene in a WT strain. Complementation determines whether the identified gene is responsible for the drug hypersensitivity phenotype. In mutants where loss of function of the mutated gene causes drug hypersensitivity, complementation of this gene will likely restore the drug sensitivity to levels similar to that seen in WT. Over-expression of these genes of interest in WT allows further characterisation of their role in drug sensitivity, such as whether overexpression results in sensitivity similar to WT or a dramatic increase in drug resistance. Complementation and over-expression experiments, along with information gleaned from the literature, can be combined to generate a more encompassing description of drug mode of action.

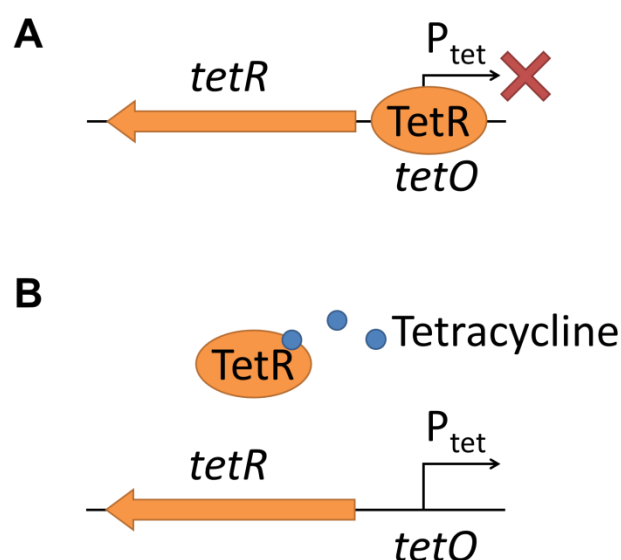
#### **4.1.1. Transposition site identification**

A major advantage of the use of transposons for random mutagenesis is that the site of insertion is labelled with a known DNA sequence (i.e. the transposon). The first step in identifying the site of mutation is to digest the mutant gDNA with a restriction enzyme to yield DNA fragments that contain the junction between the end of the transposon and the flanking gDNA sequence. Multiple techniques exist for amplifying this transposon DNA/gDNA junction; for example, inverse PCR involves ligating the hybrid transposon DNA/gDNA fragments under dilute conditions to produce circularised DNA. The flanking gDNA region can then be amplified from two primers based within the transposon DNA sequence (Billman-Jacobe et al., 2006). An alternative method is ligation-mediated PCR, where a linker is ligated to the transposon DNA/gDNA junction containing fragments and this construct is amplified using a primer from the linker and a primer from the transposon sequence

(Prod'hom et al., 1998). Sequencing of the PCR products from either inverse PCR or ligation-mediated PCR allows pinpointing of the junction between transposon and gDNA and therefore the specific transposon insertion site.

#### **4.1.2. Conditional gene expression in mycobacteria**

A number of different constitutive and conditional promoter systems have been developed to allow the extra-chromosomal or integrated expression of genes in mycobacteria (Blokpoel et al., 2005; Brown and Parish, 2006; Carroll et al., 2005, 2007; Ehrt et al., 2005; Pandey et al., 2009; Stover et al., 1991; Triccas et al., 1998). Conditional promoters come in a number of varieties including on/off type promoters and titrateable promoters, both of which can be actively induced and/or repressed by small molecules depending on the specific promoter. Tetracycline inducible promoters are routinely used in mycobacteria for conditional gene expression, and are activated when tetracycline binds to a repressor protein, allowing the RNA polymerase access to the promoter and resulting in induction of gene expression (Figure 4.1). The common limitation of the conditional expression vectors, including the tetracycline inducible vectors, is that the promoter can be leaky, with potentially high levels of basal expression in the absence of the inducer tetracycline. Newer generation vectors, such as plasmid pKW08 (Williams et al., 2010), have been constructed to limit basal expression in mycobacteria, although the vector is still leaky in *E. coli*, which is routinely used for sub-cloning. A derivative of plasmid pKW08 will be used for the conditional gene expression in *M. smegmatis* mc<sup>2</sup>155 in this thesis.



**Figure 4.1: Tetracycline inducible promoter of plasmid pKW08.** (A) The repressor protein TetR, encoded by *tetR*, binds the *tetO* operator region and prevents transcription from the promoter  $P_{tet}$ . (B) The inducer (tetracycline) binds the repressor protein (TetR) and prevents binding of TetR to *tetO*, allowing transcription from  $P_{tet}$ .

#### 4.1.3. Objectives of Chapter Four

The goal of Chapter Four was to identify the genetic basis for the drug hypersensitivity phenotype of the 12 most sensitive transposon mutants validated in each secondary assay (isoniazid, rifampicin, and bedaquiline assays for drug hypersensitivity) in Chapter Three.

To achieve this goal the following specific aims were addressed:

- Identification of the transposon insertion site in the 12 mutants most hypersensitive to isoniazid, rifampicin, and bedaquiline from Chapter Three
- Complementation of a select few transposon mutants to confirm the role of the gene containing the transposon insertion in these strains drug sensitivity
- Overexpression of genes containing or adjacent to *Tn611* insertions in drug hypersensitive mutants to further characterise their role in drug sensitivity

The site of *Tn611* insertion in the isoniazid, rifampicin, and bedaquiline hypersensitive mutants of *M. smegmatis* mc<sup>2</sup>155 was determined using either inverse PCR or ligation-mediated PCR. Genes identified as containing, or adjacent to *Tn611* insertions were

expressed from the tetracycline inducible promoter of pRC20, a derivative of plasmid pKW08, in *Tn611* mutants for complementation assays, or in WT *M. smegmatis* mc<sup>2</sup>155 for overexpression assays.

## **4.2. Methods**

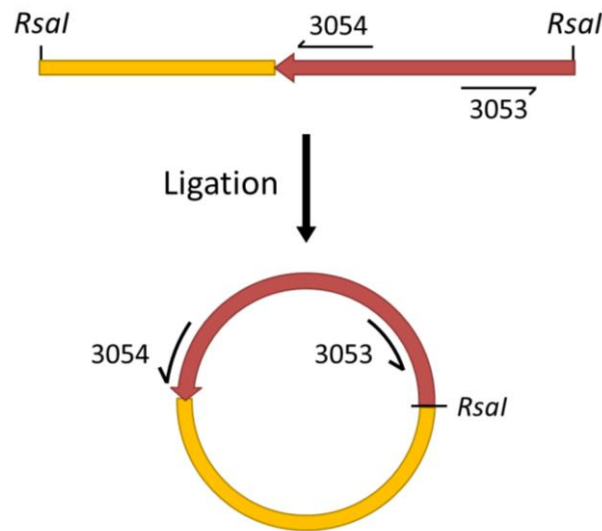
### **4.2.1. Transposon insertion site identification**

Two different methods were used to identify the insertion site of the *Tn611* in the mutant strains of *M. smegmatis* mc<sup>2</sup>155: inverse PCR or ligation-mediated PCR. Inverse PCR was performed initially, however was not successful for generating sequences for all of the mutants tested. In such cases, ligation-mediated PCR was subsequently performed to enable identification of the transposon insertion site.

#### **4.2.1.1. Inverse PCR**

Substrates for inverse PCR were generated as described in section 2.6.4, and inverse PCR performed as described in section 2.6.3.2. The products from inverse PCR were electrophoresed on a 1% agarose gel (section 2.6.1.4). Inverse PCR produced two products: one of constant size (approximately 1 Kb) that corresponded to an internal transposon PCR product; and a variable sized band that correlated to the product containing the gDNA/junction. Gel extraction was performed to isolate the variably sized band of interest as described in section 2.6.1.5. The gDNA flanking the *Tn611* insertion was subsequently sequenced using primer 3054 ( Table 2.4.

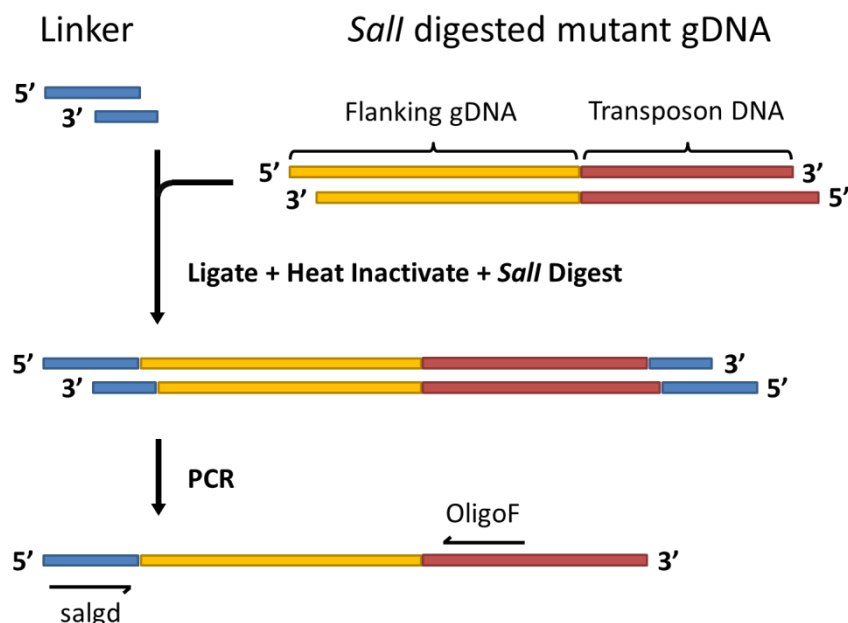
Table 2.4). If a PCR product could not be generated by inverse PCR from the *RsaI* generated fragments, or the PCR product did not provide a useful sequence, the inverse PCR process was repeated using another restriction enzyme, *EagI*. The protocol for *EagI* based inverse PCR was identical to *RsaI* based inverse PCR except that the DNA fragments were generated by *EagI* digestion instead (section 2.6.4.)



**Figure 4.2: Inverse PCR.** *RsaI* digested gDNA from a *Tn611* insertional mutant is circularised by ligating under dilute conditions. The outward facing transposon primers 3053 and 3054 are then able to amplify the gDNA/transposon DNA junction. Red bars represent *Tn611* DNA, while yellow bars represent *M. smegmatis* mc<sup>2</sup>155 gDNA.

#### 4.2.1.2. Ligation-mediated PCR

In cases where inverse PCR with either *RsaI* or *EagI* digestion failed to produce a PCR product or produced a PCR product that failed to give a useful sequence, ligation-mediated PCR was used instead. ligation-mediated PCR was performed as described previously by Prod'hom et al., (1998) and as depicted in Figure 4.3. The substrate for ligation-mediated PCR was generated as described in section 2.6.5, and ligation-mediated PCR performed as described in section 2.6.3.2. PCR products were electrophoresed on 1% agarose gels (section 2.6.1.4) and successful PCR reactions were cleaned and concentrated (section 2.6.1.6) and sequenced with salgd and OligoF (Table 2.4).



**Figure 4.3: Ligation-mediated PCR.** The linker (blue), composed of the non-phosphorylated oligos salgd and salpt, is ligated to *SalI* digested transposon mutant DNA fragments. While the longer salgd oligo strand can ligate to the DNA fragment due to the fragments 5' phosphate group, the shorter salpt strand lacks its own phosphate so cannot ligate and subsequent heating during PCR results in the salpt oligo being displaced. The second digestion with *SalI* ensures no unwanted products are amplified during PCR due to improper initial *SalI* digestion. The fragment containing the gDNA flanking the transposon mutant is selectively amplified by PCR using the linker primer salgd, and OligoF.

#### 4.2.1.3. Sequence processing

The PCR products generated by inverse PCR or ligation-mediated PCR as described previously, were sequenced as described in section 2.6.2. Sequences of the PCR products generated from inverse PCR or ligation-mediated PCR were analysed identically using the bioinformatics software Geneious 5.6.6 ([www.geneious.com](http://www.geneious.com)) as follows. The returned DNA sequence was aligned with the DNA sequence from the end of the *Tn611* transposon using the Geneious "pairwise align" function with default settings to identify the junction between the transposon and gDNA. The sequence of the gDNA from the transposon DNA/gDNA junction until the first relevant restriction site (*RsaI* or *EagI* or *SalI*), or until the end of the

sequence (whichever was shorter), was used as the input for a nucleotide Basic Local Alignment Search Tool (BLAST) analysis at the ncbi BLAST website (<http://blast.ncbi.nlm.nih.gov>). The nucleotide BLAST was performed against the non-redundant nucleotide database using default settings to identify the genomic region matching the gDNA sequence generated from inverse PCR/ligation-mediated PCR. Once identified, the corresponding genomic region was used as a reference sequence against which the PCR generated gDNA sequence was aligned in Geneious using the “align to reference” tool with default settings. From this reference alignment the exact location of the *Tn611* insertion in the *M. smegmatis* mc<sup>2</sup>155 genome was determined. The identity, function, and known *M. tuberculosis* homologues of genes containing transposon insertions, or genes adjacent to intergenic transposon insertions, was determined using databases including tuberculist (Lew et al., 2011), smegmalist (Kapopoulou et al., 2011), and the TBDB (Galagan et al., 2010). If no *M. tuberculosis* homologue was given for a *M. smegmatis* gene on any of these databases then none was reported in the tables of results for each drug later in this chapter.

#### **4.2.2. Optimisation of tetracycline concentration for induction of gene expression from plasmid pRC20**

The plasmid pRC20 was used for both the complementation and overexpression assays, and the optimal tetracycline inducer concentration was determined for each of these assays separately. Dose-response assays measuring endpoint GFP fluorescence and growth-inhibition with varying concentrations of tetracycline were performed to optimise the tetracycline concentrations (section 2.8.3). For the complementation assays, the complementation strains and empty vector controls were grown in 0, 2.5, 5, 10, 20, or 40 ng·mL<sup>-1</sup> tetracycline, under the same conditions as the complementation assays (specifically 41 °C and 20 µg·mL<sup>-1</sup> kanamycin and hygromycin B). For the overexpression assays, the empty vector control strain MRC20 was grown in 0, 5, 10, 20, 40, or 80 ng·mL<sup>-1</sup> tetracycline, under the same conditions as the overexpression assays (37 °C and 50 µg·mL<sup>-1</sup> hygromycin B). The optimal tetracycline concentration for each assay was determined as the



concentration that provided maximal GFP fluorescence, and therefore gene expression from the tetracycline inducible promoter of pRC20, while causing minimal growth-inhibition.

#### **4.2.3. Complementation of transposon mutants**

Complementation was performed using the vector pRC20 expressing the WT copy of the gene containing or adjacent to the *Tn611* insertion in the relevant mutant strain. The WT copies of the genes were amplified by PCR from *M. smegmatis* mc<sup>2</sup>155 (section 2.6.3.2) before being cloned into the *Bam*HI site in plasmid pRC20 as described in section 2.6.9.1. Sequencing was performed to check the orientation and fidelity of the insert as described in section 2.6.2. Constructs that were in the correct orientation and did not contain errors were transformed into the relevant transposon mutant strain (section 2.6.7.2). One gene used for complementation, *MSMEI\_1905*, contained a *Bam*HI site within its ORF which was removed by PCR using a long (60-mer) primer to remove the restriction site by creating a silent mutation (Table 2.5). The removal of the restriction site was confirmed by sequencing as described in section 2.6.2.

Empty vector control strains were generated for each transposon mutant strain by transforming the transposon mutant strains with pRC20 (section 2.6.9). Complementation assays were performed as dose-response assays as described in section 2.8.3. The MIC of the relevant drug was determined for the complementation strains and empty vector controls, both with and without vector induction by tetracycline.

#### **4.2.4. Overexpression of *M. smegmatis* genes**

The vectors expressing the genes of interest generated for the complementation assays were also transformed into WT *M. smegmatis* mc<sup>2</sup>155 to generate the corresponding overexpression strains. Overexpression assays were performed as dose-response assays as described in section 2.8.3. The MIC of the relevant drug was determined for the overexpression strains, both with and without vector induction by tetracycline. Control strains for the overexpression assay included an empty vector negative control strain (MRC20), and an additional negative control strain that expressed a random gene from

*M. smegmatis* mc<sup>2</sup>155. This negative control strain overexpressed *MSMEI\_4267*, the gene in which the random transposon control strain D11 contained a *Tn611* insertion. *MSMEI\_4267* encodes a putative iron-sulfur oxidoreductase. For the overexpression assays against isoniazid an additional positive control expressing the gene encoding the known target of isoniazid, *inhA* (*MSMEI\_3070*), was included.

## **4.3.Results**

### **4.3.1. Isoniazid**

#### **4.3.1.1. Transposon insertion site identification**

The transposon insertion sites were able to be identified for the 12 mutants most sensitive to isoniazid identified in Chapter Three, using either inverse PCR or ligation-mediated PCR as described in section 4.2.1. (Table 4.1).

**Table 4.1: Transposon insertion sites in isoniazid hypersensitive mutants.**

Mutant Strain	<i>Tn611</i> insertion location (ORF)	Putative Identification	Common Name	Nearest H <sub>37</sub> Rv homologue	Gene Length (bp)	POI
<i>myco0409</i>	<i>MSMEI_3684</i>	acetylornithine aminotransferase	<i>argD</i>	<i>Rv1655</i>	1173	152
<i>myco1897</i>	<i>MSMEI_5538</i>	Multiple antibiotic resistance regulator	<i>marR</i>	<i>Rv0880</i>	432	385
<i>myco2100</i>	55 bp downstream of <i>MSMEI_1210</i>	<i>MSMEI_1210</i> – PAPS reductase	-	-	909	-
	96 bp upstream of <i>MSMEI_1211</i>	<i>MSMEI_1211</i> - conserved hypothetical protein	-	-	1437	-
<i>myco2576</i>	<i>MSMEI_1904</i>	NADH pyrophosphatase	<i>nudC</i>	<i>Rv3199c</i>	936	710
<i>myco2659</i>	<i>MSMEI_0062</i>	ftsk/spoiii family protein	<i>eccCa<sub>1</sub></i>	<i>Rv3870</i>	2229	2072
<i>myco3113</i>	47 bp upstream <i>MSMEI_4423</i>	<i>MSMEI_4423</i> - conserved hypothetical protein	-	-	1278	-
	338 bp upstream of <i>MSMEI_4424</i>	<i>MSMEI_4424</i> – Major Membrane Protein 1	-	-	924	-
<i>myco5016</i>	<i>MSMEI_1905</i>	Glutaredoxin-like protein	-	<i>Rv3198A</i>	249	59
<i>myco6166</i>	<i>MSMEI_5554</i>	Conserved hypothetical protein	-	<i>Rv0862c</i>	2256	666
<i>myco6192</i>	<i>MSMEI_5244</i>	K <sup>+</sup> transporting ATPase, A subunit	<i>kdpA</i>	<i>Rv1029</i>	1671	391
<i>myco6482</i>	<i>MSMEI_5460</i>	putative transcriptional regulator	-	-	951	332
<i>myco7102</i>	103 bp upstream of <i>MSMEI_4764</i>	<i>MSMEI_4764</i> - integral membrane transporter	-	-	1323	-
	36bp downstream of <i>MSMEI_4765</i>	<i>MSMEI_4765</i> – Alkylhydroperoxidase	<i>ahpD</i>	<i>Rv2429</i>	534	-
<i>myco7437</i>	<i>MSMEI_6092</i>	Fur Family Transcriptional Regulator	-	-	465	204

Isoniazid hypersensitive mutants are organised by their location in the mutant collection in ascending order. Transposon point of insertion (POI) is counted from the start of the gene.

The *myco7437* mutant strain contained a transposon insertion in a putative ferric uptake regulator (Fur) type transcriptional regulator (*MSMEI\_6092*). KatG, the enzyme responsible for the activation of isoniazid, is regulated by the Fur type regulator FurA. Due to the relationship between a Fur type regulator and the mode of action of isoniazid, the similarity between *MSMEI\_6092* and other Fur type regulators (FurA and FurB type) from *M. smegmatis* and *M. tuberculosis* was investigated. A protein alignment (Geneious “pairwise alignment”, default settings) was performed with the two known *M. smegmatis* mc<sup>2</sup>155 homologs of FurA, FurA1<sub>SMEG</sub> (*MSMEI\_6215*) and FurA2<sub>SMEG</sub> (*MSMEI\_3379*), as well as FurB (*MSMEI\_4376*), along with FurA and FurB from *M. tuberculosis* H<sub>37</sub>Rv (*Rv1909c* and *Rv2359* respectively). The protein alignment showed that *MSMEI\_6092* is much more similar to the FurA proteins than FurB (Table 4.2). However, the two *M. smegmatis* FurA proteins are much more similar to each other and *Rv1909c* than to *MSMEI\_6092*.

**Table 4.2: Protein similarity matrix of Fur proteins from *M. smegmatis* mc<sup>2</sup>155 and *M. tuberculosis* H<sub>37</sub>Rv.**

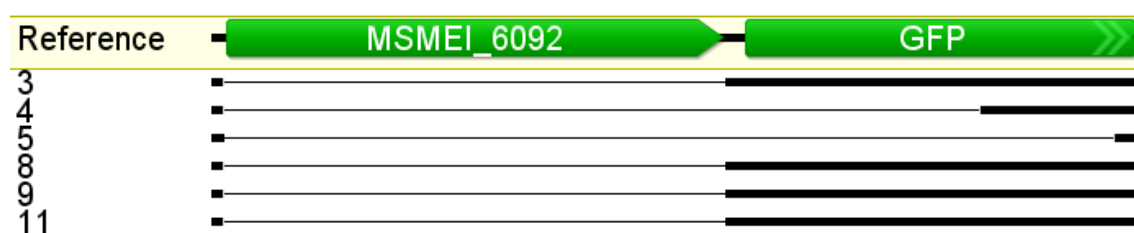
Protein	FurA <sub>TB</sub>	FurA1 <sub>SMEG</sub>	FurA2 <sub>SMEG</sub>	MSMEI_6092	FurB <sub>SMEG</sub>	FurB <sub>TB</sub>
FurA <sub>TB</sub>	-	68	69.1	56.4	24.3	24.6
FurA1 <sub>SMEG</sub>	68	-	65.1	56.6	22.1	24.6
FurA2 <sub>SMEG</sub>	69.1	65.1	-	53.4	22.1	21.6
MSMEI_6092	56.4	56.6	53.4	-	25.7	26.9
FurB <sub>SMEG</sub>	24.3	22.1	22.1	25.7	-	76.7
FurB <sub>TB</sub>	24.6	24.6	21.6	26.9	76.7	-

Percentage similarity of amino acid sequences for *M. smegmatis* mc<sup>2</sup>155 and *M. tuberculosis* H<sub>37</sub>Rv FurA and FurB proteins and the Fur-like protein encoded by *MSMEI\_6092*.

#### 4.3.1.2. Complementation of isoniazid hypersensitive mutants

The three mutants most hypersensitive to isoniazid identified in Chapter Three, *myco2576*, *myco5016*, and *myco7437*, were selected for complementation using the genes that were identified in 4.3.1.1 as containing the *Tn611* insertion in these strains. These strains were selected for complementation as they were greater than two-fold more sensitive to isoniazid than the control whereas the remaining nine hypersensitive strains were between 1.1- and 1.7-fold more sensitive (section 3.3.4.3). It was expected that the greater sensitivity of the selected strains would make it easier to determine whether or not complementation was

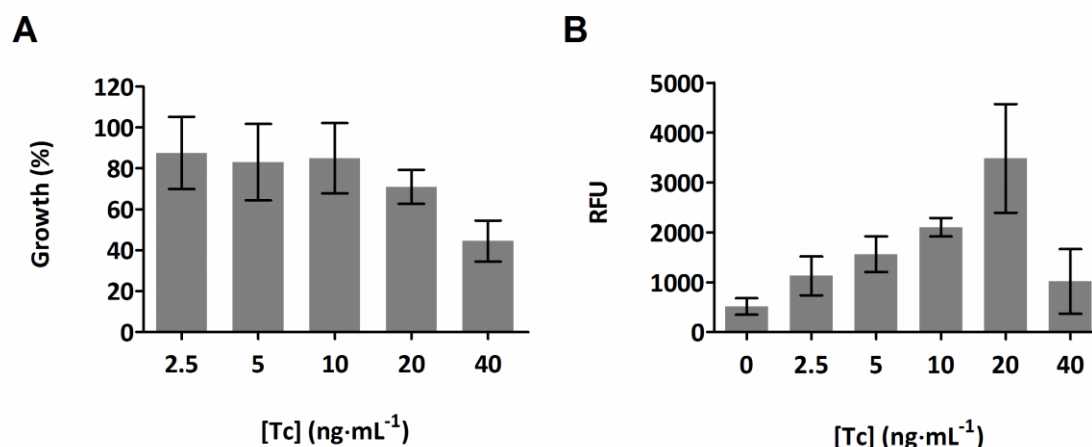
successful. The mutant strains *myco2576*, *myco5016*, and *myco7437* are henceforth referred to by the ORF containing the *Tn611* insertion: *Tn::nudC*, *Tn::MSMEI\_1905*, and *Tn::MSMEI\_6092* respectively. A complementation construct containing *MSMEI\_6092* was unable to be produced. Sequencing results showed that expression plasmids with *MSMEI\_6092* in the forward direction could be recovered, with a number of constructs containing no insert, or deletions of part of the downstream GFP gene (Figure 4.4).



**Figure 4.4: Alignments of pRC20 *MSMEI\_6092* constructs.** Sequencing results from the pRC20 constructs containing *MSMEI\_6092*, aligned with a reference sequence. Construct sequences from six recovered clones are shown, with clone number shown on the left hand side. Solid black bars represent sequence that matches the reference, while the thin black lines represent gaps in the sequence. Constructs 3, 8, 9, and 11 appear to have no insert, while constructs 4 and 5 contain deletions of part of the GFP gene. All other constructs recovered had *MSMEI\_6092* in the reverse orientation with no deletions.

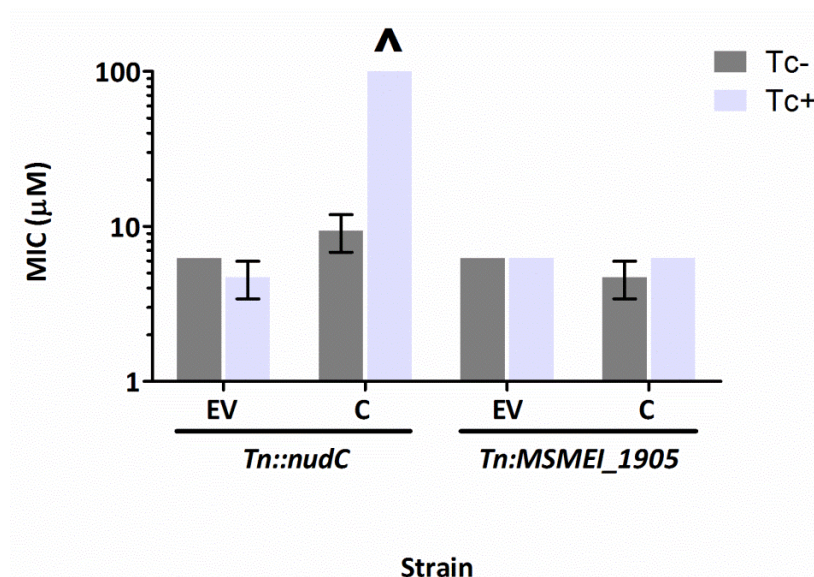
The complementation strains for *Tn::nudC* and *Tn::MSMEI\_1905* were created by transforming each mutant strain with the pRC20 vector containing either the *nudC* or *MSMEI\_1905* construct respectively. Each mutant strain was also transformed with pRC20 that did not contain a construct (i.e. empty vector controls). The inducer concentration was optimised for the complementation studies, with GFP fluorescence used as a relative measure of vector induction, as described in section 4.2.2. As there was no difference between the response of any of the mutant strains or the empty vector strains, these results were analysed together. A tetracycline concentration of 20 ng·mL<sup>-1</sup> was found to provide the highest fluorescence, however this concentration showed a substantial increase in growth-inhibition compared to the lower tetracycline concentrations (Figure 4.5). A tetracycline concentration of 10 ng·mL<sup>-1</sup> provided an approximate four-fold increase in

fluorescence, with minimal growth-inhibition, when averaging the response of the four strains, and was therefore selected as the inducer concentration to be used for the complementation assays.



**Figure 4.5: Optimisation of inducer concentration for complementation assays.** (A) Average endpoint growth relative to the untreated control, and (B) average endpoint RFU of *Tn::nudC* and *Tn::MSMEI\_1905* empty vector control and complemented strains grown in different tetracycline (Tc) concentrations. Column heights represent mean values from three independent experiments with standard error bars shown.

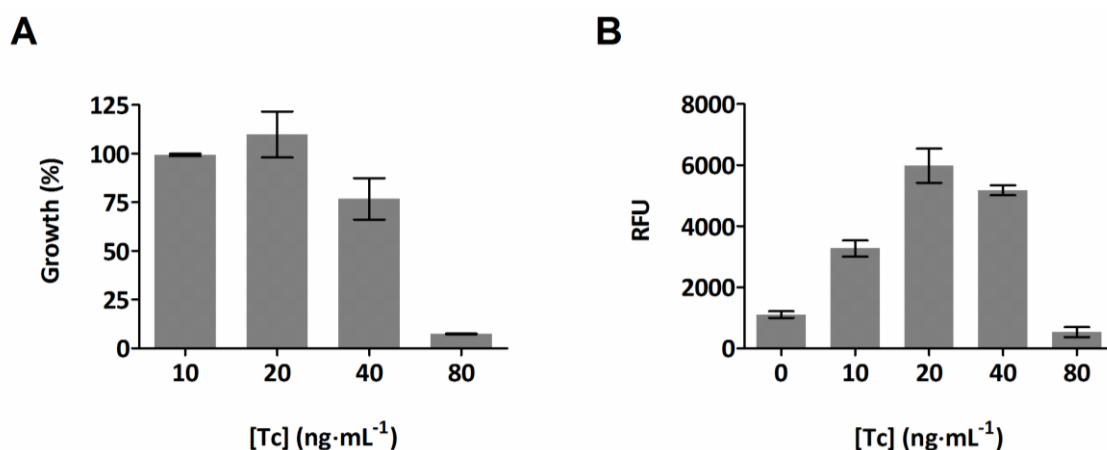
The MIC of isoniazid for the relevant complementation strains and the empty vector controls was determined by a dose-response assay (Figure 4.6). There was no change in the MIC of isoniazid for either of the empty vector controls upon induction with tetracycline. The complemented *Tn::nudC* strain showed an increased resistance to isoniazid upon induction, with a greater than 10-fold increase in the MIC, while there was no change in the MIC of isoniazid for the complemented *Tn::MSMEI\_1905* strain upon vector induction.



**Figure 4.6: Complementation of isoniazid hypersensitive transposon mutants.** The MIC of isoniazid for the *Tn::nudC* and *Tn::MSMEI\_1905* empty vector controls (EV) and complemented strains (C) was determined with and without vector induction with 10 ng·mL<sup>-1</sup> tetracycline (Tc). Column heights represent mean MIC over three independent experiments, with standard error bars shown. For those columns that have no error bars the standard error was zero. The highest tested concentration of isoniazid was 100 μM and MICs greater than the highest tested concentration are indicated by a caret (^).

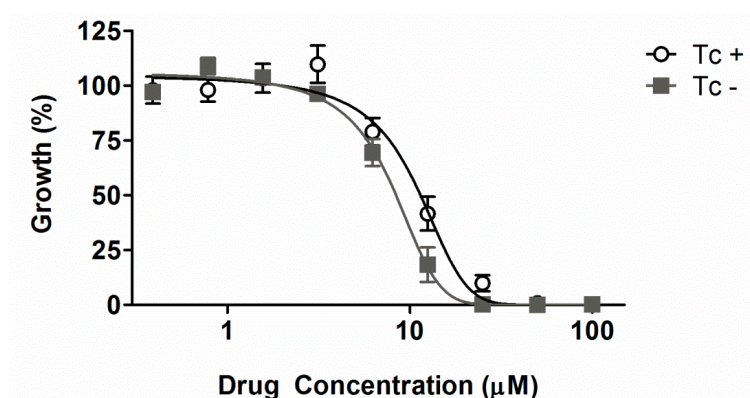
#### 4.3.1.3. Overexpression of genes related to isoniazid hypersensitivity

The inducer concentration for the overexpression assay was optimised by growing the empty vector control strain (MRC20) in different concentrations of the inducer tetracycline. It was found that a tetracycline concentration of 20 ng·mL<sup>-1</sup> gave the highest increase in fluorescence (six-fold) with minimum growth-inhibition. Therefore, 20 ng·mL<sup>-1</sup> was selected as the tetracycline concentration for the overexpression assays (Figure 4.7).



**Figure 4.7: Optimal inducer concentration for MRC20.** (A) Average endpoint growth relative to the untreated control, and (B) average endpoint RFU of the empty vector control strain MRC20 grown in different tetracycline (Tc) concentrations. Column heights represent mean values from three independent experiments with standard error bars shown.

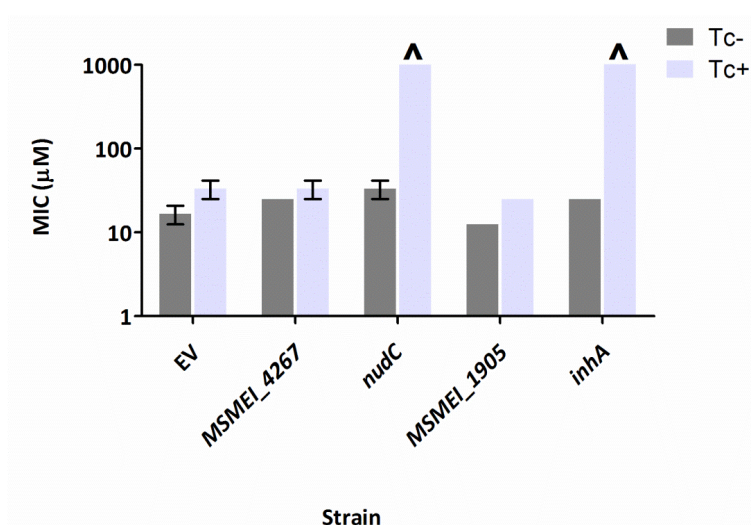
The roles of the genes *nudC* and *MSMEI\_1905* in isoniazid sensitivity were further examined by overexpressing each gene in WT *M. smegmatis* mc<sup>2</sup>155. Background sensitivity of WT *M. smegmatis* mc<sup>2</sup>155 to isoniazid upon vector induction was determined by way of a dose-response assay against the empty vector control strain MRC20. A two-fold increase in the MIC of isoniazid was observed upon vector induction with 20 ng·mL<sup>-1</sup> tetracycline (Figure 4.8). Therefore for the genes of interest, only changes in the MIC of isoniazid that were greater than two-fold after induction were considered to be biologically significant.



**Figure 4.8: Dose response curve of MRC20 versus isoniazid ± inducer.** Data points represent the mean growth of the MRC20 strain with or without 20 ng·mL<sup>-1</sup> of the inducer tetracycline (Tc) over three independent experiments with standard error bars shown.



The MICs of isoniazid for the *nudC* and *MSMEI\_1905* overexpression strains were determined by dose-response assay, along with the following control strains: an empty vector control, an *inhA* overexpression control, and an *MSMEI\_4267* random gene overexpression control (Figure 4.9). Overexpression of *nudC* and *inhA* resulted in a greater than 100-fold increase in the MIC of isoniazid, from approximately 10  $\mu$ M in the un-induced overexpression strain, to greater than the highest tested concentration of 1 mM in the induced overexpression strain. The *MSMEI\_1905* overexpression strain did not show any change in the MIC of isoniazid following induction, nor did the random gene expression control strain (*MSMEI\_4267*).



**Figure 4.9: Overexpression strains versus isoniazid.** MICs of isoniazid for gene overexpression strains including empty vector (EV) control MRC20, with and without induction with 20 ng.mL<sup>-1</sup> tetracycline (Tc). Column heights represent mean MICs over three independent experiments with standard error bars shown. For those columns that have no error bars the standard error was zero. The highest tested concentration of isoniazid was 1 mM, with MIC values greater than the highest tested concentration indicated with a caret (^).

## 4.3.2. Rifampicin

### 4.3.2.1. Transposon insertion site identification

The transposon insertion sites were able to be identified for 11 of the 12 mutants most hypersensitive to rifampicin identified in Chapter Three, using either inverse PCR or ligation-mediated PCR as described in section 4.2.1. (Table 4.3).

**Table 4.3: Transposon insertion sites in rifampicin hypersensitive mutants.**

Mutant Strain	<i>Tn611</i> insertion location (ORF)	Putative Identification	Common Name	Nearest H <sub>37</sub> Rv homologue	Gene Length (bp)	POI
<i>myco0163</i>	<i>MSMEI_6730</i>	proline-rich 28 kDa antigen	<i>mtc28</i>	<i>Rv0040c</i>	945	399
<i>myco0891</i>	Undefined	Transposase	<i>ISMsm2</i>	-	987 - 1086	97
<i>myco1030</i>	<i>MSMEI_6040</i>	penicillin binding protein	<i>ponA2</i>	<i>Rv3682</i>	2454	260
<i>myco2642</i>	19 bp downstream of <i>MSMEI_6263</i>	<i>MSMEI_6263</i> - ESX-1 transcriptional regulator	<i>espR</i>	<i>Rv3849</i>	405	-
	>1000 bp upstream of <i>MSMEI_6264</i>	<i>MSMEI_6264</i> - Conserved hypothetical protein		-	492	-
<i>myco2694</i>	<i>MSMEI_1186</i>	rifampicin ADP-ribosyl transferase	<i>arr</i>	-	429	224
<i>myco4005</i>	<i>MSMEI_3093</i>	ribosomal large subunit pseudouridine synthase D		<i>Rv1540</i>	930	528
<i>myco5826</i>	98 bp downstream of <i>MSMEI_1800</i>	<i>MSMEI_1800</i> - TetR like transcriptional regulator	-	<i>Rv3249C</i>	714	-
	52 bp upstream of <i>MSMEI_1801</i>	<i>MSMEI_1801</i> - Adenosylhomocysteinase	<i>ahcY</i>	<i>Rv3248C</i>	1458	-
<i>myco5883</i>	Undefined	Transposase	<i>ISMsm4</i>	-	1323	348
<i>myco6762</i>	<i>MSMEI_0227</i>	metallopeptidase	<i>zmp1</i>	<i>Rv0198c</i>	2001	774
<i>myco6859</i>	<i>MSMEI_6301</i>	O-methyltransferase	<i>omt</i>	<i>Rv1153c</i>	819	722
<i>myco7011</i>	<i>MSMEI_5621</i>	Cell envelope-related transcriptional attenuator	-	<i>Rv0822c</i>	2379	502

Rifampicin hypersensitive mutants are organised by their location in the mutant collection in ascending order. Transposon point of insertion (POI) is counted from the start of the gene. For the undefined mutant *myco0891* the range of gene lengths of the four possible insertion sites is given.

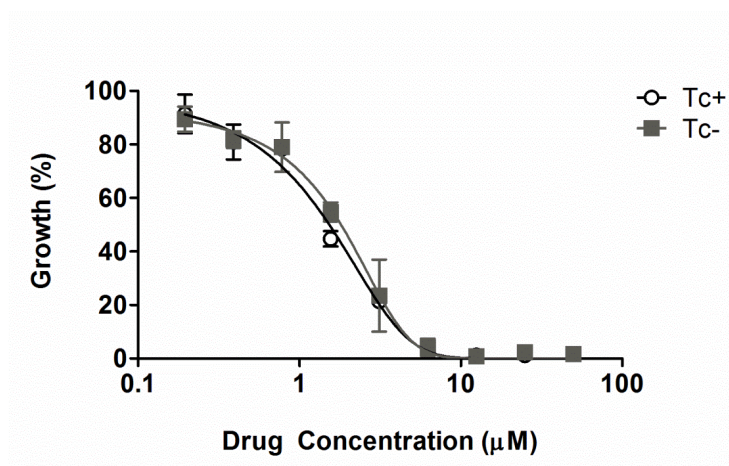
Two mutants, *myco0891* and *myco5883*, contained *Tn611* insertions in two different insertion elements, each of which is present in multiple copies within the genome of *M. smegmatis* mc<sup>2</sup>155. *Myco0891* contains a transposon insertion in an ISMsm2 transposase gene that occurs four times in the *M. smegmatis* mc<sup>2</sup>155 genome at *MSMEI\_0054*, *MSMEI\_3431*, *MSMEI\_4411*, and *MSMEI\_5518*. *Myco5883* contains a transposon insertion within an ISMsm4 transposase that occurs four times in the *M. smegmatis* mc<sup>2</sup>155 genome at *MSMEI\_0419*, *MSMEI\_1205*, *MSMEI\_2757*, and *MSMEI\_5245*. The entire sequences generated for both of these mutants were within the ORFs of the transposase genes, therefore the specific copies of ISMsm2 or ISMsm4 that contained the insertions could not be determined by inverse PCR or ligation-mediated PCR.

#### **4.3.2.2. Complementation of rifampicin hypersensitive mutants**

The mutant strains selected for complementation, *myco2694* and *myco4005*, were eight-fold and four-fold more sensitive to rifampicin respectively (Chapter Three) compared with a less than two-fold increase in sensitivity for the other mutant strains. It was expected that the greater sensitivity of these strains would make it easier to determine whether or not complementation was successful. The mutant strains *myco2694* and *myco4005* are henceforth referred to by the ORF containing the *Tn611* insertion: *Tn::arr* and *Tn::MSMEI\_3093* respectively. Although vectors for the complementation of each strain were constructed, an empty vector control strain was not constructed for *Tn::MSMEI\_3093*. No colonies grew when *Tn::MSMEI\_3093* was transformed with the empty vector pRC20, despite four experimental repeats. As there was no suitable control, complementation of *Tn::MSMEI\_3093* was not performed. Due to the already well characterised activity of Arr in *M. smegmatis*, the complementation of the *Tn::arr* mutant was to serve as a positive control for the complementation of rifampicin hypersensitive mutants. As such, complementation of *Tn::arr* was not pursued once it was decided to not pursue complementation of *Tn::MSMEI\_3093*.

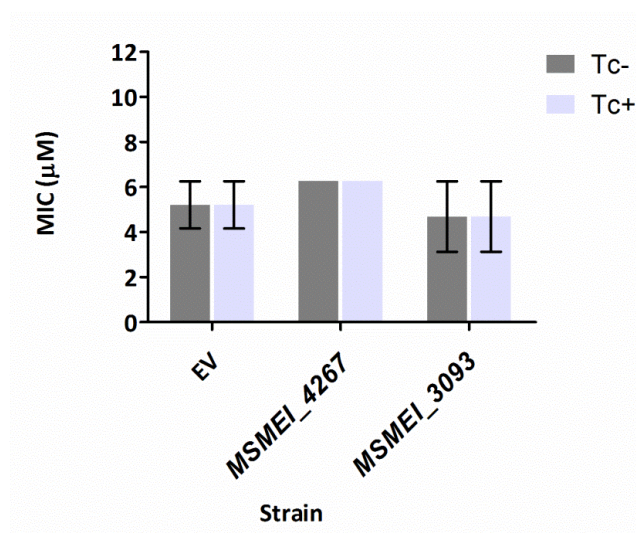
#### 4.3.2.3. Overexpression of genes related to rifampicin hypersensitivity

Background sensitivity of WT *M. smegmatis* to rifampicin upon vector induction was determined by way of a dose-response assay against the empty vector control strain MRC20. No change in the MIC of rifampicin for MRC20 was observed upon induction with 20ng·mL<sup>-1</sup> tetracycline (Figure 4.10).



**Figure 4.10: Dose response curve of MRC20 versus rifampicin ± inducer.** Data points represent the mean growth of the MRC20 strain with or without 20 ng·mL<sup>-1</sup> of the inducer tetracycline (Tc) over three independent experiments with standard error bars shown.

The role of *MSMEI\_3093* in rifampicin sensitivity was examined by overexpressing *MSMEI\_3093* in WT *M. smegmatis* mc<sup>2</sup>155. The MIC of rifampicin for the empty vector control strain MRC20, the *MSMEI\_3093* overexpression strain, and the *MSMEI\_4267* random gene overexpression control strain were determined by a dose-response assay with and without induction with 20ng·mL<sup>-1</sup> tetracycline (Figure 4.11). The MIC of rifampicin did not change for any of the three strains upon vector induction, with all strains showing an approximately equal MIC.



**Figure 4.11: Overexpression strains versus rifampicin.** MICs of rifampicin for gene overexpression strains including empty vector (EV) control MRC20, with and without induction with 20 ng·mL<sup>-1</sup> tetracycline (Tc). Column heights represent mean MICs over three independent experiments with standard error bars shown. For those columns that have no error bars the standard error was zero.

### 4.3.3. Bedaquiline

#### 4.3.3.1. Transposon insertion site identification

The transposon insertion sites were able to be identified for eight of the 12 mutants most hypersensitive to bedaquiline identified in Chapter Three, using either inverse PCR or ligation-mediated PCR. Table 4.4 summarises the sequencing results. As mentioned in Chapter Three, the decision to pursue bedaquiline was made late into the thesis and due to time constraints the study of bedaquiline hypersensitive mutants did not progress to complementation or overexpression assays.

**Table 4.4: Transposon insertion site for bedaquiline hypersensitive mutants.**

<b>Mutant Strain</b>	<b><i>Tn611</i> insertion location (ORF)</b>	<b>Putative Identification</b>	<b>Common Name</b>	<b>Nearest H<sub>37</sub>Rv homologue</b>	<b>Gene Length (bp)</b>	<b>POI</b>
<i>myco0934</i>	<i>MSMEI_3416</i>	MmpL family protein	<i>MmpL5</i>	<i>Rv0676c</i>	2910	1961
<i>myco1994</i>	<i>MSMEI_3189</i>	Glutamyl aminopeptidase	-	-	1002	931
<i>myco2176</i>	<i>MSMEI_3358</i>	Esterase	-	<i>Rv1288</i>	1353	827
<i>myco2833</i>	77 bp upstream of <i>MSMEI_2671</i>	Biotin sulfoxide reductase	<i>bisC</i>	<i>Rv1442</i>	2292	-
	181 bp upstream of <i>MSMEI_2672</i>	Conserved hypothetical protein	-	<i>Rv2721c</i>	2436	-
<i>myco2908</i>	<i>MSMEI_4815</i>	ATP synthase F <sub>0</sub> domain, A subunit	<i>atpB</i>	<i>Rv1304</i>	777	563
<i>myco3011</i>	<i>MSMEI_4123</i>	Conserved hypothetical protein	<i>yfiH</i>	<i>Rv2149c</i>	714	462
<i>myco4393</i>	<i>MSMEI_5136</i>	Transmembrane protein	-	<i>Rv1072</i>	837	770
<i>myco5040</i>	<i>MSMEI_5828</i>	PPE family protein	-	-	1107	423

Bedaquiline hypersensitive mutants are organised by their location in the mutant collection in ascending order. Transposon point of insertion (POI) is counted from the start of the gene.

## 4.4. Discussion

### 4.4.1. Identification of transposon insertion sites

Two different techniques, inverse PCR and ligation-mediated PCR, were used in the identification of the *Tn611* insertion sites in the drug hypersensitive mutants. Both inverse PCR and ligation-mediated PCR rely upon endonuclease digestion of the transposon mutant DNA to generate fragments that contain both the end of the transposon, and the adjacent gDNA into which it has inserted. Inverse PCR was initially used for identifying the *Tn611* insertion site using *RsaI* digestion as described by Billman-Jacobe et al. (2006). In this study inverse PCR was unable to generate the product containing the *Tn611* end and the flanking gDNA for some of the mutant strains, amplifying only the internal transposon product. Additionally, in some cases a PCR product was generated but the end of the transposon was too close to an *RsaI* site resulting in very short fragments from which no reliable sequence matches could be made. In order to overcome this, the inverse PCR method was repeated using *EagI* digestion for those mutant strains where *RsaI* based inverse PCR failed. Inverse PCR using these *EagI* digested samples enabled identification of the *Tn611* insertion site for several more, but not all of the transposon mutants, likely due to the same reasons as the failure of *RsaI* based inverse PCR. Ligation-mediated PCR was used as an alternative method for identifying the mutation site for those mutant strains where inverse PCR using either restriction enzyme was unsuccessful. Ligation-mediated PCR utilises *SalI* digestion to generate DNA fragments containing the transposon DNA/gDNA junction, and a DNA linker to allow selective amplification of this junction. Utilisation of ligation-mediated PCR resulted in identification of the mutation site for the majority of mutants where inverse PCR was unsuccessful. However, the mutation sites could not be identified for one rifampicin hypersensitive mutant and for five of the bedaquiline hypersensitive mutants, using either inverse PCR or ligation-mediated PCR due to an inability to generate PCR products for sequencing. The reason for the inability to generate products for these mutant strains is unknown, although due to the late inclusion of bedaquiline in the study significantly less time was spent troubleshooting the identification of *Tn611* insertion in the bedaquiline hypersensitive mutants than those for isoniazid and rifampicin. Future investigations utilising other methods such as ligating the DNA fragments containing the gDNA/transposon DNA

junction into a vector and sub-cloning into *E.coli* (Billman-Jacobe et al., 2006) may yield more information on the transposon insertion site for these remaining mutants.

#### **4.4.2. Genetic complementation**

The three mutants most sensitive to isoniazid and two mutants most sensitive to rifampicin as determined in Chapter Three were selected for complementation. These particular mutants were selected for complementation as they showed a large change in the MIC of isoniazid or rifampicin than the remainder of the 12 most sensitive mutants. These mutants were prioritised for complementation as it was expected that the large decrease in the MIC of the relevant drug for these mutants would make it easier to determine whether or not complementation was successful.

Complementation was performed for the isoniazid hypersensitive mutant strains *Tn::nudC* and *Tn::MSMEI\_1905*. Complementation of a third isoniazid hypersensitive mutant, *Tn::MSMEI\_6092*, was unable to be completed due to deletions that occurred in all of the *MSMEI\_6092* expression constructs that did not contain the gene in the reverse orientation. The deletions that occurred in the *MSMEI\_6092* construct may have been due to the expression of this gene being toxic to *E. coli*. Although expression of *MSMEI\_6092* was not induced when the vector was sub-cloned, the tetracycline inducible promoter of pRC20 is leaky in *E. coli* DH5 $\alpha$  in which the vector sub-cloning was performed.

Additionally, although a complementation strain was able to be constructed for the rifampicin hypersensitive mutant *Tn::MSMEI\_3093*, no empty vector control strain could be built (section 4.3.2.2). The mutant *Tn::MSMEI\_3093* contains the *Tn611* insertion within the ribosomal large subunit pseudouridine synthase gene and therefore may have defective translation. This mutant displayed a slow growth phenotype and it is possible that the addition of the hygromycin B antibiotic, an aminoglycoside and inhibitor of transcription, required to maintain the plasmid within the host, prevented the strain *Tn::MSMEI\_3093* containing pRC20 from growing. Interestingly, the ability to generate the *Tn::MSMEI\_3093* complementation strain suggests that it was possible to complement whatever was preventing the generation of the empty vector control e.g. hygromycin sensitivity. However, this was not examined further in the present study. As no empty vector control could be



built for *Tn::MSMEI\_3093* complementation of this strain was not completed. Consequently, it was decided to not attempt complementation of *Tn::arr* by itself, as the activity of Arr in *M. smegmatis* is already well characterised (Alexander et al., 2003; Dabbs et al., 1995; Quan et al., 1999), and the complementation of *Tn::arr* was only to serve as a control for the complementation of rifampicin hypersensitive mutants.

#### **4.4.3. Gene overexpression**

To further characterise the genetic basis of drug hypersensitivity for mutants hypersensitive to isoniazid (*Tn::nudC* and *Tn::MSMEI\_1905*), and rifampicin (*Tn::MSMEI\_3093*) the genes containing the *Tn611* insertions were overexpressed in WT *M. smegmatis* mc<sup>2</sup>155. It was found that MRC20 in the presence of the inducer tetracycline had an approximate two-fold increase in the MIC of isoniazid, while no change in the MIC of rifampicin was observed. The reason for the increased isoniazid MIC observed upon vector induction is unknown. Further investigation into the interaction between isoniazid and tetracycline may reveal whether there is an overlap between the modes of action of the two drugs or whether the expression of GFP influences susceptibility to isoniazid.

#### **4.4.4. Polar effects of *Tn611* insertion**

At least six of the hypersensitive transposon mutants contained the *Tn611* insertion within an intergenic region, suggesting that *Tn611* exerts a polar effect on the genes surrounding the insertion site. A polar effect also appears responsible for the isoniazid hypersensitive phenotype of the *Tn::MSMEI\_1905* mutant as complementation of this mutant with *MSMEI\_1905* failed to recover WT isoniazid sensitivity. Interestingly, the gene that is adjacent to *MSMEI\_1905* is *nudC*, which is known to be involved in isoniazid detoxification.

Therefore, although the most likely candidate genes responsible for the drug hypersensitivity phenotype are those that contain a transposon insertion, it is possible that polar effects on the adjacent genes also play a role. As complementation was not performed for all of the most sensitive mutants, it is not possible to say with certainty which gene is responsible for the sensitivity phenotype for the remaining hypersensitive mutants

identified in this study. Further investigations into the effect of complementing the remaining hypersensitive mutants may reveal the extent that polar effects of *Tn611* play a role in drug hypersensitivity.

#### **4.4.5. Genotypes related to isoniazid hypersensitivity**

##### **4.4.5.1. Links to known isoniazid mode of action and resistance mechanisms**

Four of the 12 mutants most hypersensitive to isoniazid, as determined in Chapter Three, had a transposon insertion in or adjacent to genetic loci connected to aspects of the known mode of action and/or resistance mechanisms for isoniazid. These genes were: *nudC*, which encodes the NADH pyrophosphatase NudC (two mutants: *Tn::nudC* and *Tn::MSMEI\_1905*); *eccCa<sub>1</sub>*, the ESX-1 conserved component Ca; and the *ahpCD* operon, which encodes the heterodimeric alkylhydro peroxide reductase AhpCD. The identification of these four mutants with known links to the mode of action of isoniazid validates the use of the assays in Chapter Three for investigating isoniazid mode of action.

NudC (*MSMEI\_1904*) is known to be involved in isoniazid detoxification in *M. smegmatis* mc<sup>2</sup>155 and *M. bovis* BCG (Wang et al., 2011). Specifically, NudC has been shown to hydrolyse the INH-NAD adduct, which is the active form of isoniazid. The mutant *Tn::nudC* generated in this thesis contains a transposon insertion within the ORF of *nudC*, and likely represents a loss of function mutation. Interestingly, the mutant *Tn::MSMEI\_1905* contained a *Tn611* insertion in the gene *MSMEI\_1905* which is immediately adjacent to the *nudC* gene in *M. smegmatis* mc<sup>2</sup>155. Complementation experiments showed that expression of *nudC* was able to complement the isoniazid hypersensitive phenotype measured in the *Tn::nudC* mutant, while expression of *MSMEI\_1905* had no effect on the isoniazid hypersensitivity of the *Tn::MSMEI\_1905* mutant. Therefore, it is possible that the isoniazid hypersensitivity of the *Tn::MSMEI\_1905* mutant was due to a polar effect on the expression of the adjacent *nudC* gene. Further investigation into this, such as measuring *nudC* gene expression levels using qPCR, would reveal whether *nudC* expression levels are lower in the *Tn::MSMEI\_1905* mutant than in WT *M. smegmatis*. To further characterise the role of *nudC* and *MSMEI\_1905* in isoniazid sensitivity each gene was overexpressed in WT *M. smegmatis* as described in

section 4.3.1.3. Overexpression of *nudC* resulted in increased resistance to isoniazid, consistent with the complementation experiments. These results corroborate those published by Wang et al. (2011), and strongly support the role of NudC in the detoxification of the INH-NAD adduct. Overexpression of *MSMEI\_1905* did not alter sensitivity to isoniazid, again consistent with the results from the complementation experiments. The overexpression results further confirm that *MSMEI\_1905* was not responsible for the isoniazid hypersensitive phenotype in this mutant strain.

*Myco2659* contained an insertion in the ESX-1 conserved component  $Ca_1$  (*eccCa<sub>1</sub>*, *MSMEI\_0062*) which is also known to be involved in the mode of action of isoniazid. ESX-1 is a type-VII secretion system that plays an important role in excreting proteins involved in virulence in mycobacterial species (Pym et al., 2002, 2003). It is loss of the ESX-1 locus, which is located in the region of difference 1 (RD1), that is partly responsible for the attenuation of the *M. bovis* BCG vaccine strain (Brosch et al., 2007; Pym et al., 2002, 2003). It has previously been shown that *EccCa<sub>1</sub>* is required for proper function of the ESX-1 system, and that loss of function mutants of *eccCa<sub>1</sub>* in a related mycobacterial species, *M. marinum*, exhibit reduced secretion of ESAT-6, a protein secreted by the ESX-1 machinery (Joshi et al., 2012). In addition, *EccCa<sub>1</sub>* interacts with components of the cell wall biosynthesis machinery, including components of the FASII system which is the pathway inhibited by isoniazid (Joshi et al., 2012). Joshi et al. (2012) demonstrated that *Tn::eccCa<sub>1</sub>* mutants produced 30% - 40% less total mycolic acid compared to WT, suggesting that *EccCa<sub>1</sub>* stabilizes mycolic acid biosynthesis. Interestingly, *Tn::eccCa<sub>1</sub>* mutants were also more sensitive to ethionamide, an analogue of isoniazid that also inhibits *InhA*. Therefore, it is likely that the *Tn::eccCa<sub>1</sub>* mutant (*myco2659*) identified in this thesis is hypersensitive to isoniazid due to a partially inhibited mycolic-acid biosynthesis pathway resulting from an absence of functional *EccCa<sub>1</sub>*.

The third genetic locus related to the mode of action of isoniazid that was identified in this thesis was the *ahpCD* operon, with the mutant *myco7102* containing a *Tn611* insertion 36 bp downstream of the *ahpCD* operon (*MSMEI\_4765/4766*). The proteins *AhpC* and *AhpD* together function as a heterodimeric alkylhydro peroxidase that protects mycobacteria from oxidative damage induced by alkylhydro peroxides (Chen et al., 1998). *M. tuberculosis* isoniazid resistant *katG* mutants often have reduced catalase activity resulting in increased oxidative stress. *AhpCD* is up regulated in *M. tuberculosis katG* mutants, where it

compensates for the reduced KatG activity and resulting increased oxidative stress (Dhandayuthapani et al., 1996; Sherman et al., 1996). Overexpression of AhpCD has been shown to increase resistance to isoniazid, while conversely, loss of function *ahpCD* mutants appear to show increased sensitivity to isoniazid, due to an altered oxidative stress response and concomitant altered *katG* expression (Zhang et al., 1996). Although *myco7102* does not contain a *Tn611* insertion within the *ahpC* or *ahpD* ORFs, its close proximity likely has a polar effect upon the expression of the *ahpCD* operon resulting in the observed isoniazid hypersensitivity. This could be confirmed by quantitative PCR to measure the expression of *ahpCD* in the *myco7102* mutant.

#### **4.4.5.2. Identification of potentially novel aspects of isoniazid's mode of action**

Other isoniazid hypersensitive mutants identified in this thesis were found to contain *Tn611* insertions in genes that represent potentially novel aspects to the aforementioned known modes of action. Other mutants contain *Tn611* insertions in genes that have no known links to the known mode of action of isoniazid, and represent either novel aspects of the known mode of action, or aspects of novel modes of action.

*Tn::MSMEI\_6092* contained a *Tn611* insertion in a gene encoding a Fur-like protein (*MSMEI\_6092*). There are two classes of Fur proteins, Fur A and Fur B, and *MSMEI\_6092* was determined to be more closely related to the FurA type proteins. Fur like regulators regulate various aspects of the interlinked process of iron metabolism and the oxidative stress response (Dussurget and Smith, 1998). FurA is the regulator for expression of KatG, a catalase/peroxidase responsible for detoxification of hydrogen peroxides, and the activation of isoniazid. *M. smegmatis* mc<sup>2</sup>155 has two copies of *katG*, each with its own *furA* regulator immediately upstream of the *katG* ORF. The *furA* like gene encoded by *MSMEI\_6092* is not near a *katG*, or *katG* like gene, and has no direct homolog in *M. tuberculosis*. As an expression construct for *MSMEI\_6092* could not be constructed in this thesis it was not possible to complement the *Tn::MSMEI\_6092* strain and confirm if the mutation of this gene was in fact responsible for the isoniazid hypersensitivity of this strain. It is possible that the *Tn611* insertion in *Tn::MSMEI\_6092* had a polar effect on a nearby gene, however the known

link between the oxidative stress response, isoniazid, and the pro-drug activating role of KatG, strongly suggests it is loss of function of the *MSMEI\_6092* gene product that results in the isoniazid hypersensitivity phenotype of this strain. The *furA* like gene encoded by *MSMEI\_6092* may have a regulatory role for one or both of the *katG* genes in *M. smegmatis*. Measurement of *katG* expression levels in the *Tn::MSMEI\_6092* mutant would reveal the relationship between this *furA* like gene and KatG. Alternatively, *MSMEI\_6092* may regulate other components of the oxidative stress response, indirectly effecting *katG* expression.

*Myco1897* and *myco6482* contained transposon insertions within transcriptional regulators that have homologs in other bacterial species that are involved in multi-drug resistant phenotypes. *Myco1897* contained an insertion in a multiple antibiotic resistance (Mar) type regulator (MarR, *MSMEI\_5538*). In *E. coli* MarR mediates multiple antibiotic resistance through regulation of the genes *marA* and *marB* (Cohen et al., 1993), for which mycobacteria lack obvious homologs. Interestingly, expression of *E. coli marA* in *M. smegmatis* has been shown to increase resistance to a range of antibiotics including isoniazid (McDermott et al., 1998). A MarRAB system was recently characterised in *M. smegmatis* that *MSMEI\_5538* was not a part of, and which showed no role in isoniazid sensitivity (Zhang et al., 2014). This suggests that *M. smegmatis* may have more than one MarRAB system, perhaps with different substrate specificities.

*Myco6482* contained a transposon insertion in *MSMEI\_5460*, which encodes a putative transcriptional regulator of unknown function, and has no clear homolog in *M. tuberculosis*. Bowman and Ghosh (2014) found that expression of *MSMEI\_5460* was up-regulated in a multi-drug resistant KO mutant of *MSMEI\_5969*, which encodes an anti-sigma factor proposed to be involved in regulating the 28 sigma factors in *M. smegmatis*. It was proposed that up-regulation of genes including *MSMEI\_5460* was responsible for the observed multi-drug resistant phenotype of this KO strain. The role of these transcriptional regulators in a multi-drug resistance phenotype could be further investigated by examining the cross-sensitivity of these strains to other antibiotics, and determining which genes they regulate.

*Myco2100* and *myco3113* contained *Tn611* insertions within gene clusters that appear to be involved in sulfur metabolism. Altered sulfur metabolism is linked to a deficient oxidative

stress response (Dussurget and Smith, 1998). These strains may compensate for the increased level of basal oxidative stress by increasing *katG* expression, resulting in an increasing sensitivity to isoniazid as in AhpCD mutants of mycobacteria (Dhandayuthapani et al., 1996; Sherman et al., 1996). Further investigation into the expression levels of *katG* in *myco2100* and *myco3113* may reveal whether this is the case.

*Myco0409* contained an insertion within *argD*, which lies in the middle of the arginine biosynthesis cluster. Because of this genetic organisation, even if the cause of isoniazid sensitivity in this strain is not due to a mutation in *argD* specifically but due to a polar effect, it is very likely that arginine biosynthesis would be disrupted. Almost all of the genes in the arginine biosynthesis cluster have been shown to be essential for *in vitro* growth of *M. tuberculosis* H<sub>37</sub>Rv by transposon based mutagenesis (Sasseti et al., 2003), with the exception of *argR*, which is a negative regulator of arginine biosynthesis (Maas, 1994). To the best of my knowledge, there has not been any literature published examining a link between arginine metabolism and isoniazid activity. In addition, arginine biosynthesis is not known to be linked to the oxidative stress pathway. Therefore, these results may represent a novel aspect of the mode of action of isoniazid and a novel role for the arginine biosynthesis machinery.

*Myco6166* contained a transposon insertion in a conserved hypothetical protein with predicted helicase and DNA binding activity (*MSMEI\_5554*). *MSMEI\_5554* likely encodes a transcriptional regulatory protein and may regulate genes involved in the isoniazid mode of action, such as oxidative stress response genes. However, the H<sub>37</sub>Rv homolog *Rv0862c* has no known reported function so the role of *MSMEI\_5554* remains unclear.

*Myco6192* contains a transposon insertion within the potassium transporter encoding gene *kdpA*. The KdpA protein functions in a complex with KdpB and KdpC (KdpABC) as a potassium transporter, and is stabilised by the co-transcribed gene product KdpF (Gannoun-Zaki et al., 2013). Overexpression of KdpF caused altered cell morphology in *M. bovis* BCG in a study by Gannoun-Zaki et al., (2013). Although, no change in isoniazid resistance was seen when KdpF was overexpressed; however, investigation into altered resistance in KdpF loss of function mutants was not performed.

#### **4.4.6. Genotypes related to rifampicin hypersensitivity**

##### **4.4.6.1. Links to known rifampicin mode of action and resistance mechanisms**

After sequencing the *Tn611* insertion sites of 11 of the 12 mutants most hypersensitive to rifampicin, as determined in Chapter Three, it was found that three mutants had a connection to known rifampicin resistance mechanisms. These three mutants had *Tn611* insertions in *arr*, which encodes the rifampicin ADP-ribosyl transferase Arr, and *ponA2*, which encodes the penicillin binding protein PonA2. The third mutant had an insertion in the gene adjacent to the lipoprotein signal peptidase *lspA*. The identification of these three mutants with known links to the mode of action of rifampicin validates the use of the assay used in Chapter Three for investigating rifampicin mode of action.

Arr is involved in a known mechanism of rifampicin inactivation in *M. smegmatis*, whereby Arr attaches a ribose moiety to rifampicin resulting in loss of activity (Dabbs et al., 1995; Quan et al., 1999; Tanaka et al., 1996). A *Tn::arr* mutant of *M. smegmatis* has previously been identified in an assay for hypersensitive rifampicin transposon mutants (Alexander et al., 2003). As the activity of *arr* in WT *M. smegmatis* is already well characterised, complementation of the *Tn::arr* mutant, and overexpression of *arr* in WT *M. smegmatis* were not performed in this thesis.

The second mutant with known links to the mode of action of rifampicin was *myco1030*, which contained a transposon insertion in *ponA2*, a penicillin binding protein. PonA2 is suspected to play a role in altering peptidoglycan cross-linking in the mycobacterial cell wall during the switch to stationary phase in *M. tuberculosis* (Vandal et al., 2009). Vandal et al. (2009), showed that a *M. tuberculosis* H<sub>37</sub>Rv *Tn::ponA2* mutant had slightly increased sensitivity to rifampicin and other lipophilic drugs, but no increased sensitivity to non-lipophilic drugs such as isoniazid. A *ponA2* KO mutant of *M. smegmatis* also previously demonstrated increased sensitivity to rifampicin, along with reduced stationary-phase survival and an altered cell wall (Patru and Pavelka, 2010). The findings from these previous studies suggest that the sensitivity of the *Tn::ponA2* mutant identified in this thesis is not rifampicin specific; however, this was not further investigated in this thesis.

*Myco4005* contained a transposon insertion in a gene encoding the ribosomal large subunit pseudouridine synthase D (*MSMEI\_3093*). *M. smegmatis* mc<sup>2</sup>155 *MSMEI\_3092* and *MSMEI\_3093* share the same genetic organisation as the H<sub>37</sub>Rv homologs, which are co-transcribed. Therefore, *MSMEI\_3093* is likely also co-transcribed with *MSMEI\_3092*, which encodes the lipoprotein signal peptidase *lspA*. A previous study demonstrated that overexpression of *lspA* in H<sub>37</sub>Rv leads to increased resistance to rifampicin (Pathak, 2013). Interestingly, Pathak (2013) also showed that overexpression of *lspA* also led to increased resistance to isoniazid in *M. tuberculosis*. In this thesis it was found that overexpression of *MSMEI\_3093* resulted in no change in the MIC of rifampicin, which may indicate that a polar effect on *lspA* is the genotypic cause for the rifampicin hypersensitivity observed in this strain. Complementation with *MSMEI\_3093* would determine the role of this gene in the rifampicin hypersensitivity of the *Tn::MSMEI\_3093* strain. Complementation of this strain was not performed in this study as no suitable empty vector control could be constructed. Future complementation of this strain with *MSMEI\_3093* and *lspA* would allow the gene responsible for hypersensitivity to be determined.

#### **4.4.6.2. Identification of potentially novel aspects of rifampicin's mode of action**

The remaining rifampicin hypersensitive mutants that the *Tn611* insertion site was identified for have either tentative links, or no clear links to the known mode of action and/or detoxification mechanisms for rifampicin, and represent potentially novel modes of action or detoxification mechanisms.

*Myco0163* contained a transposon insertion within *mtc28*, which encodes a 28 kDa secreted antigen. *Mtc28* contains large proline rich regions that have been implicated in modulating the interaction between penicillin binding proteins (PBP) and peptidoglycan (PG) metabolism (Manca et al., 1997; Patru and Pavelka, 2010). Therefore, as with the *ponA2* mutant, the hypersensitivity of this strain may not be specific to rifampicin; however, this was not further investigated in this thesis.

The mutant *myco2642* contained a *Tn611* insertion 19 bp downstream of the ESX-1 regulator EspR (*MSMEI\_6263*), and over 1000 bp upstream of *MSMEI\_6264*. EspR drives expression of



ESX-1 genes, increasing pump activity (Raghavan et al., 2008). As discussed in section 4.4.5.1, the ESX-1 system is involved in secretion of proteins that are important for mycobacterial virulence. The transposon mutant *myco2642* is predicted to have a loss of activity of the *espR* gene product and therefore decreased ESX-1 activity. To the best of my knowledge, no links between a defect in EspR and/or the ESX-1 system and rifampicin sensitivity exist within the literature. As ESX-1 is involved in pumping out many substrates the specific mechanism for rifampicin hypersensitivity in *myco2642* is unknown, however it represents a potentially novel role for EspR, and by association ESX-1, in the rifampicin mode of action, or its detoxification.

*Myco5826* contains a transposon insertion 98 bp downstream of a gene encoding a predicted TetR like transcriptional regulator (*MSMEI\_1800*). To the best of my knowledge no links between the rifampicin mode of action and this gene, or the *M. tuberculosis* homolog (*Rv3249c*), exist in the literature. Identification of the genes regulated by this TetR transcriptional regulator would facilitate understanding the basis for the rifampicin hypersensitivity of this strain

*Myco6762* contains a transposon insertion in the gene encoding the metallopeptidase Zmp1 (*MSMEI\_0227*). The *M. tuberculosis* Zmp1 homolog has been shown to be involved in pathogenicity whereby Zmp1 prevents formation of the inflammasome, a protein complex involved in modulating the host response to *M. tuberculosis* infection (Ferraris and Rizzi, 2011; Ferraris et al., 2011; Master et al., 2008). No links between this process and the mode of action of rifampicin could be identified in the literature so the mechanism of rifampicin hypersensitivity in *myco6762* remains unknown.

*Myco6859* contains a *Tn611* insertion in *MSMEI\_6301*, which encodes the O-methyltransferase (*omt*). O-methyltransferase is involved in methylation of the cell wall of *M. smegmatis* (Jeevarajah et al., 2002). No link between *omt* or the *M. tuberculosis* homolog *Rv1153c*, and altered rifampicin sensitivity could be found in the literature.

*Myco7011* contained a *Tn611* insertion in a gene encoding a cell envelope-related transcriptional attenuator (*MSMEI\_5621*). The *M. tuberculosis* homolog, *Rv0822c*, has been shown to be significantly up-regulated in an RD1 deletion mutant of H<sub>37</sub>Rv (Mostowy et al., 2004). RD1 is one of the major regions of the genome of *M. bovis* BCG that is missing

compared to the genome of *M. bovis* and *M. tuberculosis*. The absence of RD1 has been shown to be largely responsible for the attenuation of BCG, due to the loss of the ESX-1 type-VII secretion system. The relationship of this gene to the RD1 locus suggests this gene may be involved in the regulation of ESX-1, similar to the rifampicin hypersensitive *Tn::espR* mutant also identified in this thesis. Therefore, these results strongly implicate a role for ESX-1 in the rifampicin mode of action or detoxification.

#### **4.4.7. Genotypes related to bedaquiline hypersensitivity**

##### **4.4.7.1. Links to known bedaquiline mode of action and resistance mechanisms**

Characterisation of the *Tn611* insertion sites of the 12 mutants most hypersensitive to bedaquiline as determined in Chapter Three, revealed that two mutants had connections to known aspects of the mode of action and/or resistance mechanisms for bedaquiline. These two mutants had *Tn611* insertions in *atpB*, which encodes the ATP synthase F<sub>0</sub> domain A subunit, and *mmpL5*, which encodes a transmembrane transporter. The identification of these two mutants with *Tn611* insertions within or adjacent to genes with known links to the mode of action of bedaquiline validates the use of the assays used in Chapter Three for investigating bedaquiline mode of action.

*Myco2908* contained a *Tn611* insertion in the *atpB* gene, which encodes subunit A of the ATP synthase F<sub>0</sub> domain. The F-ATP synthase consists of two domains, F<sub>0</sub> and F<sub>1</sub>, which function together to generate ATP. The F<sub>0</sub> unit is composed of the A, B, and C subunits and the known target of bedaquiline is the C subunit of the ATP synthase F<sub>0</sub> domain encoded by *atpE* (Andries et al., 2005; Koul et al., 2007). In *M. tuberculosis*, *atpB* and *atpE* are co-transcribed as an operon; therefore, the *Tn::atpB* mutant identified in this thesis may also have altered *atpE* expression (Roback et al., 2007; Sala et al., 2009). Interestingly the H<sub>37</sub>Rv homolog of *atpB* has been shown to be essential in *M. tuberculosis* by transposon mutagenesis (Griffin et al., 2011; Sassetti et al., 2003). The requirement for *atpB* in *M. tuberculosis* for viability, suggests that there is some functional redundancy in *M. smegmatis* as a viable *Tn::atpB* mutant was generated in this thesis. The bedaquiline hypersensitivity of this mutant may be due to a general defect in the ATP synthase, or more

specifically due to altered expression of the target of bedaquiline *atpE*; however, this was not further investigated in this thesis.

The second mutant with links to the known mode of action of bedaquiline was *myco0934*, which contained a *Tn611* insertion in *mmpL5* (*MSMEI\_3416*). The homologous *M. tuberculosis* protein is an efflux pump that is proposed to pump bedaquiline out of the cell. Increased expression of *mmpL5* in H<sub>37</sub>Rv was found to increase bedaquiline resistance (Andries et al., 2014; Hartkoorn et al., 2014). The mutant *Tn::mmpL5* identified in this study therefore likely has increased bedaquiline sensitivity due to a loss of MmpL5 efflux activity, resulting in increased intracellular concentrations of bedaquiline.

#### **4.4.7.2. Identification of potentially novel aspects of bedaquiline's mode of action**

The remaining bedaquiline hypersensitive mutants that were sequenced were found to contain *Tn611* insertions in genes with no link to the known mode of action of bedaquiline. These therefore represent potentially novel aspects of the mode of action or detoxification mechanisms of bedaquiline.

*Myco1994* contains a transposon insertion in *MSMEI\_3189*, which encodes a M42 type glutamyl aminopeptidase for which there is no apparent *M. tuberculosis* homolog. No information in the literature relating this gene to any aspects of the bedaquiline mode of action could be found, therefore, the mechanism of bedaquiline hypersensitivity for this mutant remains unclear.

*Myco2833* contains a transposon insertion 77 bp upstream of the gene encoding the biotin sulfoxide reductase (*bisC*, *MSMEI\_2671*), and 181 bp upstream of *MSMEI\_2672*, which encodes a conserved hypothetical protein. As discussed previously, *Tn611* exerts a polar effect on nearby genes and therefore it is possible that the *Tn611* insertion in *myco2833* is disrupting the function of *bisC* or *MSMEI\_2672*. Protein BLAST results suggest the product of *MSMEI\_2672* is involved in cell wall biosynthesis. The gene product of *MSMEI\_2672* contains a conserved region consisting of four repeats of a 54 aa sequence named LGFP. The LGFP repeats are proposed to be involved in anchoring the protein to the cell wall, with these

repeats found in proteins required for stabilising the cell wall in *Methanosarcina acetivorans* (Adindla et al., 2004). Alternatively, the *Tn611* insertion in *myco2833* may be causing hypersensitivity to bedaquiline by a polar effect on *MSMEI\_2671* gene expression, although the exact mechanism of sensitivity is unclear. Generation of knock out mutants of each gene would determine which gene is responsible for the bedaquiline hypersensitivity of this strain.

*Myco3011* contained a transposon insertion within the gene *MSMEI\_4123*, which encodes a conserved hypothetical gene named *yfiH*. The genetic neighbourhood of *yfiH* includes a number of genes involved in cell division including *ftsQ* and *ftsZ*, a genetic organisation conserved in *M. tuberculosis* H<sub>37</sub>Rv (Doerks et al., 2012; Weiling Hong et al., 2013). The conserved genetic region within which *yfiH* resides suggests that YfiH is involved in the process of cell division and/or cell wall maintenance, similar to its genetic neighbours. Therefore, the bedaquiline hypersensitivity of this strain may be due to deficient cell wall division/maintenance.

*Myco4393* contained a transposon insertion in *MSMEI\_5136*, which encodes a putative transmembrane protein. Both *MSMEI\_5136*, and its *M. tuberculosis* homolog *Rv1072*, reside in a relatively conserved genomic region encoding genes related to fatty acid metabolism. Interestingly, *Rv1072* has been identified as a gene required for late stage survival of mycobacteria in a guinea pig infection model, as well as being up-regulated during oxidative stress and nutrient limitation (Betts et al., 2002; Kaushal et al., 2002; Manganeli et al., 2002; Schnappinger et al., 2003).

*Myco5040* contains a transposon insertion within the gene *MSMEI\_5828*, which encodes a PPE family protein that contains the characteristic ~180 bp proline-proline-glutamic acid motif at the N-terminus. Little is known about the function of PPE proteins, which together with PE proteins (with a characteristic 100 bp proline-glutamic acid N-terminal motif) comprise 10% of the *M. tuberculosis* genome; The *M. smegmatis* genome only contains four PPE genes (Nair et al., 2009). Adjacent to *MSMEI\_5828* is *MSMEI\_5829*, which encodes a lipid transfer protein *ltp2*, and is part of a conserved operon spanning *MSMEI\_5829* to *MSMEI\_5834* in *M. smegmatis*, and the homologs *Rv3540c* to *Rv3545c* in *M. tuberculosis* H<sub>37</sub>Rv. This conserved region has been shown to be involved in cholesterol metabolism in

both *M. smegmatis* and *M. tuberculosis* (García-Fernández et al., 2013; Uhía et al., 2012). This operon is likely defective in the *myco5040* mutant due to polar effects of the *Tn611* insertion, which would lead to dysfunctional cholesterol metabolism. Therefore, a defective cholesterol metabolism may be responsible for the bedaquiline hypersensitivity of this strain, and may represent a novel aspect of the mode of action of bedaquiline. To the best of my knowledge, no clear links between cholesterol metabolism and bedaquiline exist in the literature.

#### 4.4.8. Summary

In summary, the *Tn611* insertion site for 31 drug hypersensitive mutants of *M. smegmatis* were identified in this chapter; 12 isoniazid hypersensitive strains, 11 rifampicin hypersensitive strains, and 8 bedaquiline hypersensitive strains. Of the isoniazid hypersensitive mutants, four had links to either the known mode of action or detoxification pathways of isoniazid: *ahpC*, *eccCa1*, and *nudC* which was identified twice with two separate mutants. Of the rifampicin hypersensitive mutants, two had connections to either the known mode of action or detoxification pathways of rifampicin: *arr* and *ponA2*. Of the bedaquiline hypersensitive mutants, two mutants had links to either the known mode of action or detoxification pathways of bedaquiline: *atpB* and *mmpL5*. Collectively, these results validate the use of the assay used in this thesis for identifying genes related to drug mode of action.

The remaining 23 mutants found to be hypersensitive to isoniazid, rifampicin, or bedaquiline that the insertion sites were identified for had no clear links to the known mode of action or detoxification pathways for each drug, and therefore represent novel aspects of either drug mode of action or detoxification mechanisms. As complementation of the transposon insertion was not attempted for the majority of drug hypersensitive mutants validated in Chapter Three, it is not possible to definitively identify the gene responsible for the observed drug hypersensitivity. However, for a number of strains the genes containing or adjacent to the *Tn611* insertion site provide promising links to the mode of action of isoniazid, rifampicin, and bedaquiline respectively. Specifically, three isoniazid hypersensitive mutants contained *Tn611* insertions either within or adjacent to genes linked to the oxidative stress response, which is known to interact with isoniazid via KatG. Interestingly, two genes related to the type-VII secretion systems ESX-1 were identified as containing *Tn611* insertions in

rifampicin hypersensitive mutants. To the best of my knowledge no link between rifampicin and the ESX-1 locus exists in the literature. There were no such apparent trends in the bedaquiline hypersensitive mutants; however, this is likely a limitation of the number of mutants sequenced for each compound. Had more drug hypersensitive mutants had their *Tn611* insertion sites identified, more trends in terms of pathways containing *Tn611* insertions may have become apparent.

## **5. Characterising drug sensitivity phenotypes of *Tn611* mutants**

### **5.1.Introduction**

Identifying the cross-sensitivity of the drug hypersensitive mutants identified in Chapter Three, and the differential-sensitivity to analogues of the drug that they were first identified as being hypersensitive to, can be used to generate more information on the specific role of the genes harbouring *Tn611* insertions. Cross-sensitivity testing of the hypersensitive mutants generates information on whether the drug sensitivity of the mutants identified in Chapter Three is drug specific or a result of a general multi-drug resistance mechanism (drug non-specific). Differential-sensitivity to analogues of the drug that the mutant strain is hypersensitive to, where the mutants strains are either more or less sensitive to the analogues than the parent drug, can be used to group mutants that appear to contain insertions in genes involved in similar aspects of the drug's mode of action or drug resistance mechanisms. This approach is similar to target based whole-cell drug screening, whereby target information is integrated into screening for anti-mycobacterial activity (Ioerger et al., 2013; Nisa et al., 2010). The information from these assays for cross- and differential-sensitivity can be used to generate a more complete description of the drug mode of action.

#### **5.1.1. Analogues of anti-tuberculosis drugs**

The design and synthesis of drug analogues makes it possible to improve upon the properties of the originally isolated compound or to examine the mode of action of the drug. In the case of anti-TB drugs, analogues have been developed in an effort to improve anti-mycobacterial activity, especially against drug resistant strains, or to improve pharmacokinetic properties. For example, rifapentine is an analogue of rifampicin that has an increased half-life in the plasma of patients, allowing less frequent dosing (Acocella et al., 1971; Benator et al., 2002; Keung et al., 1999). This improves the likelihood that patients will adhere to the drug regimen, reducing the probability of rifapentine resistance occurring in the patient. Isoniazid was an intermediate generated when synthesising analogues of nicotinic acid with improved mycobacterial activity (Pansy et al., 1952). Isoniazid was found to have much greater activity than the other analogues of nicotinic acid that retained activity against TB, including pyrazinamide and ethionamide.

Analogues are also used when studying drug structure-activity relationships (SAR), whereby the differential activity of the various analogues can provide information on key parts of the drug that are required for activity. This type of study can be combined with analysis of hypersensitive mutant strains to identify analogues that are less active against the mutants than expected. Differential-sensitivity of the mutant strain to different drug analogues indicates that the mode of action of the analogue differs in some way to that of the original drug, or that the analogue is resistant to a specific detoxification mechanism that defends against the original drug. As drugs are pleiotropic their complete anti-mycobacterial activity is likely to stem from a combination of both the action against the primary target and action against lesser secondary targets. Close structural analogues are generally expected to retain the complete mode of action of the parent drug; however, the activity against the specific target that generates most of its anti-mycobacterial activity may be altered and a secondary target of the parent drug may then take over to generate most of its anti-mycobacterial activity. As such, analogues that preferentially work via these secondary targets can be used as tools to identify these secondary targets, generating information on the overall mode of action of the parent drug. As the primary goal of the research described in this thesis was to gain a better understanding of the mode of action of these drugs in *M. tuberculosis*, it is important that analogues that transposon mutants demonstrate hypersensitivity to are active in *M. tuberculosis*. Any analogues that lack activity in *M. tuberculosis* are likely to have a mode of action specific to *M. smegmatis*.

### **5.1.2. Isoniazid, rifampicin, and bedaquiline hypersensitive mutants**

The hypersensitive *M. smegmatis* mutant strains studied were the isoniazid hypersensitive mutants *Tn::nudC* and *Tn::MSMEI\_6092*; the rifampicin hypersensitive mutants *Tn::arr* and *Tn::MSMEI\_3093*; and the bedaquiline hypersensitive mutants *Tn::atpB* and *Tn::MSMEI\_3189*. NudC has recently been demonstrated to be able to hydrolyse the INH-NAD adduct responsible for the inhibition of InhA (Wang et al., 2011). *MSMEI\_6092* encodes a Fur like protein of unknown function that likely regulates some aspect of the oxidative stress response. Arr is a known rifampicin-inactivating enzyme that works by ribosylating rifampicin (Dabbs et al., 1995; Quan et al., 1999). *MSMEI\_3093* encodes the



ribosomal large subunit pseudouridine synthase D, although rifampicin hypersensitivity in the *Tn::MSMEI\_3093* strain may be due to altered transcription of the adjacent gene *lspA* (Pathak, 2013). Subunit A of the ATP synthase, encoded by *atpB*, is a subunit of the  $F_0$  domain of the ATP synthase that is inhibited by bedaquiline. *MSMEI\_3189* encodes a glutamyl aminopeptidase, although the genetic basis of bedaquiline hypersensitivity for *Tn::MSMEI\_3189* remains unclear. These mutants were selected for further characterisation as they demonstrated the largest increases in sensitivity to the drugs tested; therefore it was reasoned that any cross-sensitivities or differential-sensitivities would be easier to identify than with the other mutants that showed a small increase in sensitivity.

### 5.1.2. Objectives of Chapter Five

The goal of Chapter Five was to further characterise a selection of the drug hypersensitive mutants identified in Chapter Three. Specific focus was given to the drug hypersensitive mutants' cross-sensitivity to other drugs and their differential-sensitivity to analogues of the drug that they were initially identified as being hypersensitive to.

To achieve this goal the following specific aims were addressed:

- Determine cross-sensitivity of the isoniazid hypersensitive transposon mutants *Tn::nudC* and *Tn::MSMEI\_6092*, the rifampicin hypersensitive mutants *Tn::arr* and *Tn::MSMEI\_3093*, and the bedaquiline hypersensitive mutants *Tn::atpB* and *Tn::MSMEI\_3189*
- Determine the differential-sensitivity of the rifampicin hypersensitive mutants *Tn::arr* and *Tn::MSMEI\_3093*, and the *MSMEI\_3093* overexpression strain, to the rifampicin analogue rifapentine
- Determine the differential-sensitivity of *Tn::nudC*, and *nudC*, *inhA*, and *katG* overexpression strains, to isoniazid analogues active against *M. smegmatis* mc<sup>2</sup>155
- Confirm activity in *M. tuberculosis* of analogues that *M. smegmatis* transposon mutant strains showed differential-sensitivity to

To examine specificity of drug hypersensitivity, for each mutant that was identified in the primary testing (Chapters Three and Four) as being hypersensitive to one of the three drugs

considered (isoniazid, rifampicin, and bedaquiline), the cross-sensitivities were determined for the other two drugs. The overexpression strains created in Chapter Four were used in the differential-sensitivity assay, with the exception of the *katG* overexpression strain which was generated in this chapter. Preliminary sensitivity testing of isoniazid analogues in *M. tuberculosis* was performed against the virulent strain H<sub>37</sub>Rv.

## **5.2.Methods**

### **5.2.1. Cross sensitivity testing of transposon mutants to other drugs**

The cross-sensitivity was determined for the isoniazid hypersensitive mutants *Tn::nudC* and *Tn::MSMEI\_6092*, the rifampicin hypersensitive mutants *Tn::arr* and *Tn::MSMEI\_3093*, and the bedaquiline hypersensitive mutants *Tn::atpB* and *Tn::MSMEI\_3189* to rifampicin and bedaquiline, isoniazid and bedaquiline, and isoniazid and rifampicin, respectively. Cross-sensitivity of the hypersensitive strains was quantified by MIC using dose-response assays (section 2.8.3), and compared to the mean random transposon mutant control MIC. MICs were presented as the MIC ratio between the hypersensitive mutant and the mean control MIC.

### **5.2.2. Differential-sensitivity testing of transposon mutants to drug analogues**

The differential-sensitivities of the rifampicin hypersensitive mutant strains *Tn::arr* and *Tn::MSMEI\_3093* to rifapentine, and the differential-sensitivities of the isoniazid hypersensitive mutant *Tn::nudC* to a range of isoniazid analogues were determined. Differential-sensitivity was quantified by MIC using dose-response assays (section 2.8.3). MIC values were given as the MIC ratio between the hypersensitive mutant and the MIC for the control strain D11. Differential-sensitivity was defined as a greater than 1.5-fold difference in the MIC ratio of the analogue and the original drug (rifampicin or isoniazid).

#### **5.2.2.1. Selection of isoniazid analogues for differential-sensitivity testing**

A total of 30 randomly selected isoniazid analogues were obtained from the National Institute of Health's (NIH) Developmental Therapeutics Program (DTP) repository, along with a sample of isoniazid. All analogues were dissolved in 100% dimethyl sulfoxide (DMSO) at a concentration of 10 mg·mL<sup>-1</sup> and stored at -20 °C. A full list of the isoniazid analogues, including their structural information is listed in appendix section 8.4. The isoniazid analogues were tested against WT *M. smegmatis* mc<sup>2</sup>155 to determine their anti-mycobacterial activity (section 2.8.2), and only those analogues with sufficient activity were progressed into differential-susceptibility testing. Briefly, the analogues that showed greater than 75% growth-inhibition at a concentration of 100 µg·mL<sup>-1</sup> averaged (mean) across two separate experiments were taken to have sufficient activity for differential-sensitivity testing. The MICs of the isoniazid analogues that were active against *M. smegmatis* mc<sup>2</sup>155 were determined by dose-response assay (section 2.8.3).

#### **5.2.3. Overexpression strains versus isoniazid analogues**

The MICs of the isoniazid analogues to which *Tn::nudC* showed differential-sensitivity were determined for the *nudC* and *inhA* overexpression strains constructed in Chapter Four, along with the empty vector control and random gene overexpression control strain. Overexpression assays were performed as described in section 2.8.3. Briefly, the MIC of the relevant analogue was determined by dose-response assay for the overexpression strains, both with and without vector promoter induction by 20 ng·mL<sup>-1</sup> tetracycline.

##### **5.2.3.1. *katG* overexpression strain versus isoniazid analogues**

*M. smegmatis* mc<sup>2</sup>155 contains two homologues of *katG*, *MSMEI\_3380* and *MSMEI\_6216*, with *MSMEI\_6216* sharing the greatest amino acid identity with the *M. tuberculosis* H<sub>37</sub>Rv *katG* gene, *Rv1908c* (appendix section 8.2). Therefore, for the purposes of this study *MSMEI\_6216* was used as the *M. smegmatis* mc<sup>2</sup>155 *katG* gene (*katG<sub>sm</sub>*) for the overexpression assay and was amplified by PCR from WT *M. smegmatis* mc<sup>2</sup>155 and cloned

into the *Bam*HI restriction site in plasmid pRC20 (section 2.6.9.1). The native *katG<sub>sm</sub>* gene contains a *Bam*HI site within its ORF, therefore overlap PCR was used to remove the restriction site by creating a silent mutation that was confirmed by sequencing (Table 2.9). Constructs of pRC20 containing *katG<sub>sm</sub>* were sequenced to check orientation and fidelity before transforming into WT *M. smegmatis* mc<sup>2</sup>155 to generate the *katG* overexpression strain (section 2.6.2 and 2.6.7.2).

The *katG<sub>sm</sub>* overexpression assay was performed as described in section 2.8.3. Briefly, the MIC of the relevant analogue was determined by dose-response assay for the overexpression strain, both with and without vector promoter induction by 20 ng·mL<sup>-1</sup> tetracycline.

#### **5.2.4. *M. tuberculosis* H<sub>37</sub>Rv versus isoniazid analogues**

Preliminary determination of the sensitivity of *M. tuberculosis* H<sub>37</sub>Rv to the isoniazid analogues that the *Tn::nudC* strain showed differential-sensitivity to was performed in the PC3 laboratory at University College Dublin (Dublin, Ireland). Sensitivity was quantified by MIC determination in a dose-response assay, with one experiment performed (section 2.8.3). Briefly, MICs were determined by eye as the lowest concentration 24 hours after the addition of 50 µL 0.03% resazurin to each well of the assay plates.

## 5.3.Results

### 5.3.1. Cross-sensitivities of hypersensitive mutants

The cross-sensitivities of the hypersensitive mutants are presented in Table 5.1. The rifampicin hypersensitive mutant *Tn::MSMEI\_3093* showed a minor increase in resistance to isoniazid, and the bedaquiline hypersensitive mutants *Tn::atpB* and *Tn::MSMEI\_3189* showed minor increases in resistance to rifampicin, with *Tn::MSMEI\_3189* also showing a minor increase in resistance to isoniazid. No mutants showed an increased sensitivity to any of the other drugs tested.

**Table 5.1: Cross-sensitivity of hypersensitive strains.**

Strain	MIC ratio		
	Isoniazid	Rifampicin	Bedaquiline
<b>Isoniazid</b>			
<i>Tn::nudC</i>	-	1.2	0.67
<i>Tn::MSMEI_6092</i>	-	1	1
<b>Rifampicin</b>			
<i>Tn::arr</i>	1	-	1
<i>Tn::MSMEI_3093</i>	0.5	-	1.2
<b>Bedaquiline</b>			
<i>Tn::atpB</i>	1	0.5	-
<i>Tn::MSMEI_3189</i>	0.5	0.5	-

MIC ratios for hypersensitive mutants compared to the mean MIC of the random transposon mutant control strains for isoniazid, rifampicin, and bedaquiline. An MIC ratio of less than one (red shading) indicates increased resistance, while a ratio of more than one (green shading) indicates increased sensitivity, and a ratio of one (yellow shading) indicates no change in sensitivity for the hypersensitive mutant compared to the control strain D11.

### 5.3.2. Differential-sensitivity of hypersensitive mutants

#### 5.3.2.1. Rifapentine versus rifampicin hypersensitive transposon mutants

The differential-sensitivities of the two rifampicin hypersensitive strains *Tn::arr* and *Tn::MSMEI\_3093* to the rifampicin analogue rifapentine were determined (Table 5.2). Both of the rifampicin hypersensitive strains showed similar increases in sensitivity to rifapentine compared to the control strains as had been seen with the parent compound rifampicin.

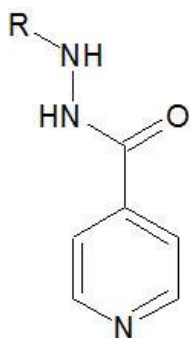
**Table 5.2: Sensitivity of rifampicin hypersensitive mutants to rifapentine.**

Drug	MIC ratio	
	<i>Tn::arr</i>	<i>Tn::MSMEI_3093</i>
Rifampicin	7.2	4.1
Rifapentine	8	5

MIC ratios for the rifampicin hypersensitive strains *Tn::arr* and *Tn::MSMEI\_3093* compared to the random transposon mutant control strain D11 for rifampicin and rifapentine. A larger MIC ratio indicates increased sensitivity of the hypersensitive mutant compared to the control strain D11.

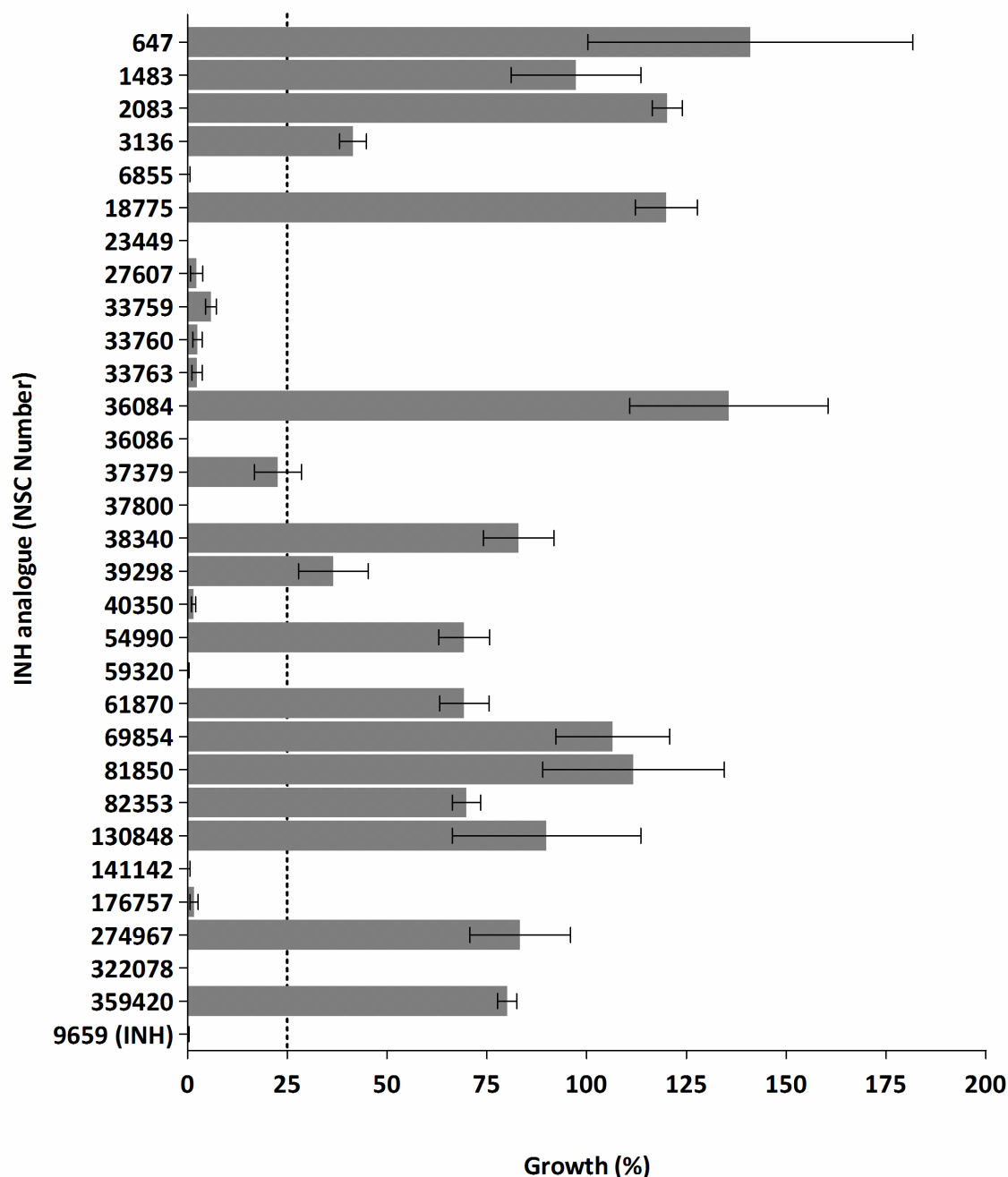
#### **5.3.2.2. Isoniazid analogues tested in isoniazid hypersensitive transposon mutants**

A selection of isoniazid analogues obtained from the DTP repository were tested for activity against WT *M. smegmatis* mc<sup>2</sup>155 at 100 µg·mL<sup>-1</sup>. A total of 14 of the 30 isoniazid analogues tested demonstrated greater than 75% growth-inhibition against WT *M. smegmatis* mc<sup>2</sup>155 and were selected for differential-sensitivity testing of the isoniazid hypersensitive mutant *Tn::nudC* (Figure 5.2). The NSC numbers of the analogues that showed growth-inhibitory activity greater than the 75% cut-off were 6855, 23449, 27607, 33759, 33760, 33763, 36086, 37379, 37800, 40350, 59320, 141142, 176757, and 322078. Information on these 14 analogues can be found in appendix section 8.4, along with structural details. Interestingly, all 14 of these analogues with activity in *M. smegmatis* had the core structure of isoniazid, varying only in their side chains (Figure 5.1). The total 30 analogues originally tested had a range of structures, with only 19 of the analogues retaining the core structure of isoniazid. Therefore, some of the analogues found to be inactive against WT *M. smegmatis* mc<sup>2</sup>155 also had the structure indicated below.



**Figure 5.1: Structure of isoniazid analogues active against *M. smegmatis* mc<sup>2</sup>155.** Structure of analogues of isoniazid that showed greater than 75% growth-inhibition of WT *M. smegmatis* mc<sup>2</sup>155 at 100  $\mu\text{g}\cdot\text{mL}^{-1}$  where R represents the various side chains that differed among the 14 analogues.

Comparison of the activity against WT *M. smegmatis* mc<sup>2</sup>155 of all 19 analogues with the structure in Figure 5.1 revealed no patterns in terms of side chains of active and inactive isoniazid analogues (appendix section 8.4).

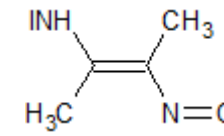

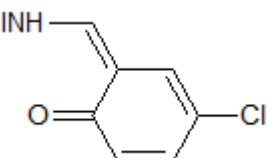
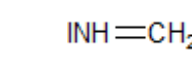
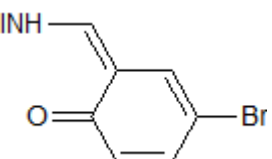
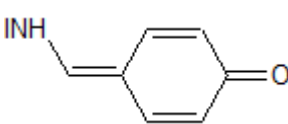
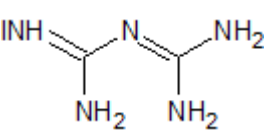
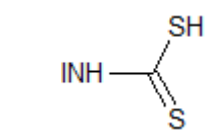


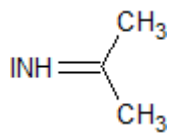
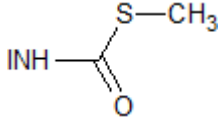
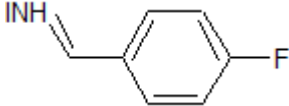
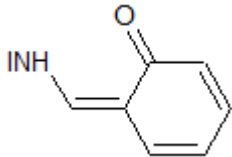
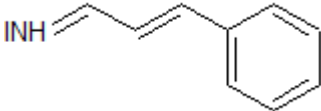
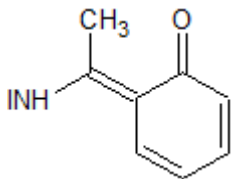
**Figure 5.2: Growth-inhibition of WT *M. smegmatis* mc<sup>2</sup>155 by isoniazid analogues.** Columns represent mean growth of WT *M. smegmatis* mc<sup>2</sup>155 in 100 µg·mL<sup>-1</sup> of each analogue across three independent experiments with standard error bars shown. Isoniazid analogues are named according to their NSC number. The dotted line at 25% growth indicates the activity cut-off of 75% growth-inhibition, with analogues that inhibited growth beyond this cut-off proceeding to the differential-sensitivity assay.



The MICs of the 14 isoniazid analogues were determined for the isoniazid hypersensitive strain *Tn::nudC* and the random transposon control strain D11, with the MIC ratios for these two strains given in Table 5.3. The *Tn::nudC* strain showed an increased sensitivity compared to D11 for all 14 isoniazid analogues tested. The *Tn::nudC* strain was 4.8-fold more sensitive to isoniazid compared to the control strain D11, and showed similar sensitivity to eight of the analogues. The *Tn::nudC* strain showed differential-sensitivity to the remaining six isoniazid analogues, showing only two – three-fold increases in sensitivity to these analogues compared to the control strain D11. The NSC numbers of the six analogues that *Tn::nudC* showed differential-sensitivity to were 27607, 33759, 37800, 40350, 141142, and 176757. There were no obvious patterns regarding the side chains of these analogues and their activity against *Tn::nudC*.

**Table 5.3: Sensitivity of *Tn::nudC* to isoniazid analogues.**

Isoniazid analogue (NSC number)	MIC Ratio	Side chain structure
37800	2.0	
40350	2.0	
27607	2.4	
141142	2.4	
33759	2.7	
176757	3.0	
6855	4.0	
23449	4.0	

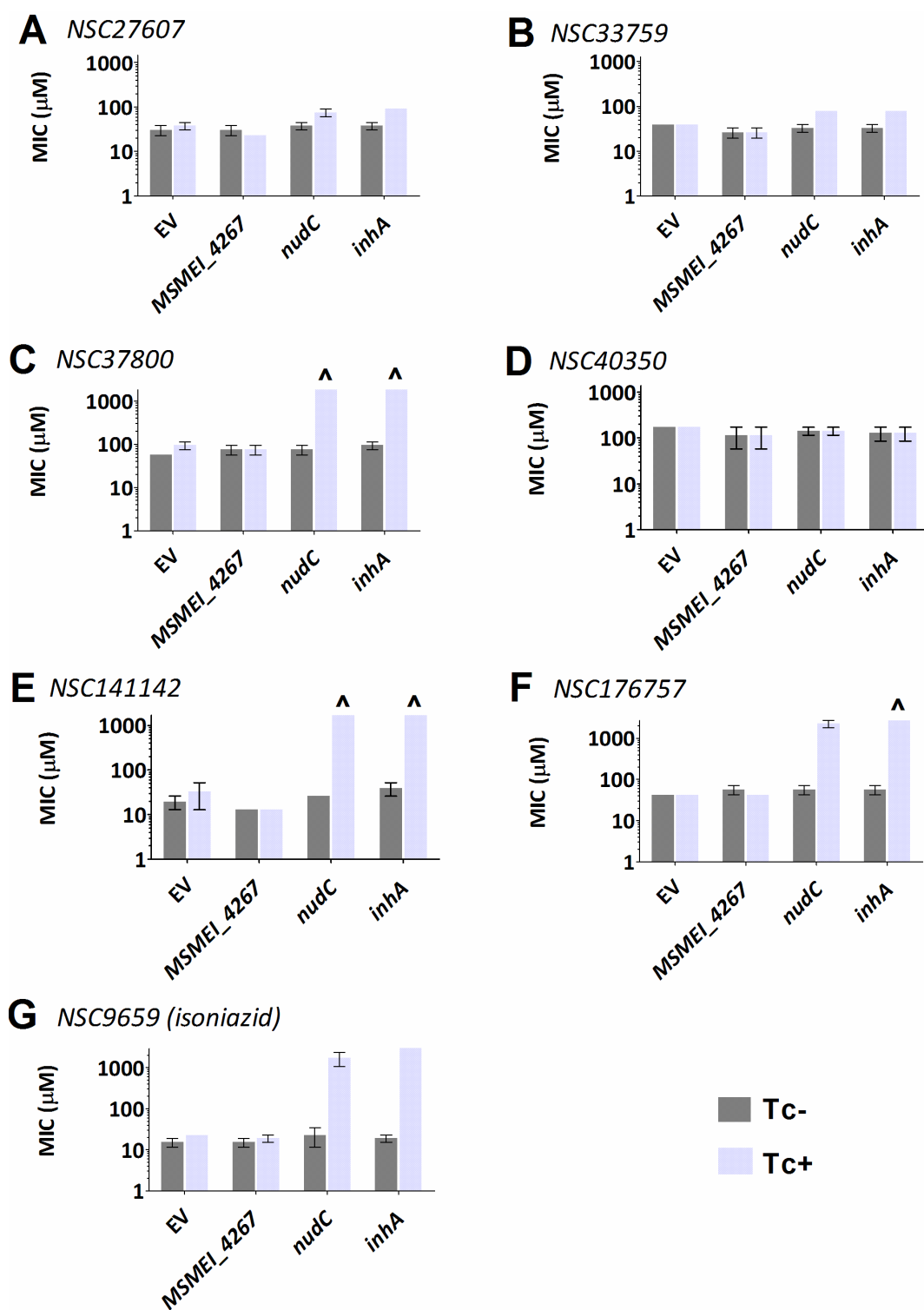
36086	4.0	
59320	4.0	
322078	4.0	
33760	4.8	
33763	4.8	
37379	4.8	
Isoniazid (9659)	4.8	INH

MIC ratios for the rifampicin hypersensitive strains *Tn::arr* and *Tn::MSMEI\_3093* compared to the control strain D11 for the 14 isoniazid analogues active against WT *M. smegmatis* mc<sup>2</sup>155. A larger MIC ratio indicates increased sensitivity of the hypersensitive mutant compared to the control strain D11. Side chains from the core isoniazid (INH) structure are shown.

### 5.1.1. Isoniazid analogues versus overexpression strains

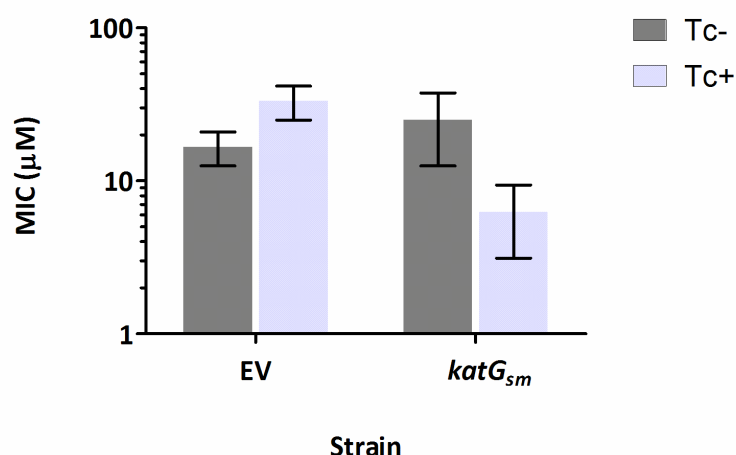
The sensitivities of the *nudC* and *inhA* overexpression strains to the six isoniazid analogues that *Tn::nudC* showed differential-sensitivity to were determined and compared to the random gene overexpression control strain and the empty vector control (Figure 5.3). Induction of expression from either the empty vector control or the random gene control *MSMEI\_4267* with 20 ng·mL<sup>-1</sup> tetracycline did not increase the MIC of any of the analogues greater than the basal two-fold increase in resistance observed for the empty vector control versus isoniazid (Figure 4.8). Induction of *inhA* expression resulted in a greater than 10-fold

increase in resistance to analogues 37800, 141142, and 176757 and to isoniazid. Similarly, induction of *nudC* expression resulted in greater than 10-fold increases in resistance to analogues 37800, 141142, and 176757 and to isoniazid. No increase above the baseline was observed for the analogues, 27607 and 33759 when expression of either *nudC* or *inhA* was induced. No change in resistance was observed for analogue 40350 in any of the overexpression strains.



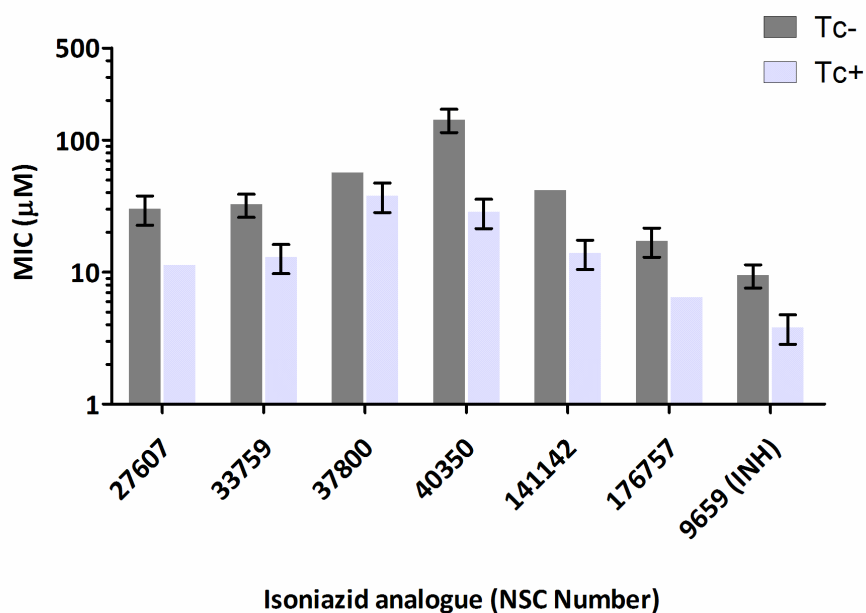
**Figure 5.3: Overexpression strains tested with isoniazid analogues.** MICs are presented for the *nudC*, *inhA*, random gene *MSMEI\_4267* control, and empty vector (EV) control overexpression strains versus isoniazid analogues with and without promoter induction by 20 ng·mL<sup>-1</sup> tetracycline (Tc). The DTP repository number for each of the analogues is written in italics. Column heights represent mean MICs across three independent experiments with standard error bars shown. MICs greater than the highest concentrations tested were indicated with the caret symbol (^).

The sensitivity of the *katG<sub>sm</sub>* (*MSMEI\_6216*) overexpression strain to isoniazid following induction with tetracycline was assessed (Figure 5.4). The *katG<sub>sm</sub>* over-expression strain was four-fold more sensitive to isoniazid following vector induction.



**Figure 5.4: *katG<sub>sm</sub>* overexpression strain versus isoniazid.** MIC of isoniazid for the empty vector (EV) control strain MRC20 and *katG<sub>sm</sub>* overexpression strain, with and without promoter induction by 20 ng·mL<sup>-1</sup> tetracycline (Tc). Columns represent the mean MIC across three independent experiments with standard error bars shown.

The MICs of the six isoniazid analogues that *Tn::nudC* showed differential-sensitivity to were determined for the *katG<sub>sm</sub>* overexpression strain (Figure 5.5). The *katG<sub>sm</sub>* overexpression strain showed increased sensitivity to all six isoniazid analogues following vector induction with tetracycline. The *katG<sub>sm</sub>* overexpression strain was five-fold more sensitive to the isoniazid analogue 40350, three-fold more sensitive to the analogues 27607, 33759, 141142, and 176757, and 2.5-fold more sensitive to the analogue 37800 following vector promoter induction.



**Figure 5.5: *katG<sub>sm</sub>* overexpression strain versus isoniazid analogues.** MICs of isoniazid analogues and isoniazid (INH), for the *katG<sub>sm</sub>* overexpression strain, with and without vector promoter induction with 20 ng·mL<sup>-1</sup> tetracycline (Tc). Columns represent mean MIC values across three independent experiments with standard error bars shown.

### 5.1.2. Activity of isoniazid analogues in wild-type mycobacterial strains

The six isoniazid analogues that showed differential activity against *Tn::nudC* (Table 5.3) were re-tested against WT *M. smegmatis* mc<sup>2</sup>155 to determine their MICs. Preliminary testing was also carried out to determine the MIC of the isoniazid analogues for *M. tuberculosis* H<sub>37</sub>Rv (Table 5.4). For *M. smegmatis* mc<sup>2</sup>155, analogues 37800 and 40350 had low activity compared to isoniazid, with MICs that were approximately three-fold and seven-fold higher than the MIC of isoniazid. The remaining analogues showed activity comparable to isoniazid, with MICs within two-fold of the MIC of isoniazid. For *M. tuberculosis* H<sub>37</sub>Rv only the two analogues 141142 and 37800 had activities comparable to isoniazid, with MICs approximately two-fold higher than the MIC of isoniazid. The remaining analogues had MICs for *M. tuberculosis* that were at least 15-fold higher than that of isoniazid.

**Table 5.4: MICs of isoniazid analogues for WT *M. smegmatis* and *M. tuberculosis*.**

INH Analogue (NSC Number)	MIC $\pm$ se ( $\mu$ M)	MIC ( $\mu$ M)
	<i>M. smegmatis</i> mc <sup>2</sup> 155	<i>M. tuberculosis</i> H <sub>37</sub> Rv
27607	45.3 $\pm$ 0.00	363
33759	58.7 $\pm$ 19.5	312
37800	113 $\pm$ 0.00	28.4
40350	257 $\pm$ 85.8	172
141142	62.9 $\pm$ 21.0	21.0
176757	25.9 $\pm$ 0.00	207
9659 (isoniazid)	34.2 $\pm$ 11.4	11.4

MICs are presented for isoniazid and isoniazid analogues for WT *M. smegmatis* mc<sup>2</sup>155 and *M. tuberculosis* H<sub>37</sub>Rv. MICs for *M. smegmatis* represent mean MICs across three independent experiments with standard error (se) presented. MICs for *M. tuberculosis* H<sub>37</sub>Rv represent results from a single preliminary experiment.

## 5.4. Discussion

The first aim of this chapter was to characterise the cross-sensitivity of selected hypersensitive mutants identified in Chapter Three to other anti-mycobacterial drugs. The second aim was to investigate whether the hypersensitive mutants displayed differential-sensitivity to analogues of the drug that they were hypersensitive to. The sensitivities of relevant overexpression strains and of *M. tuberculosis* H<sub>37</sub>Rv were also determined for the isoniazid analogues that *Tn::nudC* demonstrated differential-sensitivity to, to further characterise their anti-mycobacterial activity.

### 5.4.1. Cross-sensitivity of hypersensitive transposon mutants

The two isoniazid, two rifampicin, and two bedaquiline hypersensitive mutants examined in this chapter were all tested for cross-sensitivity to the other two compounds of the three compounds used during the initial assay for drug hypersensitivity. None of the mutants examined showed cross-sensitivity to the other two drugs. This is in keeping with the fact that none of the mutant strains were identified in either the primary or secondary assays for drug hypersensitivity for more than one compound. These results indicate that the drug hypersensitivity of these six mutants is specific to the mode of action of these compounds,

rather than a generic mechanism of drug resistance across two or more of the three drugs used (isoniazid, rifampicin, and bedaquiline). This statement is supported by the known roles of NudC and Arr in isoniazid and rifampicin sensitivity, respectively, whereby both enzymes are involved in detoxification of a specific drug (Alexander et al., 2003; Dabbs et al., 1995; Wang et al., 2011). Furthermore, these findings validate the screening process undertaken in this study as a highly specific method to identify mutants hypersensitive to a specific drug.

#### **5.4.2. Differential-sensitivities of hypersensitive transposon mutants to drug analogues**

Differential-sensitivity of the transposon mutants to analogues of the three parent drugs indicates that the analogues have modified modes of action compared to the parent drug, or that the analogues carry modifications that enable them to resist specific detoxification mechanisms. In this thesis the differential-sensitivity of transposon mutants to drug analogues was defined as a greater than 1.5-fold difference in sensitivity to the analogue compared to the parent drug, where sensitivity was quantified in terms of the MIC ratio between the drug hypersensitive mutant and the random transposon control strain D11.

Investigation into differential-sensitivities of the rifampicin hypersensitive mutants *Tn::arr* and *Tn::MSMEI\_3093* revealed that these strains showed the same increase in sensitivity to rifapentine compared to the control strain D11 as they did to rifampicin. The finding that the relative sensitivities of the mutant strains were comparable for both drugs indicates that the genes containing the *Tn611* insertion or adjacent to the insertion in these strains play similar roles in the mode of action or detoxification for rifampicin and rifapentine. Specifically, these results indicate that Arr is able to ribosylate and thereby detoxify rifapentine as well as the parent compound rifampicin. This was expected because of the structural similarity between rifapentine and rifampicin, and the fact that rifapentine is used clinically instead of rifampicin due to its increased half-life in the patient over rifampicin, rather than because it has altered activity or a different mode of action against mycobacteria (Benator et al., 2002; Keung et al., 1999).

The isoniazid hypersensitive strain *Tn::nudC* was also tested against a range of isoniazid analogues for differential-sensitivity. A total of 30 isoniazid analogues were randomly



selected and obtained from the DTP repository, as well as a sample of isoniazid as a control, and tested against WT *M. smegmatis* mc<sup>2</sup>155 to confirm their activity. Analogues that inhibited growth of WT *M. smegmatis* mc<sup>2</sup>155 by at least 75%, at a concentration of 100 µg·mL<sup>-1</sup>, were chosen for further investigation. This initial experiment was performed to remove compounds with activities that were too low to be practical for determination of an MIC. Of the original 30 analogues, 14 analogues inhibited growth of WT *M. smegmatis* mc<sup>2</sup>155 by at least 75%, and interestingly all of these analogues shared the same basic structure, retaining the core isoniazid scaffold but with modification of a side chain, as depicted in Figure 5.1. Interestingly, of the 30 isoniazid analogues tested, 19 had the structure depicted in Figure 5.1. From examining the side chains of these 19 analogues, no common motifs distinguished the 14 analogues that had activity from the five analogues that did not. It is possible that the side chains of these analogues may facilitate or inhibit the interaction of the analogue with KatG, may alter drug permeability, or may act via a combination of these and other unknown factors.

The differential-sensitivity of the *Tn::nudC* strain to these 14 isoniazid analogues was tested by determining the MIC of these analogues for the *Tn::nudC* strain compared to the control strain D11. For isoniazid and eight of the analogues, *Tn::nudC* was approximately five-fold more sensitive than the D11 control strain. This suggests that these isoniazid analogues are acting in a similar manner to isoniazid, as had been predicted (section 5.1.1). Specifically, these results suggest that these analogues are interacting with NudC in the same way as isoniazid. Interestingly, *Tn::nudC* was only two – three-fold more sensitive than the control strain for six analogues (27607, 33759, 37800, 40350, 141142, and 176757). This suggests that the interaction between NudC and these six analogues is different to that of NudC and isoniazid. The finding that *Tn::nudC* was less sensitive than expected to these six analogues suggests that the protective role of NudC is less important for these six isoniazid analogues, and that its absence therefore has less of an effect on sensitivity. Interestingly, the isoniazid analogues that *Tn::nudC* showed differential-sensitivity to showed comparable activity to isoniazid (MICs within two-fold of the MIC of isoniazid), except for analogues 37800 and 40350, which were less active (three- and seven-fold increase in MIC compared to isoniazid). The role of NudC in resistance to the six analogues that *Tn::nudC* showed differential-sensitivity to was further investigated by overexpressing *nudC* in WT

*M. smegmatis* mc<sup>2</sup>155. These six analogues were also tested against the *inhA* overexpression strain to examine if they had a modified primary target as well as a loss of interaction with NudC.

Overexpression of *nudC* and *inhA* causes an increase in resistance to isoniazid by increasing the effective concentration of isoniazid needed to inhibit growth (Banerjee et al., 1994; Wang et al., 2011). In the present study it was found that overexpression of *nudC* or *inhA* had no effect on resistance to the isoniazid analogues 27607, 33759, and 40350. Combined with the lower than expected sensitivity of the *Tn::nudC* strain to these analogues, this finding suggests that NudC does not play a protective role for *M. smegmatis* mc<sup>2</sup>155 against these particular analogues. One possibility is that the side chains of these analogues may cause steric hindrance, preventing NudC from hydrolysing any NAD adducts formed by these analogues. Alternatively, analogues 27607, 33759, and 40350 may inhibit the growth of mycobacteria by a mechanism independent of an NAD adduct. Indeed, the finding that overexpression of *inhA* does not increase resistance to these analogues suggests that InhA is not involved in the mode of action of these analogues. As mentioned previously, WT *M. smegmatis* mc<sup>2</sup>155 was much less sensitive to analogue 40350 than isoniazid; however, analogues 27607 and 33759 showed activity in *M. smegmatis* similar to isoniazid which is to be expected if they are inhibiting the growth via a similar mode of action. Interestingly, the structures of analogues 27607 and 33759 have very similar side chains, differing only in the halogen atom (chlorine and bromine, respectively). It is possible that the side chains of these three analogues have anti-mycobacterial activity independent of the core isoniazid structure. An explanation for the InhA-independent activity of these three analogues is that they may inhibit the growth of *M. smegmatis* mc<sup>2</sup>155 via secondary targets that are also part of the isoniazid mode of action. It would be of value to test the other isoniazid hypersensitive mutants identified in this thesis against isoniazid analogues 27607, 33759, 40350 to determine whether any of these strains also show differential-sensitivity. However, this was considered outside the scope of the immediate study.

The analogues 27607, 33759, and 40350 appeared to inhibit the growth of *M. smegmatis* mc<sup>2</sup>155 in an NAD adduct independent manner. It has been demonstrated that the NudC of *M. tuberculosis* species cannot hydrolyse the INH-NAD adduct, and likely does not play a protective role in this species (Wang et al., 2011). However, the same study demonstrated

that NudC from *M. bovis* BCG can hydrolyse the INH-NAD adduct and therefore may play a protective role in this species. Consequently, these analogues may have potential therapeutic applications in the treatment of *M. bovis*, which is responsible for a proportion of human TB disease, as well as disease of economically important livestock (Michel et al., 2010). Additionally, these analogues may have potential therapeutic value in the treatment of clinical isoniazid resistant *inhA* mutant or *M. tuberculosis*. Further testing of the activity of these analogues against *M. bovis* or isoniazid resistant *M. tuberculosis* was considered outside the scope of the current study.

Overexpression of *nudC* or *inhA* resulted in increased resistance to analogues 37800, 141142, and 176757, indicating that these particular analogues are likely to be working via an NAD adduct and thus inhibiting the growth of *M. smegmatis* mc<sup>2</sup>155 in an InhA-dependant manner. The finding that the *Tn::nudC* strain showed less sensitivity to these analogues than expected can be explained by alternative detoxification mechanisms for these specific analogues.

#### **5.4.2.1. Role of KatG in activation of isoniazid analogues**

Isoniazid is a pro-drug that is activated by the catalase/peroxidase gene KatG. To test whether the isoniazid analogues were also activated by KatG, the sensitivity of a *katG* overexpression strain to these analogues was determined. Only the six isoniazid analogues that *Tn::nudC* showed differential-sensitivity to were tested against the *katG* overexpression strain. *M. smegmatis* mc<sup>2</sup>155 contains two copies of *katG* encoded by *MSMEI\_3380* and *MSMEI\_6216*; whereas, *M. tuberculosis* H<sub>37</sub>Rv only contains one copy of *katG*, encoded by *Rv1908c*. Alignment of the protein sequences of *MSMEI\_3380* and *MSMEI\_6216* with *Rv1908c* revealed that *MSMEI\_6216* showed greater amino acid identity with *Rv1908c*. *MSMEI\_6216* was therefore selected as the *katG* overexpression strain for use in this study as its higher protein similarity to the *M. tuberculosis* gene suggested it would be most likely have the isoniazid activating activity. Had this assumption been incorrect and the *MSMEI\_6216* overexpression strain not shown increased sensitivity to isoniazid then a *MSMEI\_3380* overexpression strain would have been used instead, or a *Rv1908c* overexpression strain. The gene sequence for *MSMEI\_6216* contains a *BamHI* site, which

was removed by introducing a silent mutation. The product of the modified *MSMEI\_6216* (*katG<sub>sm</sub>*) was able to activate isoniazid, as demonstrated by a four-fold increase in isoniazid sensitivity compared to the control strain. This result confirmed that the KatG enzyme encoded by *MSMEI\_6216* is capable of activating isoniazid and supported the initial selection of *MSMEI\_6216* for the *katG* overexpression assay.

With the exception of the analogue 40350, the *katG* overexpression strain showed comparable levels of increased sensitivity to all the isoniazid analogues tested, indicating KatG is able to activate all six analogues. However, the overexpression strain showed a much greater increase in sensitivity to 40350 than the other five analogues suggesting that the low activity of this analogue is primarily due to reduced activation by KatG, possibly due to steric hindrance of the long side chain. Interestingly, these results indicate that although the three analogues 27607, 33759, and 40350 appear to inhibit *M. smegmatis* mc<sup>2</sup>155 independent of an NAD adduct, KatG is still able to activate these analogues. Although not pursued in this thesis, it would be valuable to know whether loss of function KatG mutants show decreased sensitivity to these analogues to confirm whether KatG is required for their activation. The apparent InhA- and NudC-independent mode of action of the three analogues 27607, 33759, and 40350 supports the idea that KatG-activated isoniazid reacts with more cellular components than just InhA (Argyrou et al., 2006; Mdluli et al., 1996, 1998; Rickman et al., 2013; Timmins and Deretic, 2006). These analogues may therefore be useful tools for elucidating what these other activated products are, and the identity of their targets.

#### **5.4.3. Activity of isoniazid analogues against *M. tuberculosis***

Preliminary testing was performed to establish the sensitivity of *M. tuberculosis* H<sub>37</sub>Rv to the six isoniazid analogues that *Tn::nudC* showed differential-sensitivity to. The two analogues 37800 and 141142 showed activity similar to isoniazid, with MICs approximately two-fold greater than isoniazid. The remaining four analogues were inactive in *M. tuberculosis* H<sub>37</sub>Rv, with MICs greater than 15-fold higher than that of isoniazid. The analogue 141142 had the most similar structure to isoniazid; however, there was no obvious connection between the structure of the side chain and the activity of the analogues. The reason for the low activity of the remaining five analogues in *M. tuberculosis* H<sub>37</sub>Rv is unclear. However, further testing

of these analogues against *M. tuberculosis* is warranted to confirm the results from the single preliminary assay performed in this study.

#### 5.4.4. Summary

None of the hypersensitive mutants tested showed cross-sensitivity to either of the other two drugs tested in this study. This indicates that the sensitivity of these mutants is specific to the original drug used in the screening process. Additionally, the two mutants identified in Chapter Three as being most hypersensitive to rifampicin showed no differential-sensitivity to the rifampicin analogue rifapentine. The isoniazid hypersensitive mutant *Tn::nudC* showed differential activity to six of the isoniazid analogues tested. Three of the six analogues likely work via an NAD adduct in an InhA-dependent manner similar to isoniazid. However, another detoxification mechanism in addition to NudC is suspected to exist for these analogues. The remaining three analogues (27607, 33759, and 40350) likely act in an InhA-independent manner that does not involve the formation of an NAD adduct. One possibility is that these analogues are inhibiting the growth of *M. smegmatis* mc<sup>2</sup>155 by mechanisms specific to their side chains. Alternatively, these analogues may be acting via a secondary isoniazid mode of action. Interestingly the results presented here suggest that all of the six isoniazid analogues that demonstrated differential-activity against *Tn::nudC* can be activated by KatG, although it remains to be demonstrated if KatG is required for their activity. These results strongly support the concept that the mode of action of isoniazid is more complex than being mediated via inhibition of InhA alone. Furthermore, this study has identified three isoniazid analogues with apparent novel modes of action (27607, 33759, and 40350). These three analogues will be useful tools in elucidating the nature of the secondary targets of isoniazid, and may have therapeutic use in the treatment of *M. bovis* and isoniazid resistant *inhA* mutant strains of *M. tuberculosis*.

## 6. General Discussion

TB is the leading cause of morbidity and mortality by a bacterial pathogen, and there is a great need for the discovery of novel drugs that can shorten the treatment regimen, and effectively treat drug resistant cases, especially MDR-TB and XDR-TB (WHO, 2014). An important step in the drug discovery pathway is the identification of drug mode of action. Knowledge of drug mode of action enables rational modification of drugs to improve efficacy against both primary and secondary targets, and to decrease unwanted interactions or harmful side effects (Balganesh et al., 2008; Ioerger et al., 2013). To date, most studies investigating the modes of action of TB drugs have revolved around study of resistance-inducing mutations and altered transcription upon drug treatment, while little work had been done investigating mutations that induce hypersensitivity. Therefore, the aim of this thesis was to develop a high-throughput assay for identifying drug hypersensitive mutants of *M. smegmatis* mc<sup>2</sup>155 in order to study the genetic basis of the drug hypersensitivity and generate information on drug mode action.

The two front-line anti-TB drugs isoniazid and rifampicin, along with bedaquiline, which is currently in phase III clinical trials, were selected for further investigation into their modes of action in this study. These drugs were selected because their primary targets are known and therefore the identification of mutations in genes already known to be involved in the drug mode or action or resistance mechanisms would validate our high-throughput screening assay for hypersensitivity mutations. Isoniazid is a prodrug that inhibits InhA, inhibiting mycolic acid biosynthesis (Banerjee et al., 1994). Isoniazid is activated by the catalase/peroxidase enzyme KatG, and reacts with NAD to form the INH-NAD adduct which binds to and inhibits InhA (Johnsson and Schultz, 1994; Rozwarski et al., 1998; Wilming and Johnsson, 1999; Zhang et al., 1992). Rifampicin inhibits transcription by binding to and inhibiting the  $\beta$  subunit of RNA polymerase (RpoB) (Levin and Hatfull, 1993; Maggi et al., 1966; Wehrli et al., 1968). Bedaquiline inhibits the production of ATP by the ATP synthase, by binding to the C subunit of the F<sub>0</sub> domain of the ATP synthase (Andries et al., 2005; Koul et al., 2007).

To the best of my knowledge, one study utilising an assay to screen for mutations that induce hypersensitivity to rifampicin has been published, albeit using a different endpoint,

but no such studies have been published for isoniazid or bedaquiline. Therefore, it was expected that the assay for drug hypersensitivity used in this research would be able to identify genes not previously linked to isoniazid, rifampicin, or bedaquiline sensitivity. These genes may represent novel aspects of the known modes of action of these drugs, or completely novel modes of action. Both types of information can be used to improve our understanding of the complete modes of action of these drugs.

## **6.1. Research summary**

### **6.1.1. Isoniazid**

The assay for hypersensitivity successfully identified mutants with significantly increased sensitivity to isoniazid. The sensitivities of the 12 most hypersensitive mutants were quantified by MIC and subsequently the *Tn611* insertion sites were determined for these mutants. Three mutants were much more sensitive to isoniazid compared to the controls than the other hypersensitive mutant strains, with two of these mutants containing a *Tn611* insertion either within the *nudC* gene or in the adjacent gene *MSMEI\_1905*. Complementation analysis suggested that the isoniazid hypersensitivity of both of these strains was due to a loss of function of *nudC*, whose protein product, NudC, is a protein recently identified in the detoxification of isoniazid. NudC hydrolyses the INH-NAD adduct that is the active form of isoniazid (Wang et al., 2011). As expected, given the role of NudC in detoxifying the INH-NAD adduct, the *Tn::nudC* mutant did not show any cross-sensitivity to either rifampicin or bedaquiline. Therefore these results strongly support a role for NudC in basal isoniazid resistance, as opposed to general multi-drug resistance. The isoniazid hypersensitive *Tn::nudC* mutant from the current study was identified prior to the publication of the results by Wang et al. (2011) and provides independent confirmation of the proposed role of NudC in basal isoniazid resistance in *M. smegmatis* mc<sup>2</sup>155 (Wang et al., 2011).

The third isoniazid hypersensitive mutant that showed a large decrease in the MIC of isoniazid compared to the control had a *Tn611* insertion within a gene (*MSMEI\_6092*) likely to be involved in the oxidative stress response. This strain showed no cross-sensitivity to either rifampicin or bedaquiline, suggesting the mechanism of drug sensitisation is isoniazid

specific. Complementation of this strain was not performed due to toxicity of the complementation vector during plasmid subcloning in *E. coli*, and therefore it is not possible to say definitively whether loss of functional *MSMEI\_6092* is responsible for the isoniazid hypersensitivity of *Tn::MSMEI\_6092*. Interestingly, three other mutants with links to the oxidative stress response were identified in the assay for isoniazid hypersensitivity, although these mutants were not as sensitive as *MSMEI\_6092*. These mutants had insertions within or adjacent to the *ahpCD* locus, and two genetic loci involved in sulfur metabolism, a process closely linked to the oxidative stress response (Dussurget and Smith, 1998). It has previously been demonstrated that mutations that retard the oxidative stress response lead to increased isoniazid sensitivity due to a compensatory increase in the expression of other oxidative stress response genes, including *katG*, resulting in increased activation of isoniazid (Sherman et al., 1996). It seems likely that this mechanism is responsible for the isoniazid hypersensitivity of mutants identified in this thesis with *Tn611* insertions within or adjacent to genes linked to the oxidative stress response.

Interestingly, only one isoniazid hypersensitive mutant that had a mutation in a gene with links to the mycolic acid biosynthesis pathway, which isoniazid inhibits, was identified. While it is possible that the transposon mutant collection generated in this thesis only contained this one mutant with an insertion in a mycolic acid biosynthesis genetic pathway, sequencing the insertion site of more mutants may have identified more hypersensitive mutants with insertions in genes related to mycolic acid biosynthesis. Strains with mutations in the mycolic acid biosynthesis pathway may have been less sensitive to isoniazid than the 12 mutants selected for further characterisation. Future investigations into the insertion sites of the other isoniazid hypersensitive mutants will reveal whether this was the case. The remaining sequenced isoniazid hypersensitive mutants had no clear links to the drug's known mode of action, or known resistance mechanisms. These genes therefore represent novel aspects of the mode of action or resistance mechanisms of isoniazid, and further study into the nature of their interaction with isoniazid will improve our understanding of the complete isoniazid mode of action.



#### 6.1.1.1. Identification of isoniazid analogues with novel modes of action

The differential-sensitivity of the *Tn::nudC* mutant was determined for 14 isoniazid analogues active against *M. smegmatis* mc<sup>2</sup>155. All 14 analogues contained the core structure of isoniazid (Figure 5.1); the analogues that did not retain the core structure were found to be inactive against *M. smegmatis*. This indicates that these 14 analogues probably also retain the core mode of action of isoniazid, implicating the core structural component as an important part of the pharmacophore of the drug. The *Tn::nudC* mutant strain showed differential-sensitivity to six of the 14 isoniazid analogues, where the *Tn::nudC* strain was less sensitive to these analogues than expected. These six analogues were subsequently tested against an *inhA* and a *nudC* overexpression strain to investigate whether overexpression of these genes would lead to resistance to the analogues as it did for isoniazid. InhA is the primary target of isoniazid and its overexpression leads to isoniazid resistance. Three of these six analogues (37800, 141142, and 176757) appeared to still inhibit the growth of *M. smegmatis* mc<sup>2</sup>155 in an InhA-dependent manner despite the structural differences, as overexpression of InhA led to increased resistance to these three analogues. Additionally, these analogues appeared to inhibit growth via an INH-NAD adduct, as overexpression of NudC was able to increase resistance to these three analogues. These results, combined with the differential-sensitivity of *Tn::nudC* to these three analogues, suggests that while NudC can detoxify these analogues, it is not the only mechanism of detoxification as the *Tn::nudC* mutant showed little to no increase in sensitivity to these analogues.

The remaining three analogues (27607, 33759, and 40350) inhibited the growth of *M. smegmatis* mc<sup>2</sup>155 in an InhA-independent manner as overexpression of InhA did not increase the resistance of *M. smegmatis* mc<sup>2</sup>155 to these analogues. Additionally, NudC appeared unable to detoxify these analogues as overexpression of *nudC* did not increase the resistance of *M. smegmatis* mc<sup>2</sup>155 to these analogues. Combined with the differential-sensitivity of *Tn::nudC* to these analogues, these results suggest that these analogues are not inhibiting the growth of *M. smegmatis* mc<sup>2</sup>155 by inhibition of InhA, and not working via the INH-NAD adduct.

A *katG* overexpression strain had increased sensitivity to all six analogues suggesting that KatG was able to metabolically activate all six isoniazid analogues. Combined with the previous observations, these results suggest that the three analogues 27607, 33759, and 40350, which were inhibiting the growth of *M. smegmatis* mc<sup>2</sup>155 in an *InhA*-independent manner, were being activated by KatG to form growth-inhibitory metabolites other than the well characterised INH-NAD adduct. However, the *Tn::nudC* mutant still showed a slight increase in sensitivity to these analogues, suggesting at least some INH-NAD adduct may be being formed. Further studies of the growth inhibitory activity of these isoniazid analogues that are acting in an *InhA*-independent manner are warranted to determine their novel mechanisms of action, and to see where that mechanism of action overlaps with that of the parent compound.

Preliminary testing of the sensitivity of *M. tuberculosis* H<sub>37</sub>Rv was performed for the six analogues that *Tn::nudC* showed differential-sensitivity to, and the MIC values compared to their activities in *M. smegmatis* mc<sup>2</sup>155. There were large differences in the relative activities of the analogues between the two species, including the three analogues that appeared to inhibit *M. smegmatis* mc<sup>2</sup>155 in an *InhA*-independent manner, with only the analogues 37800 and 141142 showing any activity in *M. tuberculosis* H<sub>37</sub>Rv. These results suggest that the target of the three *inhA*-independent analogues (27607, 33759, and 40350) may not be present in *M. tuberculosis*. Interestingly, it has been previously demonstrated that there are differences in the effect of isoniazid on *M. smegmatis* and *M. tuberculosis*, suggesting that the mode of action of isoniazid differs slightly between these two species (Mdluli et al., 1996). The NudC enzyme of *M. tuberculosis* H<sub>37</sub>Rv lacks INH-NAD hydrolysing activity, and it is predicted that the NudC of a large number of clinical isolates may also lack this hydrolysing activity (Wang et al., 2011). Despite these differences between strains, isoniazid analogues 27607, 33759, and 40350 will be useful in investigating the aspects of isoniazid's mode of action outside of the inhibition of *InhA*. Additionally, these analogues may find use in the treatment of *M. bovis*, as the NudC enzyme of *M. bovis* BCG is able to hydrolyse the INH-NAD adduct, and may play a protective role in *M. bovis* against isoniazid (Wang et al., 2011). These analogues may also have potential therapeutic value in the treatment of isoniazid resistant *inhA* mutant strains of *M. tuberculosis*.

### 6.1.2. Rifampicin

The assay for hypersensitivity successfully identified mutants with increased sensitivity to rifampicin. The *Tn611* insertion sites were successfully determined for 11 of the 12 most sensitive mutants validated in the secondary assay, and the hypersensitivities of these 12 mutants were quantified by MIC. Of these 12 mutants none showed any links to the known mode of action of rifampicin, and only three mutants had links to known rifampicin resistance mechanisms: Arr, an enzyme involved in a known rifampicin inactivation mechanism, PonA2, an enzyme involved in cell wall stability whose absence results in increased sensitivity to a range of lipophilic drugs including rifampicin, and the lipoprotein signal peptidase LspA. Two mutants had *Tn611* insertions within two different multi-copy transposase genes, but which copies contained the *Tn611* insertions, and therefore the genetic basis for the rifampicin hypersensitivity of these two mutants remains unknown. The remaining seven rifampicin hypersensitive mutants sequenced had insertions in genes with no clear links to the known mode of action of rifampicin or any of its known resistance mechanisms. These genes therefore represent novel mechanisms, and further study into the nature of their interaction with rifampicin will improve our understanding of the complete rifampicin mode of action. Of particular interest were two genes functionally related to the ESX-1 locus identified as containing *Tn611* insertions in rifampicin hypersensitive mutants. The ESX-1 locus has not previously been implicated in the rifampicin mode of action or detoxification mechanism. These results therefore suggest a novel role for the ESX-1 locus in the rifampicin mode of action or detoxification pathways.

Rifampicin inhibits the RNA polymerase  $\beta$  subunit (RpoB), inhibiting RNA transcription. Interestingly, none of the rifampicin hypersensitive mutants that were sequenced had mutations in genes that were known to be involved in transcription. This may suggest that these genes are essential in *M. smegmatis* mc<sup>2</sup>155, and therefore mutants of these genes would not have been present in the transposon mutant collection constructed in this thesis. Alternatively, sequencing of more of the rifampicin hypersensitive mutants may have revealed mutants with insertions in genes related to transcription.

The two mutants most sensitive to rifampicin identified in Chapter Three were *Tn::arr* and *Tn::MSMSEI\_3093*, which were eight- and four-fold more sensitive than the control strain,

respectively. *Tn::MSMEI\_3093* contained a *Tn611* insertion in the pseudouridine synthase D gene, which modifies selected uridine residues of the rRNA. *Tn::arr* was not complemented in this thesis as its involvement in rifampicin resistance in *M. smegmatis* is already well characterised. Complementation was also not performed for *Tn::MSMEI\_3093* due to an inability to generate a control strain for complementation and therefore the exact mechanism for this strain's rifampicin hypersensitivity remains unclear. However, it is possible that the rifampicin sensitivity may be due to altered transcription of the adjacent lipoprotein signal peptidase gene *lspA* rather than a loss of function of *MSMEI\_3093*. Overexpression of *lspA* in *M. tuberculosis* has previously been shown to increase resistance to both rifampicin and isoniazid (Pathak, 2013). Interestingly, the transposon mutant *Tn::MSMEI\_3093* did not show cross-sensitivity to isoniazid in this thesis, suggesting that altered transcription of *lspA* may not be responsible for the rifampicin hypersensitivity of this strain. Alternatively, a loss of *LspA* function may cause increased rifampicin sensitivity but not increased isoniazid sensitivity. The two strains, *Tn::arr* and *Tn::MSMEI\_3093*, were also examined for differential-sensitivity to rifapentine, an analogue of rifampicin. Both strains showed equal increases in sensitivity to rifapentine as they did to rifampicin, indicating that the role of these genes in the mode of action or resistance of rifampicin is conserved in rifapentine. Specifically, these results indicate that Arr can inactivate rifapentine, as well as its parent compound, rifampicin.

### 6.1.3. Bedaquiline

The assay for hypersensitivity successfully identified mutants with increased sensitivity to bedaquiline. The *Tn611* insertion sites were determined for eight of the 12 most sensitive mutants validated in the secondary assay, and the hypersensitivity of these 12 mutants were quantified by MIC. Of the eight mutants that the insertion site was identified for, one had a *Tn611* insertion in *mmpL5*, which encodes the transmembrane transporter MmpL5 which is known to be involved in bedaquiline detoxification (Andries et al., 2014; Hartkoorn et al., 2014). An additional validated mutant had an insertion in *atpB*, a gene that encodes the A subunit of the F<sub>0</sub> ATP synthase domain. Although this mutant was not one of the top bedaquiline sensitive strains, it was included in this thesis because *atpB* is related to the

known mode of action of bedaquiline. The work on bedaquiline was performed in collaboration with Professor Greg Cook's research group at the University of Otago. The *Tn::atpB* mutant was identified in the primary assay for drug hypersensitivity, and was not one of the 12 most sensitive mutants further characterised in this thesis. However, a number of mutant strains that were identified in the primary screen of this thesis were sent to Professor Cook, who sequenced them and identified the *Tn611* insertion site in the *Tn::atpB* mutant. Once identified it was decided to include *Tn::atpB* with the 12 most sensitive mutants for further characterisation.

Neither the most bedaquiline hypersensitive mutant, which contained a *Tn611* insertion in a glutamyl peptidase gene (*MSMEI\_3189*), nor the *Tn::atpB* mutant showed cross-sensitivity to either isoniazid or rifampicin. This result for the *Tn::atpB* mutant was expected, as it is known that the ATP synthase is related to the specific target of bedaquiline. Although the mechanism of bedaquiline hypersensitivity of the *Tn::MSMEI\_3189* mutant is unclear, it appears to be specific to bedaquiline.

## **6.2.Critical evaluation of methodology**

### **6.2.1. Limitation of using *M. smegmatis* mc<sup>2</sup>155 as the genetic model**

*M. smegmatis* mc<sup>2</sup>155 was chosen as a genetic model for investigating anti-TB drug modes of action, primarily due to the time benefits the species provides over the slow growing models *M. bovis* BCG and *M. tuberculosis* H<sub>37</sub>Ra. The fast growth rate of *M. smegmatis* increased the rate that the initial transposon mutants could be generated and then subsequently screened for drug hypersensitivity. This time benefit was offset, however, by the increased genetic differences between *M. tuberculosis* and the slow growing models such as *M. bovis* BCG. Therefore, any information on the mode of action generated from a study using *M. smegmatis* ultimately needs to be confirmed in *M. tuberculosis*. It has previously been proposed that one of the benefits of using *M. smegmatis* as a model is that it has a similar drug resistance profile as MDR-TB (Chaturvedi et al., 2007). However, the underlying genetic bases for these similar resistance phenotypes are very different. *M. smegmatis* contains drug detoxification mechanisms that *M. tuberculosis* does not have.

For example, both Arr and NudC, which were identified in this study, are mechanisms of drug detoxification present in *M. smegmatis* but not *M. tuberculosis*.

The aim of this study was not to identify specific genes involved in the drug resistance phenotype, but rather to identify pathways that were sensitised to the drugs due to the presence of transposon insertions in their genes. This was achieved for isoniazid whereby multiple genes were identified that related to the oxidative stress response, and for rifampicin whereby two genes related to the ESX-1 locus were identified. However, the bedaquiline hypersensitive mutants did not reveal any such pattern of genes in a particular pathway. As discussed below, this may be a limitation of the number of mutants sequenced or the coverage of the library. An additional factor, however, is that the genome of *M. smegmatis* is not completely annotated, with numerous hypersensitive mutants identified in this study containing insertions in conserved, but hypothetical genes. This lack of annotation confounds the results as these genes with unknown function may be involved in the pathways of interest. Without better gene annotations it is not possible to determine from the literature if this is the case. The genomes of both *M. tuberculosis* and *M. bovis* are much better annotated and had the transposon mutant collection been constructed in one of these two species it would likely have been much easier to determine the role of any specific gene product. This situation is expected to improve with time as more of the genome of *M. smegmatis* mc<sup>2</sup>155 is annotated.

### **6.2.2. Use of *Tn611* for transposon mutagenesis**

One of the advantages of random transposon mutagenesis is that the nature of the mutation is consistently a loss of function (Guilhot et al., 1994). However, after determining the transposon insertion sites for the drug hypersensitive mutants identified in this study, it was apparent that *Tn611* also exerts a significant polar effect on the surrounding genes. Specifically, the *Tn611* insertion in *MSMEI\_1905* had a polar effect on the adjacent *nudC* gene. Additionally, a number of hypersensitive mutants were identified that had intergenic *Tn611* insertions. Thus, mutants within the collection may have altered transcription of more than one genetic locus, with the potential for the hypersensitivity to be due to the combined effect, as opposed to due to loss of function of a single gene product. This altered

transcription could be down-regulation of adjacent genes or up-regulation driven by transposon internal promoters (Berg et al., 1980; Ciampi et al., 1982). To the best of my knowledge, little or no work has been done investigating the nature of the *Tn611* insertion and its potential polar effects. Because most of the hypersensitive mutants identified in this study were not complemented, it is difficult to say with any certainty what the specific genetic basis for drug hypersensitivity was for all mutants other than the complemented *Tn::nudC* mutants.

Another limitation with the *Tn611* transposon is that to the best of my knowledge the sequence into which it inserts has not been characterised. Although this transposon has previously been reported to insert in a random manner, and appears to provide good genome coverage, no studies as to which genes it can insert into have been performed. Most studies utilising transposon mutants now use a phage based transposon (*Himar1*), both for mutagenesis of *M. smegmatis* and *M. tuberculosis* (Siegrist and Rubin, 2009). The sequence where this transposon can be inserted has been characterised and, at least for *M. tuberculosis*, the genes that this transposon can insert into have been determined (Griffin et al., 2011; Sassetti et al., 2001, 2003). To the best of my knowledge no such information exists for *Tn611*. The *Tn611* transposon was used for this study as attempts to generate transposon mutants with another phage-based system were unsuccessful, and the plasmid based system of *Tn611* mutagenesis was found to be much easier for generating mutants. However, in hindsight, utilisation of the phage-based transposon *Himar1* would have been advantageous as it is much better characterised than *Tn611*.

#### **6.1.1. Transposon mutant collection coverage**

Transposon insertions inherently label the site of the genetic lesion responsible for the mutant phenotype, enabling rapid identification of the phenotype's genetic basis. For this reason, random transposon mutagenesis is routinely employed for generating collections of random mutants of mycobacteria (both *M. smegmatis* and *M. tuberculosis*) for phenotypic screening. Another characteristic of transposon mutagenesis is the largely consistent nature of the mutations generated, in which insertion within a gene results in a loss of function mutation (Guilhot et al., 1994). However, this is also a major limitation of the approach in

that only genes that are non-essential for the conditions being used can sustain transposon insertions. Mutants with insertions in genes that are essential under normal growth conditions will not be present in a random transposon mutant collection; therefore, these essential genes cannot be queried in phenotypic screening. However, the advantage of being able to rapidly identify the site of the mutation makes transposon mutagenesis a valuable methodology. As mentioned above, gene essentiality may be the reason mutants were not identified in the isoniazid or rifampicin screens that had transposon insertions within or adjacent to genes involved in fatty acid biosynthesis and transcription, respectively. The calculations estimating mutant collection coverage (section 3.2.1) assumed that the proportion of genes essential in *M. smegmatis* mc<sup>2</sup>155 was the same as that for *M. tuberculosis*. An alternate method would have been to assume that the number of essential genes was consistent between the two species. The former option was selected as it would likely result in an underestimation of the number of essential genes, and it was decided this was preferable to an overestimation. This likely resulted in a slightly larger collection that had a higher genome coverage (and therefore more redundancy), which was preferable to a smaller collection with a lower genome coverage. The number of essential genes in *M. smegmatis* mc<sup>2</sup>155 may actually be smaller than that of *M. tuberculosis* since significant portions of the *M. smegmatis* mc<sup>2</sup>155 genome are duplicated. At least one gene that is essential in *M. tuberculosis*, *atpD*, is apparently non-essential in *M. smegmatis* mc<sup>2</sup>155 due to multiple gene copies (Tran and Cook, 2005). The gene *atpB*, which was found to play a role in bedaquiline hypersensitivity, is in the same genetic region as *atpD* and may also be duplicated in the genome of *M. smegmatis* mc<sup>2</sup>155.

Another limitation of the transposon mutant collection is that collection's size is related to the genomic coverage. As the transposition is random, the distribution of the insertion sites follows a normal distribution. It was predicted that the collection of 7680 mutants created in this thesis, which has approximately 1.1-fold genome coverage, would contain at least one transposon mutant for 73.2% of the non-essential genes. The implication of this is that 26.8% of the non-essential *M. smegmatis* mc<sup>2</sup>155 genes are predicted to be excluded from the transposon mutant collection. These missing genes potentially include those related to the mode of action or resistance mechanisms of the drugs screened in this study, and may partially be responsible for the absence of mutants with insertions in pathways related to



the respective drugs modes of action. The size of the collection created in the current study was chosen for a relatively high level of coverage while keeping the collection small enough to allow high-throughput screening. Increasing the size of the collection, and therefore its coverage, would have reduced the impact the incompleteness of the mutant collection had on the results of the hypersensitivity assays, potentially increasing the number of mutants identified as hypersensitive to each drug.

### **6.1.2. Quantifying mutant hypersensitivity**

Quantification of the drug sensitivity of mutants validated in the secondary assay revealed that these mutants showed approximately two-fold or less increases in MIC compared to the controls, with the exception of the three and two most sensitive mutants from the isoniazid and rifampicin assays, respectively. As the variation in MIC was relatively small between the majority of validated hypersensitive mutants and the control strains, only the most sensitive mutants from each drug's assay were selected for complementation. Selection of only the most sensitive mutants allowed for clearer results in the complementation experiments as it was easier to determine if complementation was able to partially or completely restore WT sensitivity. Similarly, only the most sensitive mutants were selected for cross-sensitivity and differential-sensitivity testing. MICs are commonly used as the quantitative metric of drug sensitivity in the literature when discussing the sensitivity or resistance of mycobacteria to drugs and therefore were also used in this study. It was found in this thesis, however, that using MICs was not a very sensitive metric, with many of the dose-response assays showing variation close to the dilution factor used during serial dilution of the drugs (two-fold). This may have been mitigated by using smaller dilutions resulting in an improvement of the dose-response assay variation.

The recovery of mutants with only small changes in drug MIC may correlate with the essentiality of those genes. This is corroborated by the fact that no genes that are known to be directly involved in the known modes of action of isoniazid or rifampicin were identified. It may be the genes involved in the drug mode of action are essential, meaning that only mutations in genes that were less directly involved in drug mode of action were present in the collection. A strain containing a *Tn611* insertion in *atpB* which is known to be involved in

the mode of action of bedaquiline was probably only recovered because of its duplication in the genome. Interestingly, a previous study of rifampicin hypersensitive transposon mutants of *M. smegmatis* mc<sup>2</sup>155 identified a *Tn::arr* mutant similar to the one isolated in the present study (Alexander et al., 2003). However, this previously described *Tn::arr* mutant showed a 16-fold increase in MIC, compared to the eight-fold increase in MIC observed in this study. The major difference between these two studies was the use of transposon *Tn611* in the present study and the *Himar1* transposon in the study by Alexander et al. (2003) both transposons were delivered via temperature-sensitive delivery vectors; however, the non-permissive temperature for the *Tn611* delivery vector was 41 °C compared to 37 °C for the *Himar1* delivery vector (Siegrist and Rubin, 2009). Therefore, the rifampicin sensitivity of the *Himar1* *Tn::arr* mutant was assessed at 37 °C, while all assays of *Tn611* mutants were performed at 41 °C in our study. This higher temperature may also be responsible for the observed low level of sensitivity of the isolated drug hypersensitive mutants. This highlights another reason why the use of a *Himar1*-based transposon would have been advantageous over the use of *Tn611*.

### **6.1.3. Transposon mutant controls**

In the primary assay for drug hypersensitivity, the sensitivity of the mutants was expressed relative to the median sensitivity of the transposon mutant libraries, as it was assumed that the majority of mutants would have no increased sensitivity to the drug of interest. For the lower throughput secondary assay, the sensitivity of the mutants was validated, with the mutants ordered from most to least sensitive according to their growth-inhibition. Before further phenotypic and genotypic characterisation of the mutants, the hypersensitivities of the mutant strains were quantified using the MIC of the relevant drug. The selected control scheme was to use 10 mutant strains randomly selected from the mutant libraries, with the MICs of isoniazid, rifampicin, and bedaquiline averaged over the 10 strains. While WT *M. smegmatis* mc<sup>2</sup>155 or WT *M. smegmatis* mc<sup>2</sup>155 carrying a multi-copy plasmid with a kanamycin resistance gene were considered for the controls for this experiment, these strains would likely have had differing sensitivities to kanamycin compared with the transposon mutant strains. It is possible that the presence of kanamycin was altering the

absolute sensitivity of the transposon mutants to the antibiotics, and therefore ideally the control should have the same level of kanamycin sensitivity as the transposon mutants. This condition was met by utilising random transposon mutant strains as the controls. It was expected that the chance of any one of the random transposon mutants selected as controls being hypersensitive or resistant to the drugs was low. Averaging the MICs for each drug across all 10 strains would compensate for any one strain that showed an altered sensitivity. When testing the differential-sensitivity of the strains against various analogues, only one of the 10 mutant strains was used due to the logistics of the assay and the large number of analogues screened. This strain, D11, showed a similar MIC for all three original drugs compared to the other 9 random control strains and therefore it was assumed that D11 would also show similar sensitivity to all the drug analogues. It would have been advantageous to have a WT control that had a single copy of extra-chromosomally encoded *aph*, the kanamycin resistance gene, so that no assumptions needed to be made about the requirement of any of the genes in the random transposon mutant controls for drug sensitivity or resistance.

## **6.2.Future directions**

The work in this thesis has identified many novel genes that confer hypersensitivity and are potentially involved in the known modes of action or detoxification pathways of isoniazid, rifampicin, and bedaquiline. In addition, potential novel modes of action or detoxification pathways were identified, with numerous future directions for this research.

- Completion of the sequencing and complementation of the isoniazid, rifampicin, and bedaquiline hypersensitive mutants identified in this study, as well as constructing knock-out mutants of genes containing *Tn611* insertions. This would enable confirmation of the genetic basis for the hypersensitivity of these mutants. Better understanding of the genotypic basis would further improve our understanding of the complete modes of action of isoniazid, rifampicin, and bedaquiline facilitating rational drug design to improve drug treatment of TB.
- Expansion of the transposon mutant collection beyond 1.1-fold genome coverage, and screening the additional mutants against isoniazid, rifampicin, and bedaquiline

would likely provide additional information on the mode of action of these drugs. Expansion of the library to three-fold coverage would mean that approximately 95% of the genes (versus 73.2% currently) predicted to be non-essential in *M. smegmatis* would be represented in the mutant collection. Further screening of isoniazid, rifampicin, and bedaquiline, would enable the identification of more novel genes in the modes of action or resistance mechanisms of these compounds, additional to those already identified in this thesis.

- The drug hypersensitive phenotype of many of the mutants identified in this study may not directly be due to a loss of function of the gene containing the transposon, but rather as a result of a perturbation in the genetic networks interacting with the drug target. These genetic networks include genes that are functionally related to the target such as those encoding other components of the targets functional pathway, regulators of the components of the targets functional pathway, as well as genes encoding enzymes that provide functional redundancy for components of the target pathway. Genetic interaction studies would reveal how the genes identified as containing transposon insertions in the drug hypersensitive mutants are interacting with the drug target or innate resistance mechanisms. Genetic interaction studies can be performed by studying synthetic lethality, where two viable single mutants are combined to produce a non-viable double mutant (Joshi et al., 2006; Ooi et al., 2006). This loss of viability indicates the two gene containing mutations have a genetic interaction. By generating collections of these double mutants a map of genetic interactions can be generated and used to identify functional relationships. Recent advances in the efficiency of generating targeted knock out mutations using allelic exchange in mycobacteria is making studies of genetic interactions more viable (Tufariello et al., 2014). This approach could be used to introduce secondary mutations into the transposon mutant collection in genes identified in this study as being involved in drug hypersensitivity to map their genetic interaction networks, and understand their functional relationship to the drug target or innate resistance mechanisms.
- This study has demonstrated the power of screening for hypersensitivity in identifying genes related to the modes of action and resistance mechanisms of anti-mycobacterial compounds. Therefore, future research using the assay developed

in this thesis with novel anti-mycobacterial compounds would facilitate identification of their mode of action. Identification of the modes of action of novel anti-mycobacterials would enable the prioritisation of compounds with novel modes of action. Additionally, knowledge of the novel compounds modes of action would allow for rational modifications to improve their efficacy against TB. This would facilitate the discovery of new drugs with novel modes of action, and ultimately lead to an improvement in treatment of TB including MDR-TB.

- This study also identified three analogues of isoniazid that appear to inhibit the growth of *M. smegmatis* mc<sup>2</sup>155 independent of the known target or isoniazid, InhA. Future work to identify the primary targets of these analogues may identify a novel drugable target in mycobacteria. Investigation into the cross-sensitivity of the target of these three analogues to isoniazid, will determine whether the primary target of these analogues is a secondary target for isoniazid. The identification of a secondary target for isoniazid would enable rational design of co-treatment options to improve the efficacy of isoniazid therapy of TB.

### 6.3.Conclusions

The aim of this thesis was to generate information on anti-TB drug mode of action by identifying the genetic basis of drug hypersensitivity in mutants of *M. smegmatis* mc<sup>2</sup>155. The screening of a transposon mutant collection for isoniazid, rifampicin, and bedaquiline hypersensitive mutants confirmed a recently identified novel isoniazid resistance mechanism involving NudC detoxification, and highlighted a number of potentially new aspects of the modes of action of detoxification mechanisms for these drugs in *M. smegmatis* mc<sup>2</sup>155. Additionally, this thesis demonstrated that analogues of current anti-TB drugs with modified modes of action with potential therapeutic use can be identified by integrating genetic information from a screen for hypersensitivity with chemical derivatisation. Specific outcomes from this thesis were:

- Novel genes that were related to the modes of action and resistance mechanisms of isoniazid, rifampicin, and bedaquiline were identified. This included genes related to the oxidative stress response that were identified in isoniazid hypersensitive

mutants; and of particular interest, two genes (*espR* and *MSMEI\_5621*) related to ESX-1 that were identified as containing *Tn611* insertions in rifampicin hypersensitive mutants.

- NudC is responsible for detoxifying isoniazid, whereby a *Tn::nudC* mutant of *M. smegmatis* mc<sup>2</sup>155 is hypersensitive to isoniazid and overexpression of NudC in *M. smegmatis* mc<sup>2</sup>155 increases the MIC over 100-fold. This independently verifies the results of Wang et al. (2011)
- The rifampicin ribosylating enzyme Arr, which can inactivate rifampicin, appears capable of also inactivating rifapentine, an analogue of rifampicin
- The isoniazid analogues NSC27607, NSC33759, and NSC40350 appear to inhibit the growth of *M. smegmatis* mc<sup>2</sup>155 via a novel, *InhA*-independent, mode of action, with activity comparable to the parent drug in *M. smegmatis* mc<sup>2</sup>155. These analogues may have potential therapeutic use in the treatment of infections by *M. bovis* or isoniazid resistant *inhA* mutant strains of *M. tuberculosis*
- Resazurin reduction is a valid surrogate for high-throughput screening of growth-inhibition of *M. smegmatis* mc<sup>2</sup>155 when paired with a secondary OD<sub>600</sub> based validation assay



## 7. References

- Abrahams, G.L., Kumar, A., Savvi, S., Hung, A.W., Wen, S., Abell, C., Barry III, C.E., Sherman, D.R., Boshoff, H.I.M., and Mizrahi, V. (2012). Pathway-selective sensitization of *Mycobacterium tuberculosis* for target-based whole-cell screening. *Chem. Biol.* **19**, 844–854.
- Acocella, G., Pagani, V., Marchetti, M., Baroni, G.C., and Nicolis, F.B. (1971). Kinetic studies on rifampicin. *Chemotherapy* **16**, 356–370.
- Adindla, S., Inampudi, K.K., Guruprasad, K., and Guruprasad, L. (2004). Identification and analysis of novel tandem repeats in the cell surface proteins of archaeal and bacterial genomes using computational tools. *Comp. Funct. Genomics* **5**, 2–16.
- Adler, J.J., and Rose, D.N. (1996). Transmission and pathogenesis of tuberculosis. *Tuberculosis* **1**, 1002.
- Alderton, H., and Smith, D. (2001). Safety in the laboratory. In *Mycobacterium Tuberculosis Protocols*, T. Parish, and N.G. Stoker, eds. (Humana Press), pp. 367–383.
- Alexander, D.C., Jones, J.R.W., and Liu, J. (2003). A rifampin-hypersensitive mutant reveals differences between strains of *Mycobacterium smegmatis* and presence of a novel transposon, IS1623. *Antimicrob. Agents Chemother.* **47**, 3208–3213.
- Allen, B.W. (1998). *Mycobacteria: General Culture Methodology and Safety Considerations*. In *Mycobacteria Protocols*, (New Jersey: Humana Press), pp. 15–30.
- Altaf, M., Miller, C.H., Bellows, D.S., and O'Toole, R. (2010). Evaluation of the *Mycobacterium smegmatis* and BCG models for the discovery of *Mycobacterium tuberculosis* inhibitors. *Tuberculosis* **90**, 333–337.
- Andries, K., Verhasselt, P., Guillemont, J., Göhlmann, H.W.H., Neefs, J.-M., Winkler, H., Gestel, J.V., Timmerman, P., Zhu, M., Lee, E., et al. (2005). A diarylquinoline drug active on the ATP synthase of *Mycobacterium tuberculosis*. *Science* **307**, 223–227.
- Andries, K., Villellas, C., Coeck, N., Thys, K., Gevers, T., Vranckx, L., Lounis, N., de Jong, B.C., and Koul, A. (2014). Acquired resistance of *Mycobacterium tuberculosis* to bedaquiline. *PLoS ONE* **9**, e102135.
- Anton, V., Rougé, P., and Daffé, M. (1996). Identification of the sugars involved in mycobacterial cell aggregation. *FEMS Microbiol. Lett.* **144**, 167–170.
- Argyrou, A., Vetting, M.W., Aladegbami, B., and Blanchard, J.S. (2006). *Mycobacterium tuberculosis* dihydrofolate reductase is a target for isoniazid. *Nat. Struct. Mol. Biol.* **13**, 408–413.
- Azad, M.A., and Wright, G.D. (2012). Determining the mode of action of bioactive compounds. *Bioorg. Med. Chem.* **20**, 1929–1939.



- Bacon, J., and Hatch, K.A. (2009). Continuous culture of mycobacteria. In *Mycobacteria Protocols*, T. Parish, and A.C. Brown, eds. (Humana Press), pp. 153–171.
- Baker, M.A., Harries, A.D., Jeon, C.Y., Hart, J.E., Kapur, A., Lönnroth, K., Ottmani, S.-E., Goonesekera, S.D., and Murray, M.B. (2011). The impact of diabetes on tuberculosis treatment outcomes: A systematic review. *BMC Med.* 9, 81.
- Balganesh, T.S., Alzari, P.M., and Cole, S.T. (2008). Rising standards for tuberculosis drug development. *Trends Pharmacol. Sci.* 29, 576–581.
- Banerjee, A., Dubnau, E., Quemard, A., Balasubramanian, V., Um, K.S., Wilson, T., Collins, D., Lisle, G. de, and Jr., W.R.J. (1994). *inhA*, a gene encoding a target for isoniazid and ethionamide in *Mycobacterium tuberculosis*. *Science* 263, 227–230.
- Bardarov, S., Kriakov, J., Carriere, C., Yu, S., Vaamonde, C., McAdam, R.A., Bloom, B.R., Hatfull, G.F., and Jacobs, W.R. (1997). Conditionally replicating mycobacteriophages: a system for transposon delivery to *Mycobacterium tuberculosis*. *Proc. Natl. Acad. Sci.* 94, 10961–10966.
- Bassett, I.M., Lun, S., Bishai, W.R., Guo, H., Kirman, J.R., Altaf, M., and O'Toole, R.F. (2013). Detection of inhibitors of phenotypically drug-tolerant *Mycobacterium tuberculosis* using an in vitro bactericidal screen. *J. Microbiol.* 51, 651–658.
- Belanger, A.E., Besra, G.S., Ford, M.E., Mikusová, K., Belisle, J.T., Brennan, P.J., and Inamine, J.M. (1996). The *embAB* genes of *Mycobacterium avium* encode an arabinosyl transferase involved in cell wall arabinan biosynthesis that is the target for the antimycobacterial drug ethambutol. *Proc. Natl. Acad. Sci. U. S. A.* 93, 11919–11924.
- Benator, D., Bhattacharya, M., Bozeman, L., Burman, W., Cantazaro, A., Chaisson, R., Gordin, F., Horsburgh, C.R., Horton, J., Khan, A., et al. (2002). Rifapentine and isoniazid once a week versus rifampicin and isoniazid twice a week for treatment of drug-susceptible pulmonary tuberculosis in HIV-negative patients: a randomised clinical trial. *Lancet* 360, 528–534.
- Bentrup, K.H. zu, and Russell, D.G. (2001). Mycobacterial persistence: adaptation to a changing environment. *Trends Microbiol.* 9, 597–605.
- Berg, D.E., Weiss, A., and Crossland, L. (1980). Polarity of Tn5 insertion mutations in *Escherichia coli*. *J. Bacteriol.* 142, 439–446.
- Bernstein, J., Lott, A., Steinberg, B., and Yale, H. (1952). Chemotherapy of experimental tuberculosis. *Am Rev Tuberc* 357–374.
- Betts, J.C., Lukey, P.T., Robb, L.C., McAdam, R.A., and Duncan, K. (2002). Evaluation of a nutrient starvation model of *Mycobacterium tuberculosis* persistence by gene and protein expression profiling. *Mol. Microbiol.* 43, 717–731.
- Billman-Jacobe, H., Sloan, J., and Coppel, R.L. (2006). Analysis of isoniazid-resistant transposon mutants of *Mycobacterium smegmatis*. *FEMS Microbiol. Lett.* 144, 47–52.

Blokpoel, M.C.J., Murphy, H.N., O'Toole, R., Wiles, S., Runn, E.S.C., Stewart, G.R., Young, D.B., and Robertson, B.D. (2005). Tetracycline-inducible gene regulation in mycobacteria. *Nucleic Acids Res.* 33, e22.

Boshoff, H.I.M. (2004). The Transcriptional Responses of *Mycobacterium tuberculosis* to Inhibitors of Metabolism: Novel insights into drug mechanisms of action. *J. Biol. Chem.* 279, 40174–40184.

Bowman, J., and Ghosh, P. (2014). A complex regulatory network controlling intrinsic multidrug resistance in *Mycobacterium smegmatis*: Regulation of *M. smegmatis* drug resistance. *Mol. Microbiol.* 91, 121–134.

Brennan, P.J. (2003). Structure, function, and biogenesis of the cell wall of *Mycobacterium tuberculosis*. *Tuberculosis* 83, 91–97.

Brosch, R., Gordon, S.V., Garnier, T., Eiglmeier, K., Frigui, W., Valenti, P., Santos, S.D., Duthoy, S., Lacroix, C., Garcia-Pelayo, C., et al. (2007). Genome plasticity of BCG and impact on vaccine efficacy. *Proc. Natl. Acad. Sci.* 104, 5596–5601.

Brown, A.C., and Parish, T. (2006). Instability of the acetamide-inducible expression vector pJAM2 in *Mycobacterium tuberculosis*. *Plasmid* 55, 81–86.

Brown, C.A., Draper, P., and Hart, P.D. (1969). *Mycobacteria* and lysosomes: A paradox. *Nature* 221, 658–660.

Bucher, H.C., Griffith, L.E., Guyatt, G.H., Sudre, P., Naef, M., Sendi, P., and Battegay, M. (1999). Isoniazid prophylaxis for tuberculosis in HIV infection: a meta-analysis of randomized controlled trials. *Aids* 13, 501–507.

Bull, T.J., Hermon-Taylor, J., Pavlik, I., El-Zaatari, F., and Tizard, M. (2000). Characterization of IS900 loci in *Mycobacterium avium* subsp. paratuberculosis and development of multiplex PCR typing. *Microbiology* 146, 2185–2197.

Campbell, E.A., Korzheva, N., Mustaev, A., Murakami, K., Nair, S., Goldfarb, A., and Darst, S.A. (2001). Structural mechanism for rifampicin inhibition of bacterial RNA polymerase. *Cell* 104, 901–912.

Carroll, P., Muttucumaru, D.G.N., and Parish, T. (2005). Use of a tetracycline-inducible system for conditional expression in *Mycobacterium tuberculosis* and *Mycobacterium smegmatis*. *Appl. Environ. Microbiol.* 71, 3077–3084.

Carroll, P., Brown, A.C., Hartridge, A.R., and Parish, T. (2007). Expression of *Mycobacterium tuberculosis* Rv1991c using an arabinose-inducible promoter demonstrates its role as a toxin. *FEMS Microbiol. Lett.* 274, 73–82.

Caws, M., Thwaites, G., Dunstan, S., Hawn, T.R., Thi Ngoc Lan, N., Thuong, N.T.T., Stepniewska, K., Huyen, M.N.T., Bang, N.D., Huu Loc, T., et al. (2008). The influence of host and bacterial genotype on the development of disseminated disease with *Mycobacterium tuberculosis*. *PLoS Pathog* 4, e1000034.

- Chakraborty, S., Gruber, T., Barry, C.E., Boshoff, H.I., and Rhee, K.Y. (2013). Para-aminosalicylic acid acts as an alternative substrate of folate metabolism in *Mycobacterium tuberculosis*. *Science* 339, 88–91.
- Chao, M.C., and Rubin, E.J. (2010). Letting sleeping dogs lie: Does dormancy play a role in tuberculosis? *Annu. Rev. Microbiol.* 64, 293–311.
- Chaturvedi, V., Dwivedi, N., Tripathi, R.P., and Sinha, S. (2007). Evaluation of *Mycobacterium smegmatis* as a possible surrogate screen for selecting molecules active against multi-drug resistant *Mycobacterium tuberculosis*. *J. Gen. Appl. Microbiol.* 53, 333–337.
- Chen, L., Xie, Q., and Nathan, C. (1998). Alkyl hydroperoxide reductase subunit C (AhpC) protects bacterial and human cells against reactive nitrogen intermediates. *Mol. Cell* 1, 795–805.
- Chopra, I., and Brennan, P. (1998). Molecular action of anti-mycobacterial agents. *Tuber. Lung Dis.* 78, 89–98.
- Ciampi, M.S., Schmid, M.B., and Roth, J.R. (1982). Transposon Tn10 Provides a Promoter for Transcription of Adjacent Sequences. *Proc. Natl. Acad. Sci. U. S. A.* 79, 5016–5020.
- Clark-Curtiss, J.E., and Haydel, S.E. (2003). Molecular genetics of *Mycobacterium tuberculosis* pathogenesis. *Annu. Rev. Microbiol.* 57, 517–549.
- Claxton, A.J., Cramer, J., and Pierce, C. (2001). A systematic review of the associations between dose regimens and medication compliance. *Clin. Ther.* 23, 1296–1310.
- Click, E.S., Moonan, P.K., Winston, C.A., Cowan, L.S., and Oeltmann, J.E. (2012). Relationship between *Mycobacterium tuberculosis* phylogenetic lineage and clinical site of tuberculosis. *Clin. Infect. Dis.* 54, 211–219.
- Cohen, S.P., Hächler, H., and Levy, S.B. (1993). Genetic and functional analysis of the multiple antibiotic resistance (*mar*) locus in *Escherichia coli*. *J. Bacteriol.* 175, 1484–1492.
- Cole, S.T., Brosch, R., Parkhill, J., Garnier, T., Churcher, C., Harris, D., Gordon, S.V., Eiglmeier, K., Gas, S., Barry, C.E., et al. (1998). Deciphering the biology of *Mycobacterium tuberculosis* from the complete genome sequence. *Nature* 393, 537–544.
- Dabbs, E.R., Yazawa, K., Mikami, Y., Miyaji, M., Morisaki, N., Iwasaki, S., and Furihata, K. (1995). Ribosylation by mycobacterial strains as a new mechanism of rifampin inactivation. *Antimicrob. Agents Chemother.* 39, 1007–1009.
- Daugherty, A., Powers, K.M., Standley, M.S., Kim, C.S., and Purdy, G.E. (2011). *Mycobacterium smegmatis* RoxY is a repressor of *oxyS* and contributes to resistance to oxidative stress and bactericidal ubiquitin-derived peptides. *J. Bacteriol.* 193, 6824–6833.
- Davis, A.L. (1996). History of the sanatorium movement. *Tuberc. N. Y. Brownand Co.* 935–943.

- Deng, L., Mikusová, K., Robuck, K.G., Scherman, M., Brennan, P.J., and McNeil, M.R. (1995). Recognition of multiple effects of ethambutol on metabolism of mycobacterial cell envelope. *Antimicrob. Agents Chemother.* 39, 694–701.
- Deshayes, C., Perrodou, E., Gallien, S., Euphrasie, D., Schaeffer, C., Van-Dorsselaer, A., Poch, O., Lecompte, O., and Reyrat, J.-M. (2007). Interrupted coding sequences in *Mycobacterium smegmatis*: authentic mutations or sequencing errors? *Genome Biol.* 8, R20.
- Dhandayuthapani, S., Zhang, Y., Mudd, M.H., and Deretic, V. (1996). Oxidative stress response and its role in sensitivity to isoniazid in mycobacteria: characterization and inducibility of *ahpC* by peroxides in *Mycobacterium smegmatis* and lack of expression in *M. aurum* and *M. tuberculosis*. *J. Bacteriol.* 178, 3641–3649.
- Doerks, T., van Noort, V., Minguéz, P., and Bork, P. (2012). Annotation of the *M. tuberculosis* hypothetical orfeome: Adding functional information to more than half of the uncharacterized proteins. *PLoS ONE* 7, e34302.
- Dubos, R.J., and Dubos, J. (1952). *The white plague: Tuberculosis, man, and society* (Rutgers University Press).
- Duncan, K. (2003). Progress in TB drug development and what is still needed. *Tuberculosis* 83, 201–207.
- Dussurget, O., and Smith, I. (1998). Interdependence of mycobacterial iron regulation, oxidative-stress response and isoniazid resistance. *Trends Microbiol.* 6, 354–358.
- Dye, C., and Williams, B.G. (2010). The population dynamics and control of tuberculosis. *Science* 328, 856–861.
- Dye, C., Scheele, S., Dolin, P., Pathania, V., and Ravigliione, M. (1999). Global burden of tuberculosis: Estimated incidence, prevalence, and mortality by country. *JAMA* 282, 677–686.
- Ehrt, S., Guo, X.Z.V., Hickey, C.M., Ryou, M., Monteleone, M., Riley, L.W., and Schnappinger, D. (2005). Controlling gene expression in mycobacteria with anhydrotetracycline and Tet repressor. *Nucleic Acids Res.* 33, e21.
- Fernandes, P.B. (1988). Mode of action, and in vitro and in vivo activities of the fluoroquinolones. *J. Clin. Pharmacol.* 28, 156–168.
- Ferraris, D.M., and Rizzi, M. (2011). Zinc-dependent metalloprotease-1 (Zmp1). In *Encyclopedia of Inorganic and Bioinorganic Chemistry*, (John Wiley & Sons, Ltd),.
- Ferraris, D.M., Sbardella, D., Petrera, A., Marini, S., Amstutz, B., Coletta, M., Sander, P., and Rizzi, M. (2011). Crystal structure of *Mycobacterium tuberculosis* zinc-dependent metalloprotease-1 (Zmp1), a metalloprotease involved in pathogenicity. *J. Biol. Chem.* 286, 32475–32482.

- Fleischmann, R.D., Alland, D., Eisen, J.A., Carpenter, L., White, O., Peterson, J., DeBoy, R., Dodson, R., Gwinn, M., Haft, D., et al. (2002). Whole-genome comparison of *Mycobacterium tuberculosis* clinical and laboratory strains. *J. Bacteriol.* **184**, 5479–5490.
- Gagneux, S., and Small, P.M. (2007). Global phylogeography of *Mycobacterium tuberculosis* and implications for tuberculosis product development. *Lancet Infect. Dis.* **7**, 328–337.
- Gagneux, S., DeRiemer, K., Van, T., Kato-Maeda, M., Jong, B.C. de, Narayanan, S., Nicol, M., Niemann, S., Kremer, K., Gutierrez, M.C., et al. (2006). Variable host–pathogen compatibility in *Mycobacterium tuberculosis*. *Proc. Natl. Acad. Sci. U. S. A.* **103**, 2869–2873.
- Galagan, J.E. (2014). Genomic insights into tuberculosis. *Nat. Rev. Genet.* **15**, 307–320.
- Galagan, J.E., Sisk, P., Stolte, C., Weiner, B., Koehrsen, M., Wymore, F., Reddy, T.B.K., Zucker, J.D., Engels, R., Gellesch, M., et al. (2010). TB database 2010: Overview and update. *Tuberculosis* **90**, 225–235.
- Galamba, A., Soetaert, K., Wang, X.-M., Bruyn, J.D., Jacobs, P., and Content, J. (2001). Disruption of *adhC* reveals a large duplication in the *Mycobacterium smegmatis* mc2155 genome. *Microbiology* **147**, 3281–3294.
- Gallien, S., Perrodou, E., Carapito, C., Deshayes, C., Reytrat, J.-M., Van Dorsselaer, A., Poch, O., Schaeffer, C., and Lecompte, O. (2009). Ortho-proteogenomics: multiple proteomes investigation through orthology and a new MS-based protocol. *Genome Res.* **19**, 128–135.
- Gannoun-Zaki, L., Alibaud, L., Carrère-Kremer, S., Kremer, L., and Blanc-Potard, A.-B. (2013). Overexpression of the KdpF membrane peptide in *Mycobacterium bovis* BCG results in reduced intramacrophage growth and altered cording morphology. *PLoS ONE* **8**, e60379.
- García-Fernández, E., Frank, D.J., Galán, B., Kells, P.M., Podust, L.M., García, J.L., and Ortiz de Montellano, P.R. (2013). A highly conserved mycobacterial cholesterol catabolic pathway. *Environ. Microbiol.* **15**, 2342–2359.
- Gill, W.P., Harik, N.S., Whiddon, M.R., Liao, R.P., Mittler, J.E., and Sherman, D.R. (2009). A replication clock for *Mycobacterium tuberculosis*. *Nat. Med.* **15**, 211–214.
- Ginsberg, A.M., and Spigelman, M. (2007). Challenges in tuberculosis drug research and development. *Nature* **13**, 290–294.
- Girardi, E., Raviglione, M.C., Antonucci, G., Godfrey-Faussett, P., and Ippolito, G. (1999). Impact of the HIV epidemic on the spread of other diseases: the case of tuberculosis. *AIDS Lond. Engl.* **14 Suppl 3**, S47–S56.
- Goude, R., and Parish, T. (2009). Electroporation of mycobacteria. In *Mycobacteria Protocols*, T. Parish, and A.C. Brown, eds. (Humana Press), pp. 203–215.
- Griffin, J.E., Gawronski, J.D., DeJesus, M.A., Ioerger, T.R., Akerley, B.J., and Sassetti, C.M. (2011). High-resolution phenotypic profiling defines genes essential for mycobacterial growth and cholesterol catabolism. *PLoS Pathog* **7**, e1002251.

- Guilhot, C., Otal, I., Van Rompaey, I., Martin, C., and Gicquel, B. (1994). Efficient transposition in mycobacteria: construction of *Mycobacterium smegmatis* insertional mutant libraries. *J. Bacteriol.* *176*, 535.
- Gutacker, M.M., Smoot, J.C., Migliaccio, C.A.L., Ricklefs, S.M., Hua, S., Cousins, D.V., Graviss, E.A., Shashkina, E., Kreiswirth, B.N., and Musser, J.M. (2002). Genome-wide analysis of synonymous single nucleotide polymorphisms in *Mycobacterium tuberculosis* complex organisms: resolution of genetic relationships among closely related microbial strains. *Genetics* *162*, 1533–1543.
- Harisinghani, M.G., McCloud, T.C., Shepard, J.-A.O., Ko, J.P., Shroff, M.M., and Mueller, P.R. (2000). Tuberculosis from Head to Toe. *RadioGraphics* *20*, 449–470.
- Hartkoorn, R.C., Uplekar, S., and Cole, S.T. (2014). Cross-resistance between clofazimine and bedaquiline through upregulation of MmpL5 in *Mycobacterium tuberculosis*. *Antimicrob. Agents Chemother.* *58*, 2979–2981.
- Hopewell, P.C. (1992). Impact of human immunodeficiency virus infection on the epidemiology, clinical features, management, and control of tuberculosis. *Clin. Infect. Dis.* *15*, 540–547.
- Howard, S.T., and Byrd, T.F. (2000). The rapidly growing mycobacteria: saprophytes and parasites. *Microbes Infect.* *2*, 1845–1853.
- Huard, R.C., Fabre, M., Haas, P. de, Lazzarini, L.C.O., Soolingen, D. van, Cousins, D., and Ho, J.L. (2006). Novel genetic polymorphisms that further delineate the phylogeny of the *Mycobacterium tuberculosis* complex. *J. Bacteriol.* *188*, 4271–4287.
- Ioerger, T.R., O'Malley, T., Liao, R., Guinn, K.M., Hickey, M.J., Mohaideen, N., Murphy, K.C., Boshoff, H.I.M., Mizrahi, V., Rubin, E.J., et al. (2013). Identification of new drug targets and resistance mechanisms in *Mycobacterium tuberculosis*. *PLoS ONE* *8*, e75245.
- Ito, K., Yamamoto, K., and Kawanishi, S. (1992). Manganese-mediated oxidative damage of cellular and isolated DNA by isoniazid and related hydrazines: non-Fenton-type hydroxyl radical formation. *Biochemistry (Mosc.)* *31*, 11606–11613.
- Jarlier, V., and Nikaido, H. (1994). Mycobacterial cell wall: Structure and role in natural resistance to antibiotics. *FEMS Microbiol. Lett.* *123*, 11–18.
- Johnsson, K., and Schultz, P.G. (1994). Mechanistic studies of the oxidation of isoniazid by the catalase peroxidase from *Mycobacterium tuberculosis*. *J. Am. Chem. Soc.* *116*, 7425–7426.
- Joshi, S.A., Ball, D.A., Sun, M.G., Carlsson, F., Watkins, B.Y., Aggarwal, N., McCracken, J.M., Huynh, K.K., and Brown, E.J. (2012). EccA1, a component of the *Mycobacterium marinum* ESX-1 protein virulence factor secretion pathway, regulates mycolic acid lipid synthesis. *Chem. Biol.* *19*, 372–380.

- Joshi, S.M., Pandey, A.K., Capite, N., Fortune, S.M., Rubin, E.J., and Sasseti, C.M. (2006). Characterization of mycobacterial virulence genes through genetic interaction mapping. *Proc. Natl. Acad. Sci.* *103*, 11760–11765.
- Kapopoulou, A., Lew, J.M., and Cole, S.T. (2011). The MycoBrowser portal: A comprehensive and manually annotated resource for mycobacterial genomes. *Tuberculosis* *91*, 8–13.
- Kaushal, D., Schroeder, B.G., Tyagi, S., Yoshimatsu, T., Scott, C., Ko, C., Carpenter, L., Mehrotra, J., Manabe, Y.C., Fleischmann, R.D., et al. (2002). Reduced immunopathology and mortality despite tissue persistence in a *Mycobacterium tuberculosis* mutant lacking alternative  $\sigma$  factor, SigH. *Proc. Natl. Acad. Sci.* *99*, 8330–8335.
- Keung, A., Eller, M.G., McKenzie, K.A., and Weir, S.J. (1999). Single and multiple dose pharmacokinetics of rifapentine in man: Part II. *Int. J. Tuberc. Lung Dis.* *3*, 437–444.
- Kocagöz, T., Hackbarth, C.J., Unsal, I., Rosenberg, E.Y., Nikaido, H., and Chambers, H.F. (1996). Gyrase mutations in laboratory-selected, fluoroquinolone-resistant mutants of *Mycobacterium tuberculosis* H37Ra. *Antimicrob. Agents Chemother.* *40*, 1768–1774.
- Koul, A., Dendouga, N., Vergauwen, K., Molenberghs, B., Vranckx, L., Willebrords, R., Ristic, Z., Lill, H., Dorange, I., Guillemont, J., et al. (2007). Diarylquinolines target subunit c of mycobacterial ATP synthase. *Nat. Chem. Biol.* *3*, 323–324.
- Koul, A., Arnoult, E., Lounis, N., Guillemont, J., and Andries, K. (2011). The challenge of new drug discovery for tuberculosis. *Nature* *469*, 483–490.
- Krieger, I.V., Freundlich, J.S., Gawandi, V.B., Roberts, J.P., Gawandi, V.B., Sun, Q., Owen, J.L., Fraile, M.T., Huss, S.I., Lavandera, J.-L., et al. (2012). Structure-guided discovery of phenyl-diketo acids as potent inhibitors of *M. tuberculosis* malate synthase. *Chem. Biol.* *19*, 1556–1567.
- Larsen, M.H., Vilchèze, C., Kremer, L., Besra, G.S., Parsons, L., Salfinger, M., Heifets, L., Hazbon, M.H., Alland, D., Sacchettini, J.C., et al. (2002). Overexpression of *inhA*, but not *kasA*, confers resistance to isoniazid and ethionamide in *Mycobacterium smegmatis*, *M. bovis* BCG and *M. tuberculosis*. *Mol. Microbiol.* *46*, 453–466.
- Lawn, S.D., and Zumla, A.I. (2011). Tuberculosis. *The Lancet* *378*, 57–72.
- Lechartier, B., Rybníček, J., Zumla, A., and Cole, S.T. (2014). Tuberculosis drug discovery in the post-post-genomic era. *EMBO Mol. Med.* *6*, 158–168.
- Levin, M.E., and Hatfull, G.F. (1993). *Mycobacterium smegmatis* RNA polymerase: DNA supercoiling, action of rifampicin and mechanism of rifampicin resistance. *Mol. Microbiol.* *8*, 277–285.
- Lew, J.M., Kapopoulou, A., Jones, L.M., and Cole, S.T. (2011). TubercuList – 10 years after. *Tuberculosis* *91*, 1–7.

- L'homme, R.F., Nijland, H.M.J., Gras, L., Aarnoutse, R.E., van Crevel, R., Boeree, M., Brinkman, K., Prins, J.M., Juttman, J.R., and Burger, D.M. (2009). Clinical experience with the combined use of lopinavir/ritonavir and rifampicin. *AIDS Lond. Engl.* 23, 863–865.
- Lienhardt, C., Glaziou, P., Uplekar, M., Lönnroth, K., Getahun, H., and Raviglione, M. (2012). Global tuberculosis control: lessons learnt and future prospects. *Nat. Rev. Microbiol.* 10, 407–416.
- Lim, H., and Heffernan, H. (2013). Tuberculosis in New Zealand: Annual Report 2012 (Porirua: Institute of Environmental Science and Research Ltd (ESR)).
- Lönnroth, K., Roglic, G., and Harries, A.D. (2014). Improving tuberculosis prevention and care through addressing the global diabetes epidemic: from evidence to policy and practice. *Lancet Diabetes Endocrinol.* 2, 730–739.
- Maas, W.K. (1994). The arginine repressor of *Escherichia coli*. *Microbiol. Rev.* 58, 631–640.
- Maggi, N., Pasqualucci, C.R., Ballotta, R., and Sensi, P. (1966). Rifampicin: A new orally active rifamycin. *Chemotherapy* 11, 285–292.
- Manca, C., Lyashchenko, K., Colangeli, R., and Gennaro, M.L. (1997). MTC28, a novel 28-kilodalton proline-rich secreted antigen specific for the *Mycobacterium tuberculosis* complex. *Infect. Immun.* 65, 4951–4957.
- Manganelli, R., Voskuil, M.I., Schoolnik, G.K., Dubnau, E., Gomez, M., and Smith, I. (2002). Role of the extracytoplasmic-function  $\sigma$  Factor  $\sigma^H$  in *Mycobacterium tuberculosis* global gene expression. *Mol. Microbiol.* 45, 365–374.
- Manjunatha, U., Boshoff, H.I.M., and Barry, C.E. (2009). The mechanism of action of PA-824. *Commun. Integr. Biol.* 2, 215–218.
- Marais, B.J., Lönnroth, K., Lawn, S.D., Migliori, G. ni B., Mwaba, P., Glaziou, P., Bates, M., Colagiuri, R., Zijenah, L., Swaminathan, S., et al. (2013). Tuberculosis comorbidity with communicable and non-communicable diseases: integrating health services and control efforts. *Lancet Infect. Dis.* 13, 436–448.
- Martin, C., Timm, J., Rauzier, J., Gomez-Lus, R., Davies, J., and Gicquel, B. (1990). Transposition of an antibiotic resistance element in mycobacteria. *Nature* 345, 739–743.
- Martinez, A., Torello, S., and Kolter, R. (1999). Sliding motility in mycobacteria. *J. Bacteriol.* 181, 7331–7338.
- Master, S.S., Davis, A.S., Rampini, S.K., Keller, C., Ehlers, S., Springer, B., Sander, P., and Deretic, V. (2008). *Mycobacterium tuberculosis* prevents inflammasome activation. *Cell Host Microbe* 3, 224–232.
- Matsumoto, M., Hashizume, H., Tomishige, T., Kawasaki, M., Tsubouchi, H., Sasaki, H., Shimokawa, Y., and Komatsu, M. (2006). OPC-67683, a nitro-dihydro-imidazooxazole derivative with promising action against tuberculosis in vitro and in mice. *PLoS Med* 3, e466.



- Maus, C.E., Plikaytis, B.B., and Shinnick, T.M. (2005). Mutation of *tlyA* confers capreomycin resistance in *Mycobacterium tuberculosis*. *Antimicrob. Agents Chemother.* *49*, 571–577.
- McAdam, R.A., Quan, S., Smith, D.A., Bardarov, S., Betts, J.C., Cook, F.C., Hooker, E.U., Lewis, A.P., Woollard, P., Everett, M.J., et al. (2002). Characterization of a *Mycobacterium tuberculosis* H37Rv transposon library reveals insertions in 351 ORFs and mutants with altered virulence. *Microbiology* *148*, 2975–2986.
- McDermott, P.F., White, D.G., Podglajen, I., Alekshun, M.N., and Levy, S.B. (1998). Multidrug resistance following expression of the *Escherichia coli* *marA* gene in *Mycobacterium smegmatis*. *J. Bacteriol.* *180*, 2995–2998.
- Mdluli, K., Sherman, D.R., Hickey, M.J., Kreiswirth, B.N., Morris, S., Stover, C.K., and Barry, C.E. (1996). Biochemical and genetic data suggest that *InhA* is not the primary target for activated isoniazid in *Mycobacterium tuberculosis*. *J. Infect. Dis.* *174*, 1085–1090.
- Mdluli, K., Slayden, R.A., Zhu, Y., Ramaswamy, S., Pan, X., Mead, D., Crane, D.D., Musser, J.M., and Barry, C.E., 3rd (1998). Inhibition of a *Mycobacterium tuberculosis* beta-ketoacyl ACP synthase by isoniazid. *Science* *280*, 1607–1610.
- Mehta, P.K., King, C.H., White, E.H., Murtagh, J.J., and Quinn, F.D. (1996). Comparison of in vitro models for the study of *Mycobacterium tuberculosis* invasion and intracellular replication. *Infect. Immun.* *64*, 2673–2679.
- Michel, A.L., Müller, B., and van Helden, P.D. (2010). *Mycobacterium bovis* at the animal–human interface: A problem, or not? *Vet. Microbiol.* *140*, 371–381.
- Miller, C.H., Nisa, S., Dempsey, S., Jack, C., and O’Toole, R. (2009). Modifying culture conditions in chemical library screening identifies alternative inhibitors of mycobacteria. *Antimicrob. Agents Chemother.* *53*, 5279–5283.
- Moazed, D., and Noller, H.F. (1987). Interaction of antibiotics with functional sites in 16S ribosomal RNA. *327*, 389–394.
- Mostowy, S., Cleto, C., Sherman, D.R., and Behr, M.A. (2004). The *Mycobacterium tuberculosis* complex transcriptome of attenuation. *Tuberculosis* *84*, 197–204.
- Mudenda, V., Lucas, S., Shibemba, A., O’Grady, J., Bates, M., Kapata, N., Schwank, S., Mwaba, P., Atun, R., Hoelscher, M., et al. (2012). Tuberculosis and tuberculosis/HIV/AIDS–associated mortality in Africa: The urgent need to expand and invest in routine and research autopsies. *J. Infect. Dis.* *jir859*.
- Murray, C.J., Styblo, K., and Rouillon, A. (1990). Tuberculosis in developing countries: burden, intervention and cost. *Bull. Int. Union Tuberc. Lung Dis.* *65*, 6–24.
- Mwandumba, H.C., Russell, D.G., Nyirenda, M.H., Anderson, J., White, S.A., Molyneux, M.E., and Squire, S.B. (2004). *Mycobacterium tuberculosis* resides in nonacidified vacuoles in endocytically competent alveolar macrophages from patients with tuberculosis and HIV infection. *J. Immunol.* *172*, 4592–4598.

- Nair, S., Ramaswamy, P.A., Ghosh, S., Joshi, D.C., Pathak, N., Siddiqui, I., Sharma, P., Hasnain, S.E., Mande, S.C., and Mukhopadhyay, S. (2009). The PPE18 of *Mycobacterium tuberculosis* interacts with TLR2 and activates IL-10 induction in macrophage. *J. Immunol.* *183*, 6269–6281.
- Niemi, M., Backman, J.T., Fromm, M.F., Neuvonen, P.J., and Kivistö, K.T. (2003). Pharmacokinetic interactions with rifampicin : Clinical relevance. *Clin. Pharmacokinet.* *42*, 819–850.
- Nisa, S., Blokpoel, M.C.J., Robertson, B.D., Tyndall, J.D.A., Lun, S., Bishai, W.R., and O’Toole, R. (2010). Targeting the chromosome partitioning protein ParA in tuberculosis drug discovery. *J. Antimicrob. Chemother.* *65*, 2347–2358.
- Oatway Jr., W.H., and Steenken Jr., W. (1936). The pathogenesis and fate of tubercle produced by dissociated variants of tubercle bacilli. *J. Infect. Dis.* *59*, 306–325.
- O’Brien, R.J., and Nunn, P.P. (2001). The need for new drugs against tuberculosis. *Am. J. Respir. Crit. Care Med.* *163*, 1055–1058.
- Ooi, S.L., Pan, X., Peyser, B.D., Ye, P., Meluh, P.B., Yuan, D.S., Irizarry, R.A., Bader, J.S., Spencer, F.A., and Boeke, J.D. (2006). Global synthetic-lethality analysis and yeast functional profiling. *Trends Genet.* *22*, 56–63.
- Orme, I.M. (2014). A new unifying theory of the pathogenesis of tuberculosis. *Tuberculosis* *94*, 8–14.
- Palomino, J.C., and Portaels, F. (1999). Simple procedure for drug susceptibility testing of *Mycobacterium tuberculosis* using a commercial colorimetric assay. *Eur. J. Clin. Microbiol. Infect. Dis.* *18*, 380–383.
- Pandey, A.K., Raman, S., Proff, R., Joshi, S., Kang, C.M., Rubin, E.J., Husson, R.N., and Sassetti, C.M. (2009). Nitrile-inducible gene expression in mycobacteria. *Tuberculosis* *89*, 12–16.
- Pansy, F., Stander, H., and Donovan, R. (1952). In vitro studies on isonicotinic acid hydrazide. *Am. Rev. Tuberc.* *65*, 761–764.
- Parrish, N.M., Dick, J.D., and Bishai, W.R. (1998). Mechanisms of latency in *Mycobacterium tuberculosis*. *Trends Microbiol.* *6*, 107–112.
- Parsons, A.B., Brost, R.L., Ding, H., Li, Zhijiang, Zhang, Chaoying, Sheikh, B., Brown, Grant W., Kane, Patricia M., Hughes, Timothy R., and Boone, C. (2004). Integration of chemical genetic and genetic interaction data links bioactive compounds to cellular target pathways. *Nat Biotech* *22*, 62–69.
- Parsons, A.B., Lopez, A., Givoni, I.E., Williams, D.E., Gray, C.A., Porter, J., Chua, G., Sopko, R., Brost, R.L., Ho, C.-H., et al. (2006). Exploring the mode-of-action of bioactive compounds by chemical-genetic profiling in yeast. *Cell* *126*, 611–625.

- Parwati, I., Alisjahbana, B., Apriani, L., Soetikno, R.D., Ottenhoff, T.H., Zanden, A.G.M. van der, Meer, J. van der, Soolingen, D. van, and Crevel, R. van (2010). Mycobacterium tuberculosis Beijing genotype is an independent risk factor for tuberculosis treatment failure in Indonesia. *J. Infect. Dis.* 201, 553–557.
- Pathak, R. (2013). Role of *lspA* gene in the biology and pathogenesis of mycobacterium tuberculosis. University of Delhi.
- Patru, M.-M., and Pavelka, M.S. (2010). A role for the class A penicillin-binding protein PonA2 in the survival of Mycobacterium smegmatis under conditions of nonreplication. *J. Bacteriol.* 192, 3043–3054.
- Payne, D.J., Gwynn, M.N., Holmes, D.J., and Pompliano, D.L. (2007). Drugs for bad bugs: confronting the challenges of antibacterial discovery. *Nat. Rev. Drug Discov.* 6, 29–40.
- Perrodou, E., Deshayes, C., Muller, J., Schaeffer, C., Van Dorsselaer, A., Ripp, R., Poch, O., Reytrat, J.-M., and Lecompte, O. (2006). ICDS database: interrupted CoDing sequences in prokaryotic genomes. *Nucleic Acids Res.* 34, D338–D343.
- Pethe, K., Sequeira, P.C., Agarwalla, S., Rhee, K., Kuhen, K., Phong, W.Y., Patel, V., Beer, D., Walker, J.R., Duraiswamy, J., et al. (2010). A chemical genetic screen in Mycobacterium tuberculosis identifies carbon-source-dependent growth inhibitors devoid of in vivo efficacy. *Nat. Commun.* 1, 57.
- Pitulle, C., Dorsch, M., Kazda, J., Wolters, J., and Stackebrandt, E. (1992). Phylogeny of rapidly growing members of the genus Mycobacterium. *Int. J. Syst. Bacteriol.* 42, 337–343.
- Prod'homme, G., Lagier, B., Pelicic, V., Hance, A.J., Gicquel, B., and Guilhot, C. (1998). A reliable amplification technique for the characterization of genomic DNA sequences flanking insertion sequences. *FEMS Microbiol. Lett.* 158, 75–81.
- Prosser, G.A., and de Carvalho, L.P.S. (2013). Metabolomics reveal d-alanine:d-alanine ligase as the target of d-cycloserine in Mycobacterium tuberculosis. *ACS Med. Chem. Lett.*
- Protopopova, M., Hanrahan, C., Nikonenko, B., Samala, R., Chen, P., Gearhart, J., Einck, L., and Nacy, C.A. (2005). Identification of a new antitubercular drug candidate, SQ109, from a combinatorial library of 1,2-ethylenediamines. *J. Antimicrob. Chemother.* 56, 968–974.
- Pyle, M.M. (1947). Relative numbers of resistant tubercle bacilli in sputa of patients before and during treatment with streptomycin. *Proc. Staff Meet. Mayo Clin.* 22, 465–473.
- Pym, A.S., Brodin, P., Brosch, R., Huerre, M., and Cole, S.T. (2002). Loss of RD1 contributed to the attenuation of the live tuberculosis vaccines Mycobacterium bovis BCG and Mycobacterium microti. *Mol. Microbiol.* 46, 709–717.
- Pym, A.S., Brodin, P., Majlessi, L., Brosch, R., Demangel, C., Williams, A., Griffiths, K.E., Marchal, G., Leclerc, C., and Cole, S.T. (2003). Recombinant BCG exporting ESAT-6 confers enhanced protection against tuberculosis. *Nat. Med.* 9, 533–539.

- Quan, S., Imai, T., Mikami, Y., Yazawa, K., Dabbs, E.R., Morisaki, N., Iwasaki, S., Hashimoto, Y., and Furihata, K. (1999). ADP-Ribosylation as an Intermediate Step in Inactivation of Rifampin by a Mycobacterial Gene. *Antimicrob. Agents Chemother.* **43**, 181–184.
- Raghavan, S., Manzanillo, P., Chan, K., Dovey, C., and Cox, J.S. (2008). Secreted transcription factor controls *Mycobacterium tuberculosis* virulence. *Nature* **454**, 717–721.
- Ramaswamy, S., and Musser, J.M. (1998). Molecular genetic basis of antimicrobial agent resistance in *Mycobacterium tuberculosis*: 1998 update. *Tuber. Lung Dis.* **79**, 3–29.
- Reed, M.B., Pichler, V.K., McIntosh, F., Mattia, A., Fallow, A., Masala, S., Domenech, P., Zwerling, A., Thibert, L., Menzies, D., et al. (2009). Major *Mycobacterium tuberculosis* Lineages Associate with Patient Country of Origin. *J. Clin. Microbiol.* **47**, 1119–1128.
- Rengarajan, J., Bloom, B.R., and Rubin, E.J. (2005). Genome-wide requirements for *Mycobacterium tuberculosis* adaptation and survival in macrophages. *Proc. Natl. Acad. Sci. U. S. A.* **102**, 8327–8332.
- Von Reyn, C.F., Kimambo, S., Mtei, L., Arbeit, R.D., Maro, I., Bakari, M., Matee, M., Lahey, T., Adams, L.V., Black, W., et al. (2011). Disseminated tuberculosis in human immunodeficiency virus infection: ineffective immunity, polyclonal disease and high mortality. *Int. J. Tuberc. Lung Dis.* **15**, 1087–1092.
- Rickman, K.A., Swancutt, K.L., Mezyk, S.P., and Kiddle, J.J. (2013). Isoniazid: Radical-induced oxidation and reduction chemistry. *Bioorg. Med. Chem. Lett.* **23**, 3096–3100.
- Riley, R. (1957). Aerial dissemination of pulmonary tuberculosis—the Burns Amberson Lecture. *Am Rev Tuberc Pulm. Dis* **76**, 931–941.
- Roback, P., Beard, J., Baumann, D., Gille, C., Henry, K., Krohn, S., Wiste, H., Voskuil, M.I., Rainville, C., and Rutherford, R. (2007). A predicted operon map for *Mycobacterium tuberculosis*. *Nucleic Acids Res.* **35**, 5085–5095.
- Rozwarski, D.A., Grant, G.A., Barton, D.H.R., Jacobs, W.R., and Sacchettini, J.C. (1998). Modification of the NADH of the Isoniazid Target (InhA) from *Mycobacterium tuberculosis*. *Science* **279**, 98–102.
- Sala, C., Haouz, A., Saul, F.A., Miras, I., Rosenkrands, I., Alzari, P.M., and Cole, S.T. (2009). Genome-wide regulon and crystal structure of Blal (Rv1846c) from *Mycobacterium tuberculosis*. *Mol. Microbiol.* **71**, 1102–1116.
- Sambrook, J., Russell, D.W., and Russell, D.W. (2001). *Molecular cloning: a laboratory manual* (3-volume set) (Cold spring harbor laboratory press Cold Spring Harbor, New York:).
- Sassetti, C.M., Boyd, D.H., and Rubin, E.J. (2001). Comprehensive identification of conditionally essential genes in mycobacteria. *Proc. Natl. Acad. Sci.* **98**, 12712–12717.
- Sassetti, C.M., Boyd, D.H., and Rubin, E.J. (2003). Genes required for mycobacterial growth defined by high density mutagenesis. *Mol. Microbiol.* **48**, 77–84.

Saunders, B.M., and Cooper, A.M. (2000). Restraining mycobacteria: Role of granulomas in mycobacterial infections. *Immunol. Cell Biol.* 78, 334–341.

Saunders, N.J., Trivedi, U.H., Thomson, M.L., Doig, C., Laurenson, I.F., and Blaxter, M.L. (2011). Deep resequencing of serial sputum isolates of *Mycobacterium tuberculosis* during therapeutic failure due to poor compliance reveals stepwise mutation of key resistance genes on an otherwise stable genetic background. *J. Infect.* 62, 212–217.

Saviola, B., and Bishai, W. (2006). The Genus *Mycobacterium*--Medical. In *The Prokaryotes*, M.D.P. Dr, S. Falkow, E. Rosenberg, K.-H. Schleifer, and E. Stackebrandt, eds. (Springer New York), pp. 919–933.

Schnappinger, D., Ehrt, S., Voskuil, M.I., Liu, Y., Mangan, J.A., Monahan, I.M., Dolganov, G., Efron, B., Butcher, P.D., Nathan, C., et al. (2003). Transcriptional adaptation of *Mycobacterium tuberculosis* within macrophages insights into the phagosomal environment. *J. Exp. Med.* 198, 693–704.

Selwyn, P.A., Hartel, D., Lewis, V.A., Schoenbaum, E.E., Vermund, S.H., Klein, R.S., Walker, A.T., and Friedland, G.H. (1989). A prospective study of the risk of tuberculosis among intravenous drug users with human immunodeficiency virus infection. *N. Engl. J. Med.* 320, 545–550.

Shenoi, S., and Friedland, G. (2009). Extensively drug-resistant tuberculosis: a new face to an old pathogen. *Annu. Rev. Med.* 60, 307.

Sherman, D.R., Mdluli, K., Hickey, M.J., Arain, T.M., Morris, S.L., III, C.E.B., and Stover, C.K. (1996). Compensatory *ahpC* Gene Expression in Isoniazid-Resistant *Mycobacterium tuberculosis*. *Science* 272, 1641–1643.

Shi, W., Zhang, X., Jiang, X., Yuan, H., Lee, J.S., Barry, C.E., Wang, H., Zhang, W., and Zhang, Y. (2011). Pyrazinamide inhibits trans-translation in *Mycobacterium tuberculosis*. *Science* 333, 1630–1632.

Shiloh, M.U., and DiGiuseppe Champion, P.A. (2010). To catch a killer. What can mycobacterial models teach us about *Mycobacterium tuberculosis* pathogenesis? *Curr. Opin. Microbiol.* 13, 86–92.

Shinnick, T.M., and Good, R.C. (1994). Mycobacterial taxonomy. *Eur. J. Clin. Microbiol. Infect. Dis.* 13, 884–901.

Siegrist, M.S., and Rubin, E.J. (2009). Phage transposon mutagenesis. In *Mycobacteria Protocols*, T. Parish, and A.C. Brown, eds. (Humana Press), pp. 311–323.

Singh, R., Manjunatha, U., Boshoff, H.I.M., Ha, Y.H., Niyomrattanakit, P., Ledwidge, R., Dowd, C.S., Lee, I.Y., Kim, P., Zhang, L., et al. (2008). PA-824 kills nonreplicating *Mycobacterium tuberculosis* by intracellular NO release. *Science* 322, 1392–1395.

Smith, N.H., Kremer, K., Inwald, J., Dale, J., Driscoll, J.R., Gordon, S.V., van Soolingen, D., Glyn Hewinson, R., and Maynard Smith, J. (2006). Ecotypes of the *Mycobacterium tuberculosis* complex. *J. Theor. Biol.* 239, 220–225.

Snapper, S.B., Melton, R.E., Mustafa, S., Kieser, T., and Jr, W.R.J. (1990). Isolation and characterization of efficient plasmid transformation mutants of *Mycobacterium smegmatis*. *Mol. Microbiol.* 4, 1911–1919.

Srivastava, V., Rouanet, C., Srivastava, R., Ramalingam, B., Loch, C., and Srivastava, B.S. (2007). Macrophage-specific *Mycobacterium tuberculosis* genes: identification by green fluorescent protein and kanamycin resistance selection. *Microbiology* 153, 659.

Steenken, W., Oatway, W.H., and Petroff, S.A. (1934). Biological studies of the tubercle bacillus. *J. Exp. Med.* 60, 515–540.

Stop TB Partnership (2006). The Global Plan to Stop TB 2006-2015: Actions for Life: Towards a World Free of Tuberculosis (Stop TB Partnership).

Stover, C.K., de la Cruz, V.F., Fuerst, T.R., Burlein, J.E., Benson, L.A., Bennett, L.T., Bansal, G.P., Young, J.F., Lee, M.H., Hatfull, G.F., et al. (1991). New use of BCG for recombinant vaccines. *Nature* 351, 456–460.

Stover, C.K., Warren, P., VanDevanter, D.R., Sherman, D.R., Arain, T.M., Langhorne, M.H., Anderson, S.W., Towell, J.A., Yuan, Y., McMurray, D.N., et al. (2000). A small-molecule nitroimidazopyran drug candidate for the treatment of tuberculosis. *Nature* 405, 962–966.

Suthar, A.B., Lawn, S.D., del Amo, J., Getahun, H., Dye, C., Sculier, D., Sterling, T.R., Chaisson, R.E., Williams, B.G., Harries, A.D., et al. (2012). Antiretroviral therapy for prevention of tuberculosis in adults with HIV: A systematic review and meta-analysis. *PLoS Med* 9, e1001270.

Tahlan, K., Wilson, R., Kastrinsky, D.B., Arora, K., Nair, V., Fischer, E., Barnes, S.W., Walker, J.R., Alland, D., Barry, C.E., et al. (2012). SQ109 targets MmpL3, a membrane transporter of trehalose monomycolate involved in mycolic acid donation to the cell wall core of *Mycobacterium tuberculosis*. *Antimicrob. Agents Chemother.* 56, 1797–1809.

Tanaka, Y., Yazawa, K., Dabbs, E.R., Nishikawa, K., Komaki, H., Mikami, Y., Miyaji, M., Morisaki, N., and Iwasaki, S. (1996). Different rifampicin inactivation mechanisms in nocardia and related taxa. *Microbiol. Immunol.* 40, 1–4.

Timmins, G.S., and Deretic, V. (2006). Mechanisms of action of isoniazid. *Mol. Microbiol.* 62, 1220–1227.

Timmins, G.S., Master, S., Rusnak, F., and Deretic, V. (2004). Nitric oxide generated from isoniazid activation by KatG: Source of nitric oxide and activity against *Mycobacterium tuberculosis*. *Antimicrob. Agents Chemother.* 48, 3006–3009.

Timperio, A.M., Rinalducci, S., and Zolla, L. (2005). Hydrazide derivatives produce active oxygen species as hydrazine. *Bioorganic Chem.* 33, 459–469.

- Tran, S.L., and Cook, G.M. (2005). The F1Fo-ATP synthase of *Mycobacterium smegmatis* is essential for growth. *J. Bacteriol.* **187**, 5023–5028.
- Triccas, J.A., Parish, T., Britton, W.J., and Gicquel, B. (1998). An inducible expression system permitting the efficient purification of a recombinant antigen from *Mycobacterium smegmatis*. *Fems Microbiol. Lett.* **167**, 151–156.
- Tufariello, J.M., Malek, A.A., Vilchèze, C., Cole, L.E., Ratner, H.K., González, P.A., Jain, P., Hatfull, G.F., Larsen, M.H., and Jacobs, W.R. (2014). Enhanced Specialized Transduction Using Recombineering in *Mycobacterium tuberculosis*. *mBio* **5**, e01179–14.
- Udwadia, Z.F., Amale, R.A., Ajbani, K.K., and Rodrigues, C. (2012). Totally drug-resistant tuberculosis in India. *Clin. Infect. Dis.* **54**, 579–581.
- Uhía, I., Galán, B., Kendall, S.L., Stoker, N.G., and García, J.L. (2012). Cholesterol metabolism in *Mycobacterium smegmatis*. *Environ. Microbiol. Rep.* **4**, 168–182.
- Uplekar, M., Figueroa-Munoz, J., Floyd, K., Getahun, H., and Jaramillo, E. (2006). The Stop TB Strategy: building on and enhancing DOTS to meet the TB-related Millennium Development Goals.
- Vandal, O.H., Roberts, J.A., Odaira, T., Schnappinger, D., Nathan, C.F., and Ehrt, S. (2009). Acid-Susceptible Mutants of *Mycobacterium tuberculosis* Share Hypersusceptibility to Cell Wall and Oxidative Stress and to the Host Environment. *J. Bacteriol.* **191**, 625–631.
- Villemagne, B., Crauste, C., Flipo, M., Baulard, A.R., Déprez, B., and Willand, N. (2012). Tuberculosis: The drug development pipeline at a glance. *Eur. J. Med. Chem.* **51**, 1–16.
- Wang, F., Jain, P., Gulten, G., Liu, Z., Feng, Y., Ganesula, K., Motiwala, A.S., Ioerger, T.R., Alland, D., Vilchèze, C., et al. (2010). *Mycobacterium tuberculosis* Dihydrofolate Reductase Is Not a Target Relevant to the Antitubercular Activity of Isoniazid. *Antimicrob. Agents Chemother.* **54**, 3776–3782.
- Wang, X.-D., Gu, J., Wang, T., Bi, L.-J., Zhang, Z.-P., Cui, Z.-Q., Wei, H.-P., Deng, J.-Y., and Zhang, X.-E. (2011). Comparative analysis of mycobacterial NADH pyrophosphatase isoforms reveals a novel mechanism for isoniazid and ethionamide inactivation. *Mol. Microbiol.* **82**, 1375–1391.
- Wang, X.-M., Galamba, A., Warner, D.F., Soetaert, K., Merkel, J.S., Kalai, M., Bifani, P., Lefèvre, P., Mizrahi, V., and Content, J. (2008). IS1096-mediated DNA rearrangements play a key role in genome evolution of *Mycobacterium smegmatis*. *Tuberculosis* **88**, 399–409.
- Wehrli, W., Knüsel, F., Schmid, K., and Staehelin, M. (1968). Interaction of rifamycin with bacterial RNA polymerase. *Proc. Natl. Acad. Sci.* **61**, 667–673.
- Weiling Hong, Wanyan Deng, and Jianping Xie (2013). The Structure, Function, and Regulation of *Mycobacterium* FtsZ. *Cell Biochem. Biophys.* **65**, 97–105.

Wengenack, N.L., and Rusnak, F. (2001). Evidence for Isoniazid-Dependent Free Radical Generation Catalyzed by *Mycobacterium tuberculosis* KatG and the Isoniazid-Resistant Mutant KatG(S315T). *Biochemistry (Mosc.)* 40, 8990–8996.

WHO (2010). The Global Plan to Stop TB 2011-2015: Transforming the fight towards the elimination of tuberculosis.

WHO (2014). Global tuberculosis report 2014.

Williams, K.J., Joyce, G., and Robertson, B.D. (2010). Improved mycobacterial tetracycline inducible vectors. *Plasmid* 64, 69–73.

Wilming, and Johnsson (1999). Spontaneous formation of the bioactive form of the tuberculosis drug isoniazid. *Angew. Chem. Int. Ed Engl.* 38, 2588–2590.

Yen, S., Bower, J.E., Freeman, J.T., Basu, I., and O’Toole, R.F. (2013). Phylogenetic lineages of tuberculosis isolates in New Zealand and their association with patient demographics. *Int. J. Tuberc. Lung Dis.* 17, 892–897.

Young, D.B., Perkins, M.D., Duncan, K., and Barry, C.E. (2008). Confronting the scientific obstacles to global control of tuberculosis. *J. Clin. Invest.* 118, 1255–1265.

Zhang, H., Gao, L., Zhang, J., Li, W., Yang, M., Zhang, H., Gao, C., and He, Z.-G. (2014). A Novel *marRAB* Operon Contributes to the Rifampicin Resistance in *Mycobacterium smegmatis*. *PLoS ONE* 9, e106016.

Zhang, Y., Heym, B., Allen, B., Young, D., and Cole, S. (1992). The catalase—peroxidase gene and isoniazid resistance of *Mycobacterium tuberculosis*. 358, 591–593.

Zhang, Y., Dhandayuthapani, S., and Deretic, V. (1996). Molecular basis for the exquisite sensitivity of *Mycobacterium tuberculosis* to isoniazid. *Proc. Natl. Acad. Sci. U. S. A.* 93, 13212–13216.

Van Zyl, J.M., and Van Der Walt, B.J. (1994). Apparent hydroxyl radical generation without transition metal catalysis and tyrosine nitration during oxidation of the anti-tubercular drug, isonicotinic acid hydrazide. *Biochem. Pharmacol.* 48, 2033–2042.



## **8. Appendix**

### **8.1.Solutions**

All solutions with the exception of proteinase K were stored at room temperature. Proteinase K was stored at -20 °C.

#### **Tris-HCl (pH 7.5)**

121.1 g of Tris Base was dissolved in 900 mL deionised water, and the pH adjusted to 7.5 with the addition of HCl. Once at the desired pH the volume was topped up to 1 L.

#### **0.5 M EDTA (pH 8.0)**

186.2g of EDTA was added to 900 mL deionised water, and the pH adjusted to 8.0 with the addition of NaOH. Once at the desired pH the volume was topped up to 1 L.

#### **TE Buffer**

A 10x stock of TE buffer was made up containing 100 mM Tris-HCl and 10 mM EDTA in deionised water and sterilised by autoclaving at 121 °C for 30 minutes on a liquid cycle. Working stocks of 1x TE buffer were made up using a 1/10 dilution of the 10x stock in deionised water and sterilised as above.

#### **TAE Buffer**

A 50x stock was made by dissolving 242 g Tris base in 1 L of deionised water containing 57.1 mL glacial acetic acid and 50 mM EDTA. The solution was diluted to a 1x working stock in deionised water.

#### **CTAB**

10 g CTAB and 4 g NaCl were added to 100 mL deionised water. The solution was heated at 65 °C in a water bath, with frequent agitation until dissolved. The CTAB solution was then stored at 4 °C.

#### **Proteinase K**

The proteinase K stock was made up by dissolving 1 mg of proteinase K powder (Sigma Aldrich) in 1mM Tris-HCl (pH 8.0) and 1.5 mM calcium acetate in deionised water.

## **Resazurin**

The resazurin stock solution was made up as a 0.3% (w/v) solution in ddH<sub>2</sub>O and stored at 4 °C. A working solution of resazurin at a concentration of 0.03% (w/v) was made up by diluting the stock solution in ddH<sub>2</sub>O and filter sterilising before storing at 4 °C.

## **8.2.Routine laboratory procedures**

### **Cleaning electroporation cuvettes**

Electroporation cuvettes were cleaned for reuse after each transformation. Cuvettes were soaked 12.5% bleach for 30 minutes with agitation, rinsed in ddH<sub>2</sub>O, soaked in 1 M HCl for 30 minutes with agitation, rinsed in ddH<sub>2</sub>O, and then rinsed in 75% ethanol three times. Cuvettes were dried, and stored. Immediately prior to use cuvettes were sterilised with UV for 10 minutes in a laminar flow hood.

### **Cleaning 384-pin RePads®**

RePads® were cleaned after each use. RePads® were soaked in 12.5% bleach overnight, and then soaked in a mixture of dishwashing detergent and water overnight. RePads® were then rinsed under tap water and scrubbed thoroughly with a dish-brush, and then dried on the bench. RePads® were then dipped in 100% ethanol and left to dry in a laminar flow hood. Dry RePads® were stored in large zip-lock plastic bags.

### **Cleaning metal 96-pin tool**

The pinning tool was dipped in 12.5% bleach (v/v) for one minute, then dipped in ddH<sub>2</sub>O for a further minute, before being dipped in 100% ethanol and flamed to sterilise between pinning each plate, and after use.

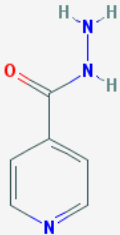
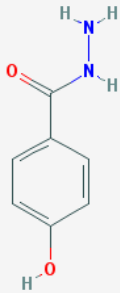
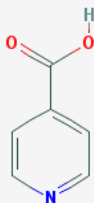
### 8.3. *MSMEI* and *MSMEG* annotations

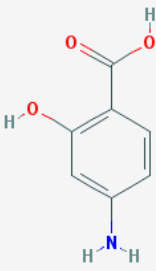
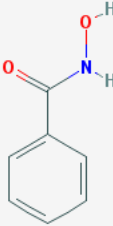
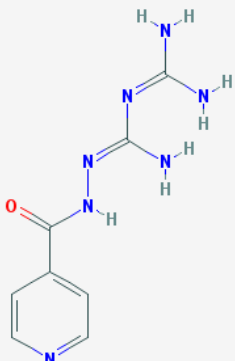
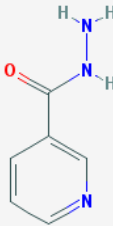
This study used the *M. smegmatis* mc<sup>2</sup>155 reference genome using the *MSMEI* annotations. The older *MSMEG* annotations are provided for each of the *M. smegmatis* mc<sup>2</sup>155 genes mentioned in this study.

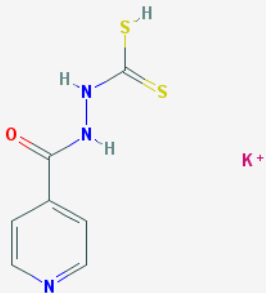
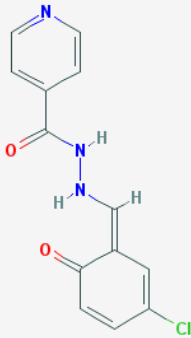
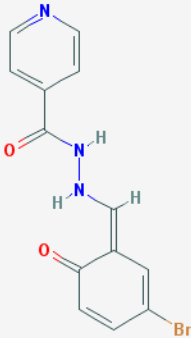
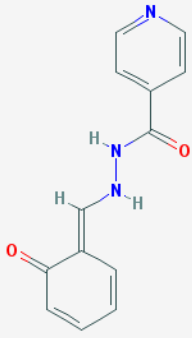
<b><i>MSMEI</i> annotation</b>	<b><i>MSMEG</i> annotation</b>
0062	0061
0227	0234
1186	1221
1210	1245
1211	1246
1800	1842
1801	1843
1904	1946
1905	1947
2671	2738
2672	2739
3093	3175
3189	3273
3358	3437
3380	3461
3416	3496
3684	3773
4123	4221
4267	4371
4423	4536
4424	4537
4764	4889
4765	4890
4815	4942
5136	5275
5244	5392
5460	5610
5538	5688
5554	5705
5621	5775
5828	5989
6040	6201
6092	6253
6216	6384
6263	6430

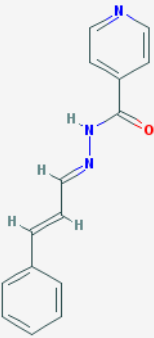
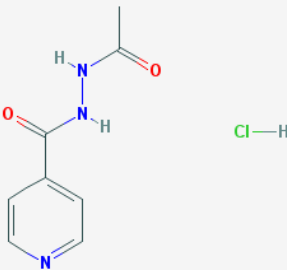
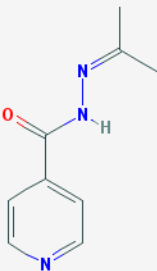
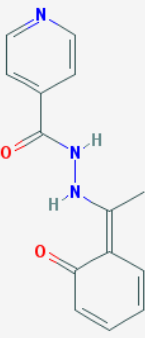
6264	6431
6301	6473
6730	6919

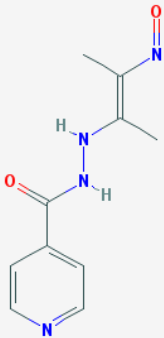
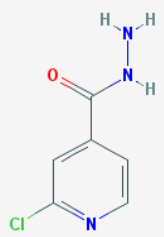
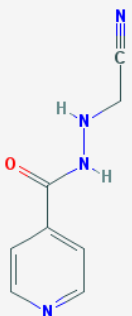
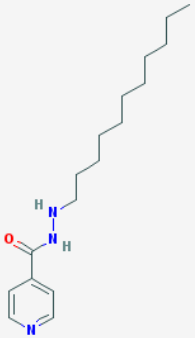
## 8.4. Isoniazid analogues

Drug (NSC)	Structure	Active against WT <i>M. smegmatis</i> mc2155 (>75% Growth-Inhibition at 10mg·mL <sup>-1</sup> )	Differential Activity versus <i>Tn::nudC</i>
Isoniazid (9659)		Yes	No
647		No	n/a
1483		No	n/a

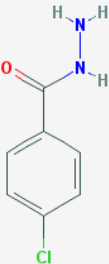
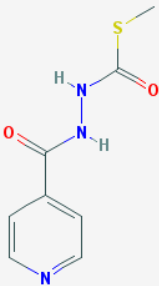
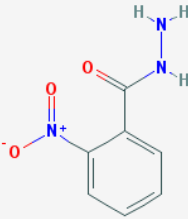
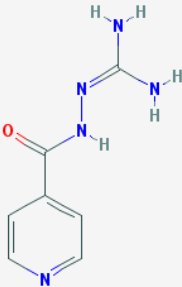
2083		No	n/a
3136		No	n/a
6855		Yes	No
18775		No	n/a

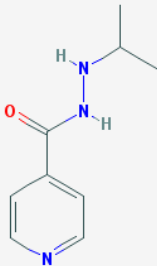
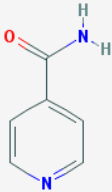
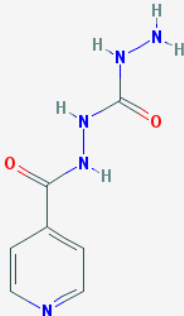
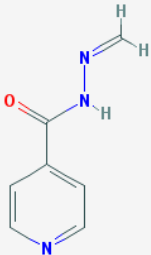
23449		Yes	No
27607		Yes	Yes
33759		Yes	Yes
33760		Yes	No

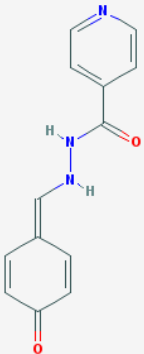
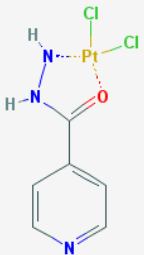
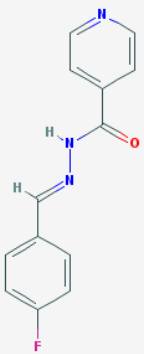
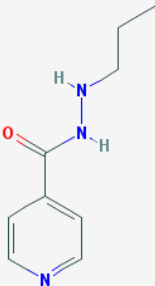
33763		Yes	No
36084		No	n/a
36086		Yes	No
37379		Yes	No

37800		Yes	Yes
38340		No	n/a
39298		No	n/a
40350		Yes	Yes



54990		No	n/a
59320		Yes	No
61870		No	n/a
69854		No	n/a

81850	 <chem>CC(C)NNC(=O)c1cccnc1</chem>	No	n/a
82353	 <chem>NC(=O)c1cccnc1</chem>	No	n/a
130848	 <chem>NC(=O)NNC(=O)c1cccnc1</chem>	No	n/a
141142	 <chem>C=NNC(=O)c1cccnc1</chem>	Yes	Yes

176757		Yes	Yes
274967		No	n/a
322078		Yes	No
359420		No	n/a

## 8.5.katG protein alignments

Consensus	1	10	20	30	40	50
	M	XXXXXXXXXX	EE	XXXXXXXXXX	XXXXXX	XXXXXX
1. Rv1908c	1	5	10	15	20	25
2. MSMEI_6126	1	5	10	15	20	25
3. MSMEI_3380	1	5	10	15	20	25
Consensus	60	70	80	90	100	110
1. Rv1908c	60	70	80	90	100	110
2. MSMEI_6126	60	70	80	90	100	110
3. MSMEI_3380	60	70	80	90	100	110
Consensus	120	130	140	150	160	170
1. Rv1908c	120	130	140	150	160	170
2. MSMEI_6126	120	130	140	150	160	170
3. MSMEI_3380	120	130	140	150	160	170
Consensus	180	190	200	210	220	230
1. Rv1908c	180	190	200	210	220	230
2. MSMEI_6126	180	190	200	210	220	230
3. MSMEI_3380	180	190	200	210	220	230
Consensus	240	250	260	270	280	290
1. Rv1908c	240	250	260	270	280	290
2. MSMEI_6126	240	250	260	270	280	290
3. MSMEI_3380	240	250	260	270	280	290
Consensus	300	310	320	330	340	350
1. Rv1908c	300	310	320	330	340	350
2. MSMEI_6126	300	310	320	330	340	350
3. MSMEI_3380	300	310	320	330	340	350
Consensus	360	370	380	390	400	410
1. Rv1908c	360	370	380	390	400	410
2. MSMEI_6126	360	370	380	390	400	410
3. MSMEI_3380	360	370	380	390	400	410
Consensus	420	430	440	450	460	470
1. Rv1908c	420	430	440	450	460	470
2. MSMEI_6126	420	430	440	450	460	470
3. MSMEI_3380	420	430	440	450	460	470
Consensus	480	490	500	510	520	530
1. Rv1908c	480	490	500	510	520	530
2. MSMEI_6126	480	490	500	510	520	530
3. MSMEI_3380	480	490	500	510	520	530
Consensus	540	550	560	570	580	590
1. Rv1908c	540	550	560	570	580	590
2. MSMEI_6126	540	550	560	570	580	590
3. MSMEI_3380	540	550	560	570	580	590
Consensus	600	610	620	630	640	650
1. Rv1908c	600	610	620	630	640	650
2. MSMEI_6126	600	610	620	630	640	650
3. MSMEI_3380	600	610	620	630	640	650
Consensus	660	670	680	690	700	710
1. Rv1908c	660	670	680	690	700	710
2. MSMEI_6126	660	670	680	690	700	710
3. MSMEI_3380	660	670	680	690	700	710
Consensus	720	730	740	750	760	770
1. Rv1908c	720	730	740	750	760	770
2. MSMEI_6126	720	730	740	750	760	770
3. MSMEI_3380	720	730	740	750	760	770
Consensus	780	790	800	810	820	830
1. Rv1908c	780	790	800	810	820	830
2. MSMEI_6126	780	790	800	810	820	830
3. MSMEI_3380	780	790	800	810	820	830
Consensus	840	850	860	870	880	890
1. Rv1908c	840	850	860	870	880	890
2. MSMEI_6126	840	850	860	870	880	890
3. MSMEI_3380	840	850	860	870	880	890
Consensus	900	910	920	930	940	950
1. Rv1908c	900	910	920	930	940	950
2. MSMEI_6126	900	910	920	930	940	950
3. MSMEI_3380	900	910	920	930	940	950

## **8.6.Publications**

Campen, R.L., Ackerley, D.F., Cook, G.M., and O'Toole, R.F. (2015). Development of a *Mycobacterium smegmatis* transposon mutant array for characterising the mechanism of action of tuberculosis drugs: Findings with isoniazid and its structural analogues. *Tuberculosis Article In Press*.